

**THE BEHAVIOUR OF A HEADED STUD
CONNECTION IN A 'NEW' PUSH TEST
INCLUDING A RIBBED SLAB.**

Tests: Background report.

ir. P.G.F.J. van der Sanden.
BKO-report 95-16, March 1996.

RAPPORT

**THE BEHAVIOUR OF A HEADED STUD
CONNECTION IN A 'NEW' PUSH TEST
INCLUDING A RIBBED SLAB.**

Tests: Background report.

ir. P.G.F.J. van der Sanden.
BKO-report 95-16, March 1996.

PREFACE.

A 'new' push test has been developed including a 'new' push specimen in which a single headed stud connection was embedded in a composite slab. In total twenty-three push tests were carried out. These 'new' push tests and the results are described in two reports: the 'main report' and the 'background report'. In the 'background report' detailed information is presented which is necessary to be able to reproduce the 'new' push tests, to analyse the measurements as well as a justification of several aspects.

Eindhoven, March 1996,

Pieter van der Sanden.

CONTENTS.

1	Concrete composition.	1.
2	Fabrication of the push specimens.	5.
3	Material properties headed stud connectors.	13.
4	Material properties profiled steel sheeting.	15.
5	Concrete properties.	19.
6	Supports of the push specimen.	23.
7	Technical information used equipment.	29.
8	Installation push specimen: only mechanical aspects.	31.
9	Configuration of the measurements.	33.
10	Complete installation push specimen.	41.
11	Graphical representation of the original measurements.	45.
	11.1 Introduction.	45.
	11.2 Forces in the x-direction: F_1 , F_2 , $Q_{x2,1}$, $Q_{x2,2}$ & ΣF_x .	48.
	11.3 Forces in the z-direction: $N_{z2,1}$, $N_{z2,2}$, $N_{z2,3}$ and $\Sigma N_{z2,i}$, N_{z3} , N_{z4} , N_{z5} & ΣF_z .	70.
	11.4 Strains of the headed stud connector: ϵ_{z1} , ϵ_{z2} & ϵ_{z3} .	92.
	11.5 Displacements: $u_{xc,a}$, $u_{ux,b}$, $u_{xf,1}$, $u_{xf,2}$, $u_{xh,1}$ & $u_{xh,2}$.	114.

1. CONCRETE COMPOSITION.

The maximum diameter of the aggregate was chosen 16 mm ($D = 16$ mm) dependent on the sizes of the specimens and the mesh reinforcement. The (little) amounts of concrete were mixed and cast at the university. Preventing water to be extracted from the mixture the inside of the mixer was moistened with 1 l water at the beginning of each casting day. The fractions sand and gravel (river gravel, not broken) in the mixture were as much as possible distributed according to sieve-line B₁₆ of the aggregate group 0-16 of the Dutch code NEN 5950 (VBT 1986); see Fig. 1.1. The percentages of the separate fractions were: 8-16 (24 %), 4-8 (20 %), 2-4 (14 %), 1-2 (10 %), 0.5-1 (12 %), 0.25-0.5 (12 %) and 0-0.25 (8 %). The concrete for the specimens 2 and 3 was composed out of sand and gravel out of bunkers. It appeared hardly possible to realise the before mentioned distribution of the fractions in the mixture, even if some additional aggregates were used. Moreover the humidity of the aggregates in the bunkers varied a lot. From then, the concrete was composed out of the separate fractions for the remaining specimens so that more or less the same concrete was obtained.

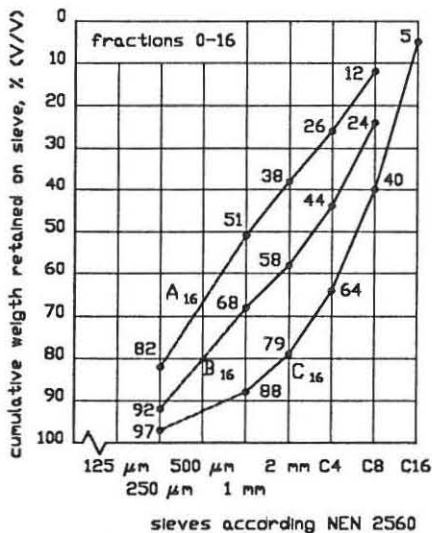


Fig. 1.1: Sieve-lines for 0-16.

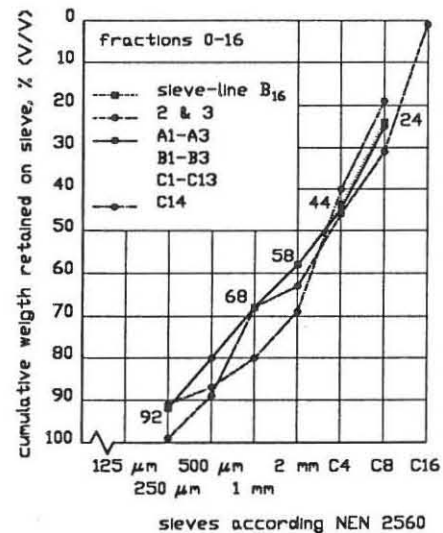


Fig. 1.2: Composition mixtures.

Unfortunately, as not all the fractions were available, some alternative fractions had to be used: quartz sand instead of 0-0.25, 0.2-0.63 instead of 0.25-0.5 and the combination of 3-5 and 5-8 instead of 4-8. Moreover, it appeared that the delivered fraction 8-16 contained also about 10 % 4-8. See Table 1.1 for the final ordered composition of the mixtures, in which each column represents a different mixture or a different casting day. For clarity's sake this subdivision will be maintained. In table 1.2 the measured composition of the aggregates in the mixture is presented (see also Fig. 1.2). Due to mainly two reasons mostly 'blast-furnace cement' was used instead of 'portland cement'. Firstly the unit mass of blast-furnace cement (2.95 kg/l) was less than the unit mass of portland cement (3.15 kg/l). Using blast-furnace cement the minimum amount

(0.125 m³/m³ concrete) of fine material (< 250 µm) could be realised without adding extra fine material. Secondly the surface of the concrete using blast-furnace cement became 'white' instead of 'grey' as portland cement would have been used. Consequently, using blast furnace cement cracks at the surface of the concrete would be more easy to detect visually.

Table 1.1: Ordered composition mixtures.

		2&3	A3,B3	A1,A2 B1,B2	C1-C6	C7-C12	C13	C14
blast-furnace cement grade A	kg/m ³	340	340	342	342	342		
portland cement grade C	kg/m ³						360	360
water-cement ratio	-	0.5	0.514	0.503	0.483	0.483	0.35	0.45
estimated air volume	%	1	1	1	1	1	3	3
sand out bunker	%	34.3						
gravel out bunker	%	42.3						
quartz sand	%		8	8	8	8	8	
0.2-0.63	%		12	12	12	12	12	
0.5-1	%		12	12	12	12	12	
1-2	%		10	10	10	10	10	
2-4	%	11.4	14	14	14	14	14	
3-5	%		3.4	3.4	3.4	3.4	3.4	
5-8	%	12.1	13.6	13.6	13.6	13.6	13.6	
8-16	%		27	27	27	27	27	
lytag 0-4 (broken)	%							60
lytag 4-8 (broken)	%							15
lytag 6-12 (not broken)	%							25
Tillman OFT-3 (*)	%						1.65	1.65

*: Superplasticizer based on naphthalene; $\rho = 1.19$ kg/l. Amount compared to the mass of the cement.

Table 1.2: Measured composition mixture of aggregates.

		2&3	A3,B3	A1,A2 B1,B2	C1-C6	C7-C12	C13	C14
0.0-0.25	%	1	8	8	8	8	8	10
0.25-0.5	%	10	12	12	12	12	12	4
0.5-1	%	21	12	12	12	12	12	7
1-2	%	5	10	10	10	10	10	11
2-4	%	17	13	13	13	13	13	29
4-8	%	15	20	20	20	20	20	21
8-16	%	30	25	25	25	25	25	19
≥16	%	1	-	-	-	-	-	-

Concrete for the specimens 2 & 3.

The mixture of just sand and gravel out of bunkers was adapted by adding some amounts of the fractions 2-4 and 5-8. As can be seen in Fig. 1.2 the distribution of the fractions still differed from sieve-line B₁₆. The specimens 2 and 3 were compacted with a vibration table (5000 Hz). The formwork absorbed a lot of the vibration energy. To get enough compaction of the mixture it was therefore necessary to compact during quite some time. A vibration needle (15000 Hz) was used for the remaining specimens so that a better compaction was obtained in less time.

Concrete for the specimens A1-A3 & B1-B3.

It was intended that these specimens would fail due to failure of the concrete. Therefore, the water-cement ratio was increased to 0.514 so that the concrete quality would become less. Accidentally the specimens A3 and B3 were cast first. Although it was not intended the amount of water for the specimens A1, A2, B1 and B2 was reduced with 0.5 l. In table 1.1 this decreased amount of water is taken into account.

Concrete for the specimens C1-C12.

No remarks, see Table 1.1.

Concrete for specimen C13.

The concrete quality is increased by using 'portland cement' grade C and a less water-cement ratio (0.35). Getting an easy to cast mixture 1.65 % superplasticizer (Tillman OFT-3) was added.

Concrete for specimen C14.

Getting a lightweight concrete both sand and gravel were replaced with Lytag in order to get a unit mass as little as possible. The Lytag particles were made out of fly-ash and had an unit mass of about 1.4 kg/l. Two fractions 0-4 (broken particles) and 6-12 (not broken particles) were used. The delivered fraction 0-4 appeared to contain a fraction 4-8 also. The delivered fraction 0-4 was splitted into the fractions 0-4 and 4-8 (both broken). The latter fractions (broken) and the fraction 6-12 (not broken) were used to compose the mixture (Table 1.1). It is known that the concrete quality decreases as the unit mass of the concrete becomes less. Therefore, maintaining a reasonable concrete quality 'portland cement' grade C was used, and the water-cement ratio was decreased (0.45). It was considered that the Lytag particles would absorb about 15 % of their dry mass. Designing the mixture the effects of the absorption were taken into account. Due to the little unit mass of the Lytag particles it seemed difficult to get a good compaction. Moreover, it was hard to get an easy to handle mixture. Therefore, 1.65 % superplasticizer (Tillman OFT-3) was added. (Afterwards, testing some cubes it became obvious that the compaction had been good.) The unit mass of the (wet) concrete mixture was about 1780 kg/m³.

(empty)

2. FABRICATION OF THE PUSH SPECIMENS.

An overview of aspects concerning the fabrication of the specimens is reported hereafter.

1. Before fabricating the specimens five parts were prefabricated. Three parts are shown in Fig. 2.1.

- A steel plate (150*160*30 mm³ for the specimens 2 and 3, 150*160*40 mm³ for the remaining specimens) with 3 holes with screw-thread M20 (Fig. 2.2) was made at the workshop of the university. This steel plate was used to fasten the specimen to the loading-frame.
- A longitudinal hole with screw-thread M3 (10 mm length) was made in the head of the stud. During the test a bolt was connected to this hole. The bolt (M3) was used to connect two transducers for determining the displacement of the head.
- Mostly flat two-sided galvanised steel sheets (1500*3000 mm²) were used as basic material. Usually before press-braking the steel sheet, four holes (numbered 1 to 4 in Fig. 2.3) were made in the steel sheet. The holes were used to pass measurement devices or measurement cables. The direction of the ribs corresponded with the rib direction of profiled steel sheets which commonly are made by roll-forming (Fig. 2.4). The steel sheets used in the series B were already roll-formed. Standard these sheets (industrial sheet "SUPERFLOOR", made by Metal Profil, Belgium,) were provided with 4 ribs. Now, the superfluous fourth rib was cut away.
- The reinforcement was made.
- The formwork was made.

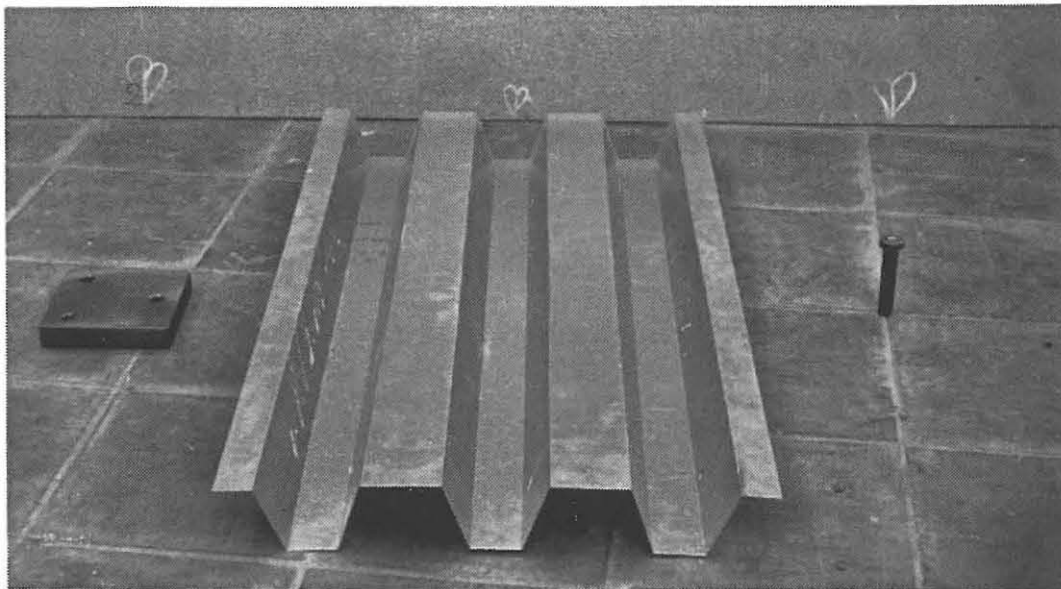
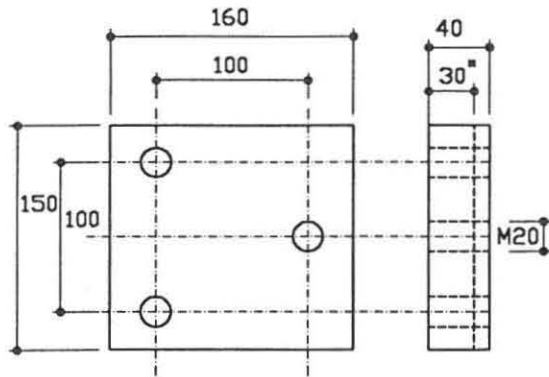


Fig 2.1: Steel plate, profiled steel sheeting and headed stud connector.



*1 just for specimens 2 & 3
 Fig. 2.2: Steel plate used to fasten specimen at the loading frame.

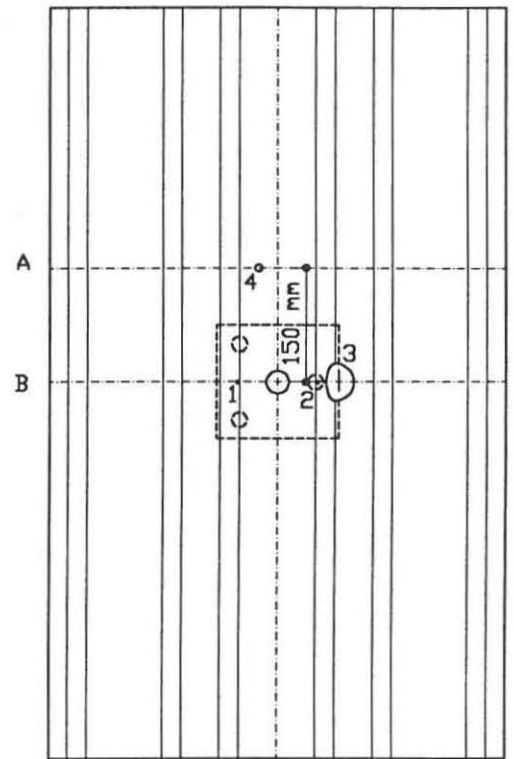


Fig. 2.3: Specimen just after welding the headed stud connector.

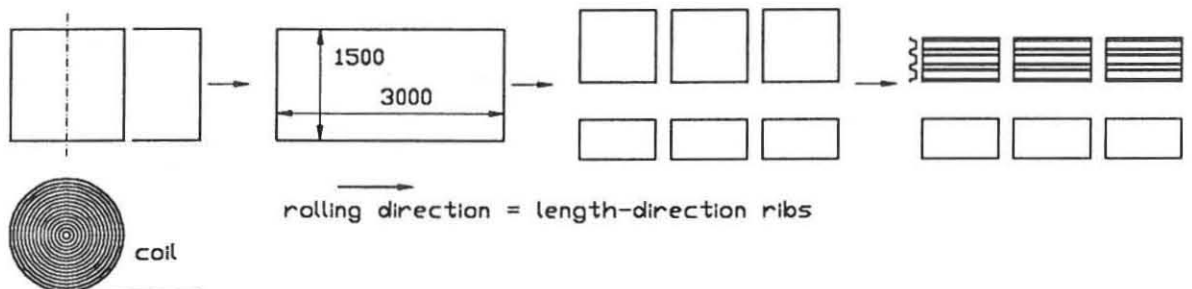


Fig. 2.4: Equal length directions of ribs made by roll-forming and by press-braking.

2. The steel plate was centred in the welding mould.
3. The thin profiled steel sheeting was centred in the welding mould.
4. The headed stud connector was welded to the steel plate by through deck welding (except the specimens 3 and C10).
5. At the shaft of the headed stud connector strain gauges were applied. The wires that were connected to the strain gauges were put through hole 4 (Fig. 2.3 & 2.5).

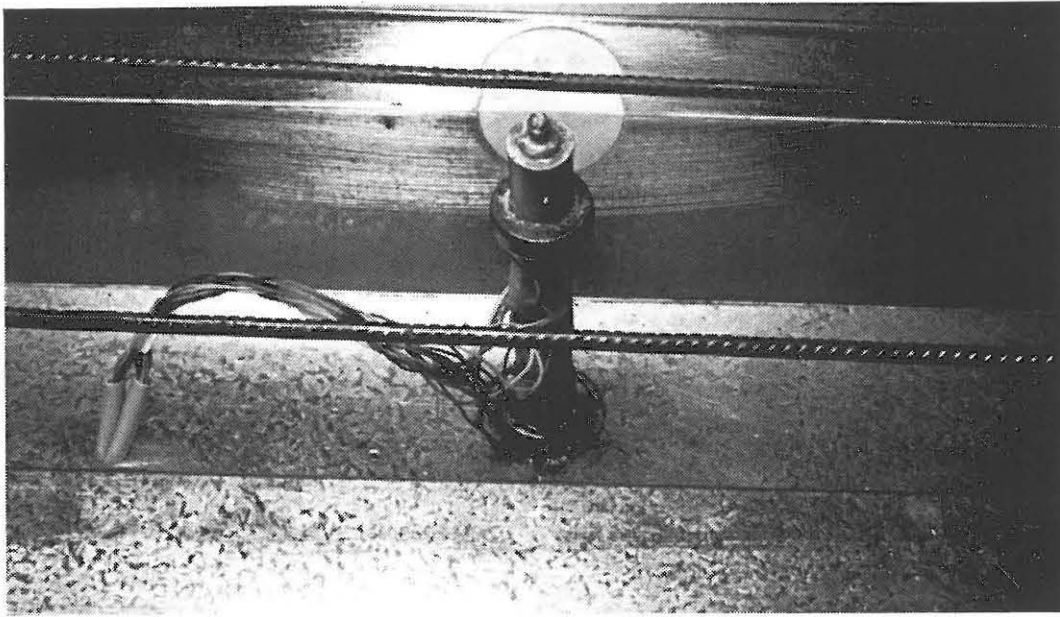


Fig. 2.5: Headed stud connector just before casting.

6. Bond between the hardened concrete and the strain gauges was prevented by applying teflon (self-adhesive at one side) at the surface of the strain gauges (Fig. 2.5). At the specimens 2 and 3 wax was used instead of teflon.
7. Hole 3 (Fig. 2.3) in the steel sheet was temporarily closed by a thin steel sheet (Fig. 2.6b) that was placed at and fixed onto the outside of the sheet.
8. The combination (steel plate, steel sheet, stud) was placed in the formwork (Fig. 2.7).
9. The temporarily closed hole 3 was filled with gypsum (Fig. 2.5 & 2.6c). Special attention was paid to the crossing of the gypsum surface to the surrounding surface of the steel sheet being smooth.
10. Thin steel wires (Fig. 2.6d) were placed in the holes at the front side and at the rear side of the headed stud connector. The wires were used to fasten measurement devices. After casting the steel wires were partly embedded in the hardened concrete. The holes 1, 2 and 4 were temporarily filled with putty (Fig. 2.6e).
11. All surfaces (steel sheet, headed stud connector, inside formwork) were rubbed with demoulding-oil.
12. The reinforcement was positioned in the formwork (Fig. 2.7).
13. Temporarily a stick (20 mm length, 15 mm diameter) was fastened in the hole (Fig. 2.6a) in the head of the stud (Fig. 2.6f), so that some room remained after casting to connect a measuring device to the head of the stud (Fig. 2.5).
14. The inside of the concrete mixer was moistened.
15. The aggregates (sand and gravel) and the cement were mixed (dry).
16. During the mixing water was added.
17. The concrete was cast and compacted. The specimens 2 and 3 were compacted with a vibration table (5000 Hz). With the vibration table it was difficult to get enough

- compaction due to the energy absorption of the formwork. Therefore, all other specimens were compacted with a vibration needle (15000 Hz).
18. During the first days after casting the specimens were covered by a plastic sheet.
 19. After a few days the plastic sheet and the formwork were removed and the specimens were stored in a climate-room ($T = 20\text{ }^{\circ}\text{C}$, relative humidity = 65 %).
 20. In the climate-room the specimens were prepared further. The parts a, b, c, e and f (Fig. 2.6) were removed. At the specimens 2 and 3 as well as the specimens in the series A and B two strain gauges each were applied at the concrete at hole 3. (After the tests it appeared that the measurements of these strains were unreliable!) At the surface of the specimens the centre lines of the ribs were marked.

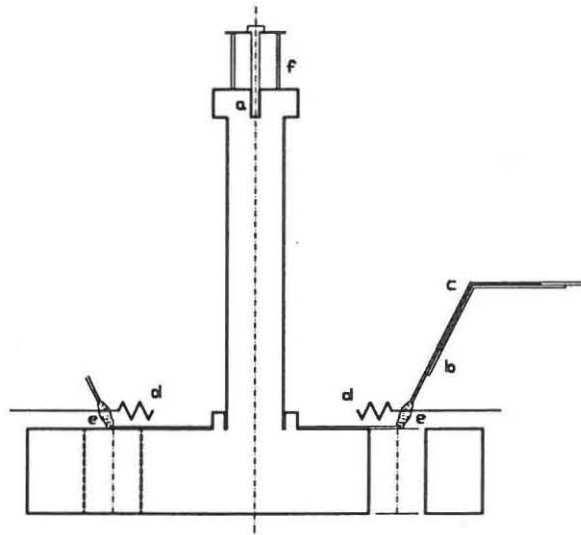


Fig. 2.6: Cross-section over the headed stud connector just before casting.

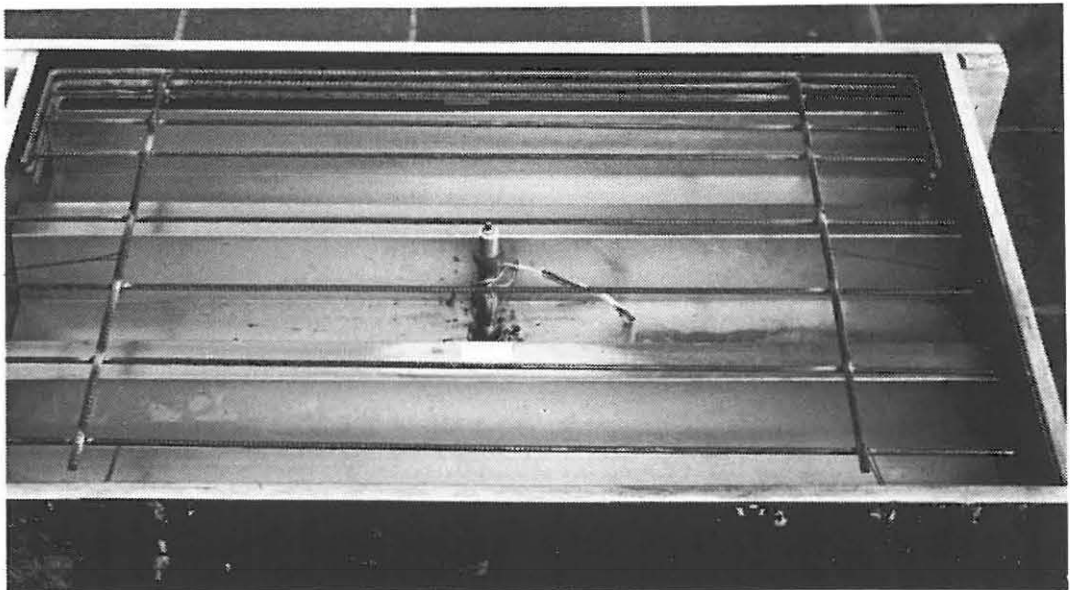


Fig. 2.7: Specimen just before casting.

Hereafter time-schedules from casting to testing of the specimens are presented. Also it is presented at what date the standard specimens (cubes and prisms) were tested. The time-schedules were necessary to be able to calculate the concrete properties at the day the push tests were carried out. The reason for this was that the standard specimens were not cast for each push specimen but for a series of push specimens. Cubes ($150 \times 150 \times 150 \text{ mm}^3$) and prisms ($100 \times 100 \times 500 \text{ mm}^3$) were used to determine the concrete properties. The mean concrete cube compressive strength (f_{ccm}) and the mean concrete cube splitting strength ($f_{ctm,sp}$) were mostly determined with three cubes. Two prisms were used to determine the mean concrete secant modulus of elasticity (E_{cm}).

Time-schedule specimens 2 & 3:

date	day	activities carried out
04-11-'93	0	Cast order: specimen 2; specimen 3; 6 cubes (no. c1-c6); 2 prisms (no. p1-p2); 2 cubes (no. c7-c8) (no more concrete left in mixer!). Wet clothes and plastic were put at the specimens including the standard specimens.
05-11-'93	1	All cubes (c1-c8) and prisms (p1-p2) were demoulded. Two cubes (c7-c8) were stored in the water-reservoir. The remaining stayed covered with wet clothes and plastic.
08-11-'93	4	The wet clothes and plastic were removed. The specimens were demoulded. The temporarily steel sheet of specimen 3 was not yet removed! The specimens, the remaining cubes (c1-c6) and the prisms (p1-p2) were stored in the climate-room.
22-11-'93	18	The temporarily steel sheet of specimen 3 was removed.
03-12-'93	29	The water-cured cubes (c7-c8, f_{ccm}) (only 2!) were tested.
08-12-'93	34	Specimen 2 was tested.
09-12-'93	35	Specimen 3 was tested.
10-12-'93	36	Six cubes (c1-c3, f_{ccm} ; c4-c6, $f_{ctm,sp}$) and two prisms were tested.

Time-schedule specimens series A & B:

date	day	activities carried out
18-02-'94	0	Cast order: batch 1: specimen A3, B3, 6 cubes (no. c31-c36); batch 2: specimen A2, B2, 3 cubes (no. c21-c23), 2 prisms (no. p21-p22); batch 3: specimen A1, B1, 6 cubes (no. c11-c16).

18-02-'94	0	The specimens, cubes and prisms were covered with plastic.
21-02-'94	3	Three cubes (c21-c23) were demoulded. These cubes (c21-c23) were stored in the water-reservoir. The remaining stayed covered with plastic.
22-02-'94	4	The specimens, the remaining cubes (c11-c16, c31-c36) and the prisms (p21-p22) were demoulded. The plastic was not yet removed.
23-02-'94	5	The plastic was removed. All specimens, cubes (c11-c16, c31-c36) and prisms (p21-p22) were moved to the climate-room.
10-03-'94	20	All specimens, cubes (c11-c16, c31-c36) and prisms (p21-p22) were moved from the climate-room to the laboratory.
14-03-'94	24	Specimen A1 was tested.
15-03-'94	25	Three air-cured cubes (c31-c33, f_{ccm}) were tested.
16-03-'94	26	Specimen A2 was tested.
17-03-'94	27	Specimen A3 was tested.
18-03-'94	28	Three water-cured cubes (c21-c23, f_{ccm}) were tested. The prisms were tested.
21-03-'94	31	Specimen B1 was tested.
22-03-'94	32	Specimen B2 was tested.
23-03-'94	33	Specimen B3 was tested. Six air-cured cubes (c11-c13, f_{ccm} ; c14-c16, $f_{ctm,sp}$) were tested.
29-03-'94	39	Three air-cured cubes (c34-c36, f_{ccm}) were tested.

Time-schedule specimens C1-C6:

date	day	activities carried out
03-06-'94	0	Cast order: batch 1: specimen C1, C2, 3 cubes (no. c11-c13); batch 2: specimen C3, C4, 6 cubes (no. c21-c26), 2 prisms (no. p21-p22); batch 3: specimen C5, C6, 6 cubes (no. c31-c36), 2 prisms (no. p31-p32). All specimens and standard specimens were covered with plastic.
06-06-'94	3	Three cubes (c11-c13) were demoulded These cubes (c11-c13) were stored in the water-reservoir. The remaining stayed covered with plastic.
08-06-'94	5	The specimens, the cubes (c21-c26, c31-c36) and the prisms (p21-p22, p31-p32) were demoulded. The plastic was removed. The specimens, cubes (c21-c26, c31-c36) and prisms (p21-p22, p31-p32) were stored in the climate-room.

01-07-'94	28	The water-cured cubes (c11-c13, f_{ccm}) were tested.
06-07-'94	33	Specimen C1 was tested. (In series C each specimen including the cubes and prisms remained in the climate-room until testing.) Six air-cured cubes (c21-c23, f_{ccm} ; c24-c26, $f_{ctm,sp}$) and two prisms (p21-p22) were tested.
08-07-'94	35	Specimen C2 was tested.
12-07-'94	39	Specimen C3 was tested.
14-07-'94	41	Specimen C4 was tested.
15-07-'94	42	Specimen C5 was tested.
18-07-'94	45	Six air-cured cubes (c31-c33, f_{ccm} ; c34-c36, $f_{ctm,sp}$) and two prisms (p31-p32) were tested.
19-07-'94	46	Specimen C6 was tested.

Time-schedule specimens C7-C12:

date	day	activities carried out
17-06-'94	0	Cast order: batch 1: specimen C7, C8, 3 cubes (no. c11-c13); batch 2: specimen C9, C10, 6 cubes (no. c21-c26), 2 prisms (no. p21-p22); batch 3: specimen C11, C12, 6 cubes (no. c31-c36), 2 prisms (no. p31-p32). All specimens were covered with plastic.
20-06-'94	3	Three cubes (c11-c13) were demoulded. These cubes (c11-c13) were stored in the water-reservoir. The remaining stayed covered with plastic.
22-06-'94	5	The specimens, the cubes (c21-c26, c31-c36) and the prisms (p21-p22, p31-p32) were demoulded. The plastic was removed. All specimens, cubes (c21-c26, c31-c36) and prisms (p21-p22, p31-p32) were stored in the climate-room.
15-07-'94	28	Three water-cured cubes (c11-c13, f_{ccm}) were tested.
18-07-'94	31	Six air-cured cubes (c21-c23, f_{ccm} ; c24-c26, $f_{ctm,sp}$) and two prisms (p21-p22) were tested.
21-07-'94	34	Specimen C7 was tested. Specimen C8 was tested.
22-07-'94	35	Specimen C9 was tested. Specimen C10 was tested.
25-07-'94	38	Specimen C11 was tested.
26-07-'94	39	Specimen C12 was tested. Six air-cured cubes (c31-c33, f_{ccm} ; c34-c36, $f_{ctm,sp}$) and two prisms (p31-p32) were tested.

Time-schedule specimen C13:

date	day	activities carried out
29-06-'94	0	Cast order: specimen C13; 9 cubes (no. c11-c19); 2 prisms (no. p11-p12). All specimens were covered with plastic.
30-06-'94	1	Three cubes (c11-c13) were demoulded. These cubes (c11-c13) were stored in the water-reservoir. The remaining stayed covered with plastic.
04-07-'94	5	The specimens and the remaining cubes (c14-c19) and prisms (p11-p12) were demoulded. The plastic was removed. The specimens, cubes (c14-c19) and prisms (p11-p12) were stored in the climate-room.
26-07-'94	27	Three water-cured cubes (c11-c13, f_{ccm}) were tested. Six air-cured cubes (c14-c16, f_{ccm} ; c17-c19, $f_{ctm,sp}$) and two prisms (p11-p12) were tested.
27-07-'94	28	Specimen C13 was tested.

Time-schedule specimen C14:

date	day	activities carried out
29-06-'94	0	Cast order: specimen C14; 9 cubes (no. c11-c19); 2 prisms (no. p11-p12). All specimens were covered with plastic.
30-06-'94	1	Three cubes (c11-c13) were demoulded. These cubes (c11-c13) were stored in the water-reservoir. The remaining stayed covered with plastic.
04-07-'94	5	The specimens, the cubes (c14-c19) and the prisms (p11-p12) were demoulded. The plastic was removed. The specimens, cubes (c14-c19) and prisms (p11-p12) were stored in the climate-room.
26-07-'94	27	Three water-cured cubes (c11-c13, f_{ccm}) were tested. Six air-cured cubes (c14-c16, f_{ccm} ; c17-c19, $f_{ctm,sp}$) and two prisms (p11-p12) were tested.
27-07-'94	28	Specimen C14 was tested.

3. MATERIAL PROPERTIES HEADED STUD CONNECTORS.

The headed stud connectors were fabricated out of the basic material St 37-3k. The specified material properties according the German code DIN 17100 were: yield strength $f_y \geq 350 \text{ N/mm}^2$, ultimate tensile strength $f_u \geq 450 \text{ N/mm}^2$, ultimate tensile strength $f_u \leq 600 \text{ N/mm}^2$ and ultimate strain at failure $\epsilon_u \geq 15 \%$. The actual material properties have been determined according to the Standard EN 10 002-1. Each time three standard specimens (numbered 1, 2 and 3) with diameter d were used to determine the material properties. The mean diameter d_m was determined with a digital vernier callipers ($\Delta = 0.01 \text{ mm}$) out of three measurements each. The standard deviation of the diameter did not exceed 0.01 mm . The maximum capacity of the used tensile testing machine was 100 kN . Therefore, to be able to load the standard specimens unto failure the diameter of the headed stud connectors was decreased to nominal 10 mm . In total five series of each 3 standard specimens (types I, II and III; see Fig. 3.1) were used:

- series 1: headed stud connectors used in the specimens 2 and 3 (type I);
- series 2: headed stud connectors used in the specimens A1-A3 and B1-B3 (type I);
- series 3: headed stud connectors used in the specimens C1 and C4-C14 (type I);
- series 4: headed stud connector used in specimen C2 (type II);
- series 5: headed stud connector used in specimen C3 (type III).

See table 3.1 and 3.2 for the measured and the mean material properties respectively.

Measurement of the yield strength (f_y).

As the headed stud connectors were cold-formed the yield strength was determined at a strain of 0.2% . Determining the yield strength the speed of the cross-head of the testing machine was maintained at 0.2 mm/min . During loading the test specimens, the load and the elongation were recorded with a chart recorder. The elongation was measured with an extensometer with a fixed original gage length (L_0) of 50 mm . With this extensometer the displacement of two pairs of knife edges that were fit to the standard specimen were determined. Using this method a maximum strain of 4% could be calculated out of the recorded elongation. It appeared not possible to determine the yield strength for the standard specimens in series 1 because accidentally the adjustments of the chart recorder were changed.

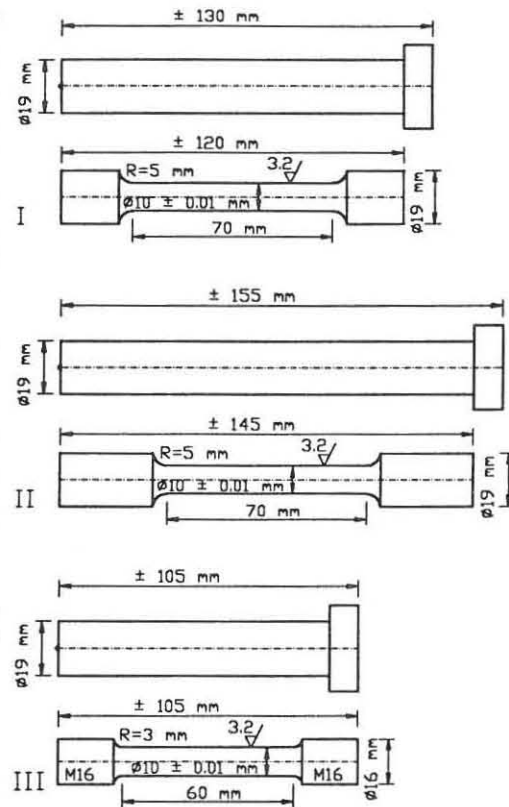


Fig. 3.1: Standard specimens.

Measurement of the ultimate tensile strength (f_u).

After an elongation of about 0.5 mm the speed of the cross-head of the testing machine was increased to 2.0 mm/min. This speed was kept constant unto failure. The maximum load was recorded by the testing machine and used to calculate the ultimate tensile strength.

Measurement of the ultimate strain at failure (ϵ_u).

The elongation at failure of a marked part (initial length 50 mm) was determined with a normal vernier callipers ($\Delta = 0.01$ mm). This elongation was used to calculate the ultimate strain at failure. Testing the standard specimens in series 1 it appeared that all three headed stud connectors failed at the same position near the crossing of the outer and inner part of the standard specimen, probably due to a locally less diameter.

Table 3.1: Mean diameter and material properties of the headed stud connectors.

	d_m	f_y	f_u	ϵ_u
	mm	N/mm ²	N/mm ²	%
series 1-1*	9.95	424.4	506.7	14.4
-2*	9.90	?	524.4	15.2
-3*	9.95	?	500.3	17.2
series 2-1	10.00	356.5	458.4	18.4
-2	10.00	354.2	443.4	29.4
-3	10.00	411.3	515.7	?
series 3-1	10.00	398.8	489.3	21.2
-2	10.00	448.5	555.5	20.8
-3	9.99	401.6	493.4	19.8
series 4-1	10.00	277.6	450.7	29.2
-2	9.99	290.7	455.2	29.4
-3	10.00	287.9	454.8	29.4
series 5-1	9.97	425.0	522.3	17.6
-2	9.99	420.0	515.8	16.6
-3	9.98	400.1	499.8	16.6

*: diameter determined just once instead of three times.

Table 3.2: Mean material properties of the headed stud connectors.

	f_{ym}	f_{um}	ϵ_{um}
	N/mm ²	N/mm ²	%
series 1	?	511	16
series 2	374	472	24
series 3	416	513	21
series 4	285	454	29
series 5	415	513	17

4. MATERIAL PROPERTIES PROFILED STEEL SHEETING.

The basic material used for all specimens was a two-sided senzimir zinc coated steel sheet. The material specifications of the steel sheet for the specimens 2, 3 and C12 were unknown. The basic material for the specimens A1-A3, C1-C11, C13 and C14 was FE P02 G Z275 NA-C according to the Standard EN 10142. The specified material properties were: yield strength $f_y \geq 140 \text{ N/mm}^2$, the ultimate tensile strength $f_u \geq 270 \text{ N/mm}^2$, $f_u \leq 500 \text{ N/mm}^2$ and the ultimate strain at failure $\epsilon_u \geq 22 \%$. Specimens in series B were made out of Fe E 350 according Euronorm 147-70. The specified material properties were: $f_y \geq 350 \text{ N/mm}^2$, $f_u \geq 460 \text{ N/mm}^2$ and $\epsilon_u \geq 16 \%$. The real material properties have been determined according to the Standard EN 10 002-1. Three standard specimens (numbered 1, 2 and 3) were used to determine the material properties. Two-sided zinc coated specimens were used to determine the material properties. These material properties were related

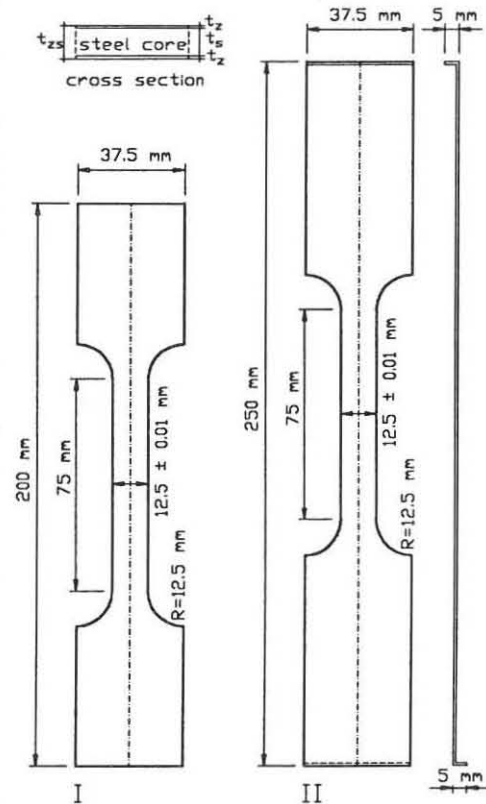


Fig. 4.1: Standard specimens.

to the thickness of just the steel core (t_s , see also cross-section in Fig. 4.1) as is done commonly. The mean thickness of the steel core (t_{sm}) was defined as the difference of the mean total thickness of the zinc coated steel sheet (t_{zsm}) and twice the mean thickness of the zinc layer (t_{zm}). The mean width b_m of the middle part of the standard specimen and the mean total thickness (t_{zsm}) were determined with a micrometer callipers ($\Delta = 0.01 \text{ mm}$) out of three measurements each. The standard deviation of both b and t_{zsm} did not exceed 0.01 mm . The thickness of the zinc layer was determined in a non-destructive way with a so-called 'elcometer', in which the measurement of the thickness was based on a magnetic principle. The mean thickness of the zinc layer (t_{zm}) was determined out of 6 measurements of the thickness (t_z) in the middle of the standard specimen. At both sides of the standard specimen 3 measurements were taken. The standard deviation of t_z varied from 1 to $4 \mu\text{m}$. Two types (I and II) of standard specimens were used (Fig. 4.1). The material properties of the steel sheet used for the specimens 2 and 3 were determined with standard specimens type I. Due to problems with the initial grip alignment which might result in bending moments in the plane of the standard specimen the remaining standard specimens were of type II. Hereafter, 8 series of 3 standard specimens each are described. The measured material properties and the mean material properties are tabulated in the tables 4.1 and 4.2 respectively.

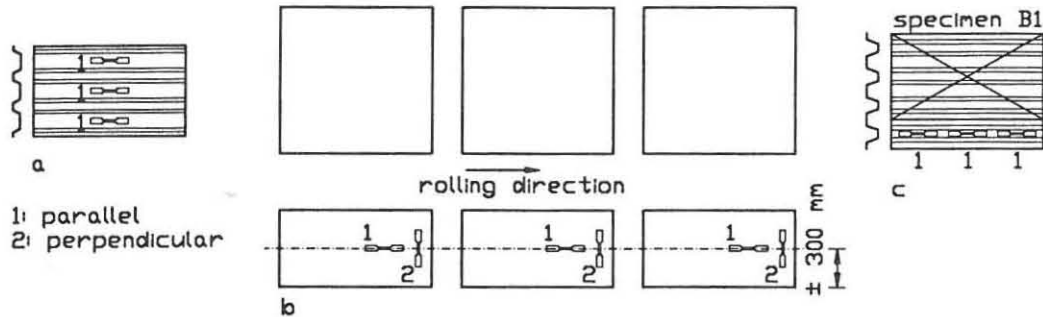


Fig. 4.2: Position standard specimens in basic steel sheets.

series 1:

- Material properties of the steel sheets of the specimens 2 and 3.
- The standard specimens (type I) were cut from the under flange of an already press-braked steel sheet (Fig. 4.2a).
- The length-direction of the standard specimens was parallel to the rolling-direction of the hot-rolled steel sheet that initially was flat.

series 2, 3, 4 and 5:

- Material properties of the steel sheets of the specimens A1-A3, C1-C11, C13 and C14.
- The standard specimens (type II) were cut from the original flat steel sheets (1500*3000*1.0 mm³). As the steel sheets of the series A and C were all of the same coil the standard specimens were cut out of some reserve sheets which were not used for the press-braking (Fig. 4.2b). Both the material properties parallel and perpendicular to the rolling-direction of the steel sheet were determined.
- Verifying the variation of the material properties within one coil the material properties were determined of two reserve flat steel sheets instead of just one.
- series 2: Flat steel sheet 1, parallel to the rolling direction.
- series 3: Flat steel sheet 1, perpendicular to the rolling direction.
- series 4: Flat steel sheet 2, parallel to the rolling direction.
- series 5: Flat steel sheet 2, perpendicular to the rolling direction.

series 6 and 7:

- Material properties of the steel sheet of the specimens C12 (nominal thickness 0.75 mm).
- The standard specimens (type II) were cut from the original flat steel sheet (1500*3000*0.75 mm³) that was used to press-brake the steel sheet for specimen C12. Both the material properties parallel and perpendicular to the rolling-direction of the steel sheet were determined (Fig. 4.2b).
- series 6: Parallel to the rolling direction.
- series 7: Perpendicular to the rolling direction.

series 8:

- Material properties of the steel sheets of the specimens B1-B3.
- The standard specimens (type II) were cut from the under flange of a remaining part of the profiled steel sheet of specimen B1, which had already been roll-formed (Fig. 4.2c). Therefore the length-direction of the standard specimens was parallel to the rolling-direction.

Measurement of the yield strength (f_y).

Determining the yield strength the speed of the cross-head of the testing machine was maintained at 0.2 mm/min. During loading the test specimens the load and the displacement of the cross-head of the testing machine were recorded with a chart recorder. The basic material of the profiled steel sheeting was hot-rolled. Therefore, it was easy to localise the part of the relation load versus cross-head displacement at which yielding occurred. The yield strength was directly determined out of the load/cross-head displacement diagram. The yield strength was taken as the upper yield strength.

Measurement of the ultimate tensile strength (f_u).

After yielding the speed of the cross-head of the testing machine was increased to 2.2 mm/min. This speed was kept constant unto failure. The maximum load was determined by means of the chart and was used for calculating the ultimate tensile strength.

Measurement of the ultimate strain at failure (ϵ_u).

The elongation of a marked part (initial length 50 mm) at failure was determined with a normal vernier callipers ($\Delta = 0.01$ mm). This elongation was used to calculate the ultimate strain at failure.

Table 4.1: Mean sizes and material properties of the profiled steel sheeting.

	b_m	t_{zsm}	t_{zm}	t_{em}	f_y	f_u	ϵ_u
	mm	mm	μm	mm	N/mm ²	N/mm ²	%
series 1-1*	12.54	1.02	19	0.98	282.7	381.8	29.0
-2*	12.53	1.00	20	0.96	285.9	387.6	29.5
-3*	12.54	1.00	20	0.96	286.8	389.6	28.0
series 2-1	12.47	1.00	21	0.98	292.2	382.8	38.6
-2	12.50	1.01	22	0.98	290.9	382.7	39.4
-3	12.51	0.99	23	0.97	292.6	384.4	40.2
series 3-1	12.47	0.98	22	0.96	317.8	392.1	38.4
-2	12.47	1.00	22	0.97	316.0	390.1	37.6
-3	12.48	0.98	21	0.96	316.8	384.5	37.6
series 4-1	12.50	0.99	21	0.97	290.6	383.1	41.4
-2	12.48	1.00	22	0.98	296.5	389.9	37.8
-3	12.49	0.99	19	0.97	290.9	383.7	40.0
series 5-1	12.48	0.98	20	0.96	324.2	384.6	35.8
-2	12.47	0.99	20	0.97	311.6	380.2	38.0
-3	12.49	0.98	21	0.96	317.9	382.8	39.4
series 6-1	12.50	0.74	19	0.72	318.0	396.4	34.0
-2	12.50	0.75	21	0.73	318.2	399.3	33.8
-3	12.50	0.75	20	0.73	318.5	393.8	34.8
series 7-1	12.50	0.74	20	0.72	333.2	404.3	34.4
-2	12.50	0.75	20	0.73	334.2	402.2	32.6
-3	12.50	0.75	23	0.73	347.6	411.4	31.8
series 8-1	12.50	0.99	20	0.97	346.4	447.0	32.2
-2	12.50	0.99	20	0.97	346.8	447.7	34.4
-3	12.49	0.99	19	0.97	346.2	445.1	33.0

*: b and t_{zs} determined just once instead of three times each.

Table 4.2: Mean material properties of the profiled steel sheeting.

	f_{ym}	f_{um}	ϵ_{um}
	N/mm ²	N/mm ²	%
series 1	285	386	29
series 2	292	383	39
series 3	317	389	38
series 4	293	386	40
series 5	318	383	38
series 6	318	397	34
series 7	338	406	33
series 8	346	447	33

5. CONCRETE PROPERTIES.

The determination of the concrete properties was split in two parts. In both parts a subdivision of the concrete properties was made according to the different casting-days (see chapter 1 & 2). In part 1 the compressive cube strength (f_{cc}) was determined of three water-cured cubes ($150*150*150 \text{ mm}^3$), in order to determine the strength class of the concrete used. In part 2 standard specimens (cubes $150*150*150 \text{ mm}^3$ and prisms $100*100*500 \text{ mm}^3$) were used to calculate the mean concrete properties at the day that a specific push specimen was tested. Therefore, these cubes and prisms were kept with and treated like the push specimens. The concrete properties that were used to calculate the mean concrete properties were: the compressive cube strength (f_{cc}), the cube splitting strength ($f_{ct,sp}$) and the secant modulus of elasticity (E_c). The mean compressive cube strength (f_{ccm}) and the mean cube splitting strength ($f_{ctm,sp}$) were determined out of three cubes each. Two prisms were used to determine the mean secant modulus of elasticity (E_{cm}). Due to practical aspects the standard specimens (cubes and prisms) were not cast with each push specimen but with a series of push specimens. Therefore, the standard specimens were seldom tested at the same day that the push tests were carried out. Mostly the standard specimens were tested both at the beginning of a series push tests and at the end of the same series push tests. The concrete properties changed just a little if the age of the concrete exceeded 28 days. Therefore, the concrete properties of the standard specimens at the days that the push specimens were tested, were determined by linear interpolation between the results at the beginning and at the end of the corresponding series push tests. For the linear interpolation, the amount of days after casting was needed for each specimen. These amounts are given in the tables 5.1 to 5.4 (see also chapter 2).

Part 1.

Measurement of compressive cube strength (f_{cc}): water-cured cubes.

Three water-cured cubes (numbered 1, 2 and 3) have been tested according the Dutch code NEN 5968. Mostly after 28 days the cubes were tested on a hydraulic testing machine with a maximum capacity of 2000 kN. The load was applied at a speed of 500 kN/min. In table 5.1 the compressive cube strengths (measured and mean) are given. The strength class was related to the characteristic compressive strength (f_{ck}). The characteristic compressive strength was calculated out of the mean compressive strength f_{cm} : ($f_{ck} = f_{cm} - 8 \text{ N/mm}^2$) in which, analogous to a similar relation in Eurocode 2, the following relation was assumed: $f_{cm} = 0.8*f_{ccm}$. The unit mass (Table 5.1) was the mean of the three water-cured cubes.

Table 5.1: Compressive cubes strengths of water-cured cubes after 28 days.

specimen	days	ρ	f_{cc}			f_{ccm}	f_{ck}
			cube 1	cube 2	cube 3		
			kg/m ³	N/mm ²	N/mm ²		
2&3	29	2379	38.7	38.2	-	38.5	22.8
A1,B1,A2,B2	28	2332	26.9	24.9	29.6	27.1	13.7
A3,B3*							≈13.7
C1-C6	28	?	40.4	43.6	41.1	41.8	25.4
C7-C12	28	2320	40.9	39.1	40.4	40.1	24.1
C13	27	2392	73.3	77.8	70.7	73.9	51.1
C14	27	1788	51.8	52.9	49.3	51.3	33.0

*: The compressive cube strength of the concrete of the specimens A3 and B3 was a little less than the strength for the specimens A1, B1, A2 and B2. This was caused by the somewhat increased use of water at casting the specimens A3 and B3 (see chapter 1). Therefore, the four specimens A1, B1, A2 and B2 and the two specimens A3 and B3 are separately treated throughout this chapter.

Part 2.

Measurement of compressive cube strength (f_{cc}); air-cured cubes.

Three air-cured cubes (numbered 1, 2 and 3) have been tested according the Dutch code NEN 5968. The cubes were tested on a hydraulic testing machine with a maximum capacity of 2000 kN. The load was applied at a speed of 500 kN/min. In the tables 5.2 (measured) and 5.3 (mean) the compressive cube strengths are given. The unit mass was the mean of three or six air-cured cubes.

Measurement of cube splitting strength ($f_{ct,sp}$); air-cured cubes.

Three air-cured cubes (numbered 1, 2 and 3) have been tested according the Dutch code NEN 5969. The cubes were tested on a hydraulic testing machine with a maximum capacity of 2000 kN. The load was supplied at a speed of 500 kN/min. In tables 5.2 and 5.3 the cube splitting strengths are given.

Measurement of secant modulus of elasticity (E_c); air-cured prisms.

Two prisms were tested in a 2.5 MN testing machine under speed-control. The speed of the cross-head of the testing machine was maintained at 0.001 mm/s. Both the load and the elongation were recorded on a chart recorder. The elongation was measured with two extensometers with an original gage length (L_0) of about 200 mm. The two extensometers were fit to two opposite faces of the prism. The secant modulus of elasticity was determined as the tangent at the chart load versus elongation. The tangent was taken at a third part of the maximum load applied. In the tables 5.2 and 5.3 the secant modulus of elasticity is given.

Table 5.2: Concrete properties of cubes and prisms (both air-cured).

specimen	days	ρ kg/m ³	f_{cc}			$f_{ct,sp}$			E_c	
			cube 1	cube 2	cube 3	cube 1	cube 2	cube 3	prism 1	prism 2
			N/mm ²							
2&3	36	?	36.3	36.1	36.7	2.3	2.1	2.0	31500	32400
A1,B1,A2,B2	28	?	*	*	*	*	*	*	25760	27650
A1,B1,A2,B2	33	2298	32.2	32.0	30.2	2.1	1.8	1.9	*	*
A3,B3	25	2285	29.1	26.9	30.2	*	*	*	*	*
A3,B3	39	2279	28.9	31.8	31.1	*	*	*	*	*
C1-C6	33	2303	43.8	37.1	40.2	2.8	2.1	2.6	26460	29390
C1-C6	45	?	46.7	43.1	42.4	2.7	2.4	3.5	28820	29290
C7-C12	31	?	43.6	44.4	40.2	3.1	2.1	3.1	28670	30540
C7-C12	39	2317	47.6	42.4	44.0	1.7	2.8	2.8	30370	30960
C13	27	2359	79.1	76.0	73.3	4.0	3.3	3.7	35820	35160
C14	27	1671	52.4	52.7	49.3	1.7	1.8	1.7	15260	15290

*: Due to a temporarily lack of moulds for cubes and prisms these concrete properties were not determined.

Table 5.3: Mean concrete properties of cubes and prisms (both air-cured).

specimen	days	ρ	f_{ccm}	$f_{ctm,sp}$	E_{cm}
		kg/m ³	N/mm ²	N/mm ²	N/mm ²
2&3	36	?	36.4	2.1	31950
A1,B1,A2,B2	28	?	30.8*	1.9*	26710
A1,B1,A2,B2	33	2298	31.5	1.9	26910*
A3,B3	25	2285	28.7	1.8*	26090*
A3,B3	39	2279	30.6	1.9*	26650*
C1-C6	33	2303	40.4	2.5	27930
C1-C6	45	?	44.1	2.9	29060
C7-C12	31	?	42.7	2.8	29610
C7-C12	39	2317	44.7	2.4	30670
C13	27	2359	76.1	3.7	35490
C14	27	1671	51.5	1.7	15280

*: These values were calculated out of the mean concrete properties that could directly be determined out of the results of the standard specimens (see next paragraph).

Calculation of the missing concrete properties in the series A and B.

The mean compressive cube strength (f_{ccm}) for the specimens A3 and B3 varied from 28.7 N/mm² (25 days) to 30.6 N/mm² (39 days). Therefore, the mean compressive cube strength increased at a rate of 0.136 N/mm²/day. Considering both f_{ccm} for the specimens A1, B1, A2 and B2 at 33 days and the rate of 0.136 N/mm²/day the mean compressive cube strength at 28 days for the same specimens was calculated: 30.8 N/mm². The mean compressive cube strengths were used to calculate the missing mean cube splitting strengths and the missing mean secant moduli of elasticity. Analogous to a similar relation in Eurocode 2 the following relation between the mean compressive cube strength (f_{ccm}) and the mean cube splitting strength ($f_{ctm,sp}$) was assumed: $f_{ctm,sp} = a (f_{ccm})^{0.667}$. The factor a was calculated for the specimens A1, B1, A2 and B2 after 33 days ($f_{ccm} = 31.5$ N/mm², $f_{ctm,sp} = 1.9$ N/mm²): $a = 0.19049$. Considering the factor a , the

mean cube splitting strength for the specimens A1, B1, A2 and B2 (28 days) as well as for the specimens A3 and B3 (25 and 39 days) were calculated out of the corresponding mean compressive cube strengths. In accordance with a relation used in Eurocode 2, a similar relation between the mean compressive cube strength and the mean secant modulus of elasticity (E_{cm}) was assumed. The assumed relation was: $E_{cm} = b \cdot (f_{ccm})^{0.333}$. The factor b was calculated for the specimens A1, B1, A2 and B2 after 28 days ($f_{ccm} = 30.8 \text{ N/mm}^2$, $E_{cm} = 26710 \text{ N/mm}^2$): $b = 8521$. With the factor b the mean secant moduli for the specimens A1, B1, A2 and B2 (33 days) and the specimens A3 and B3 (25 and 39 days) were calculated out of the corresponding mean compressive cube strengths.

Table 5.4 shows the calculated mean concrete properties at the days that the push specimens were tested. Note: the mean concrete properties at the days that the specimens 2, 3, C13 and C14 were tested, were assumed to be equal to the mean concrete properties at the days that the standard specimens were tested.

Table 5.4: Calculated mean concrete properties at the days that the push specimens were tested.

specimen	days	f_{ccm}	$f_{ctm,sp}$	E_{cm}
		N/mm ²	N/mm ²	N/mm ²
2	34	36.4	2.1	31950
3	35	36.4	2.1	31950
A1	24	30.2	1.9	26550
A2	26	30.5	1.9	26630
B1	31	31.2	1.9	26830
B2	32	31.4	1.9	26870
A3	27	29.0	1.8	26170
B3	33	29.8	1.9	26410
C1	33	40.4	2.5	27930
C2	35	41.0	2.6	28120
C3	39	42.3	2.7	28500
C4	41	42.9	2.8	28680
C5	42	43.2	2.8	28780
C6	46	44.4	2.9	29150
C7	34	43.5	2.7	30010
C8	34	43.5	2.7	30010
C9	35	43.7	2.6	30140
C10	35	43.7	2.6	30140
C11	38	44.5	2.5	30540
C12	39	44.7	2.4	30670
C13	28	76.1	3.7	35490
C14	28	51.5	1.7	15280

6. SUPPORTS OF THE PUSH SPECIMEN.

The supports (Fig. 6.1) of the push specimen were composed out of several parts that are described below. Photos are shown on the next pages. Fig. 6.2 shows the position of the strips teflon (width 10 or 20 mm) at the supports 3, 4 and 5. The teflon strips at support 6 were $10 \times 300 \text{ mm}^2$.

- (a) Steel structure with a circular bar.
- (b) Steel bar (diameter 20 mm) welded to a steel plate ($20 \times 80 \text{ mm}^2$). Both parts were 350 mm long.
- (c) Steel plate ($40 \times 60 \times 350 \text{ mm}^3$).
- (d) Steel plates of different sizes.
- (e) Steel bar, 15 mm diameter in the centre, provided with mortise-and-tenon joints at both sides.
- (f) Steel plate ($30 \times 60 \times 300 \text{ mm}^3$) with two excavations (30 mm diameter, 10 mm depth). The excavations were rubbed with grease.
- (g) Steel bar (diameter 30 mm).
- (h) Half ball (diameter 30 mm) with two flat surfaces.
- (i) Load cell ($F_{\max} = 80 \text{ kN}$).
- (j) Steel plate ($30 \times 80 \times 150 \text{ mm}^3$).
- (k) Steel sheeting ($1 \times 150 \times 150 \text{ mm}^3$, galvanised).
- (l) Steel plate ($5 \times 60 \times 150 \text{ mm}^3$).
- (m) Steel plate ($10 \times 50 \times 150 \text{ mm}^3$).
- (n) Steel plate ($30 \times 100 \times 150 \text{ mm}^3$).

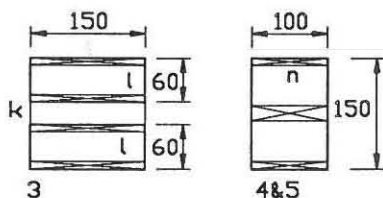
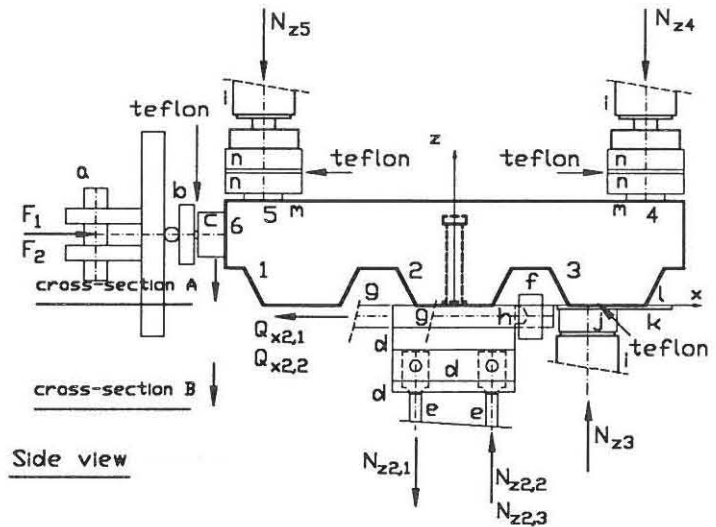
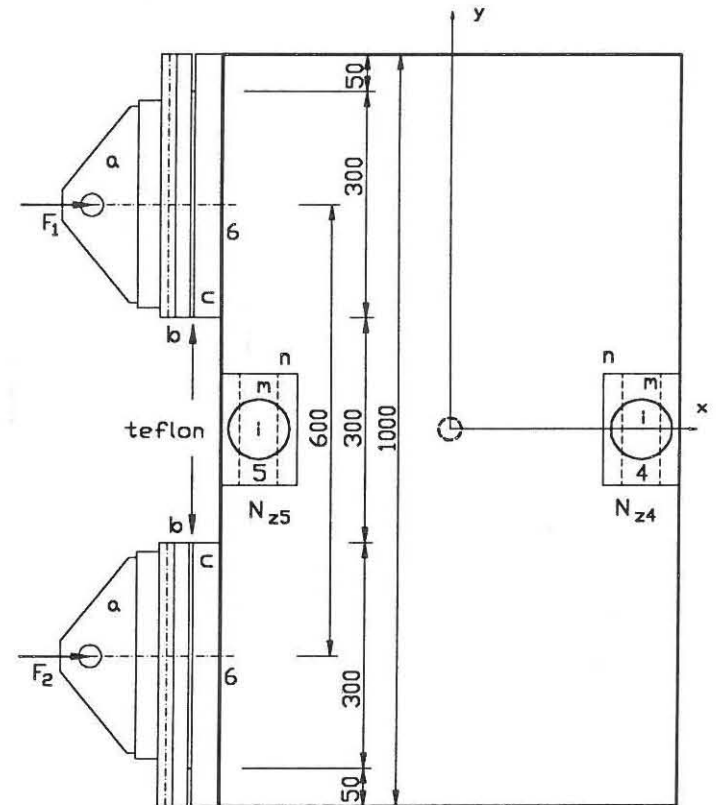


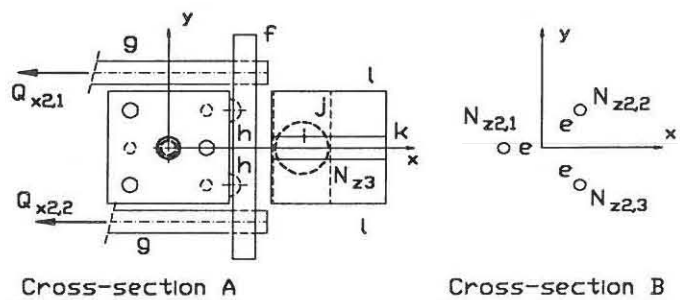
Fig. 6.2: Teflon strips



Side view



Top view



Cross-section A

Cross-section B

Fig. 6.1: Test set-up with the codes of the parts used.

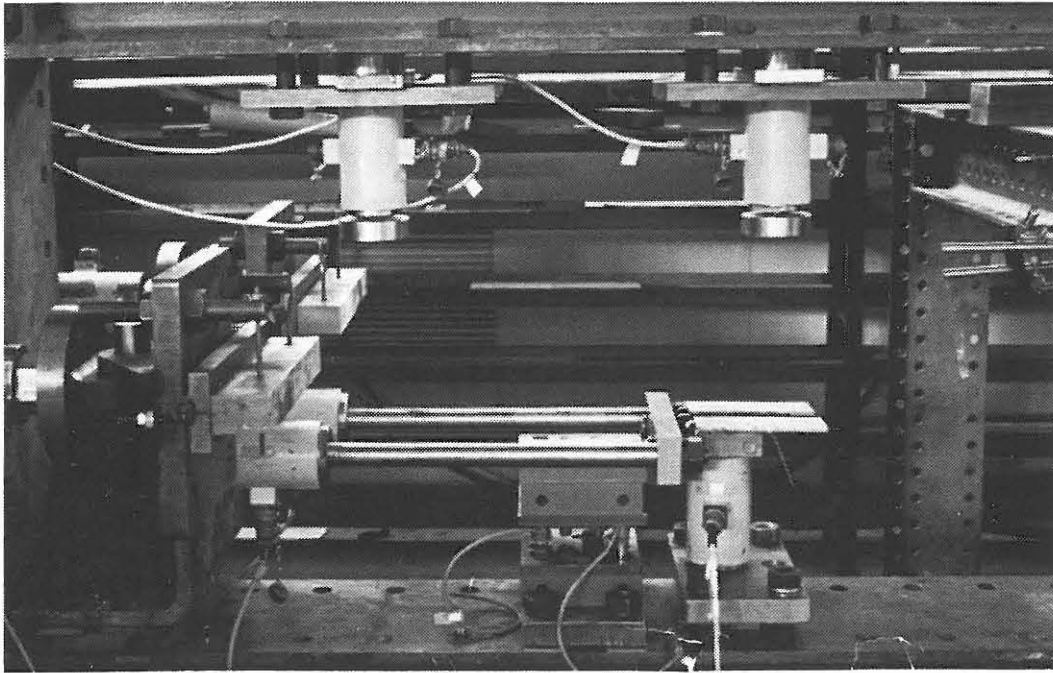


Fig. 6.3: Loading-frame and supports.

(Steel plates m and n of the supports 4 and 5 are not shown.)

Fig. 6.3 shows the loading-frame with all supports. There was no support with number 1. The part that was used to apply the load to the specimen was considered to be a support also (support 6). The composition of the supports is explained hereafter. The codes of the parts used refer to Fig. 6.1 and to Fig. 6.2.

Support 2.

Support 2 (Fig. 6.4) was composed out of two parts: one part that transferred just the shear force (Q_{x2}) and one part (called 'load-table') that transferred the normal force (N_{z2}) and the moment (M_{y2}). The shear force Q_{x2} was transferred via the steel plate to which the headed stud connector was welded to an other steel plate (part f). The latter steel plate (Fig. 6.5) was connected via two bars (part g) to two load cells ($F_{\max} = 80 \text{ kN}$) that were connected to the loading frame. The shear force Q_{x2} was transferred from the specimen to part f via two half balls (part h). The half balls (Fig. 6.5) could freely rotate in all directions in two excavations in part f. The excavations were rubbed with grease (Molykote BR2 plus). The half balls only made contact with the steel plate to which the headed stud connector was welded and not with the upper steel plate of the load-table. The half balls were used to be certain at which yz -position the shear force was transferred to part f. The upper steel plate of the load-table and therefore the complete load-table was connected to the steel plate of the push specimen with 3 bolts M20. The load-table (Fig. 6.6) consisted out of several steel plates (part d) and three bars (part e). The bars were connected to the steel plates with mortise-and-tenon joints (in theory: without any clearance). Due to the joints the bars were only suitable to transfer axial forces.

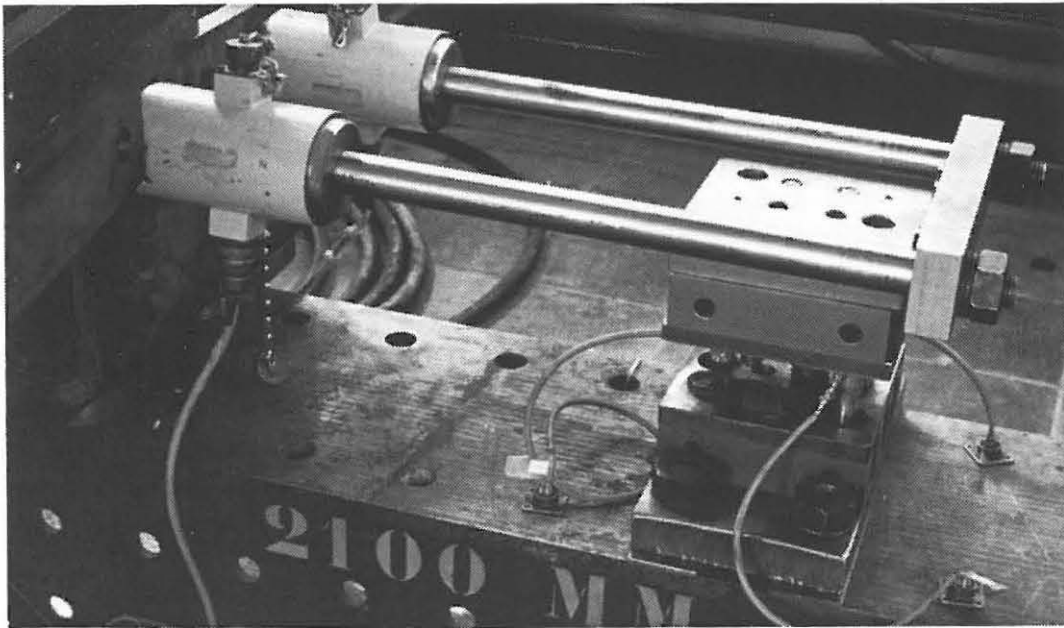


Fig. 6.4: Support 2.

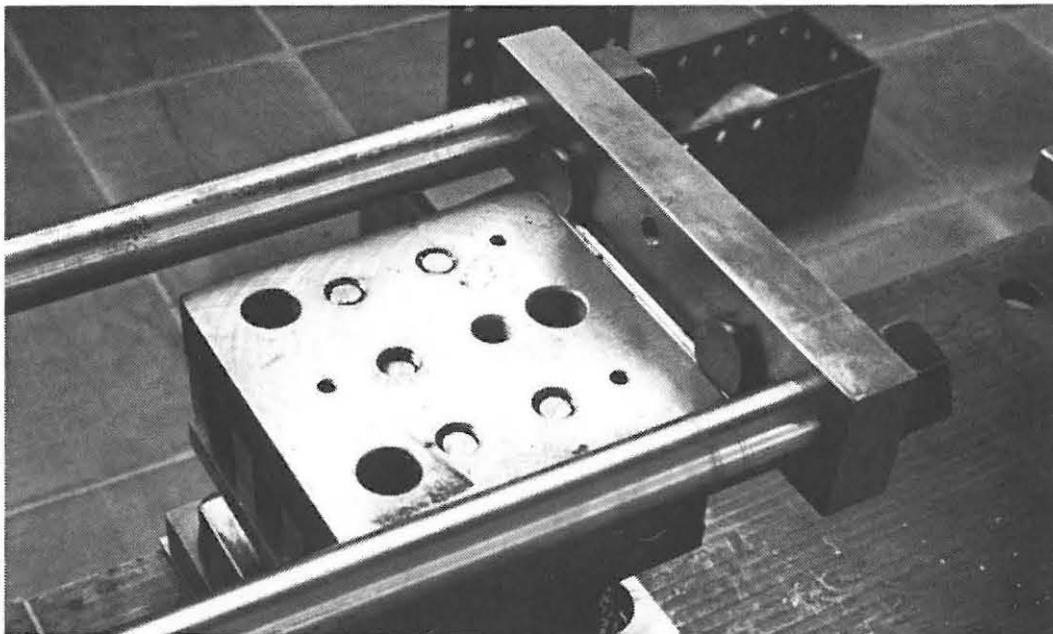


Fig. 6.5: Detail support 2.

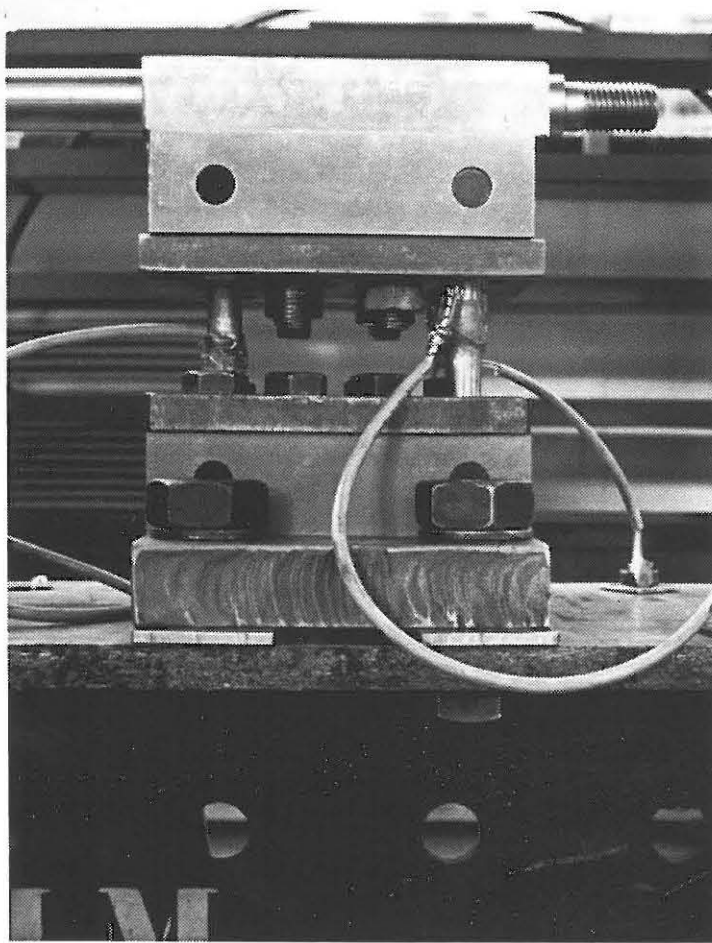


Fig. 6.6: Load-table.

Support 3.

From below to above this support (Fig. 6.7) was composed out of a load cell (part i, $F_{\max} = 80 \text{ kN}$), a steel plate (part j), a thin flat galvanised steel sheeting (part k), 4 strips teflon and two steel plates (part l). The teflon formed the intermediate layer between the thin galvanised steel sheeting and the two steel plates and was rubbed with grease (Molykote BR2 plus). The length-direction of the teflon strips was parallel to the loading-direction. The strips teflon were used to decrease possible frictional forces in the x and y-direction. The teflon was 0.1 mm thick and self-adhesive at one side. The friction was even more reduced by rubbing the teflon strips with grease. With regard to teflon it is known that the coefficient of friction decreases at increasing the compressive stress normal to the plane in which friction arises. Therefore, small teflon strips (Fig. 6.2) were used so that the compressive stresses in the teflon would increase. The coefficient of friction of the teflon rubbed with grease varied from 3% ($\sigma \approx -3 \text{ N/mm}^2$), 2% ($\sigma \approx -6 \text{ N/mm}^2$) to 1% ($\sigma \approx -18 \text{ N/mm}^2$). Only near the load cell the teflon strips were really loaded in compression (see Fig. 6.1).

Supports 4 and 5.

From above to below both supports were composed out of a load cell (part i, $F_{\max} = 80 \text{ kN}$), a steel plate (part n), 3 strips teflon (thickness 0.1 mm), a steel plate (part n) and a small steel plate (part m). Similar to support 3 the strips teflon were parallel to the loading-direction and rubbed with grease. Fig. 6.8 shows support 5 and 6.

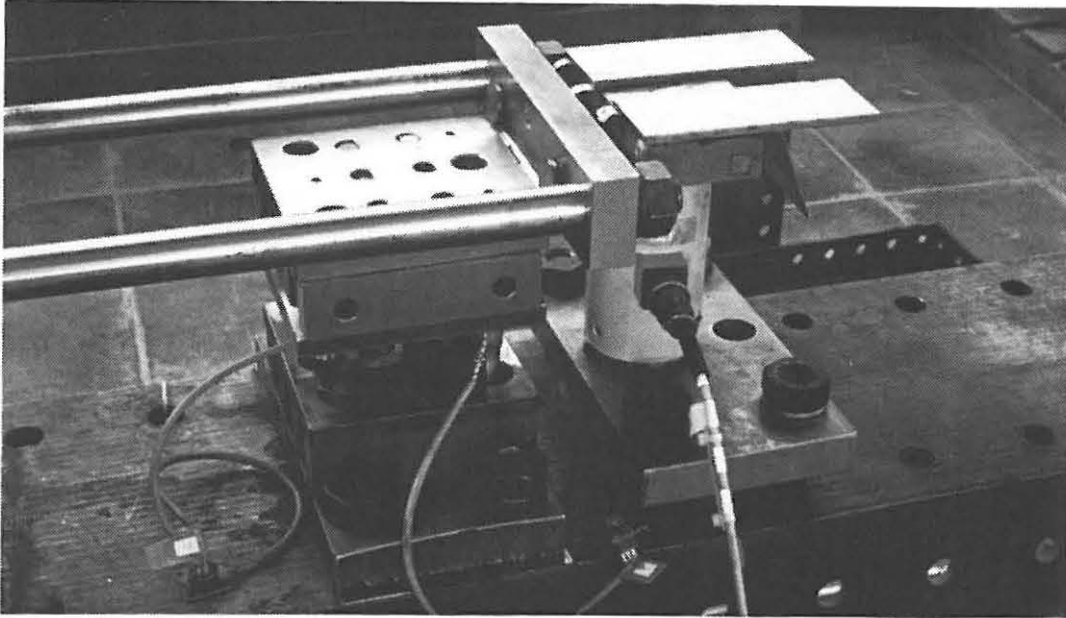


Fig. 6.7: Support 2 and 3 (right).

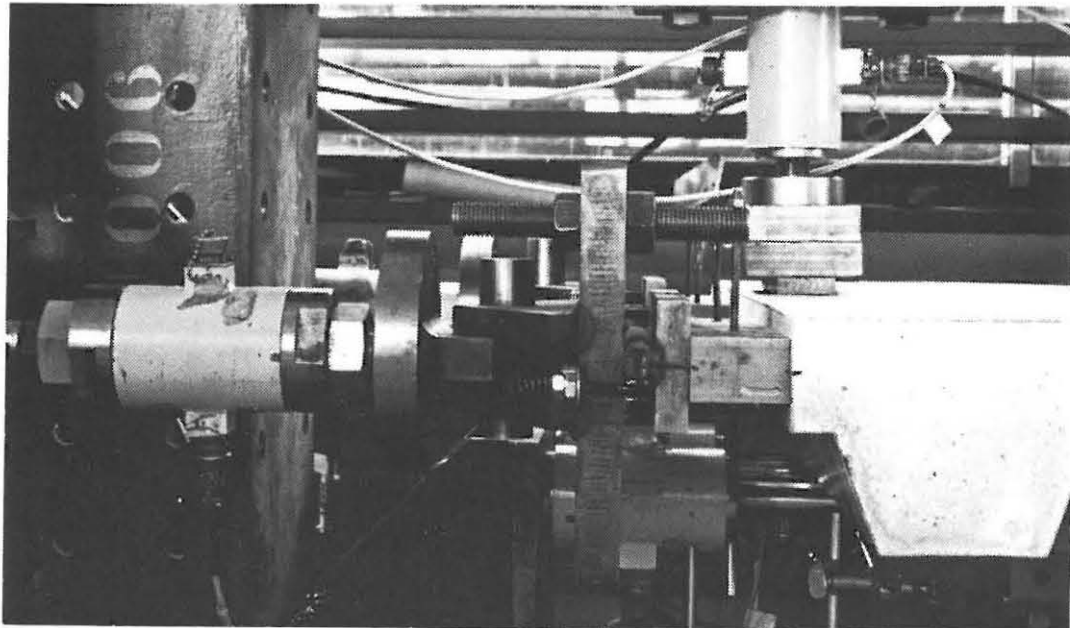


Fig. 6.8: Support 5 (right; support 4 = identical) and support 6 (loading part).

Support 6 (Loading part).

Two hydraulic jacks ($F_{\max} = 150 \text{ kN}$) were used to apply the load to the specimen via two load cells (Fig. 6.8, $F_{\max} = 150 \text{ kN}$) and via two intermediate structures (Fig. 6.8). Each intermediate structure consisted out of 3 steel parts (parts a, b and c). The parts a were used to transfer the concentrated loads (F_1 & F_2) to two non-uniform distributed loads. A circular bar was used to connect part a to the load cell. Therefore, part a could freely rotate around the z-axis (φ_z), which resulted in equal lines of action for the concentrated load and the resultant of the distributed load. Part b was used to apply the load at the centre of the solid part of the specimen. Part c distributed the load over the left side face of the specimen. Part c directly made contact with the specimen. Decreasing possible frictional forces in the y and z-direction the plane between part b and c was provided with a strip teflon ($10 \times 300 \text{ mm}^3$) rubbed with grease (Molykote BR2 plus).

7. TECHNICAL INFORMATION USED EQUIPMENT.

Used abbreviations:

- TUE Made or composed at the central workshop of the Eindhoven University of Technology.
- LVDT Linear Variable Displacement Transducer.

Description	Manufacturer	Type	Capacity/Remarks
<i>Preparation specimens:</i>			
Concrete mixer	ZYKLOS	ZK 250 (E)	250 l, counter-current mixer
Vibration table	GUTZ WEISS	938	0.8*1.2 m ² , 5000 Hz
Vibration needle	LIEVERS		25 mm diameter, 15000 Hz
<i>Determining material properties:</i>			
testing machine	Schenck-Trebel	M1600	100 kN (tension)
testing machine	HYGRAUMA		2000 kN (compression)
testing machine	Schenck-Trebel	RBU 2500-2	2500 kN (compression)
<i>Loading and supports:</i>			
hydraulic jack	TUE		150 kN
load cell	TUE		80 kN
load cell	TUE		150 kN
<i>Measurements devices:</i>			
strain gauge	TOKYO SOKKI	FLK 6-11	$\epsilon_{\max} = 3\%$, foil gauge
displacement meter	HBM	LVDT, w 10-k	from -10 mm to +10 mm
displacement meter	HBM	LVDT, w 20-k	from -20 mm to +20 mm
<i>Load control:</i>			
control unit	Schenck	System 59	3 signals (only 2 used)
control unit	Schenck	System 59	2 signals (at series C only)
signal generator	MTS	MTS 418.91	
<i>Analogue recording signals:</i>			
signal amplifier	HBM	KWS 3073	
xyy't-recorder	KIPP & Zonen	BD 91	
<i>Digital recording signals:</i>			
data logger	Peekel Instr. b.v.	autolog 2005	
computer	Tulip	AT	640 kB RAM, 20 Mb Harddisk
software	Peekel Instr. b.v.	Autosoft 2.3	

(empty)

8. INSTALLATION PUSH SPECIMEN: ONLY MECHANICAL ASPECTS.

With regard to the complete push test four major parts are distinguished:

1. the push test specimen was moved from the climate-room into the loading-frame;
2. some load was applied under manual control of the hydraulic jacks (preloading);
3. the measurement devices were installed;
4. finally the push test was carried out.

The parts 1, 2 and 3 were carried out simultaneously. Nevertheless, for clarity's sake only the first two parts are described at the moment. In chapter 10 the interrelationship of these three parts is described. Two definitions are introduced. If the position to which the cross-head of the hydraulic jack had to move was directly set by humans then it is said to be *Manual controlled*. *Automatic control* means that the imposed displacements were controlled by a signal generator. Fig. 8.1 shows the specimen and the supports. Many parts of the supports can be seen clearer at the photos in chapter 6.

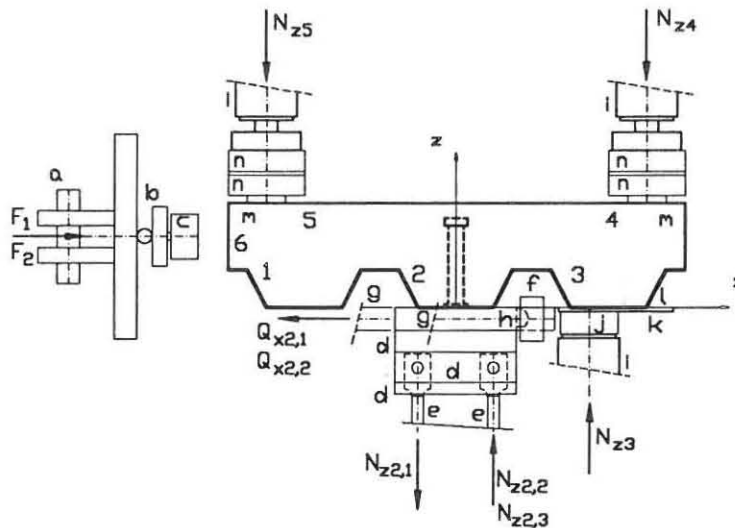


Fig. 8.1: Specimen with the supports.

Part 1: the specimen was moved into the loading-frame (see Fig. 8.1).

1. The load-table was fastened to the steel plate of the specimen by screw-threaded bars and nuts (M20). The load-table consisted out of steel plates, bars and mortise-and-tenon joints. The combination formed one part.
2. With a forklift the specimen including the fastened load-table was positioned between the beams that formed the loading-frame.
3. Whilst the specimen still made no contact with the loading frame it was suspended in a crane, and the forklift was removed.
4. Whilst the specimen hung just above the lower beam of the loading-frame the load-table was fastened to the loading-frame with bolts. The nuts were fastened only by hand. (By hand meant without any tools.)

5. One temporarily released bar (part g) was fastened to the loading-frame again. The steel plate (part f) including the two half balls (part h) was fastened to the two bars (part g) with nuts.
6. Support 3 including the steel plates (parts k & l) was positioned under rib 3 and fastened to the loading-frame by firmly screwed down nuts. (Firmly meant with a ring spanner.)
7. The hanging in the crane was removed. The mortise-and-tenon joints of the load-table caused that the upper steel plate of the load-table and so the specimen could move in the negative x-direction without any control. If this movement would exceed 9 mm then the load-table would be loaded by a shear force. This and the possible uncontrolled movement were prevented by a temporary support in the x-direction between the left side-face of the specimen and the loading-frame.
8. The nuts at the bars (part g) were equally turned until the bars of the load-table (part e) were vertical. For the moment the nuts were only fastened by hand.
9. The half balls were positioned so that they supported the steel plate to which the headed stud connector was welded only. Consequently, they made no contact with the upper steel plate of the load-table.
10. The steel plates (parts m & n) of the supports 4 and 5 were put on the upper-surface of the specimen.
11. The parts c of the loading part were suspended on part a.

Part 2: some load was applied under manual control (preloading).

1. Both the supports 4 and 5 had an adjustable part that was screwed down until the clearance between these supports and the specimen was zero.
2. The temporary support was removed (see point 7 above).
3. Under manual control a load of 1 kN at each side was applied to the specimen ($F_1 = F_2 = 1 \text{ kN}$) by increasing the imposed displacements step by step.
4. It was verified whether the forces $Q_{x2,1}$ and $Q_{x2,2}$ were equal to each other. Screwing down the nuts at the bars (part g), decreasing and/or increasing the imposed displacements resulted finally in equal forces in the x-direction ($F_1 = F_2 = Q_{x2,1} = Q_{x2,2} \approx 1 \text{ kN}$).
5. The nuts of the load-table were firmly screwed down so that the load-table was fastened to the loading-frame.
6. It was verified whether the forces in the x-direction were still equal to each other. If this was not the case (as was most likely) equal forces were restored in the way described at point 4. Anyhow, it was ensured that these forces did not exceed 2 kN.
7. Both displacements were decreased by the same amount until the forces in both hydraulic jacks became zero. Large torsional moments (M_x) at the load-table were prevented by decreasing the imposed displacements alternately and just with little amounts each time.

9. CONFIGURATION OF THE MEASUREMENTS.

Fig. 9.1 shows a schematization of the test set-up. Fig. 9.2 shows the positive directions. Each index used in this chapter refers to the number of the measurement channel of the data-logger that was used to digitise and to record the corresponding measurement. The figures 9.3, 9.4 and 9.5 show the lay-out of the measurements and the position of the measurement devices. Extensive information of the measurements is shown in the tables 9.1, 9.2 and 9.3. The multiplication factor in these tables was necessary to transfer the measurements from the measurement units to the right mechanical units and to the positive signs according to Fig. 9.2. Strains due to tension were assumed to be positive. All measurements were written to two files at the hard-disk of a computer. The tables show also which data was written to each file (= diskgroup 1 & 2). The sequence of the data in the two files was from above to below as is shown in the tables. Just for the completeness the measured strains of the concrete (specimen 2 & 3: ϵ_{38} & ϵ_{39} ; specimens in series A & B: ϵ_{30} & ϵ_{31}) are also incorporated at the next pages, although the results of these measurements were poor. Therefore, they were left out of consideration in the main report.

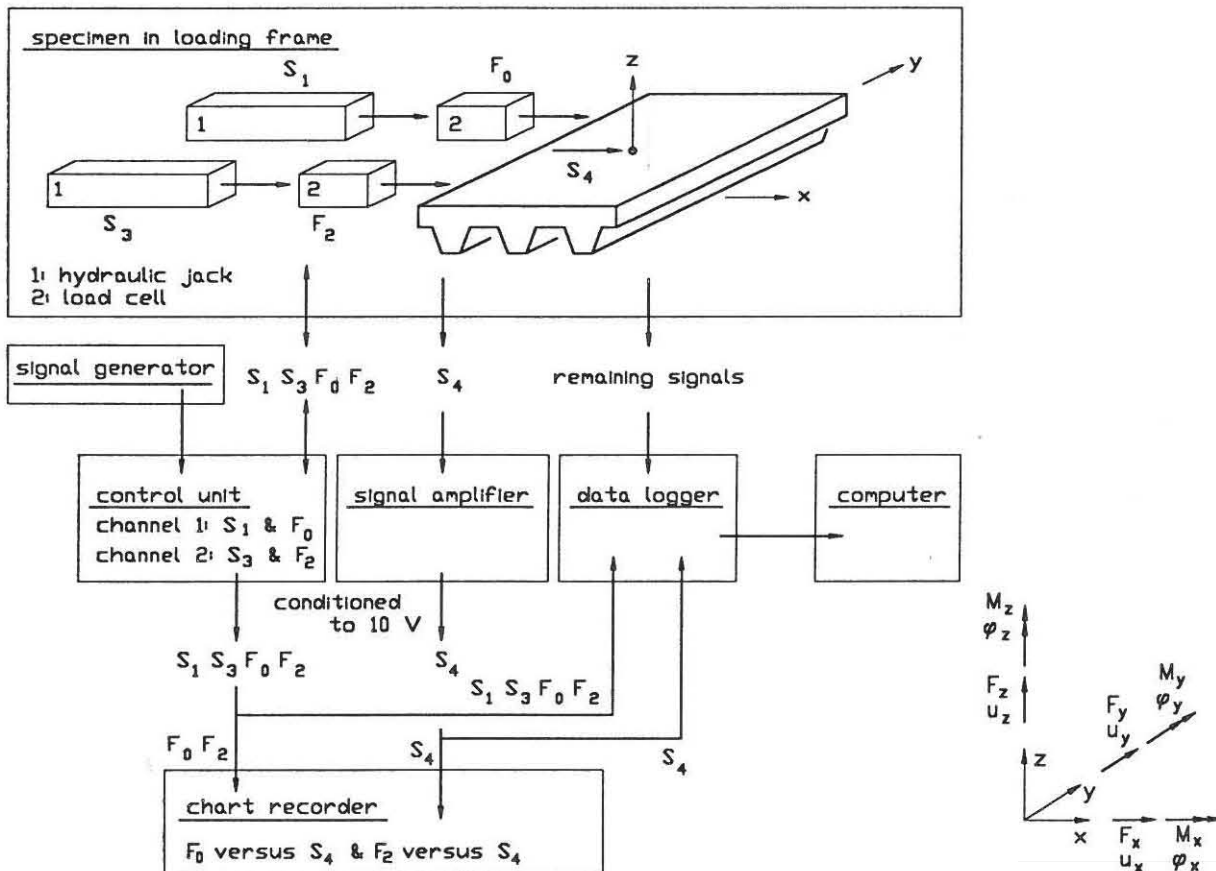


Fig. 9.2:

Sign convention.

Fig. 9.1: Schematization of the complete test set-up.

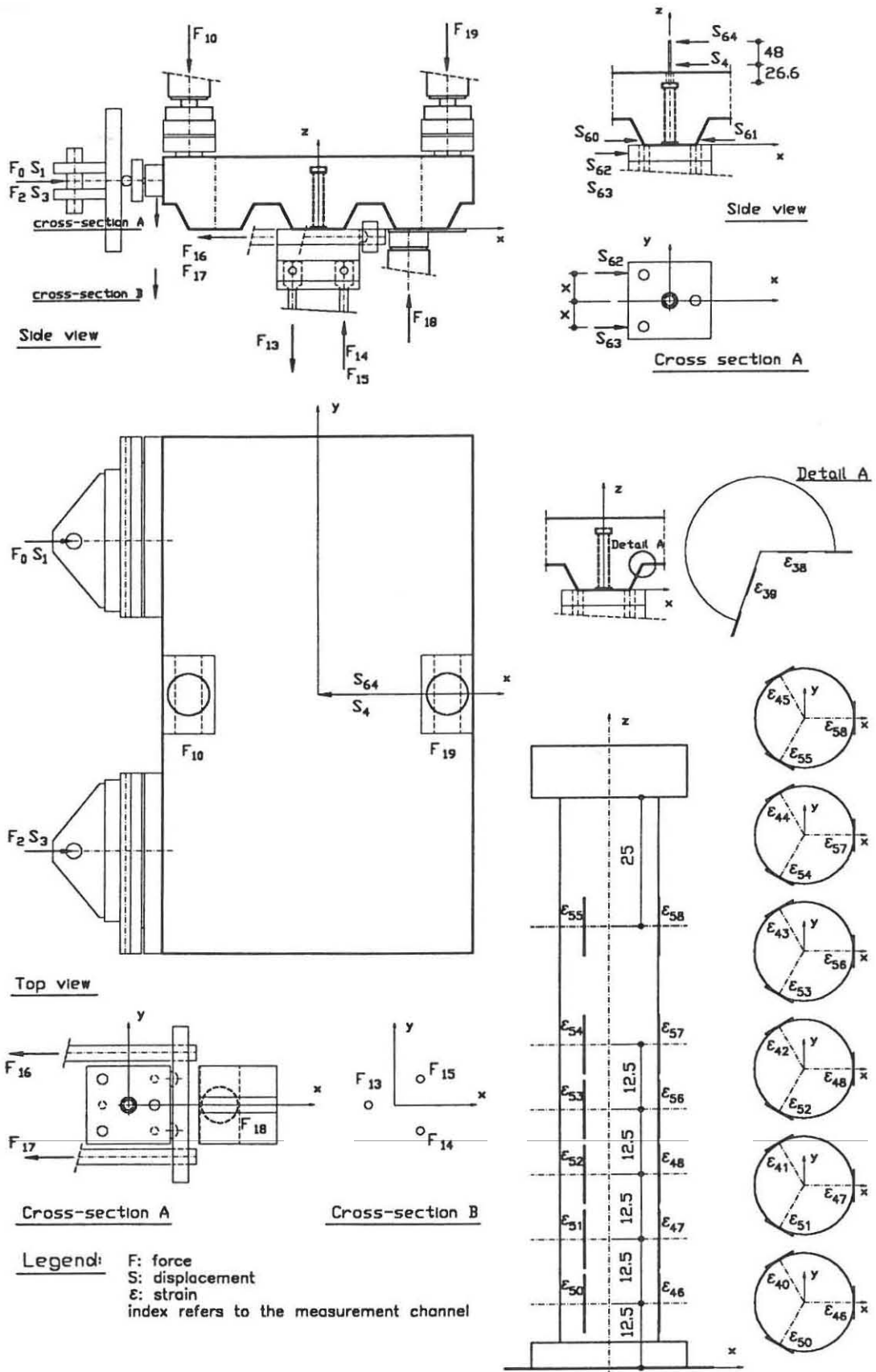


Fig 9.3: Measurements tests 2 & 3.

Table 9.1: Measurements tests 2 & 3.

type*	measurement			multiplication factor		disk group	
	channel	unit	device**	size	unit	1	2
						time	time
F	0	mV	load cell (150 kN)	-15.2721	N/mV	x	-
S	1	mV	LVDT in hydraulic jack	-5.000403E-3	mm/mV	x	-
F	2	mV	load cell (150 kN)	-14.9784	N/mV	x	-
S	3	mV	LVDT in hydraulic jack	-5.000990E-3	mm/mV	x	-
S	4	mV	LVDT (w 20-k)	-0.00183	mm/mV	x	-
F	10	-	load cell (80 kN)	+12543.78	N	x	-
F	13	-	load-table	-6203.79	N	x	-
F	14	-	load-table	-6302.20	N	x	-
F	15	-	load-table	-6438.28	N	x	-
F	16	-	load cell (80 kN)	-12215.85	N	x	-
F	17	-	load cell (80 kN)	-12539.67	N	x	-
F	18	-	load cell (80 kN)	-12522.42	N	x	-
F	19	-	load cell (80 kN)	+12418.81	N	x	-
ϵ	38	-	strain gauge (FLK 6-11)	+1.00503	$\mu\text{m/m}$	-	x
ϵ	39	-	strain gauge (FLK 6-11)	+1.00503	$\mu\text{m/m}$	-	x
ϵ	40	-	strain gauge (FLK 6-11)	+1.00503	$\mu\text{m/m}$	-	x
ϵ	41	-	strain gauge (FLK 6-11)	+1.00503	$\mu\text{m/m}$	-	x
ϵ	42	-	strain gauge (FLK 6-11)	+1.00503	$\mu\text{m/m}$	-	x
ϵ	43	-	strain gauge (FLK 6-11)	+1.00503	$\mu\text{m/m}$	-	x
ϵ	44	-	strain gauge (FLK 6-11)	+1.00503	$\mu\text{m/m}$	-	x
ϵ	45	-	strain gauge (FLK 6-11)	+1.00503	$\mu\text{m/m}$	-	x
ϵ	46	-	strain gauge (FLK 6-11)	+1.00503	$\mu\text{m/m}$	-	x
ϵ	47	-	strain gauge (FLK 6-11)	+1.00503	$\mu\text{m/m}$	-	x
ϵ	48	-	strain gauge (FLK 6-11)	+1.00503	$\mu\text{m/m}$	-	x
ϵ	50	-	strain gauge (FLK 6-11)	+1.00503	$\mu\text{m/m}$	-	x
ϵ	51	-	strain gauge (FLK 6-11)	+1.00503	$\mu\text{m/m}$	-	x
ϵ	52	-	strain gauge (FLK 6-11)	+1.00503	$\mu\text{m/m}$	-	x
ϵ	53	-	strain gauge (FLK 6-11)	+1.00503	$\mu\text{m/m}$	-	x
ϵ	54	-	strain gauge (FLK 6-11)	+1.00503	$\mu\text{m/m}$	-	x
ϵ	55	-	strain gauge (FLK 6-11)	+1.00503	$\mu\text{m/m}$	-	x
ϵ	56	-	strain gauge (FLK 6-11)	+1.00503	$\mu\text{m/m}$	-	x
ϵ	57	-	strain gauge (FLK 6-11)	+1.00503	$\mu\text{m/m}$	-	x
ϵ	58	-	strain gauge (FLK 6-11)	+1.00503	$\mu\text{m/m}$	-	x
S	60	-	LVDT (w 20-k)	+0.52281	mm	x	-
S	61	-	LVDT (w 20-k)	-0.50150	mm	x	-
S	62	-	LVDT (w 10-k)	+0.30355	mm	x	-
S	63	-	LVDT (w 10-k)	+0.29467	mm	x	-
S	64	-	LVDT (w 20-k)	+0.55861	mm	x	-

*: F means force, S means displacement and ϵ means strain.

** : More information is reported in chapter 7. LVDT means: Linear Variable Displacement Transducer.

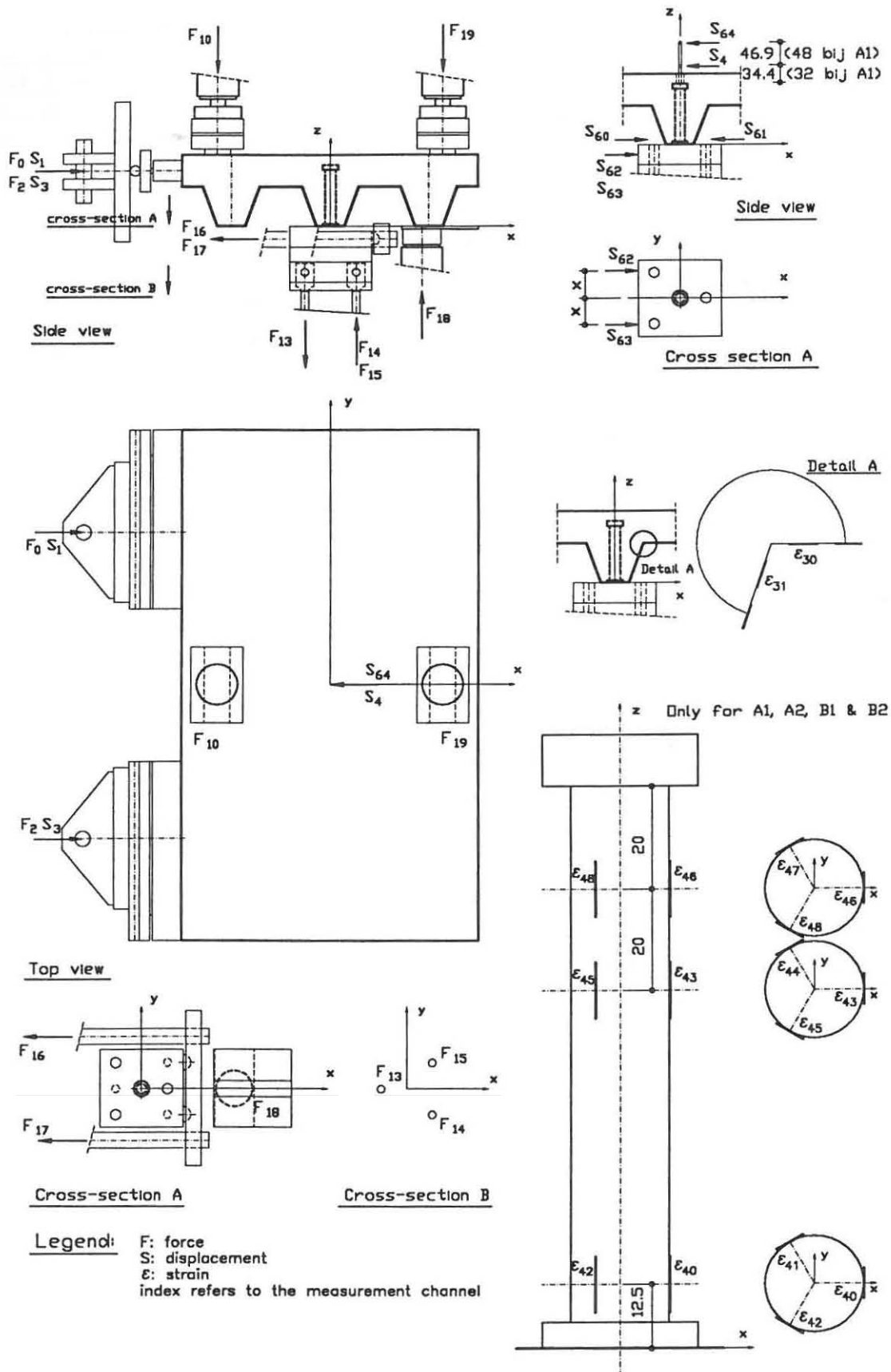


Fig. 9.4: Measurements tests in the series A & B.

Table 9.2: Measurements tests in the series A & B.

type*	measurement			multiplication factor		disk group	
	channel	unit	device**	size	unit	1	2
						time	time
F	0	mV	load cell (150 kN)	-15.2721	N/mV	x	x
S	1	mV	LVDT in hydraulic jack	-5.000403E-3	mm/mV	x	-
F	2	mV	load cell (150 kN)	-14.9784	N/mV	x	x
S	3	mV	LVDT in hydraulic jack	-5.000990E-3	mm/mV	x	-
S	4	mV	LVDT (w 20-k)	-0.00183	mm/mV	x	-
F	10	-	load cell (80 kN)	+12543.78	N	x	-
F	13	-	load-table	-6203.79	N	x	-
F	14	-	load-table	-6302.20	N	x	-
F	15	-	load-table	-6438.28	N	x	-
F	16	-	load cell (80 kN)	-12215.85	N	x	-
F	17	-	load cell (80 kN)	-12539.67	N	x	-
F	18	-	load cell (80 kN)	-12522.42	N	x	-
F	19	-	load cell (80 kN)	+12418.81	N	x	-
ϵ	30	-	strain gauge (FLK 6-11)	+1.00503	$\mu\text{m}/\text{m}$	-	x
ϵ	31	-	strain gauge (FLK 6-11)	+1.00503	$\mu\text{m}/\text{m}$	-	x
ϵ^{***}	40	-	strain gauge (FLK 6-11)	+1.00503	$\mu\text{m}/\text{m}$	-	x
ϵ^{***}	41	-	strain gauge (FLK 6-11)	+1.00503	$\mu\text{m}/\text{m}$	-	x
ϵ^{***}	42	-	strain gauge (FLK 6-11)	+1.00503	$\mu\text{m}/\text{m}$	-	x
ϵ^{***}	43	-	strain gauge (FLK 6-11)	+1.00503	$\mu\text{m}/\text{m}$	-	x
ϵ^{***}	44	-	strain gauge (FLK 6-11)	+1.00503	$\mu\text{m}/\text{m}$	-	x
ϵ^{***}	45	-	strain gauge (FLK 6-11)	+1.00503	$\mu\text{m}/\text{m}$	-	x
ϵ^{***}	46	-	strain gauge (FLK 6-11)	+1.00503	$\mu\text{m}/\text{m}$	-	x
ϵ^{***}	47	-	strain gauge (FLK 6-11)	+1.00503	$\mu\text{m}/\text{m}$	-	x
ϵ^{***}	48	-	strain gauge (FLK 6-11)	+1.00503	$\mu\text{m}/\text{m}$	-	x
S	60	-	LVDT (w 20-k)	+0.52281	mm	x	-
S	61	-	LVDT (w 20-k)	-0.50150	mm	x	-
S	62	-	LVDT (w 20-k)	+0.58254****	mm	x	-
S	63	-	LVDT (w 10-k)	+0.29467	mm	x	-
S	64	-	LVDT (w 20-k)	+0.55861	mm	x	-

*: F means force, S means displacement and ϵ means strain.

** : More information is reported in chapter 7. LVDT means: Linear Variable Displacement Transducer.

***: Not measured for the specimens A3 and B3.

****: With respect to the tests 2 and 3 the LVDT was replaced and consequently the multiplication factor changed.

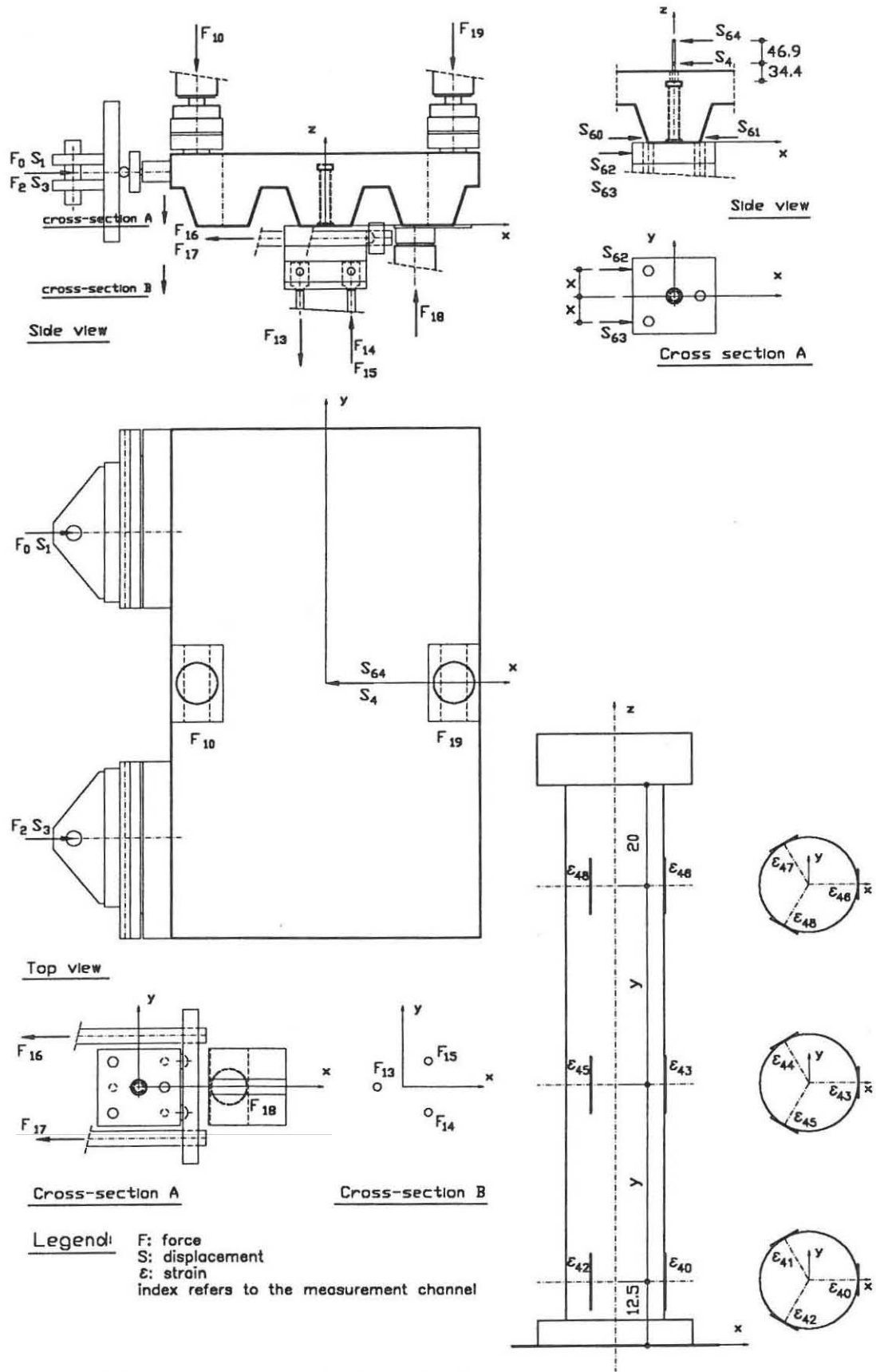


Fig. 9.5: Measurements tests in the series C.

Table 9.3: Measurements tests in the series C.

measurement				multiplication factor		disk group	
type*	channel	unit	device**	size	unit	1	2
						time	time
F	0	mV	load cell (150 kN)	-14.94602***	N/mV	x	x
S	1	mV	LVDT in hydraulic jack	-5.010810E-3***	mm/mV	x	-
F	2	mV	load cell (150 kN)	-14.94878***	N/mV	x	x
S	3	mV	LVDT in hydraulic jack	-5.007501E-3***	mm/mV	x	-
S	4	mV	LVDT (w 20-k)	-0.00183	mm/mV	x	-
F	10	-	load cell (80 kN)	+12543.78	N	x	-
F	13	-	load-table	-6203.79	N	x	-
F	14	-	load-table	-6302.20	N	x	-
F	15	-	load-table	-6438.28	N	x	-
F	16	-	load cell (80 kN)	-12215.85	N	x	-
F	17	-	load cell (80 kN)	-12539.67	N	x	-
F	18	-	load cell (80 kN)	-12522.42	N	x	-
F	19	-	load cell (80 kN)	+12418.81	N	x	-
ε	40	-	strain gauge (FLK 6-11)	+1.00503	μm/m	-	x
ε	41	-	strain gauge (FLK 6-11)	+1.00503	μm/m	-	x
ε	42	-	strain gauge (FLK 6-11)	+1.00503	μm/m	-	x
ε	43	-	strain gauge (FLK 6-11)	+1.00503	μm/m	-	x
ε	44	-	strain gauge (FLK 6-11)	+1.00503	μm/m	-	x
ε	45	-	strain gauge (FLK 6-11)	+1.00503	μm/m	-	x
ε	46	-	strain gauge (FLK 6-11)	+1.00503****	μm/m	-	x
ε	47	-	strain gauge (FLK 6-11)	+1.00503	μm/m	-	x
ε	48	-	strain gauge (FLK 6-11)	+1.00503	μm/m	-	x
S	60	-	LVDT (w 20-k)	+0.52281	mm	x	-
S	61	-	LVDT (w 20-k)	+0.50150*****	mm	x	-
S	62	-	LVDT (w 20-k)	+0.58254	mm	x	-
S	63	-	LVDT (w 10-k)	+0.29467	mm	x	-
S	64	-	LVDT (w 20-k)	+0.55861	mm	x	-

*: F means force, S means displacement and ε means strain.

** : More information is reported in chapter 7. LVDT means: Linear Variable Displacement Transducer.

***: Changed with respect to the tests 2, 3 and those in the series A and B due to the use of another control unit in series C (see also chapter 7).

****: Only for specimen C1 a multiplication factor of 10.44188 instead of 1.00503 was used.

*****: Sign (positive) was changed due to using a different cable at this LVDT in series C.

(empty)

10. COMPLETE INSTALLATION PUSH SPECIMEN.

With regard to the complete push test four major parts are distinguished:

1. the push test specimen was moved from the climate-room into the loading-frame;
2. some load was applied under manual control of the hydraulic jacks (preloading);
3. the measurement devices were installed;
4. finally the push test was carried out.

First the first three parts and their interrelationship in particular are described as well as the verification of some aspects (see also Fig. 10.1). Many parts of the supports can be seen clearer at the photos in chapter 6. The mechanical aspects were extensively described in chapter 8 already and therefore are only repeated here briefly. Secondly some details about the test control are given.

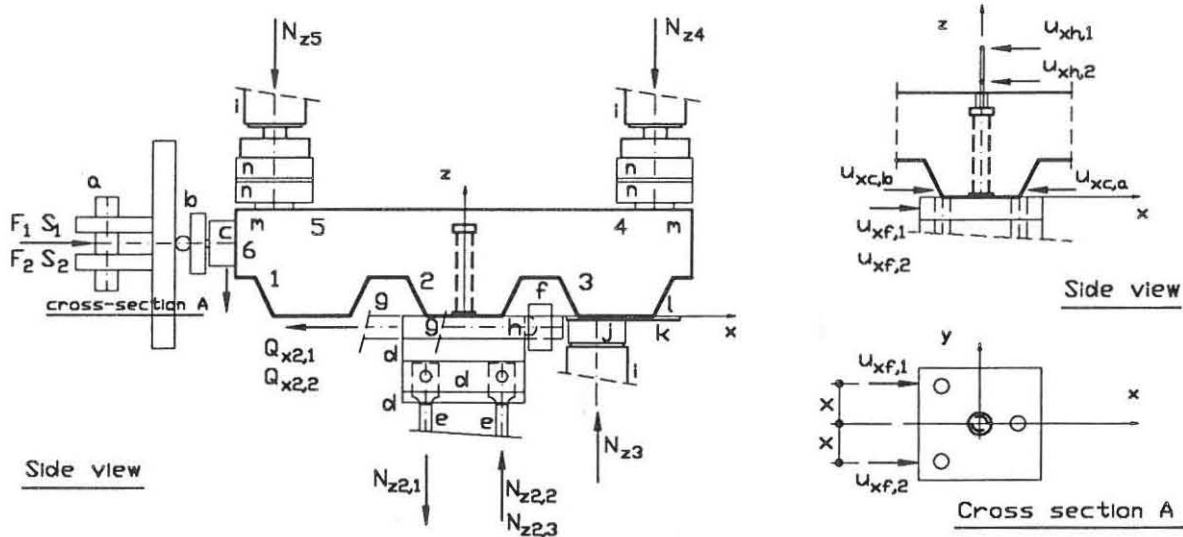


Fig. 10.1: Installation of both the specimen and the measurement devices.

List of actions:

1. It was verified whether there was any clearance between the steel plate of the specimen and the thin profiled steel sheeting at the rear side of the headed stud connector. Any clearance was filled up with a thin steel sheeting.
2. A damaged strip teflon was replaced. Even if the strips were not damaged they were all replaced after the tests 3, B3, C6 and C12. Then new grease was applied also.
3. The load-table was fastened to the steel plate of the specimen.
4. The specimen including the fastened load-table was positioned between the beams that formed the loading-frame. Whilst the specimen hung just above the lower beam of the loading-frame the load-table was fastened to the loading-frame with bolts. The nuts were only fastened by hand.

5. The temporarily released bar (part g) was fastened to the loading-frame. The steel plate (part f) including the two half balls (part h) was fastened to the two bars (part g) with nuts.
6. The connectors of the strain gauges, the load cells and the strain gauges at the bars of the load-table were connected to the measurement system.
7. The measurement was started. However, the measurements were just previewed on the screen of the computer and not yet recorded at the harddisk of the computer.
8. During the time that the specimen hung in the crane the measurement signals (strains, load cells and load-table) were set to zero.
9. The recording of the measurements was started.
10. Support 3 including the steel plates (parts k & l) was positioned under rib 3 and fastened to the loading-frame by firmly screwed down nuts.
11. The hanging in the crane was released. It was verified whether support 3 was loaded in compression due to the mass of the specimen. Any clearance between support 3 and the specimen was filled up with thin steel sheetings.
12. The hanging in the crane was removed. Due to the mortise-and-tenon joints the specimen could move in the negative x-direction. This was hindered by a temporary support in the x-direction between the left side-face of the specimen and the loading-frame.
13. The nuts at the bars (part g) were equally turned until the bars of the load-table (part e) became vertical. For the moment, the nuts were only fastened by hand.
14. The half balls were positioned so that they only supported the steel plate to which the headed stud connector was welded. So, they made no contact with the upper steel plate of the load-table.
15. The steel plates (parts m & n) of the supports 4 and 5 were put on the upper-surface of the specimen.
16. The parts c of the loading part were suspended on part a.
17. All displacement meters (LVDT's) were positioned. The LVDT's $u_{xc,b}$ and $u_{xc,a}$ were fixed to the steel wires that were embedded in the concrete. The LVDT's $u_{xf,1}$ and $u_{xf,2}$ were fixed to the steel plate to which the headed stud connector was welded. The latter two LVDT's were symmetrically positioned to the plane $y=0$. The other sides of the LVDT's ($u_{xc,b}$, $u_{xc,a}$, $u_{xf,1}$ & $u_{xf,2}$) were stuck to the lower beam (HE 300 B) of the loading-frame to which also the supports 2 and 3 were fastened. It was expected that the elongation of this beam was negligible and therefore did not effect the measured displacements. The LVDT's $u_{xh,2}$ and $u_{xh,1}$ were fixed to a bolt M3 that was fully clasped to the head of the stud. The connections of the LVDT's with the bolt were provided with a kind of mortise-and-tenon joints. Doing this it was prevented that the LVDT's were loaded in bending due to a possible rotation of the head of the headed stud connector. The other sides of the LVDT's $u_{xh,2}$ and $u_{xh,1}$ were stuck to a apart measurement frame that made no contact with the specimen and the loading-frame. Also the cables of the LVDT's did not make any contact with the specimen, even not during the test.

18. Both the supports 4 and 5 had an adjustable part that was screwed down until there was no more clearance between these supports and the specimen.
19. The temporary support was removed (see point 12 above).
20. With the control unit a load of 1 kN at each side was applied to the specimen ($F_1 = F_2 \approx 1$ kN) under manual control by increasing step by step the imposed displacements.
21. It was verified whether the forces $Q_{x2,1}$ and $Q_{x2,2}$ were equal to each other. Screwing down the nuts at the bars (part g), decreasing and/or increasing the imposed displacements resulted finally in equal forces in the x-direction ($F_1 = F_2 = Q_{x2,1} = Q_{x2,2}$).
22. The nuts of the load-table were firmly screwed down so that the loading table was fastened to the loading-frame.
23. It was verified whether the forces in the x-direction were still equal to each other. If this was not the case (as was most likely) equal forces were restored in the way described at point 21. These forces did not exceed 2 kN.
24. The at both hydraulic jacks imposed displacements (S_1 & S_2) were decreased by the same amount until the forces in both load cells (F_1 & F_2) became zero. The imposed displacements were alternately decreased with only little amounts each time. Consequently, the torsional moments (M_z) at the load-table remained little.
25. The chart recorder was installed.
26. The measurements during the installation were finished.
27. New measurements just for the real push test were started. This resulted in new data-files with just the measurements of the push test.
28. The push test was started (displacement-control, automatic control).
29. If during the first part of the push test appeared that the load was asymmetrically distributed over the specimen a symmetric distribution was restored whilst the push test was continued. In this case just the nuts at the bars (part g) were screwed down or were somewhat released.

Details with regard to the test control are summarised hereafter. The load was applied by displacement-control so that the test could be continued after the maximum shear force was reached. This also caused the stable control of the test that would hardly had been possible if force-control had been used. Initially the rate at which the displacements were imposed was 12.4 mm/h. At large slips (> 5 mm) the rate was increased to 24.8 mm/h and even to 49.7 mm/h.

The progress of the push test was directly and continuously monitored by a chart recorder and by previewing the measurements at the screen of a computer simultaneously. Consequently, it was possible to observe the distribution of the applied load and the magnitude of the axial forces in the bars of the load-table. The load was adapted if the distribution was asymmetrical ($F_1 \neq F_2$ and/or $Q_{x2,1} \neq Q_{x2,2}$). Whilst the load was adapted the test was normally continued. If an axial force in the load-table exceeded 35 kN (mostly $N_{z2,1}$) the test was prematurely stopped.

A data logger was used to digitise all measurements 6 times each minute. Simultaneously maximal 12 measurements at the time were previewed at the screen of the computer. Before the test all measurements were divided in some groups of 12 measurements each. It was possible to switch between these groups during the previewing. On the same computer all measurements were recorded in two files on the harddisk.

11. GRAPHICAL REPRESENTATION OF THE ORIGINAL MEASUREMENTS.

11.1 Introduction.

The original measurements were used to determine several relations between the relevant parameters and formed the basis for the calculation of these relevant parameters. The relevant parameters are reported in the 'main report'. The figures given here (original measurements versus slip) were used to verify the reliability of the measurements and the test. The conclusions of these figures are described hereafter (see also Fig. 11.1). In the next sections the figures are given. Table 11.1 shows an overview of the figures of each specimen that are given. See chapter 9 for the sign convention used. Strains due to tension are positive.

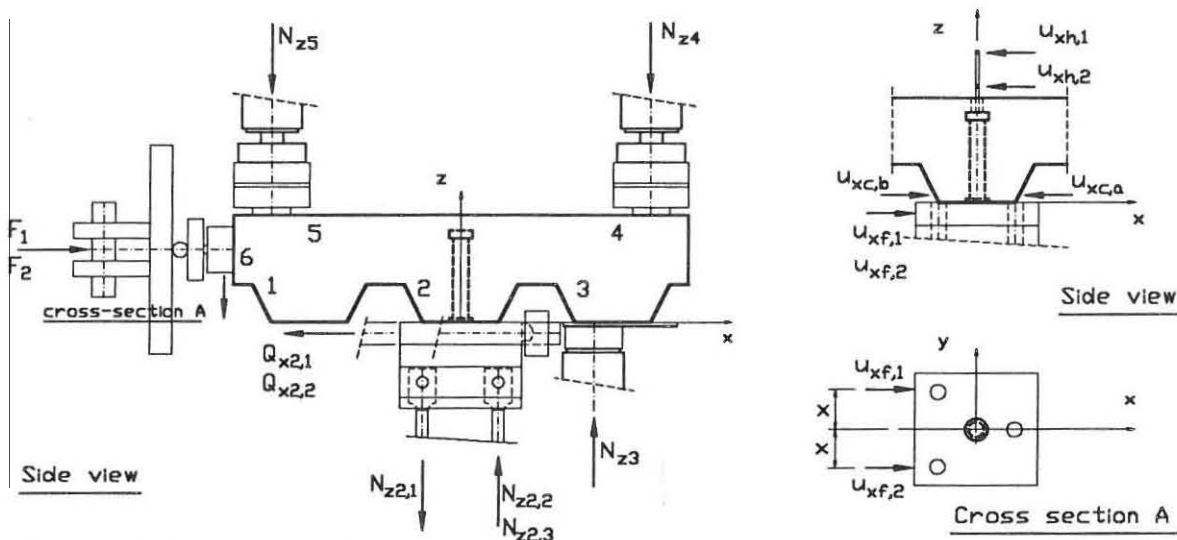


Fig. 11.1: Test set-up and measurements.

Forces in the x-direction: F_1 , F_2 , $Q_{x2,1}$, $Q_{x2,2}$ & ΣF_x (section 11.2).

Main conclusion was that 97 % of the applied load was transferred to support 2 and so to the headed stud connection. The remaining part (3 %) was transferred by frictional forces in the other supports. Comparing the forces $Q_{x2,1}$ and $Q_{x2,2}$ it could be seen that the load was not complete symmetrically distributed to the plane $y=0$. It seemed that the behaviour was hardly influenced by the little differences between $Q_{x2,1}$ and $Q_{x2,2}$.

Forces in the z-direction: $N_{z2,1}$, $N_{z2,2}$, $N_{z2,3}$ and $\Sigma N_{z2,i}$, N_{z3} , N_{z4} , N_{z5} & ΣF_z (section 11.3).

- The forces $N_{z2,2}$ and $N_{z2,3}$ were not equal. So there had to be a moment M_x . This was expected as the symmetry to the plane $y=0$ originated in theory only. As the moment remained 'small' it was expected that it did not influence the behaviour.
- Equilibrium in the z-direction was quite well satisfied. The measurements included the dead weight of the specimen. So the sum of the vertical forces should be equal to the dead weight of the specimen and some parts of the supports (about 2 kN).

- It was verified whether N_{z3} increased immediately at the first moment that the load was applied. If this was not the case there had to be some clearance between rib 3 and the support under this rib. It was expected that this clearance would influence the behaviour in an undesirable way. Unfortunately this clearance appeared at push test C4.

Strains of the headed stud connector: ϵ_{z1} , ϵ_{z2} & ϵ_{z3} (section 11.4).

The strains of the headed stud connector (Fig. 11.2; ϵ_{z1} , ϵ_{z2} & ϵ_{z3}) were measured at several levels (3 or 6, (see chapter 9)) with different z co-ordinates. The z co-ordinate of the levels increased with increasing level-number. At each level all three strains were necessary to be able to calculate the internal forces in the headed stud connector (Fig. 11.2; N_{zs} , M_{xs} & M_{ys}). The 'yield' strain was 0.2 % (= 2000 $\mu\text{m}/\text{m}$). The figures show that at level 1 (near the foot of the stud: $z=12.5$ mm) yielding originated at small slips (about 1 mm) already. Yielding originated at both the front side of the stud (tension at level 1) and at the rear side (compression at level 1). Approximately at 2 mm slip first yielding at level 2 (near the middle of the stud length) originated. At level 2 the yielding mostly originated just at the rear side and was caused by tension.

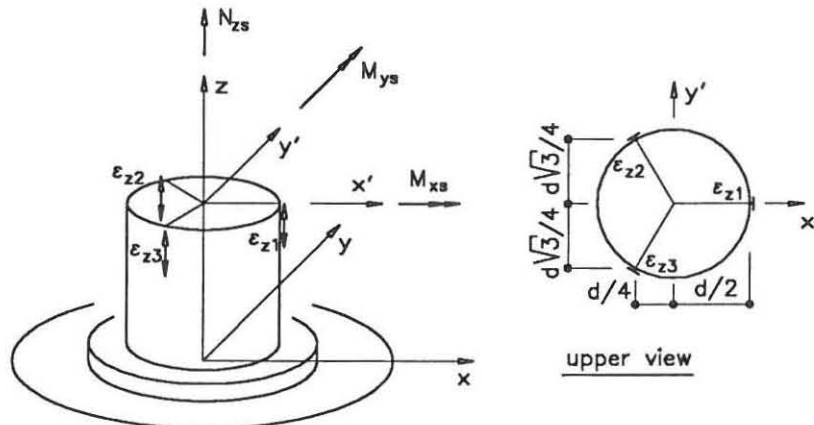


Fig. 11.2: Strains of the connector.

In spite of the caution during casting some strain gauges appeared to be damaged before the push test was started. Moreover, the strains could not be measured during the complete push test due to failure of the strain gauges at strains (mostly far) less than the capacity of the stain gauges (30.000 $\mu\text{m}/\text{m}$). Therefore, only strains not exceeding 5000 $\mu\text{m}/\text{m}$ were given, although the internal forces were calculated with strains just less than the 'yield' strain (2000 $\mu\text{m}/\text{m}$). Also just the strains were given at slips less than 7.5 mm. If complete symmetry in the plane $y=0$ originated then the strains ϵ_{z2} and ϵ_{z3} should be equal. The strains for the specimens 2 and 3 were given just for the completeness as after these tests it appeared that the strain gauges were stucked to the concrete and not anymore to the shaft of the connector. This was caused by the bond between the concrete and the surface of the strain gauge. This surface

was covered with wax to prevent damage of the strain gauge during casting. For the remaining specimens teflon was used instead of wax.

Displacements: $u_{xc,b}$, $u_{xc,a}$, $u_{xf,1}$, $u_{xf,2}$, $u_{xh,1}$ & $u_{xh,2}$ (section 11.5).

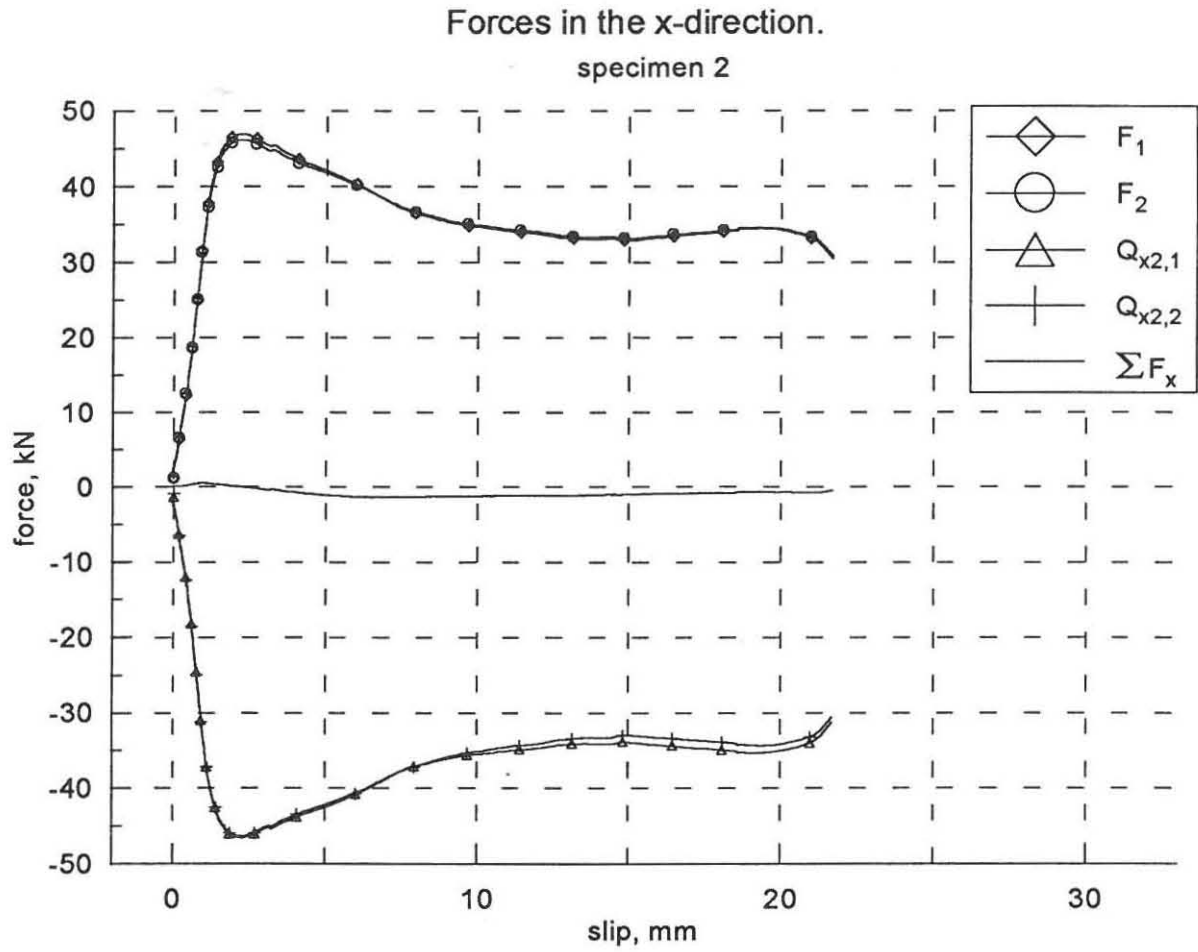
The specimen hardly rotated around the z-axis as there was no significant difference between $u_{xf,1}$ and $u_{xf,2}$. A difference between $u_{xh,1}$ and $u_{xh,2}$ pointed to a rotation of the head of the stud (φ_{yh}). Only in the series A and B this rotation became significant. For the specimens 3 (without steel sheeting) and C10 (stud in precut hole) the displacement at the rear side of rib 2 ($u_{xc,a}$) was almost equal to the displacements of the head of the stud ($u_{xh,1}$ & $u_{xh,2}$).

Table 11.1: Figures that are reported in the next sections (marked with x).

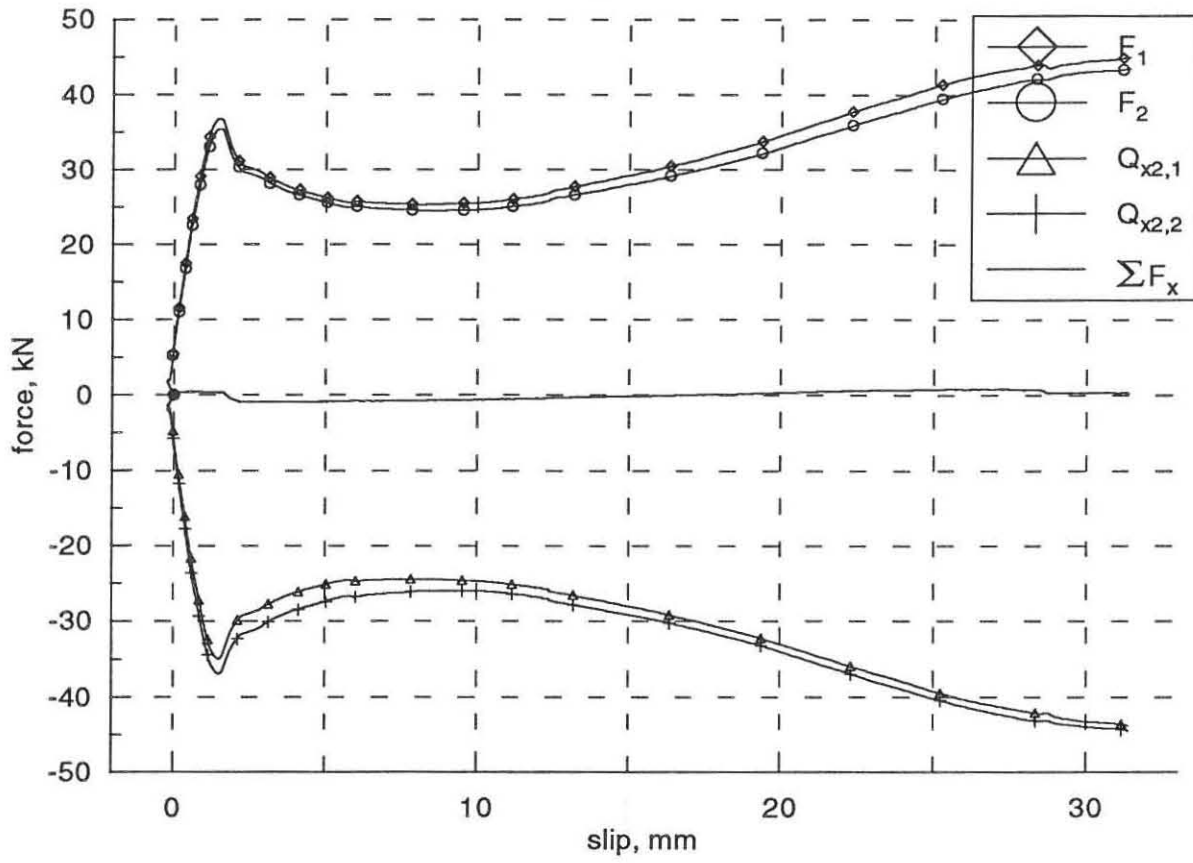
code	F ₁ , F ₂ Q _{x2,1} , Q _{x2,2} Σ F _x	N _{z2,1} , N _{z2,2} , N _{z2,3} and Σ N _{z2,1} , N _{z3} , N _{z4} , N _{z5} , Σ F _z	ε _{z1} , ε _{z2} , ε _{z3} at level						u _{xc,b} , u _{xc,a} u _{xf,1} , u _{xf,2} u _{xh,1} , u _{xh,2}
			1	2	3	4	5	6	
2*	x	x	x	x	x	x	x	x	x
3*	x	x	x	x	x	x	x	x	x
A1	x	x	x	x					x
A2	x	x	x	x					x
A3**	x	x							x
B1	x	x	x	x					x
B2	x	x	x	x					x
B3**	x	x							x
C1	x	x	x	x					x
C2	x	x	x	x					x
C3	x	x	x	x					x
C4	x	x	x	x					x
C5	x	x	x	x					x
C6	x	x	x	x					x
C7	x	x	x	x					x
C8	x	x	x	x					x
C9	x	x	x	x					x
C10	x	x	x	x					x
C11	x	x	x	x					x
C12	x	x	x	x					x
C13	x	x	x	x					x
C14	x	x	x	x					x

*: Just for the specimens 2 and 3 the strains of the headed stud connector were measured at 6 levels instead of 3 levels.

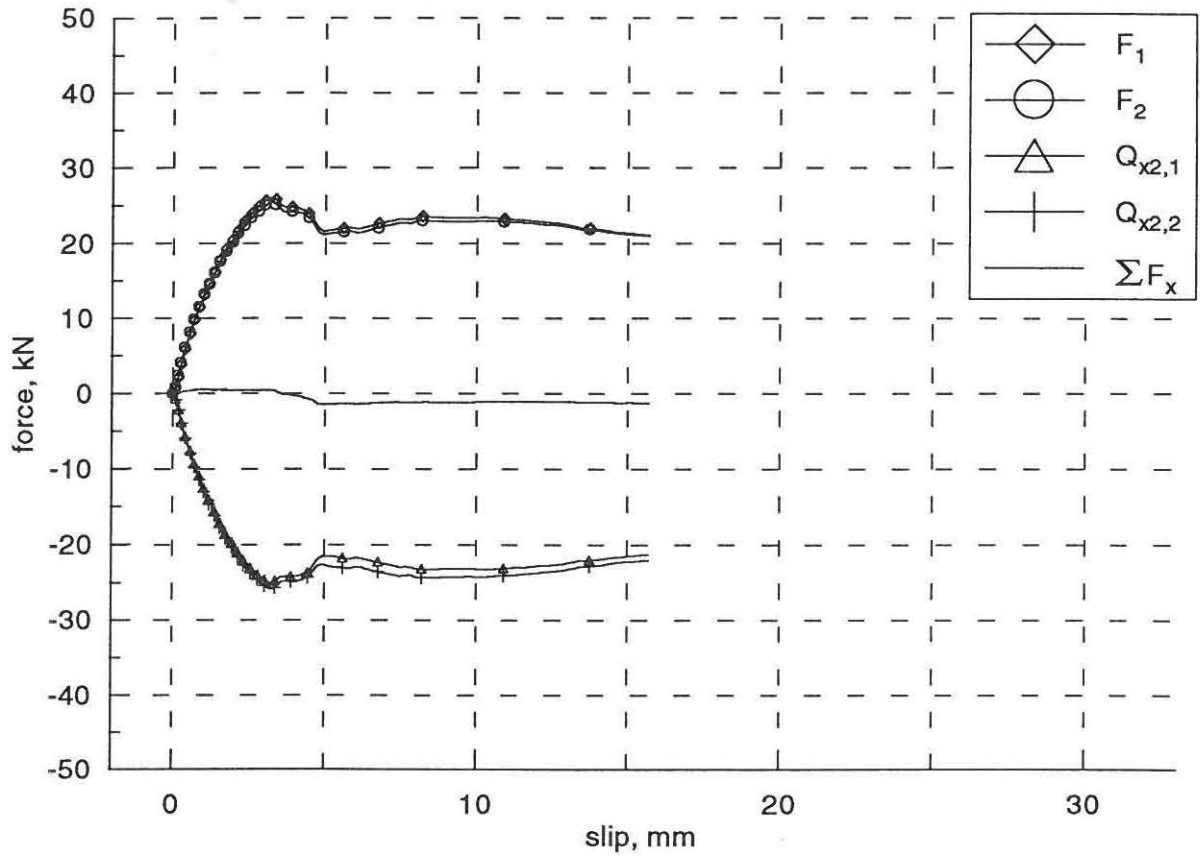
** : The strains of the headed stud connector were not measured.

11.2 Forces in the x-direction: F_1 , F_2 , $Q_{x2,1}$, $Q_{x2,2}$ & ΣF_x .

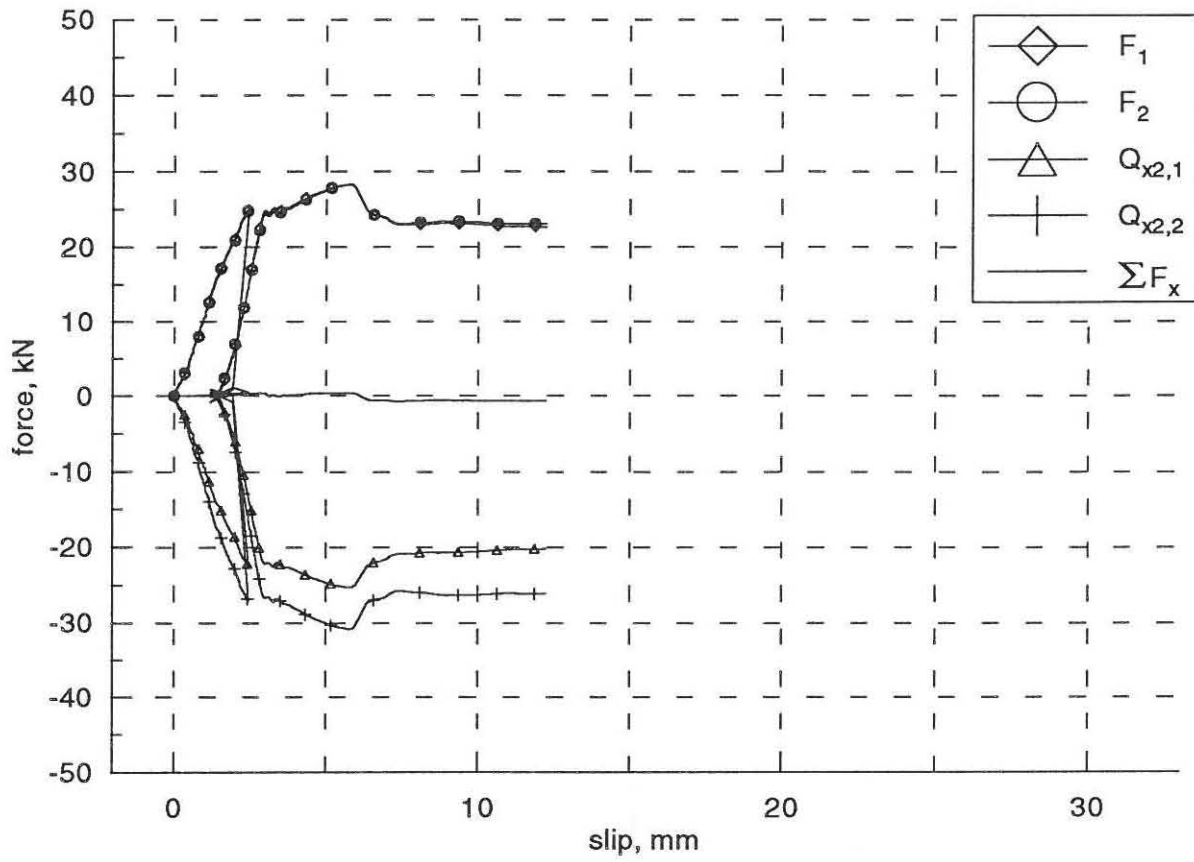
Forces in the x-direction.
specimen 3



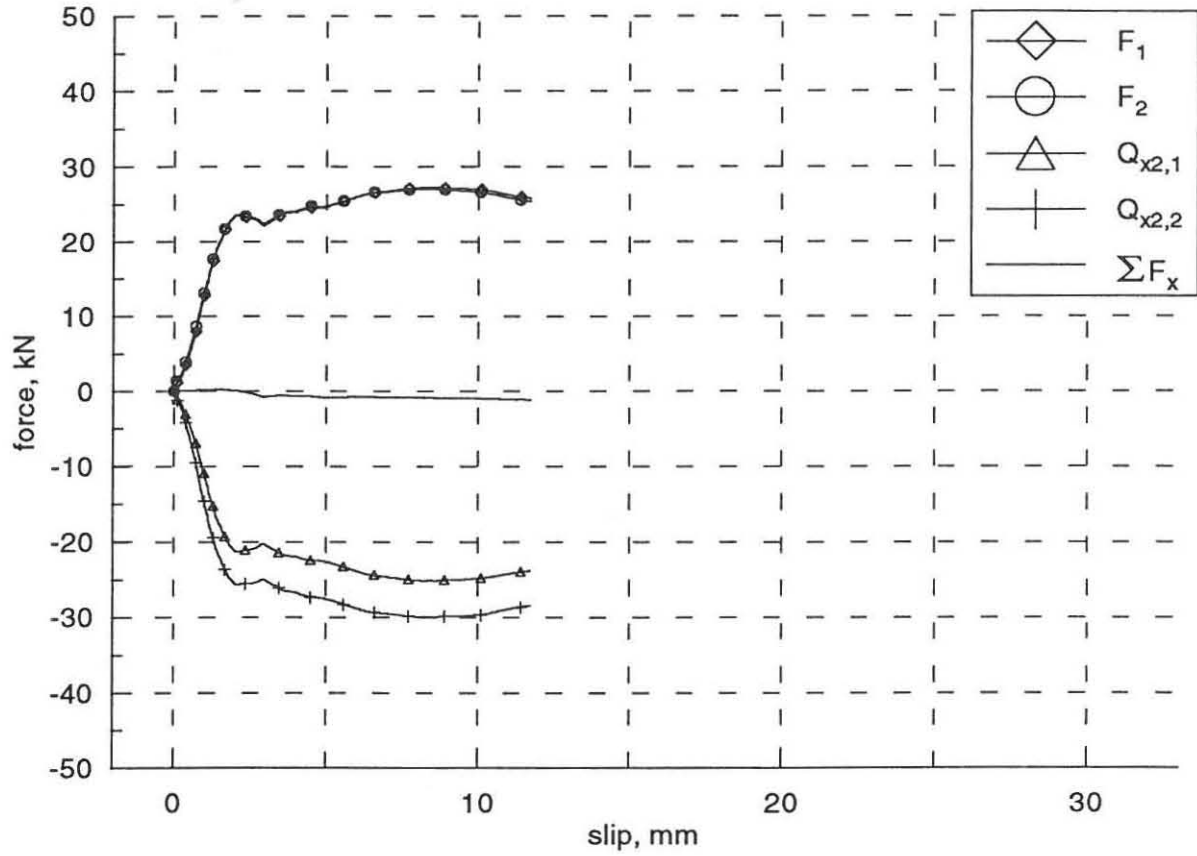
Forces in the x-direction.
specimen A1



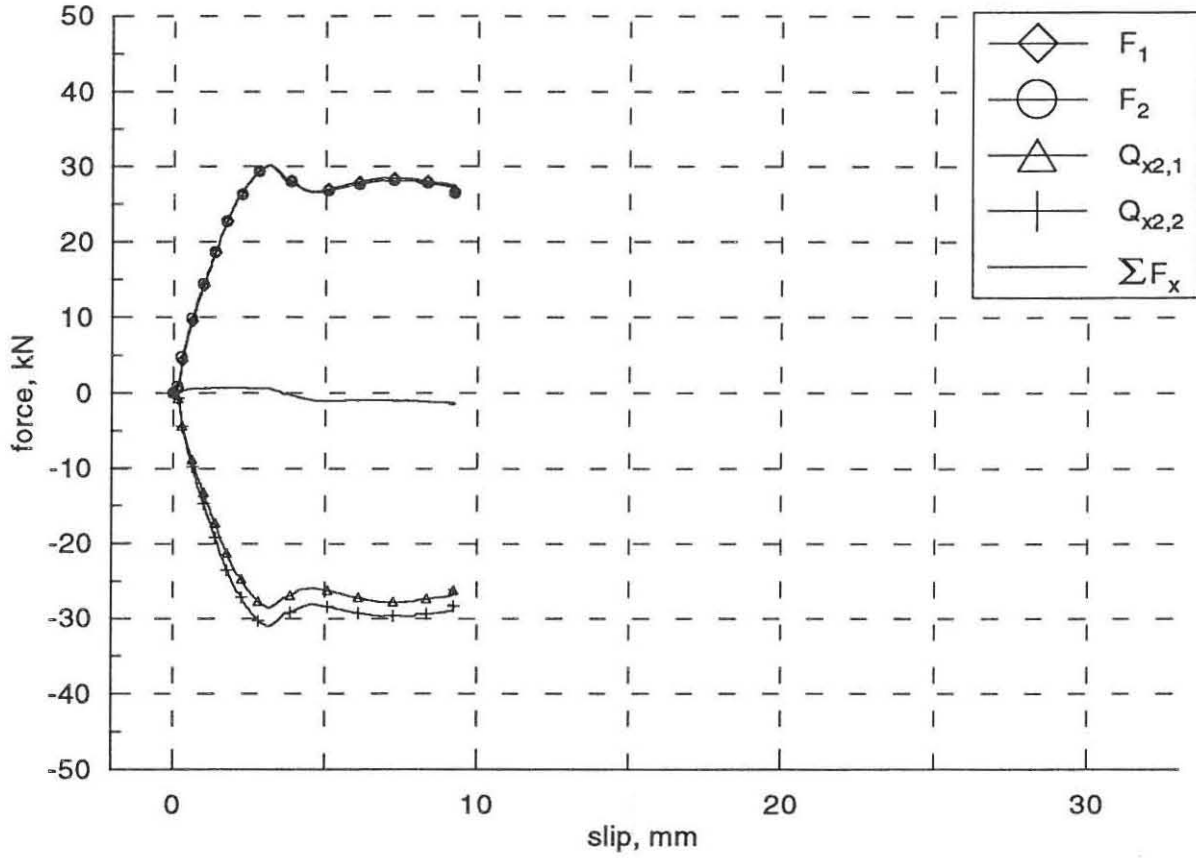
Forces in the x-direction.
specimen A2



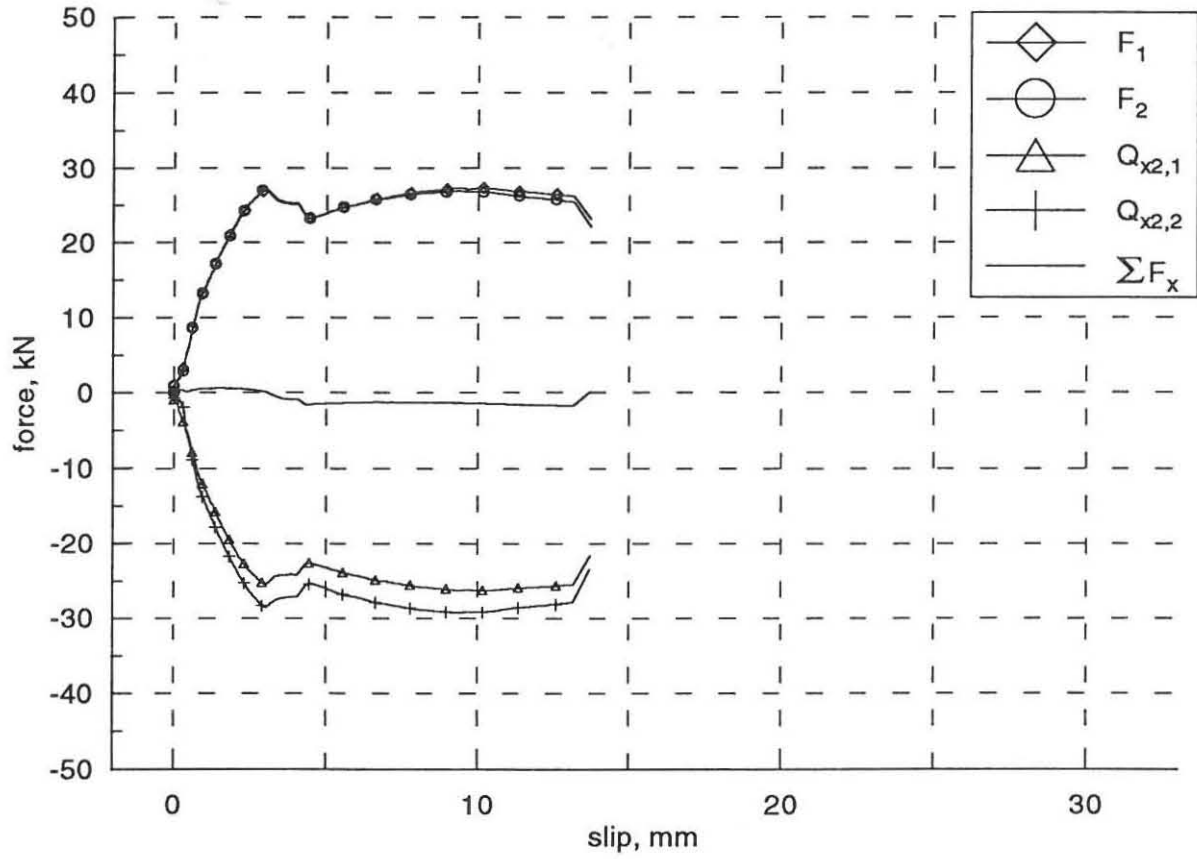
Forces in the x-direction.
specimen A3



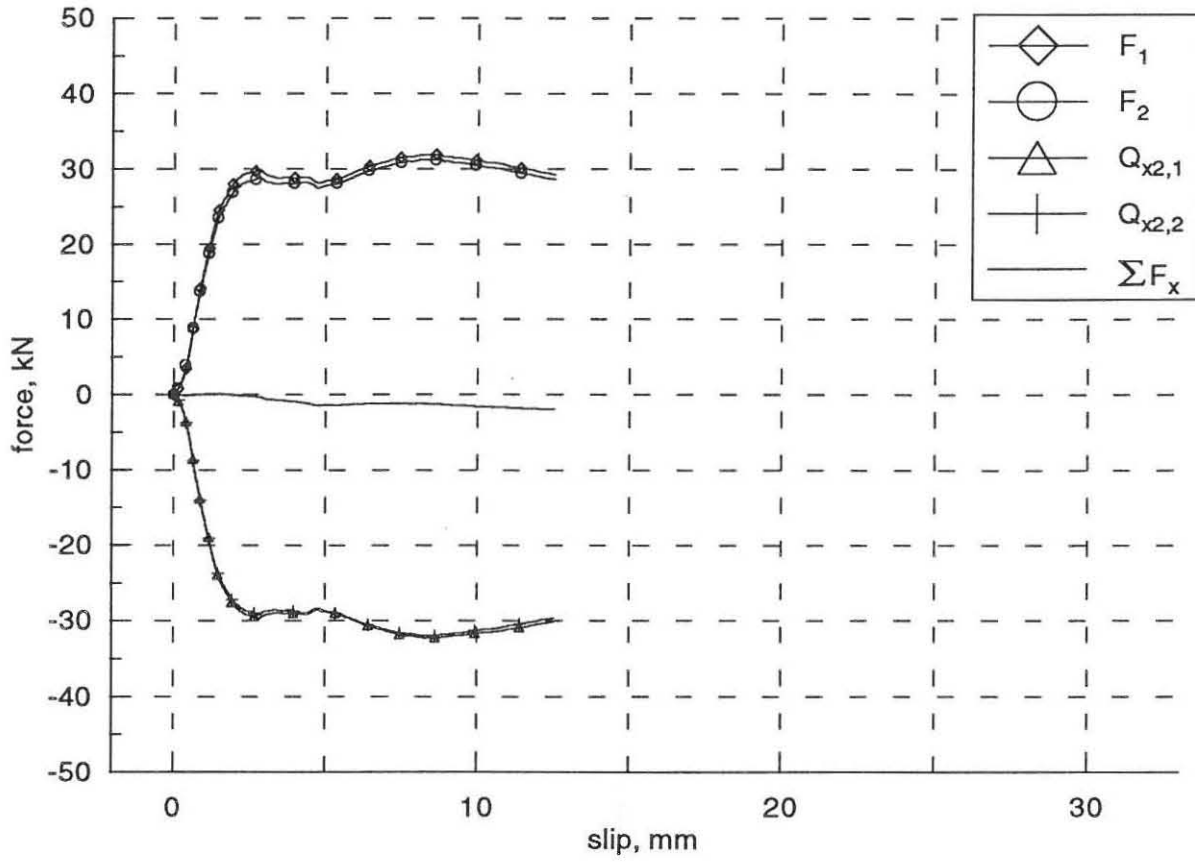
Forces in the x-direction.
specimen B1



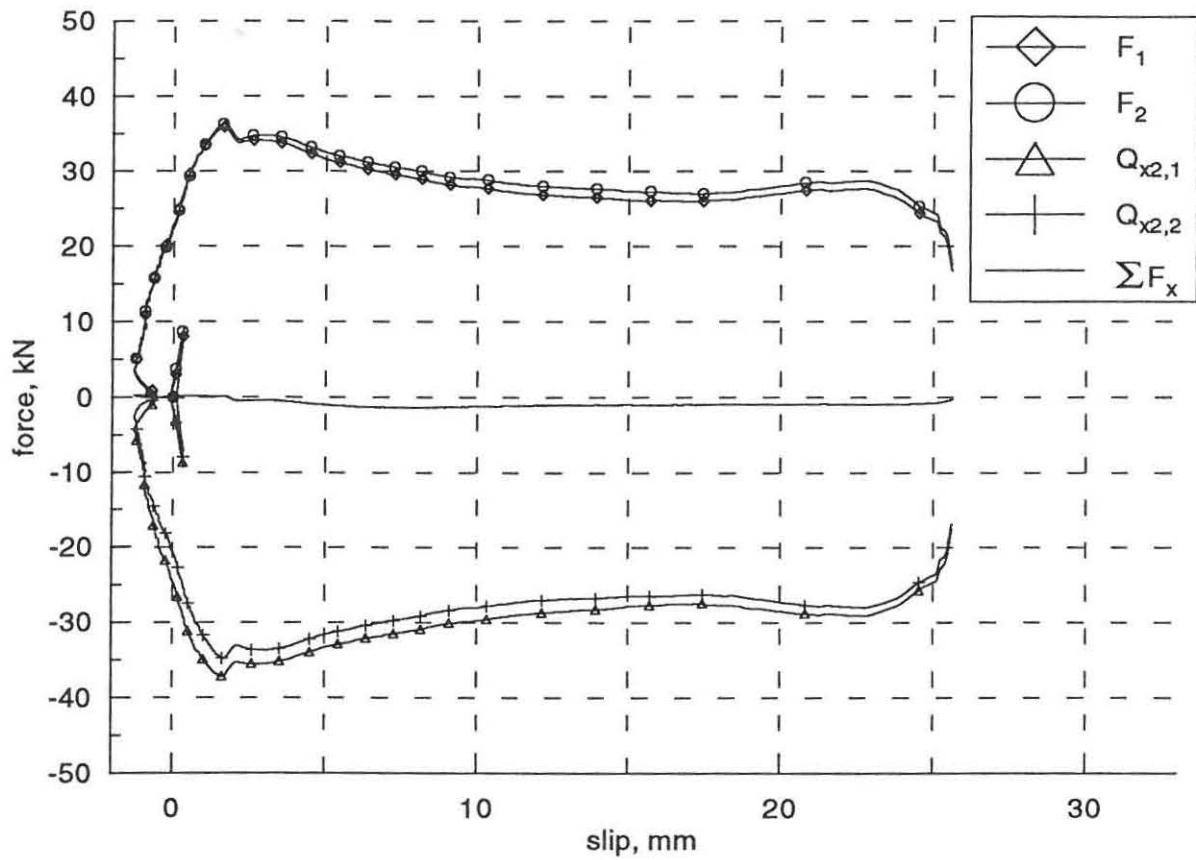
Forces in the x-direction.
specimen B2



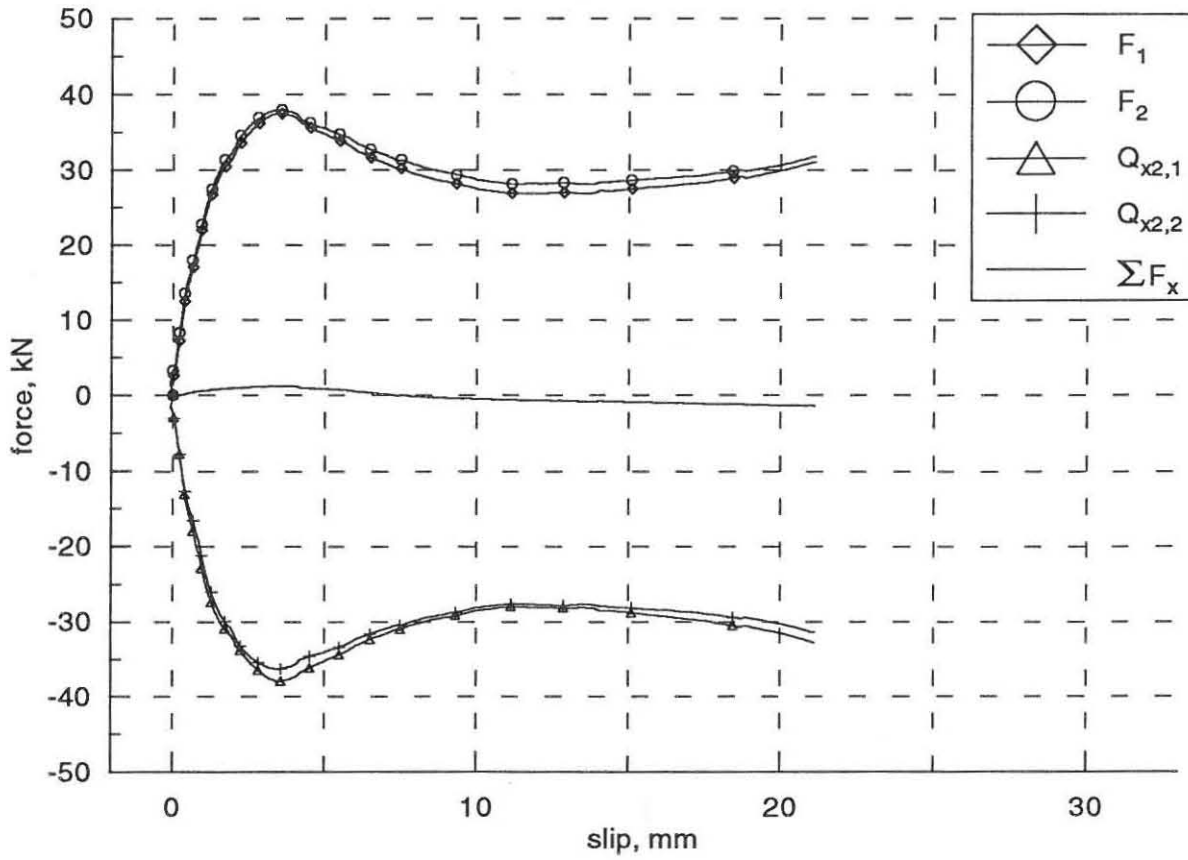
Forces in the x-direction.
specimen B3



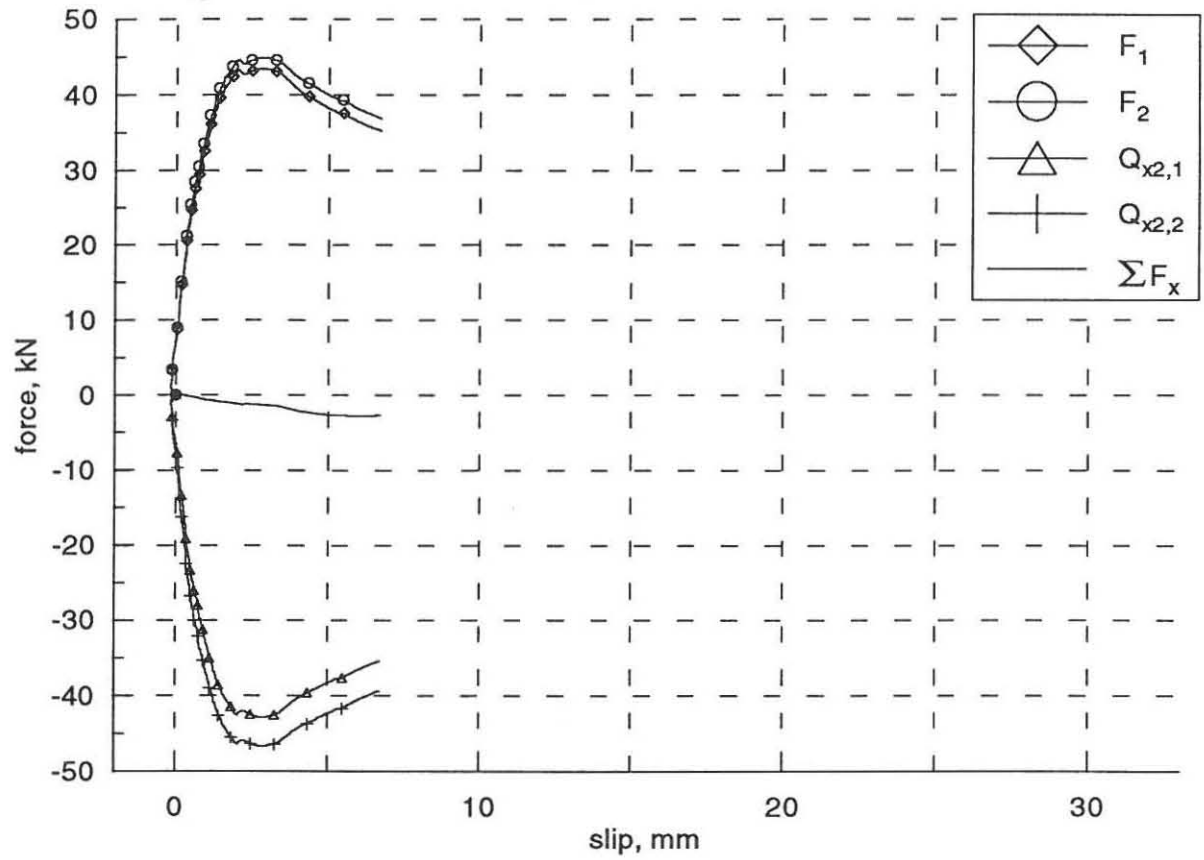
Forces in the x-direction.
specimen C1



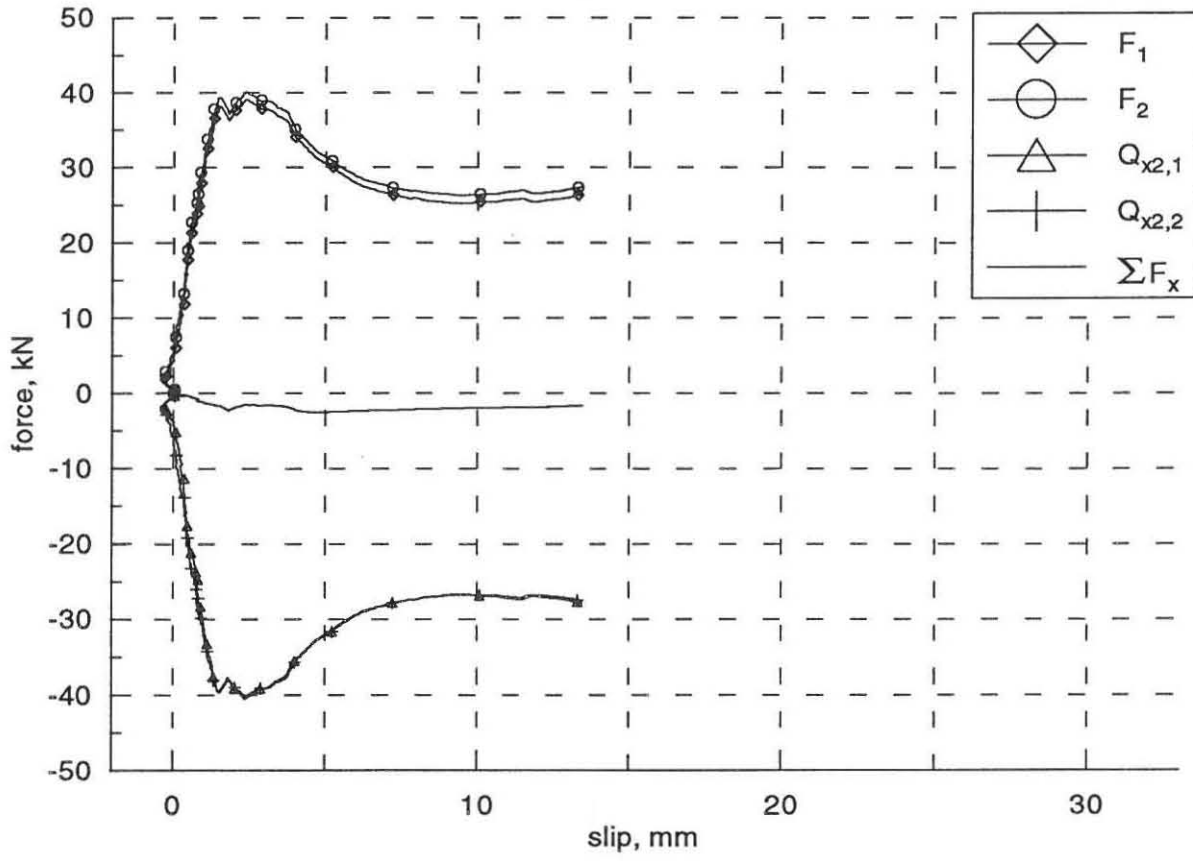
Forces in the x-direction.
specimen C2



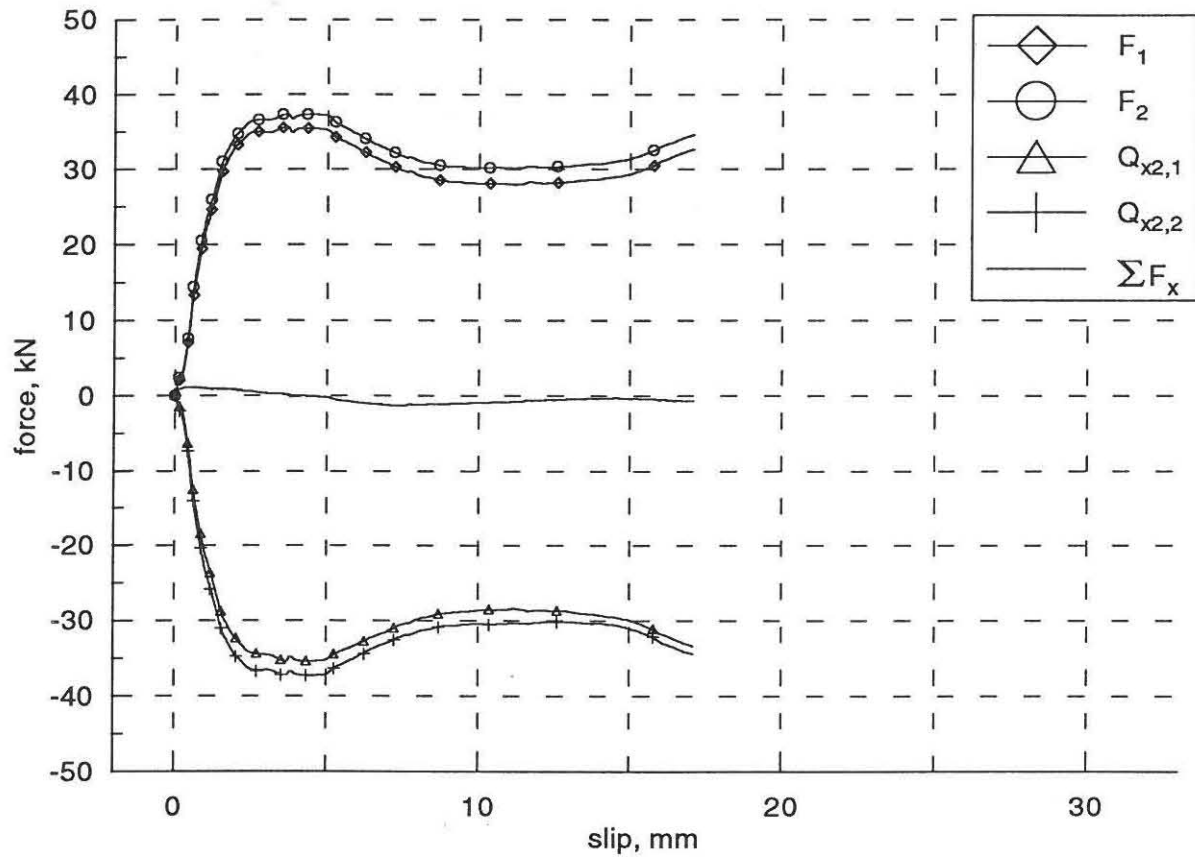
Forces in the x-direction.
specimen C3



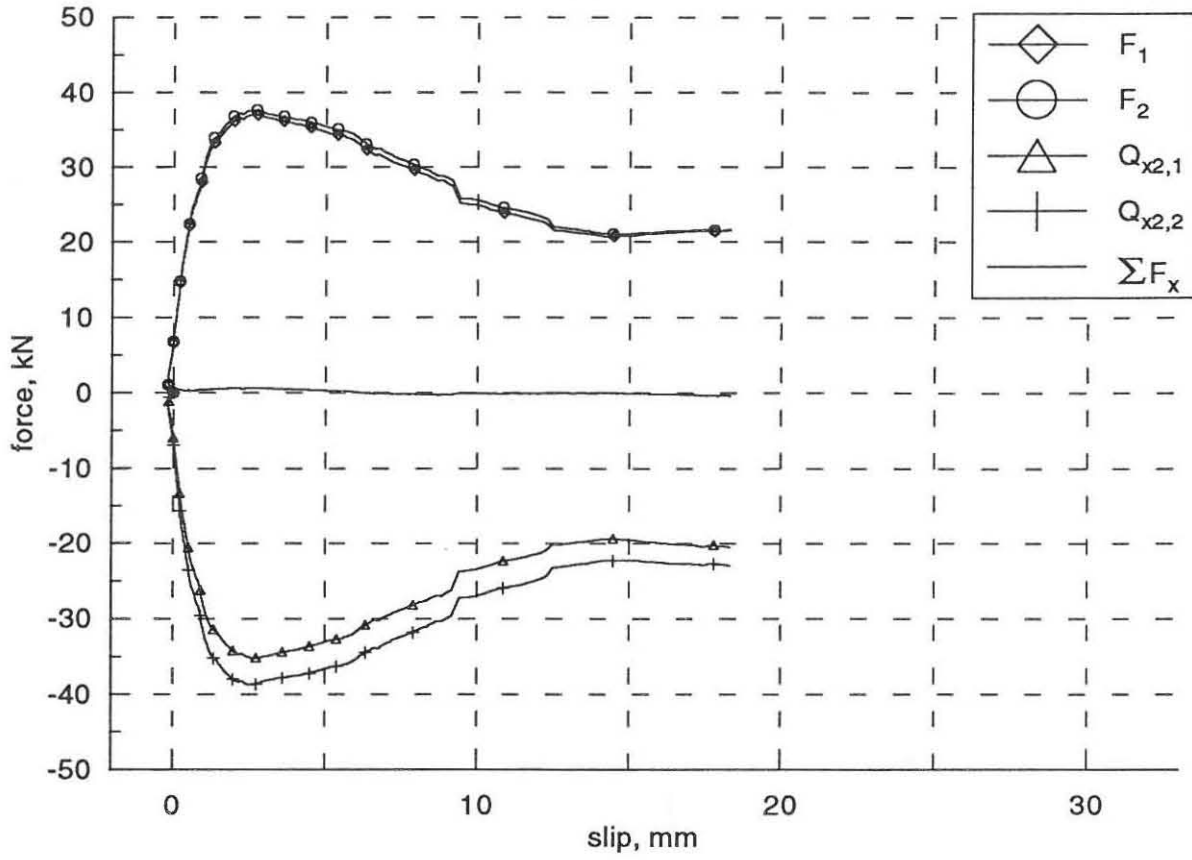
Forces in the x-direction.
specimen C4



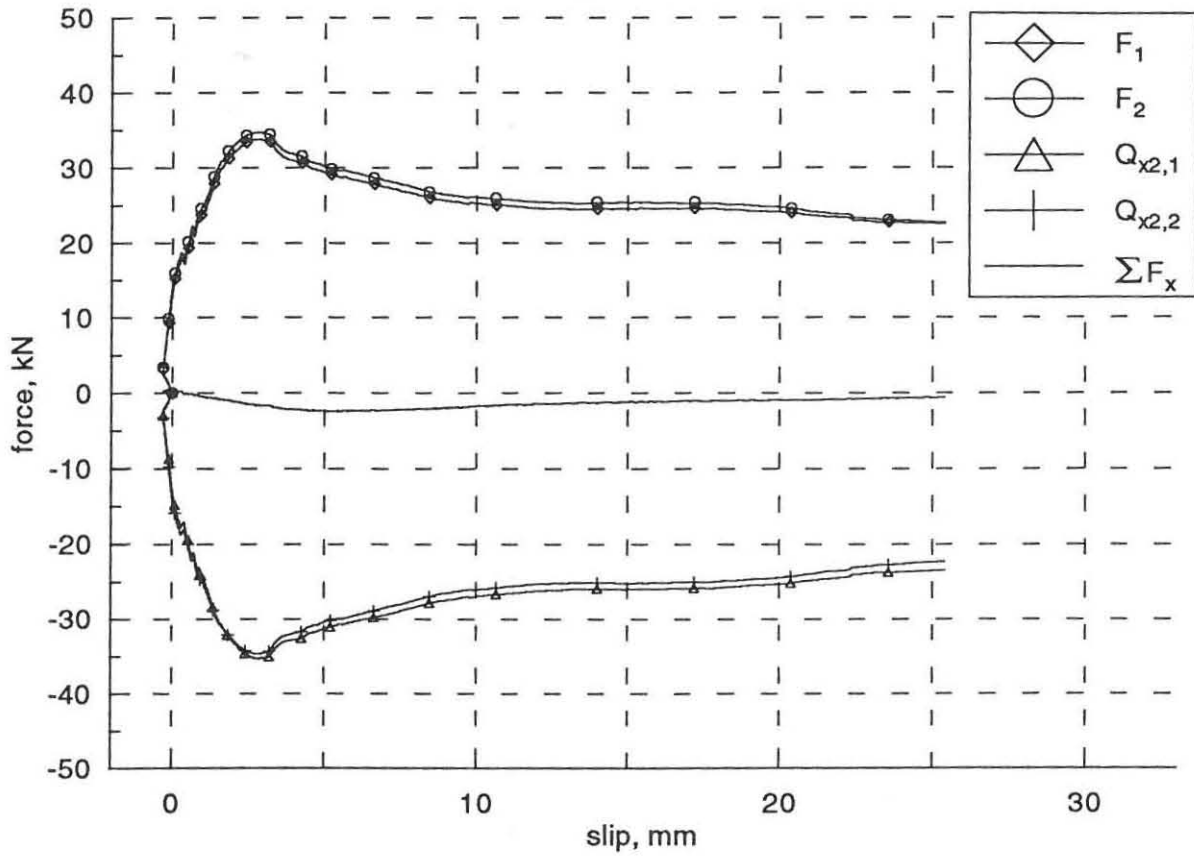
Forces in the x-direction.
specimen C5



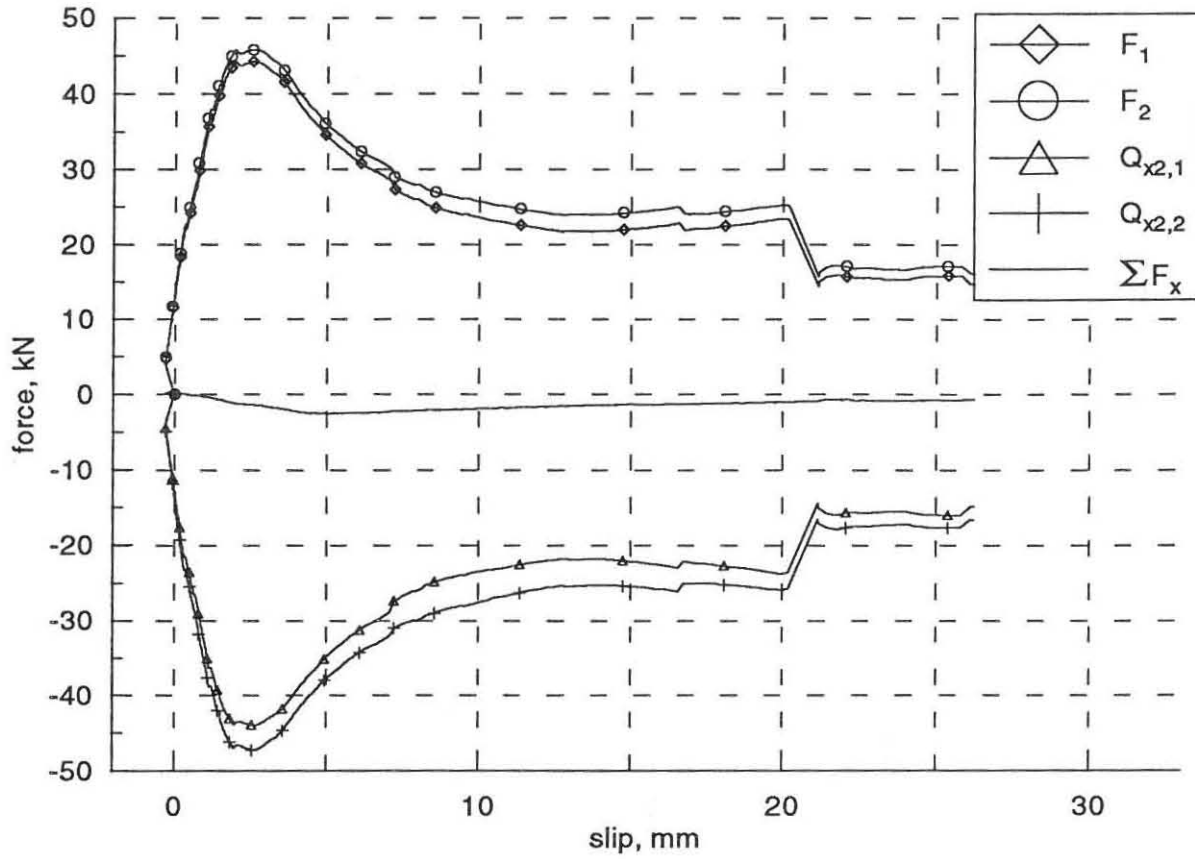
Forces in the x-direction.
specimen C6



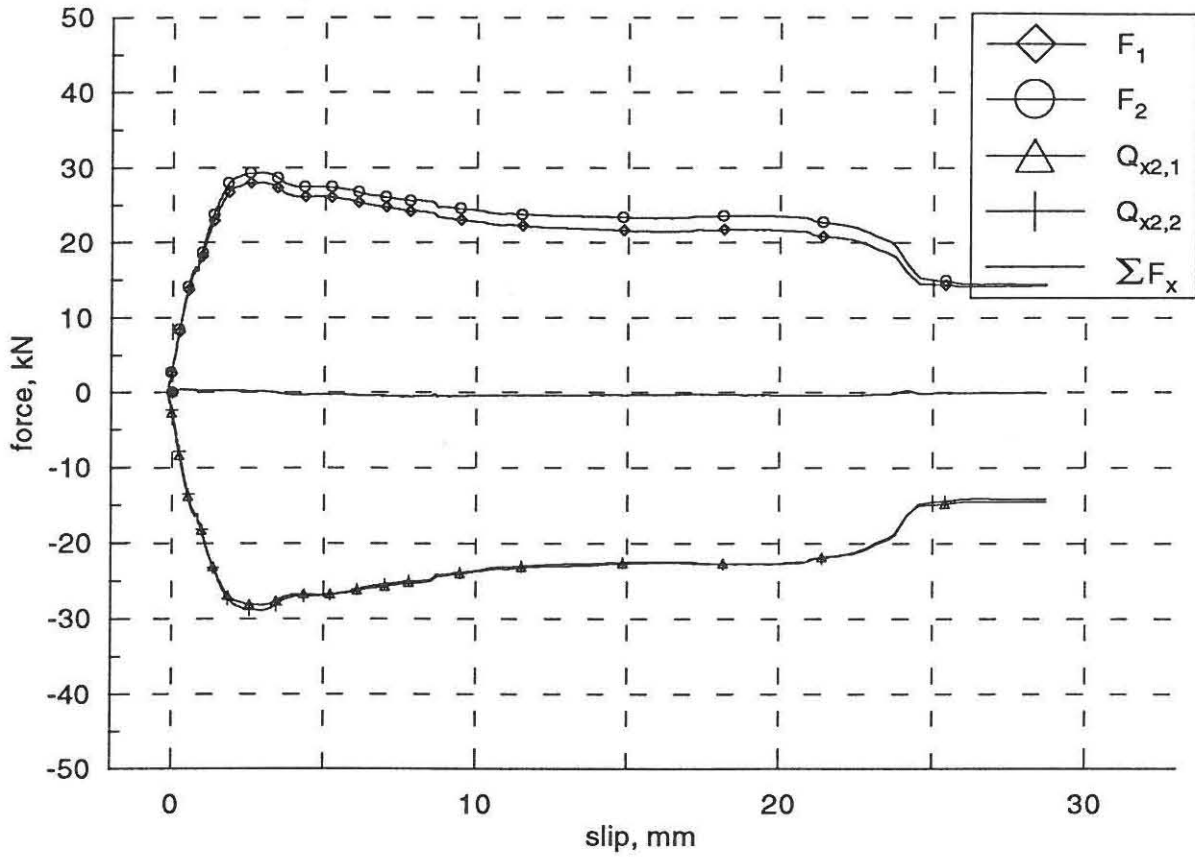
Forces in the x-direction.
specimen C7



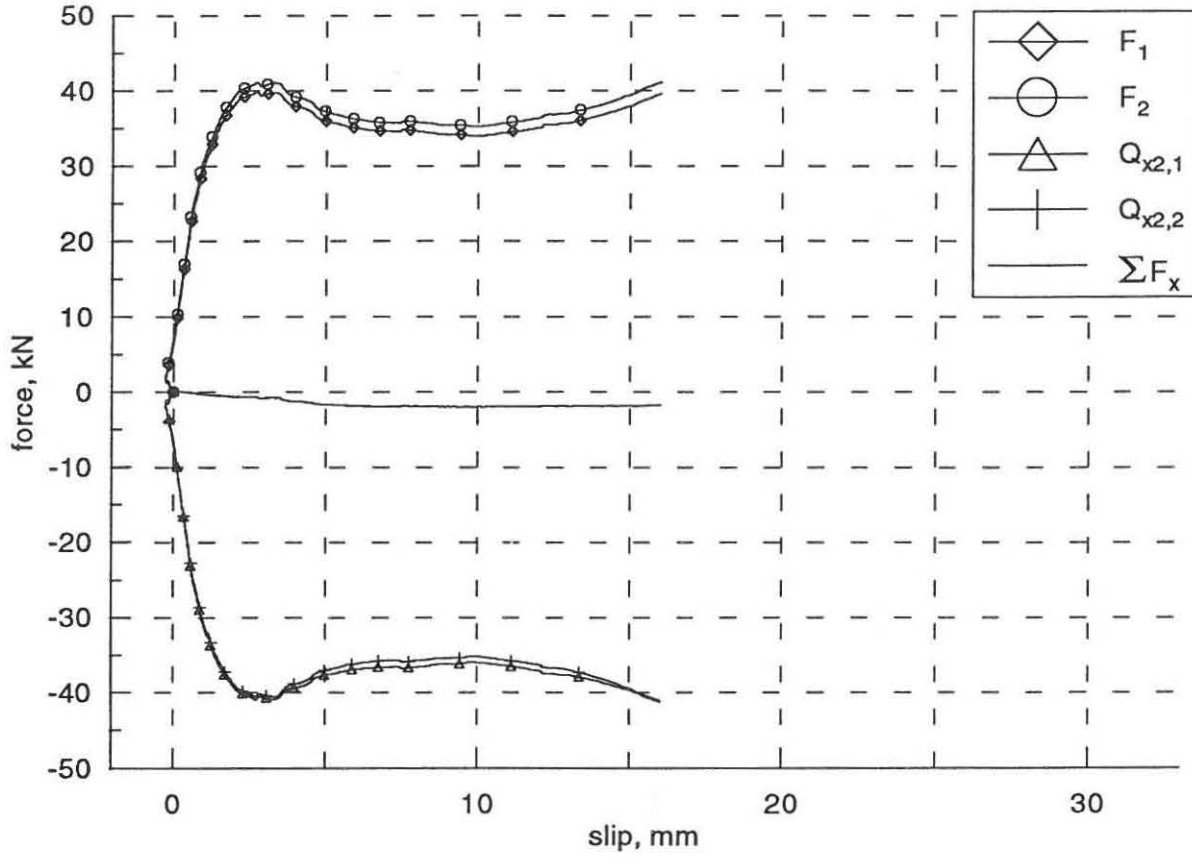
Forces in the x-direction.
specimen C8



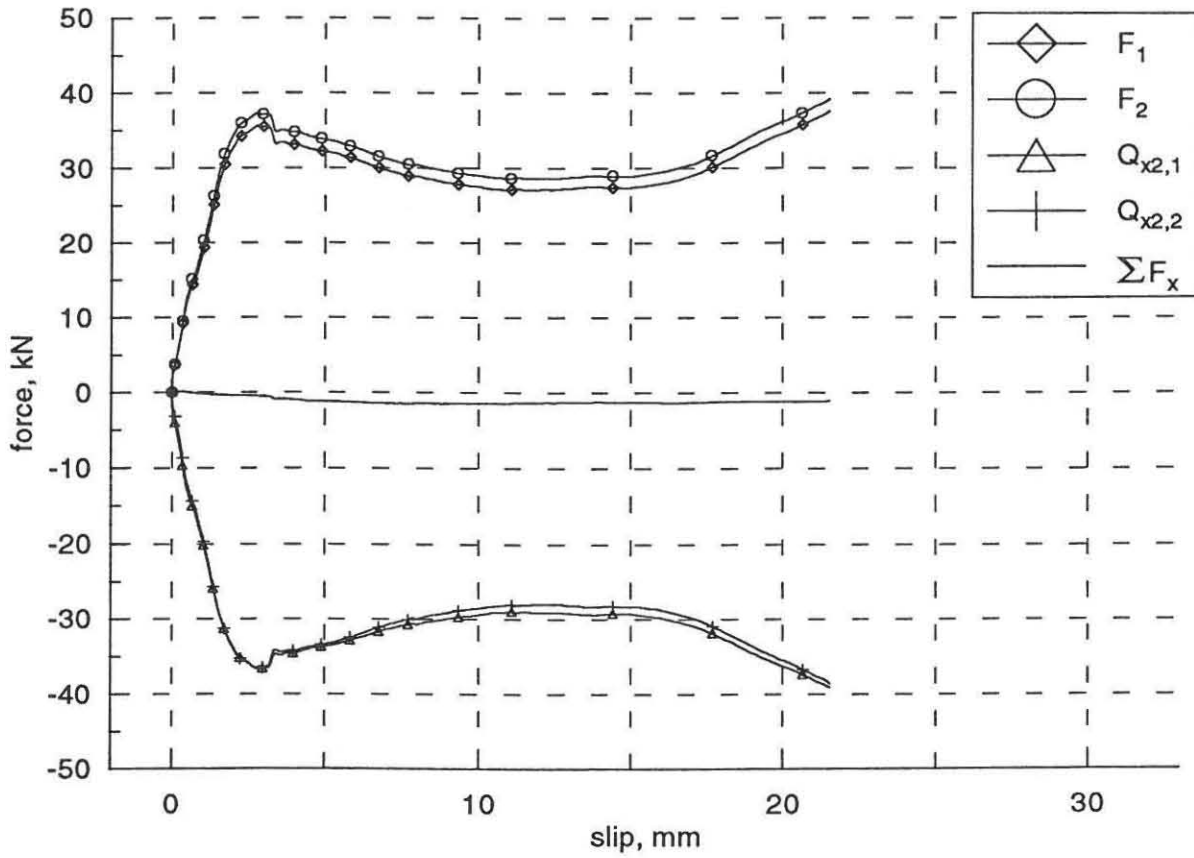
Forces in the x-direction.
specimen C9



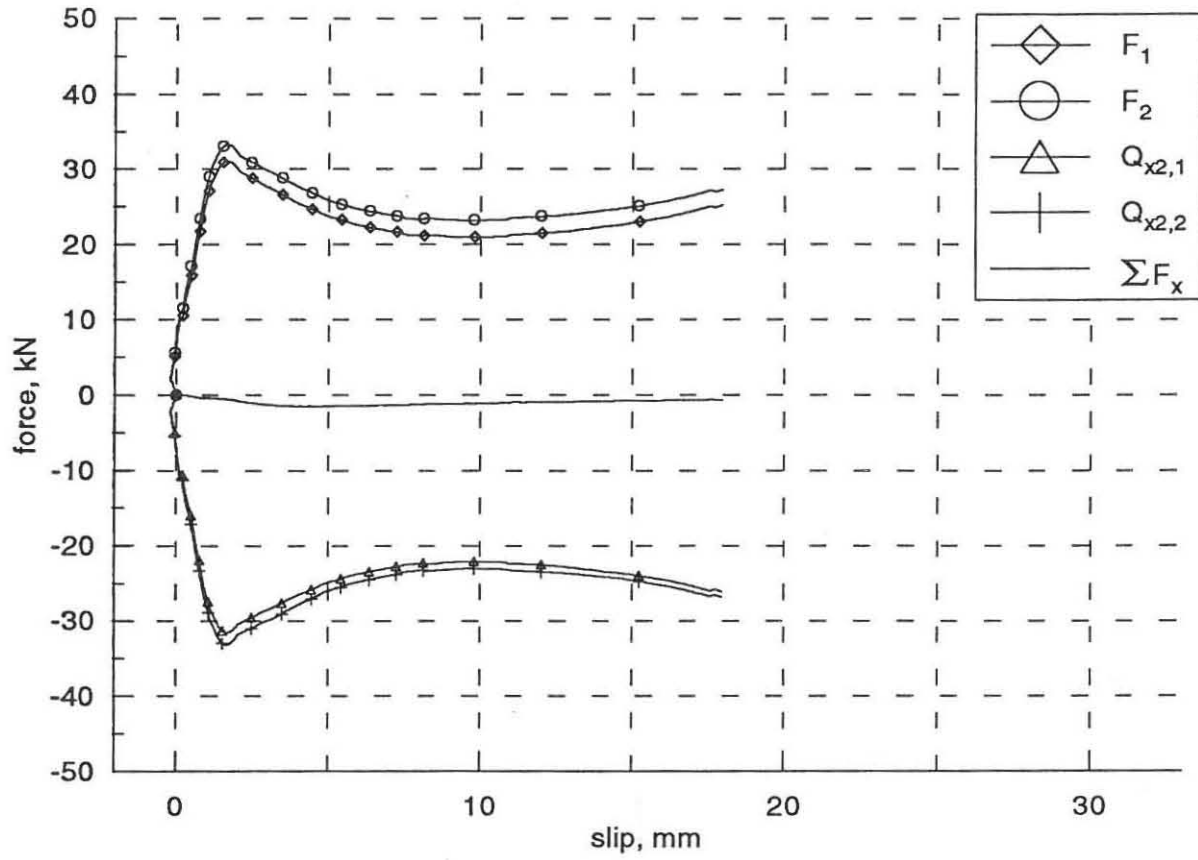
Forces in the x-direction.
specimen C10



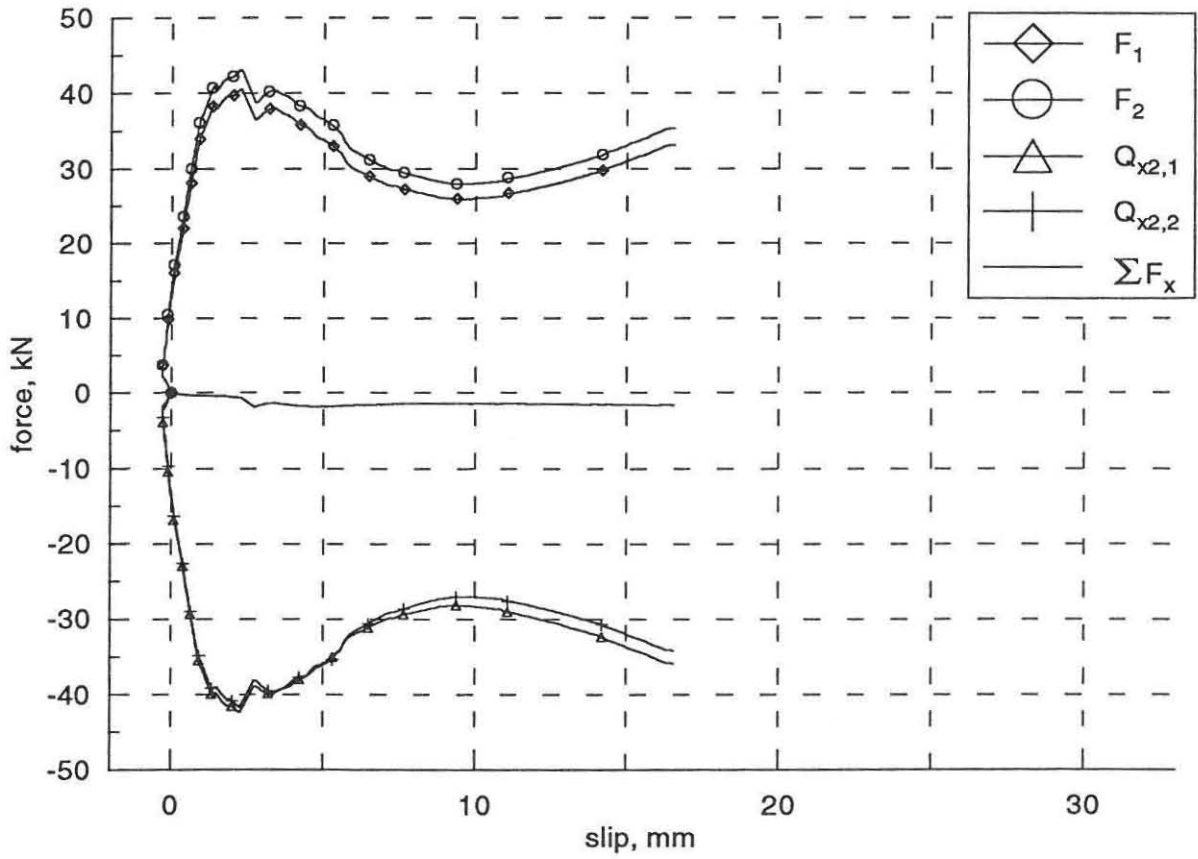
Forces in the x-direction.
specimen C11



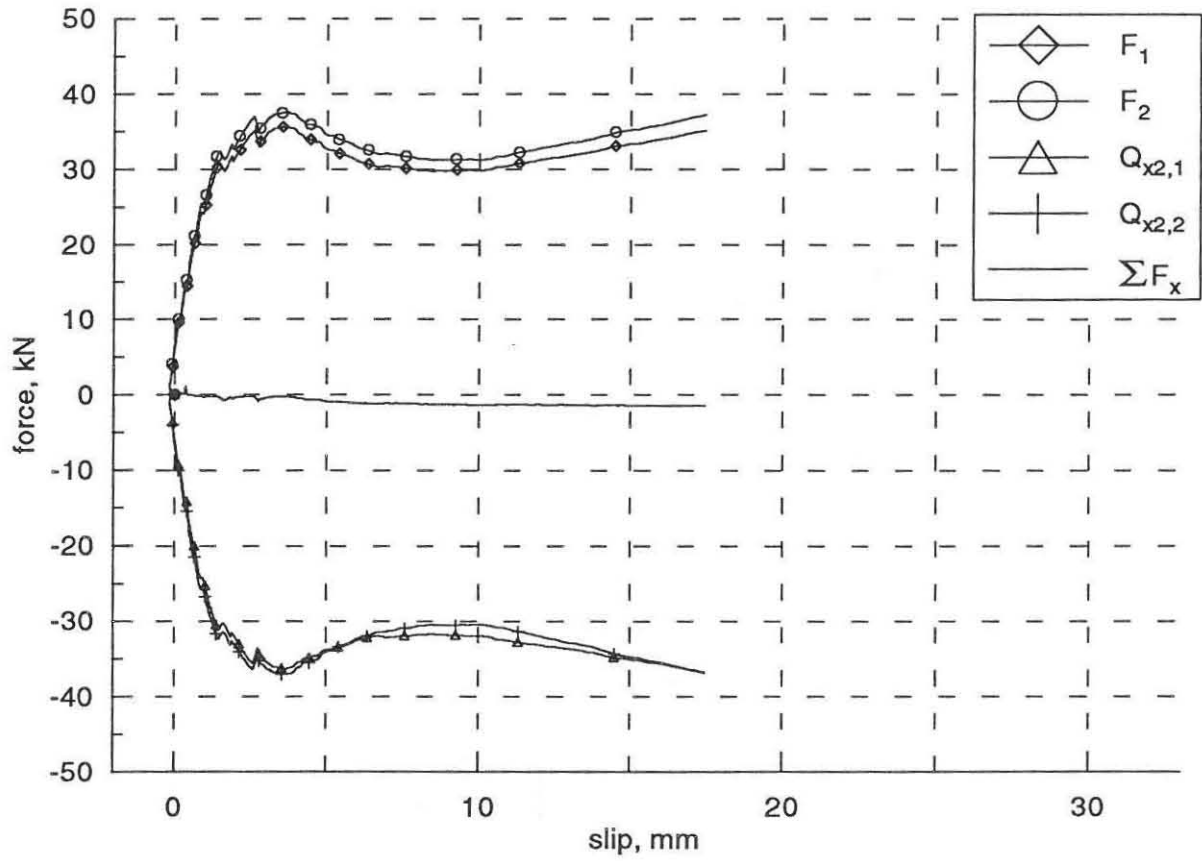
Forces in the x-direction.
specimen C12



Forces in the x-direction.
specimen C13

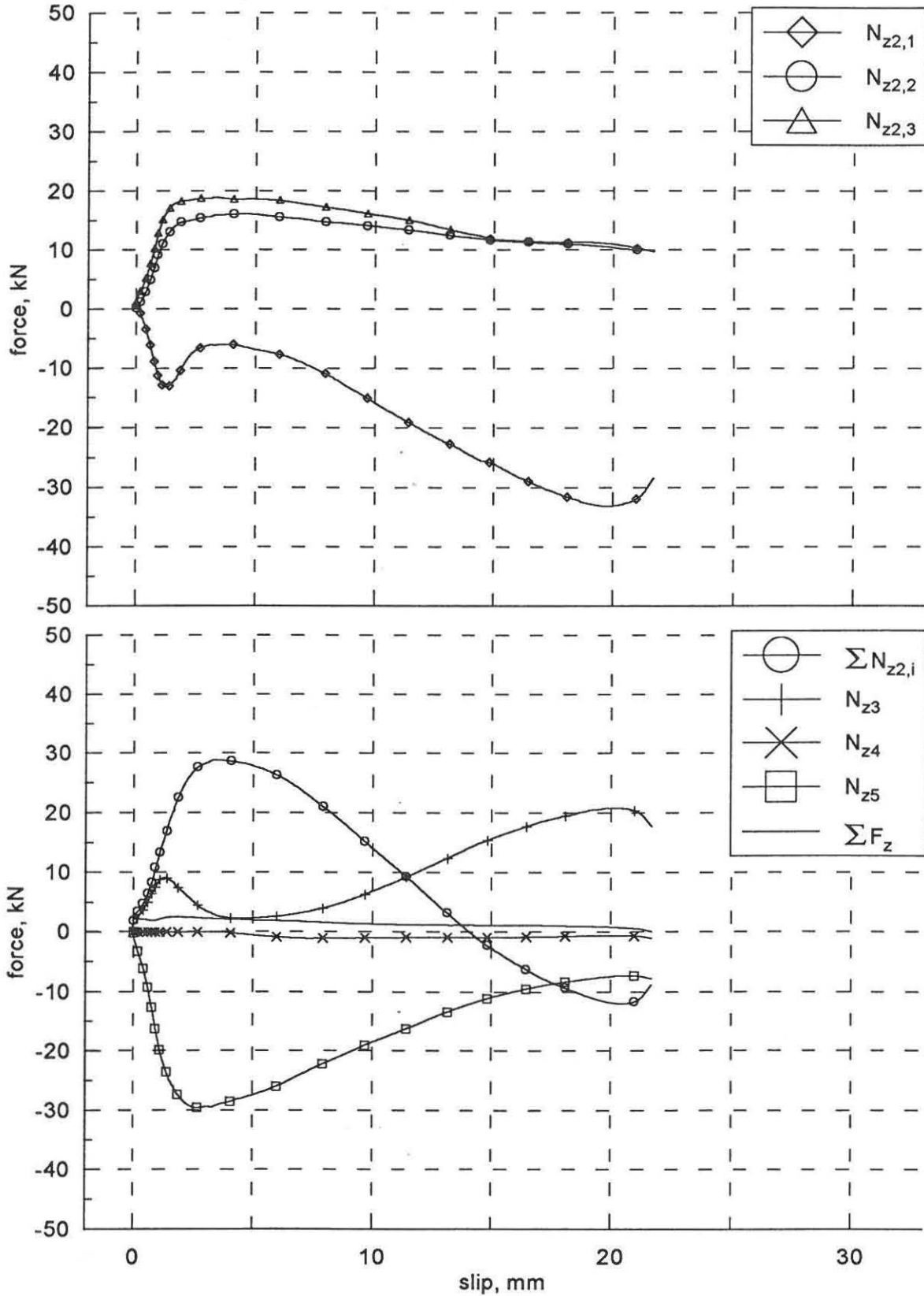


Forces in the x-direction.
specimen C14

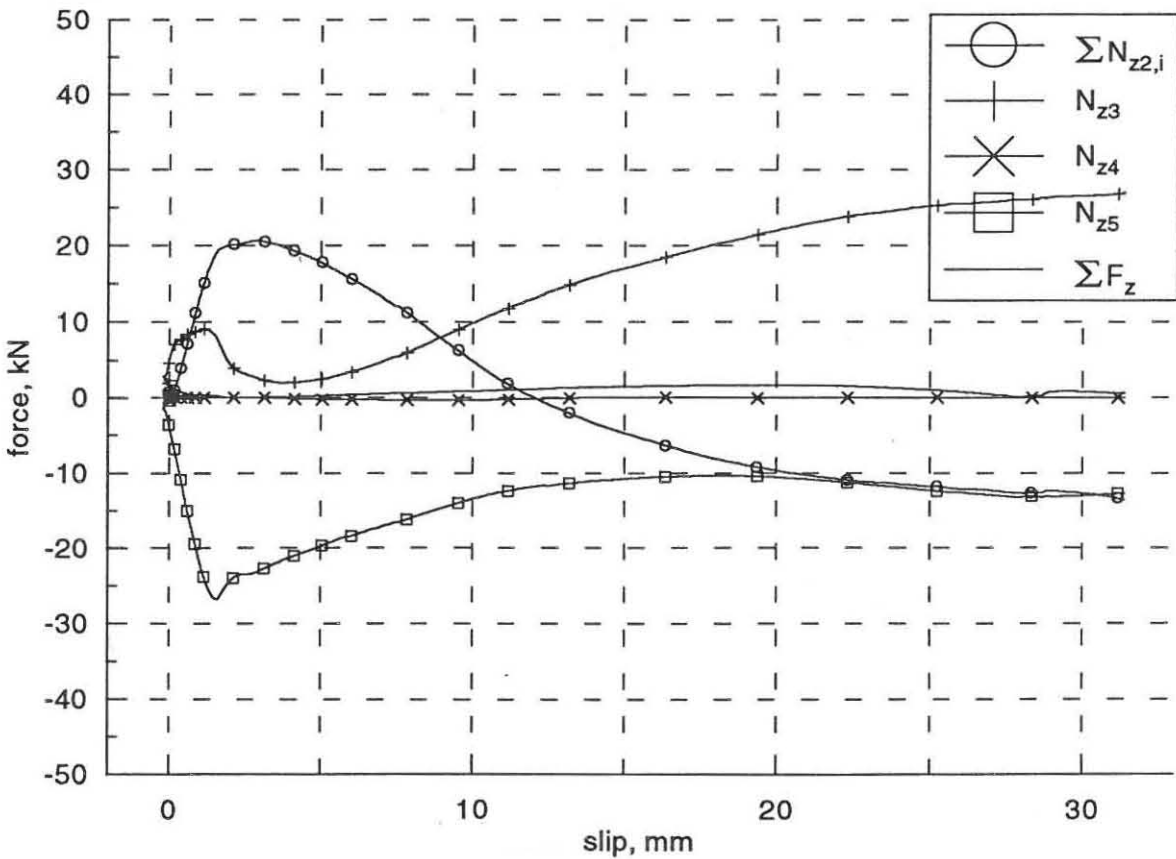
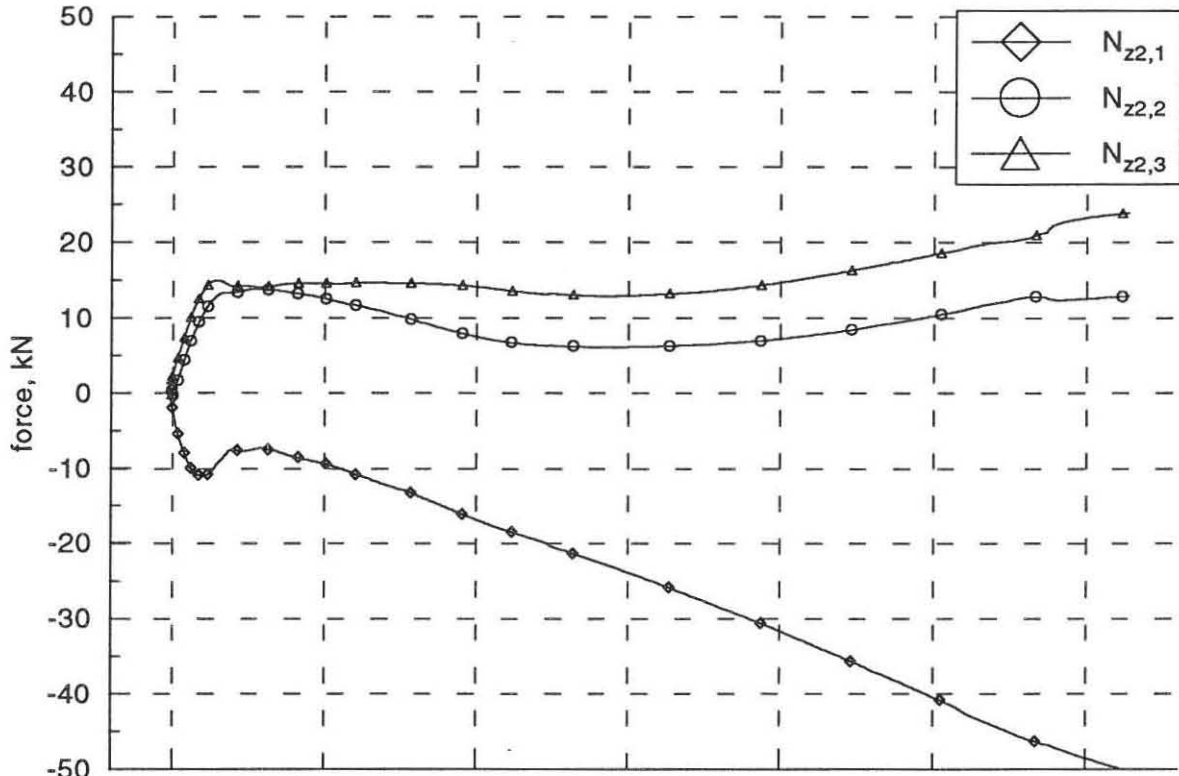


11.3 Forces in the z-direction: $N_{z2,1}$, $N_{z2,2}$, $N_{z2,3}$ and $\Sigma N_{z2,i}$, N_{z3} , N_{z4} , N_{z5} & ΣF_z

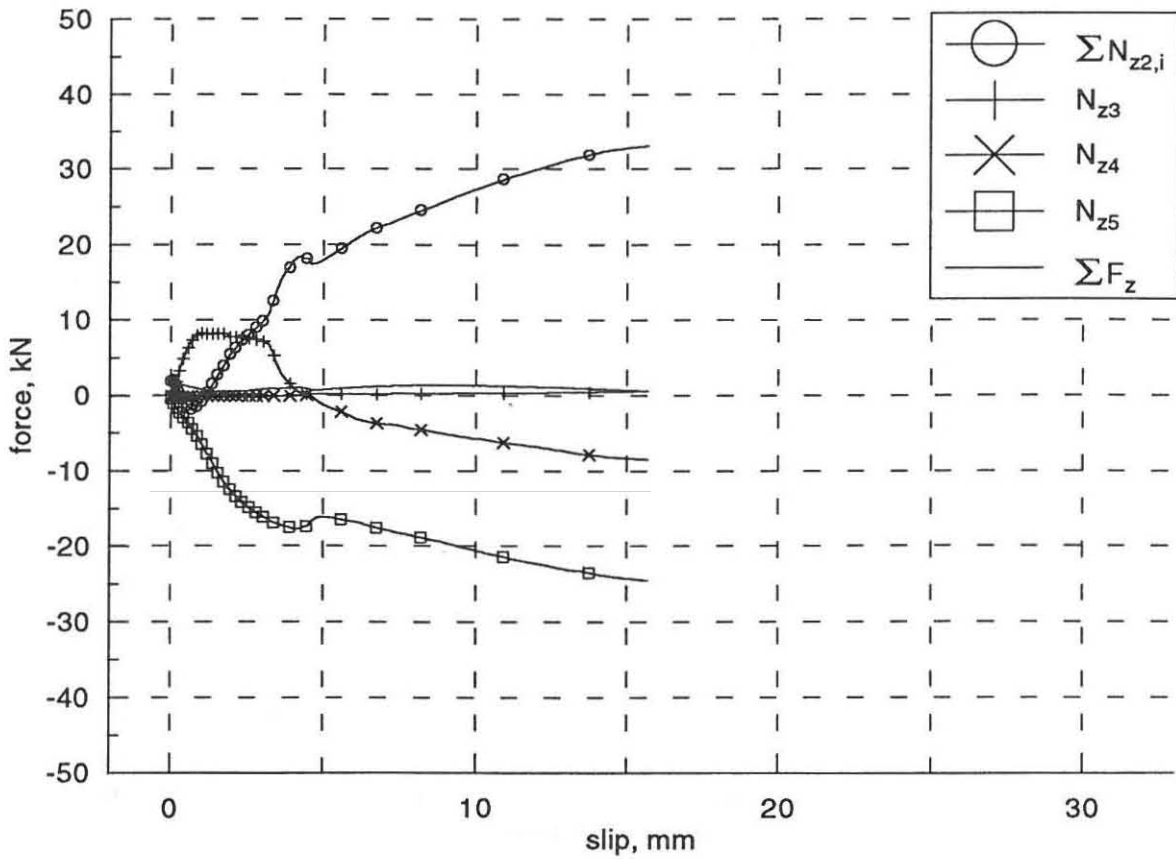
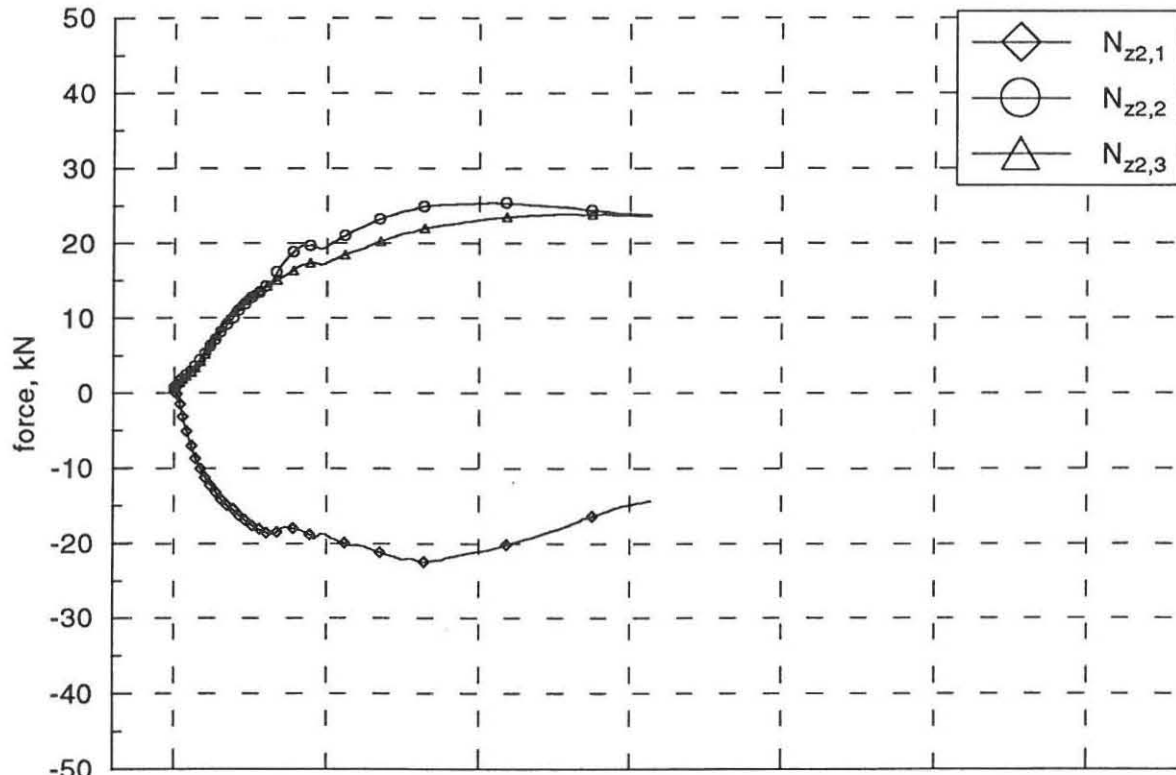
Forces in the z-direction.
specimen 2



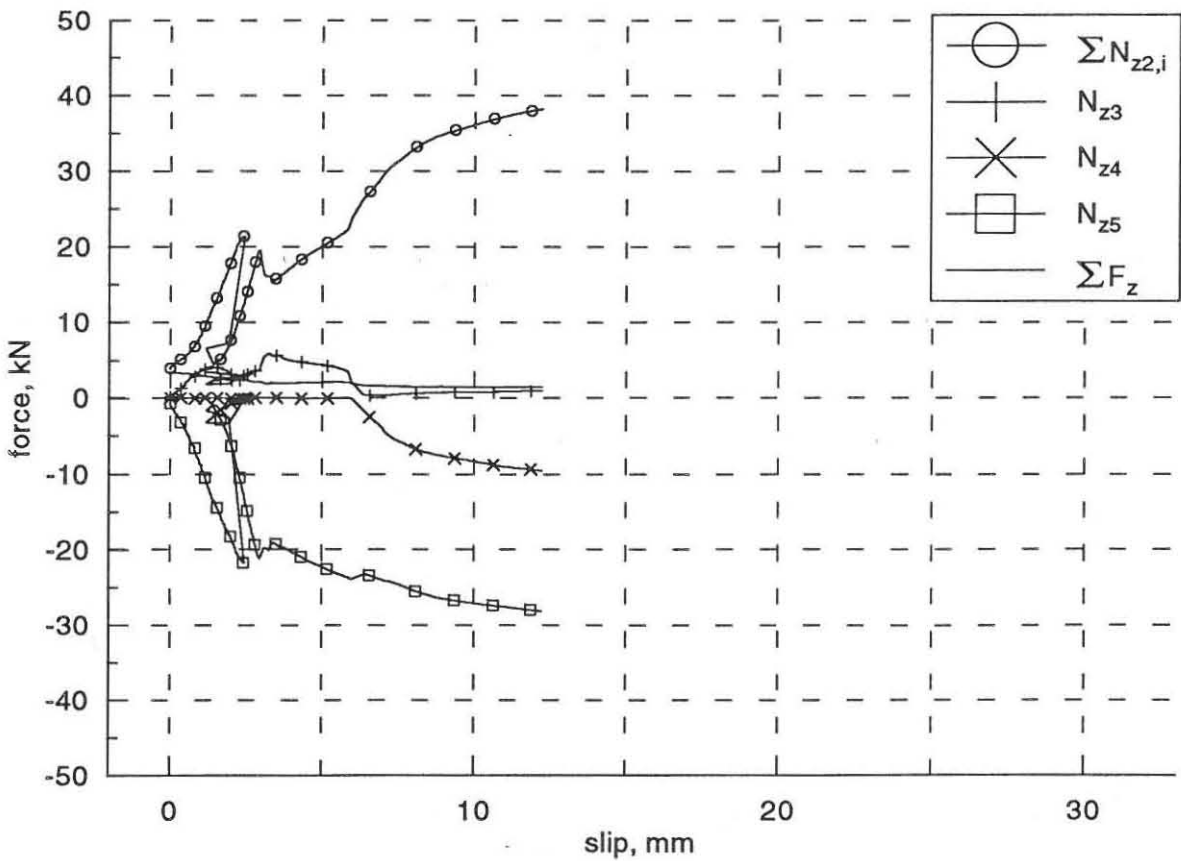
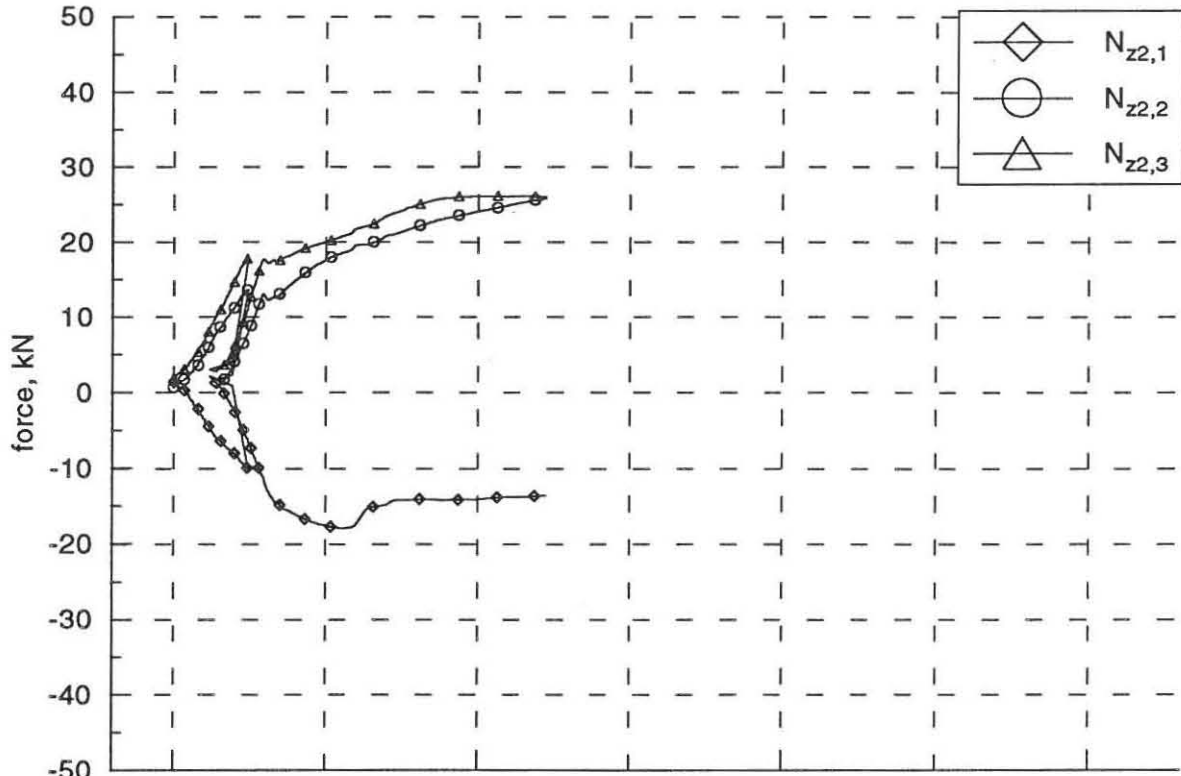
Forces in the z-direction.
specimen 3



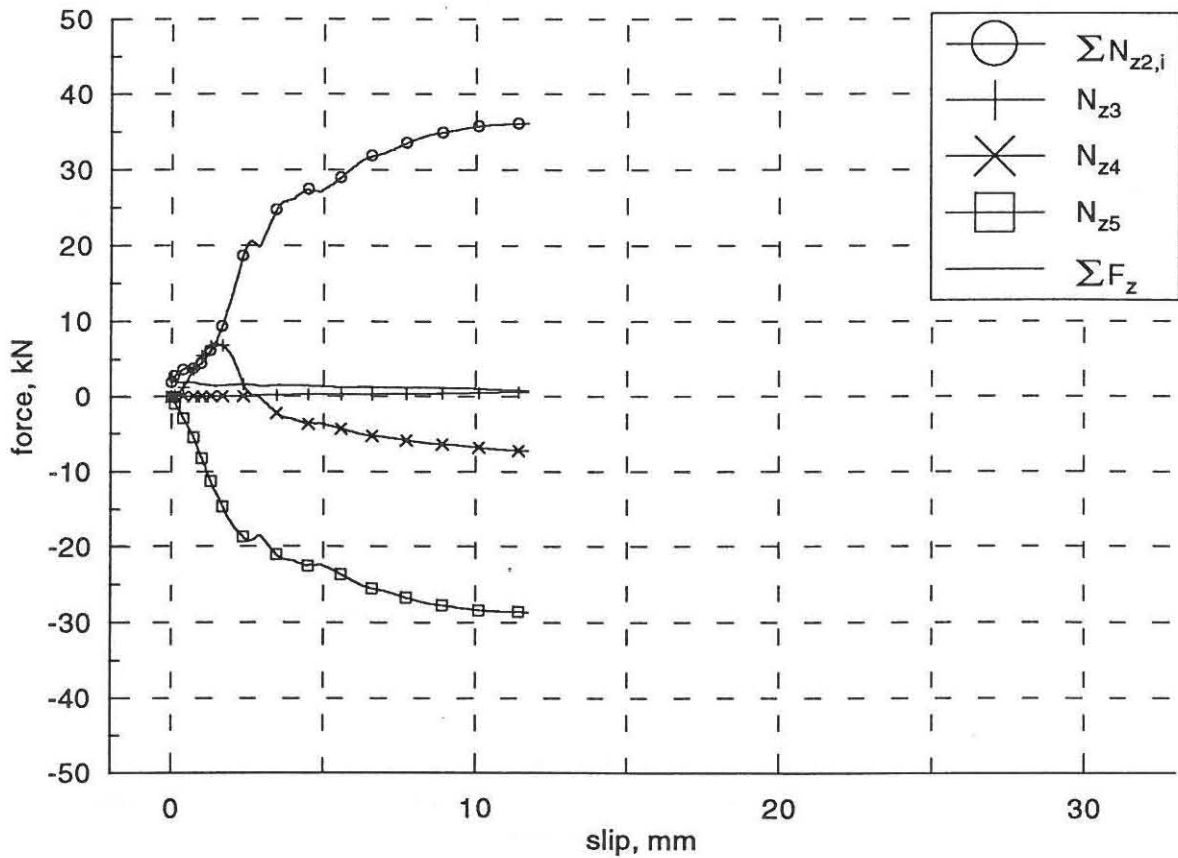
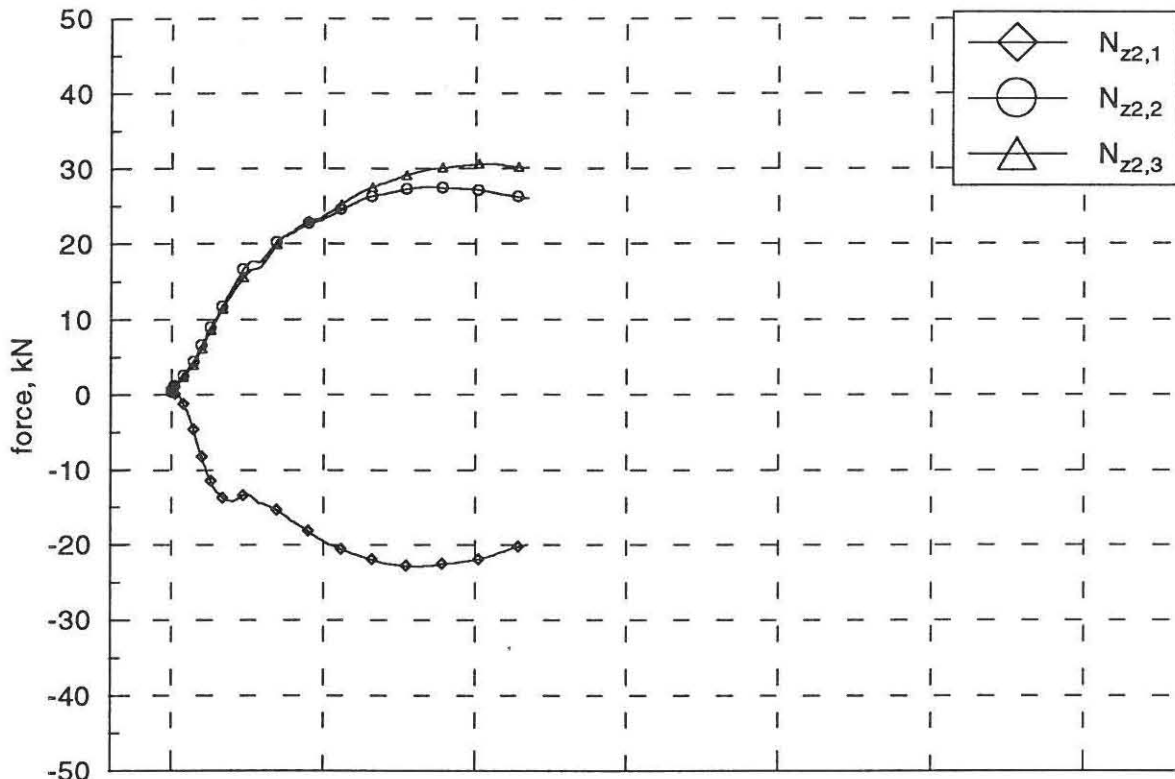
Fores in the z-direction.
specimen A1



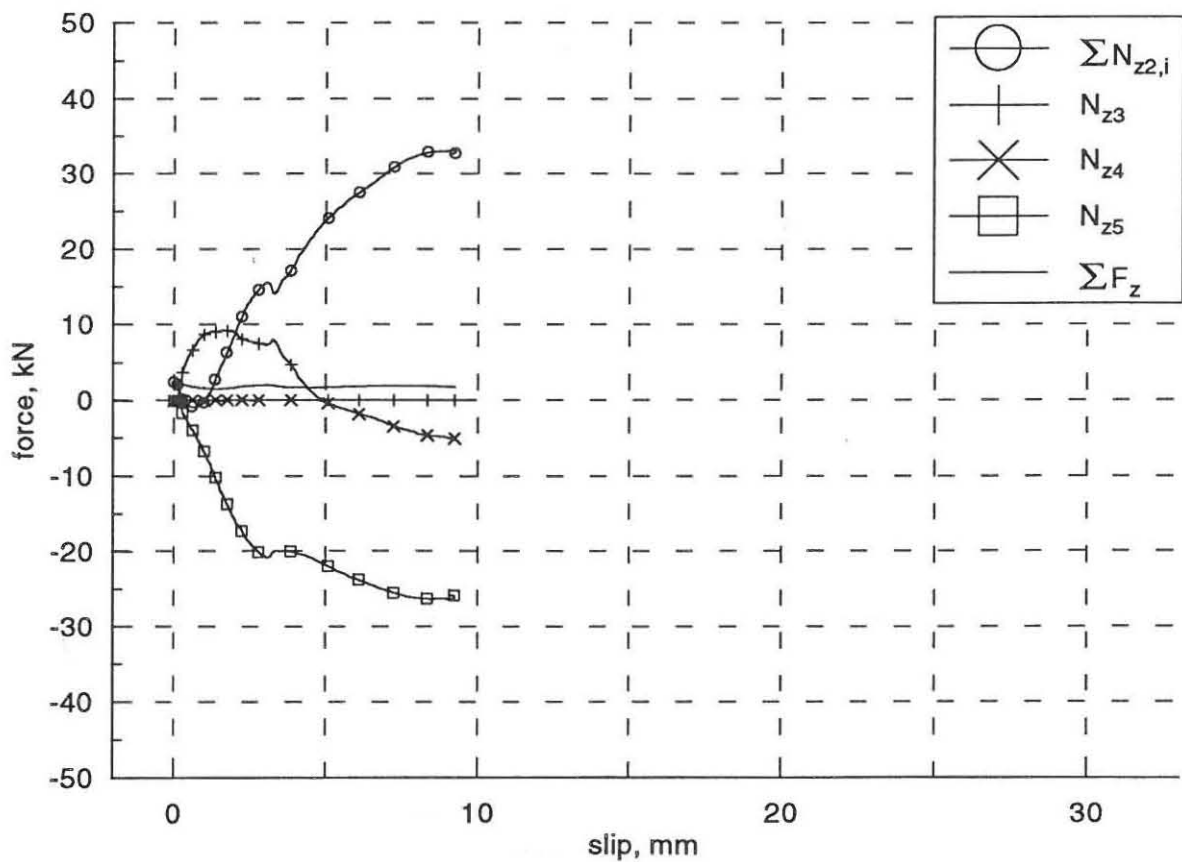
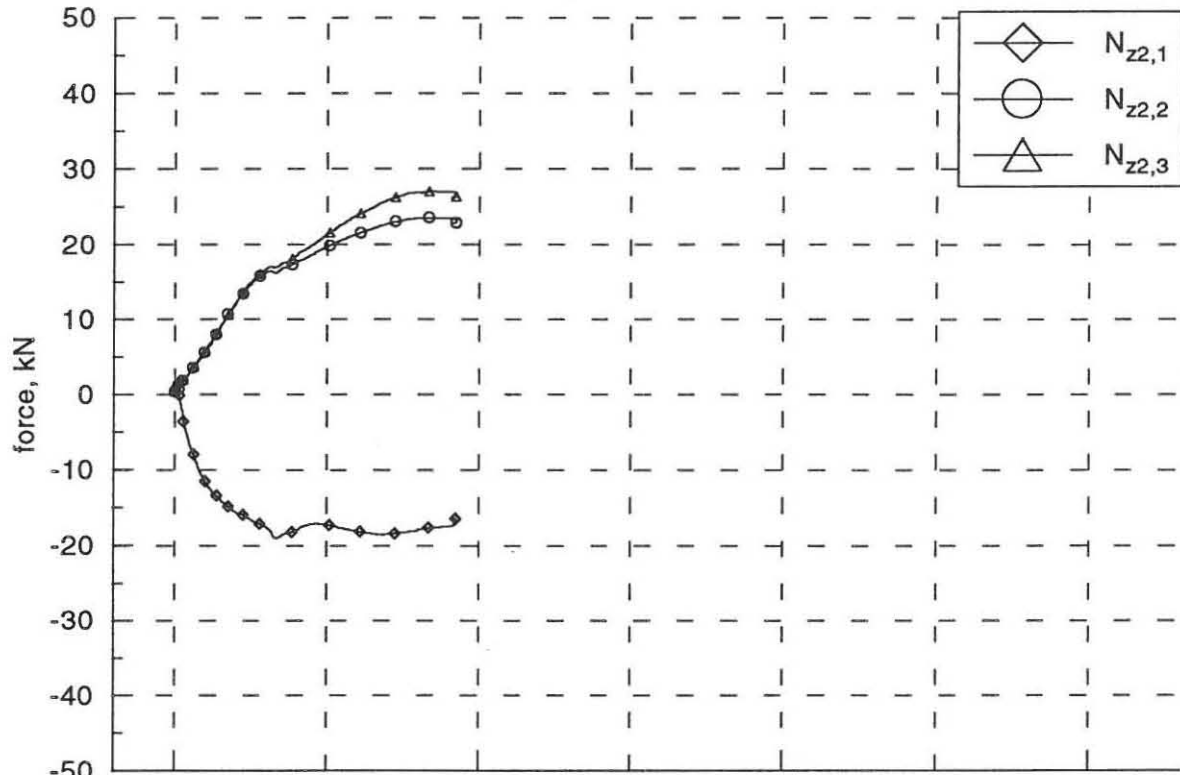
Forces in the z-direction.
specimen A2



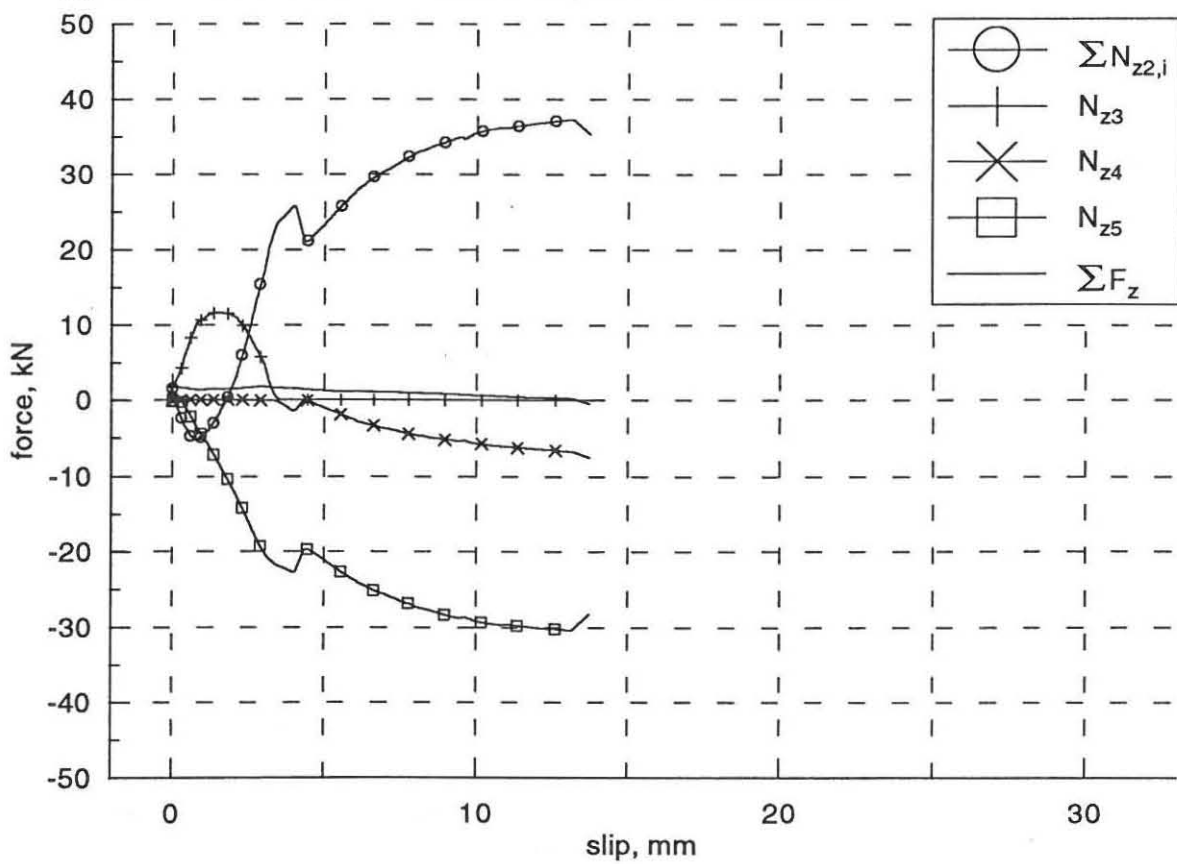
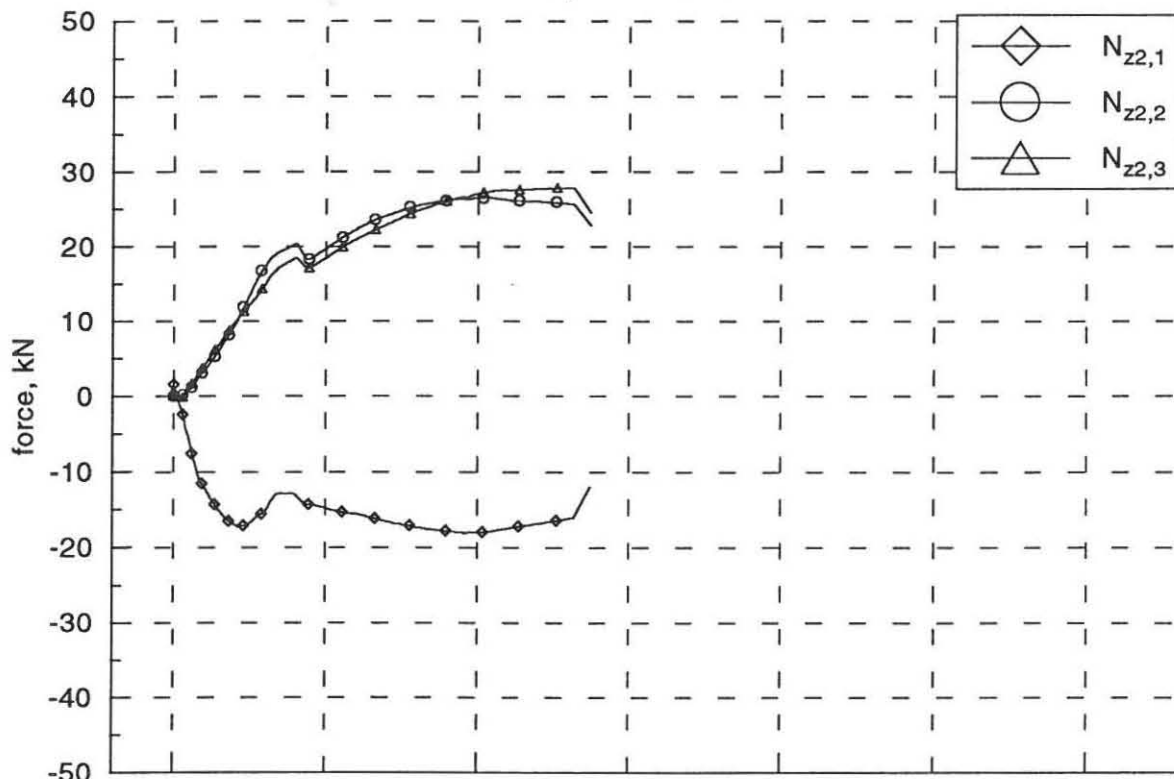
Forces in the z-direction.
specimen A3



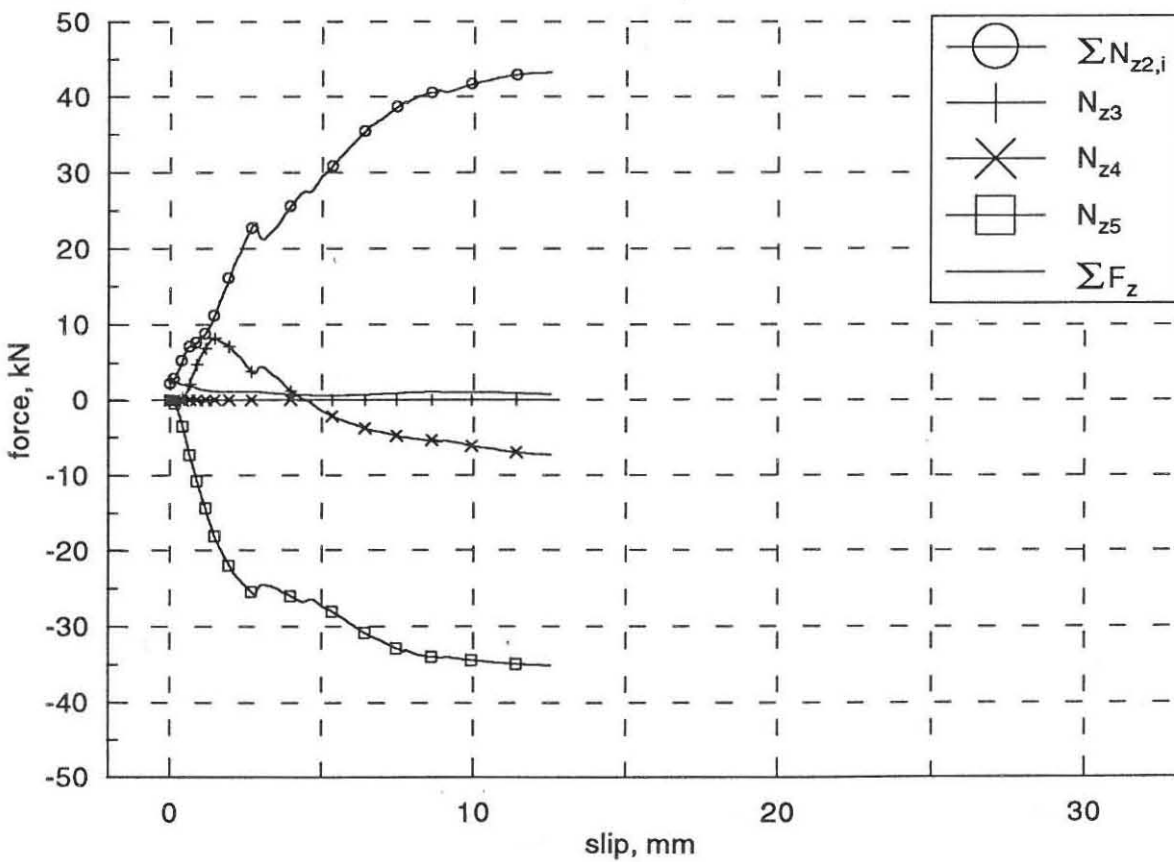
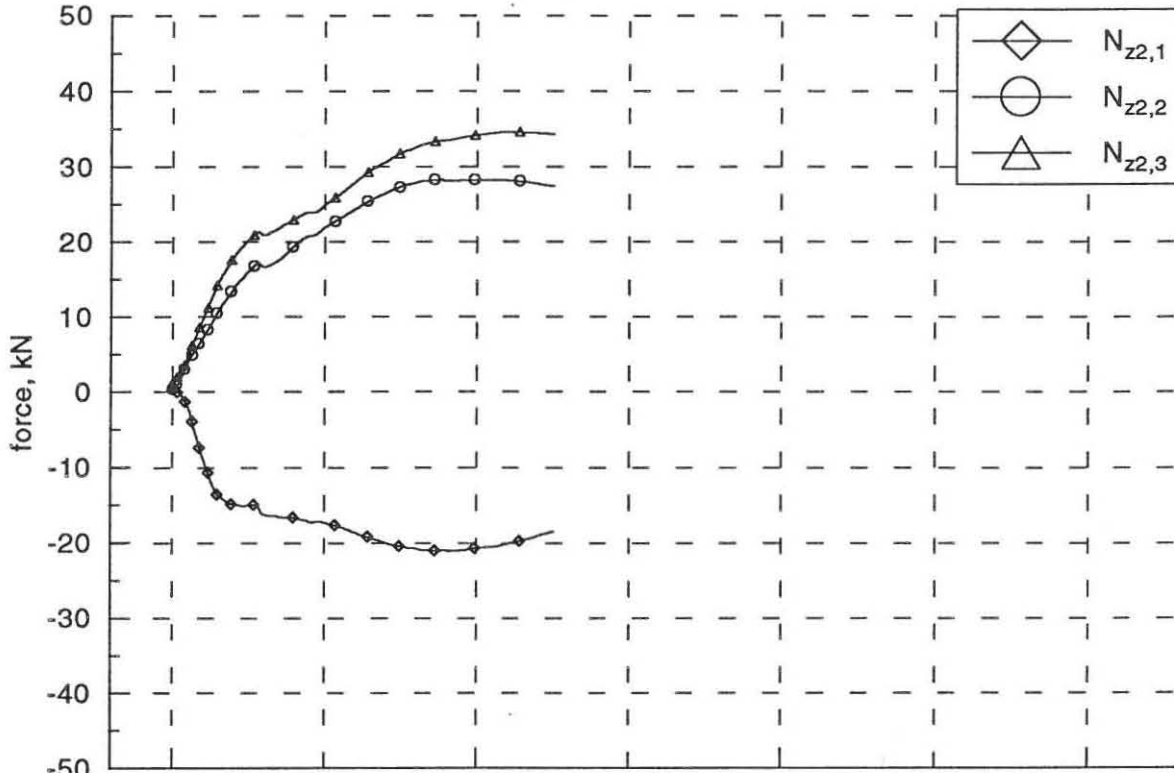
Forces in the z-direction.
specimen B1



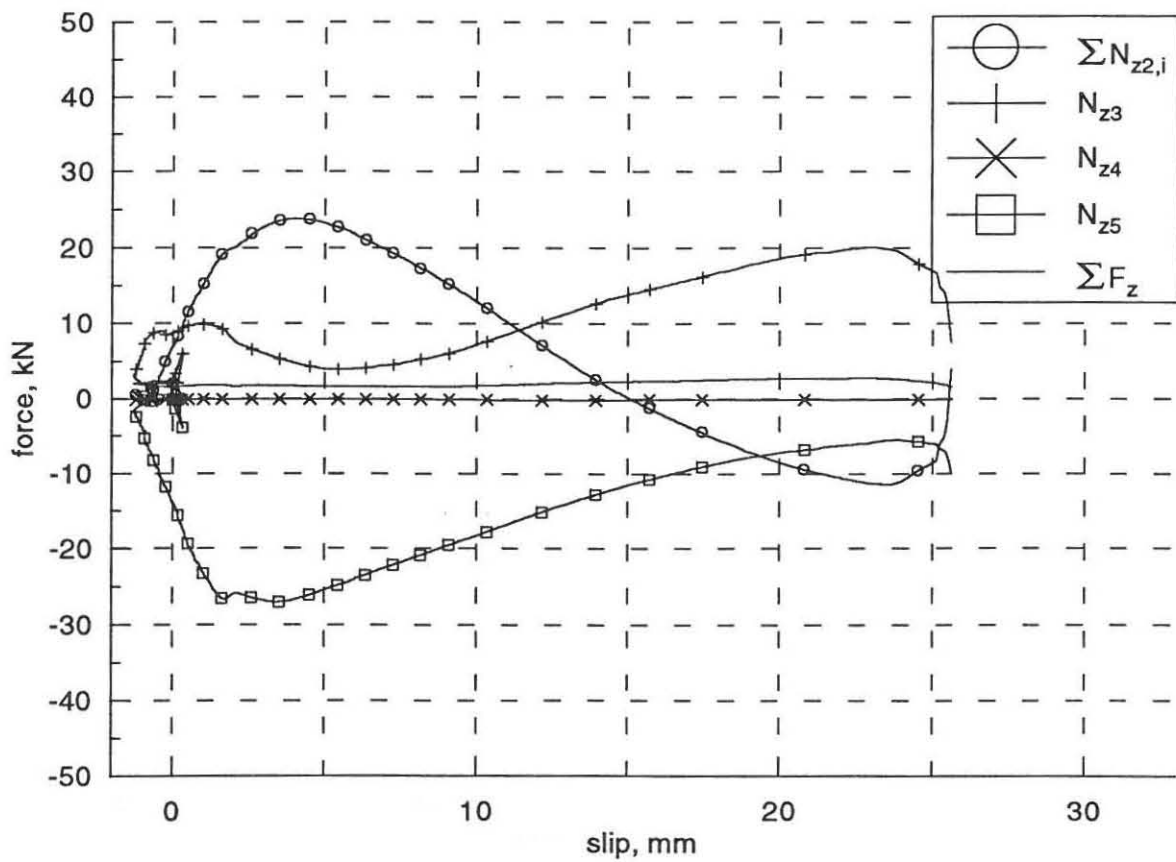
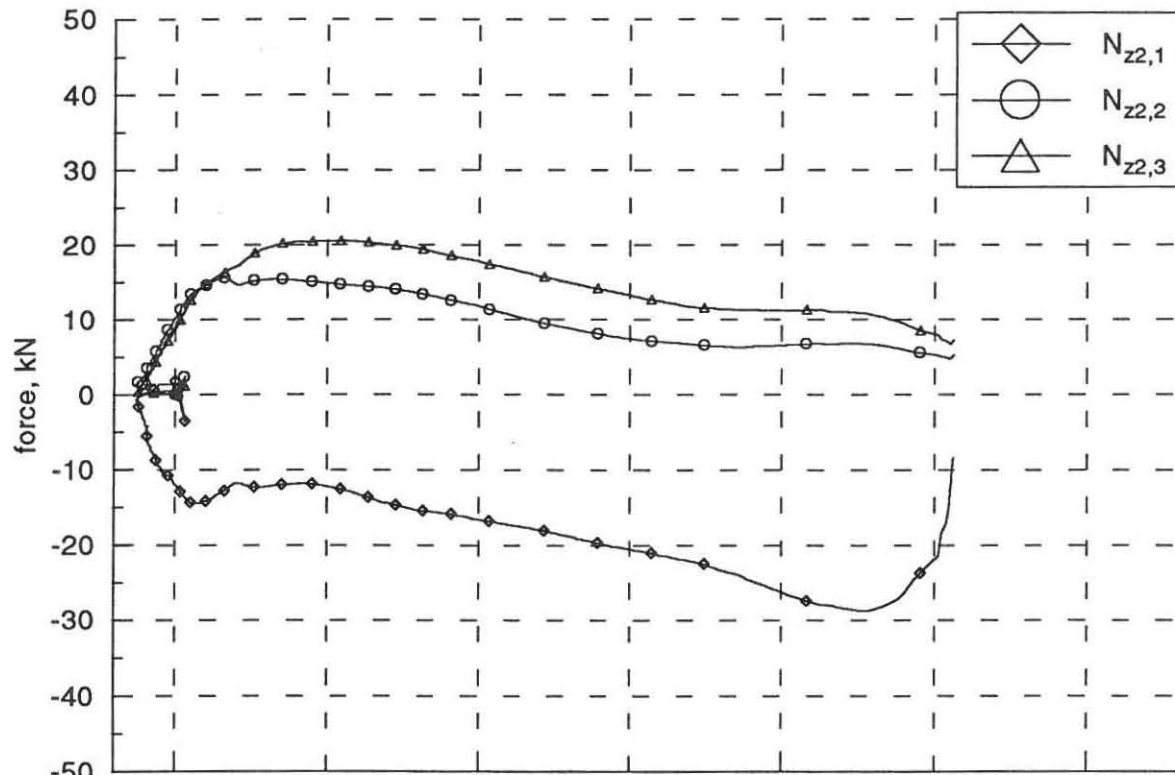
Forces in the z-direction.
specimen B2



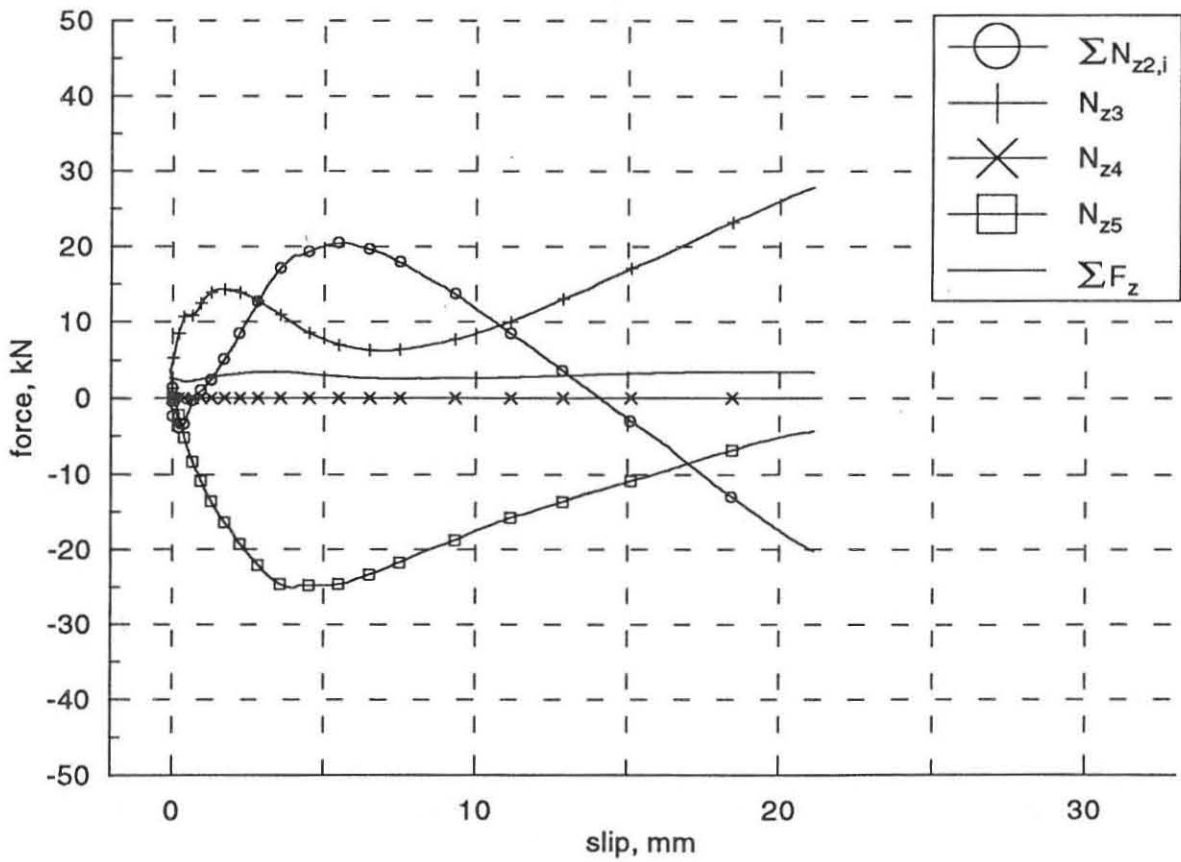
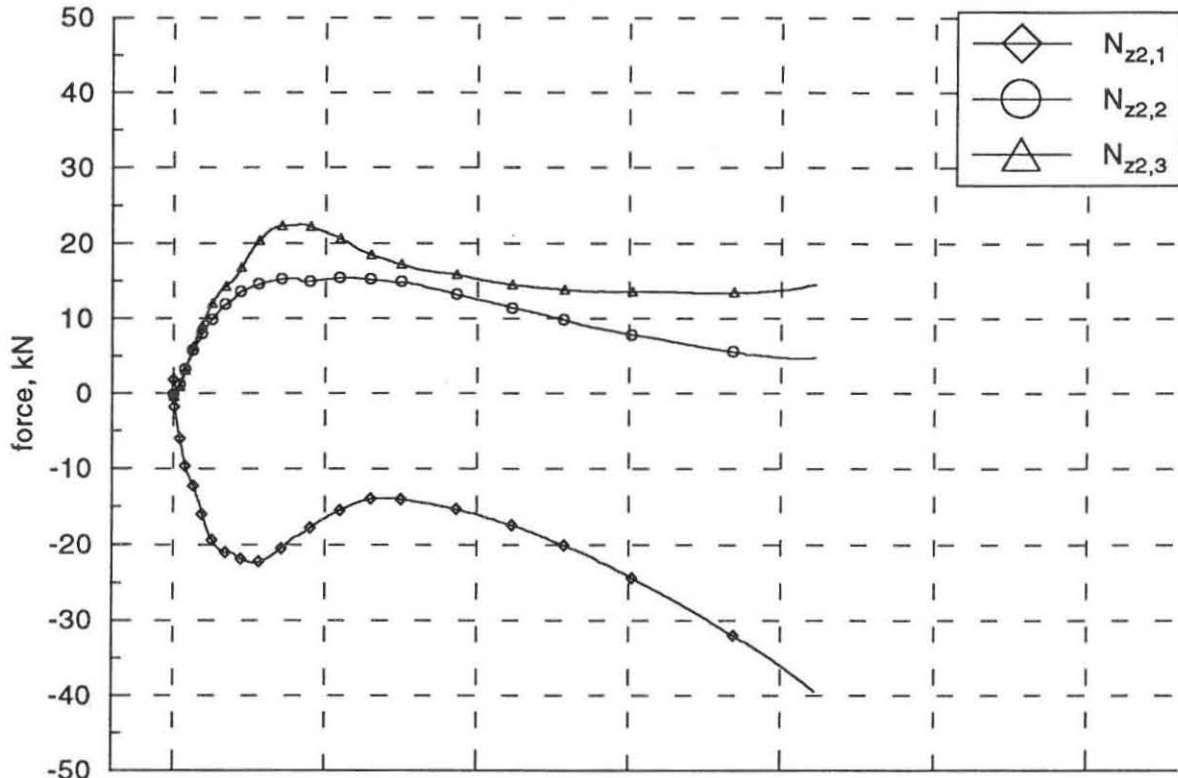
Forces in the z-direction.
specimen B3



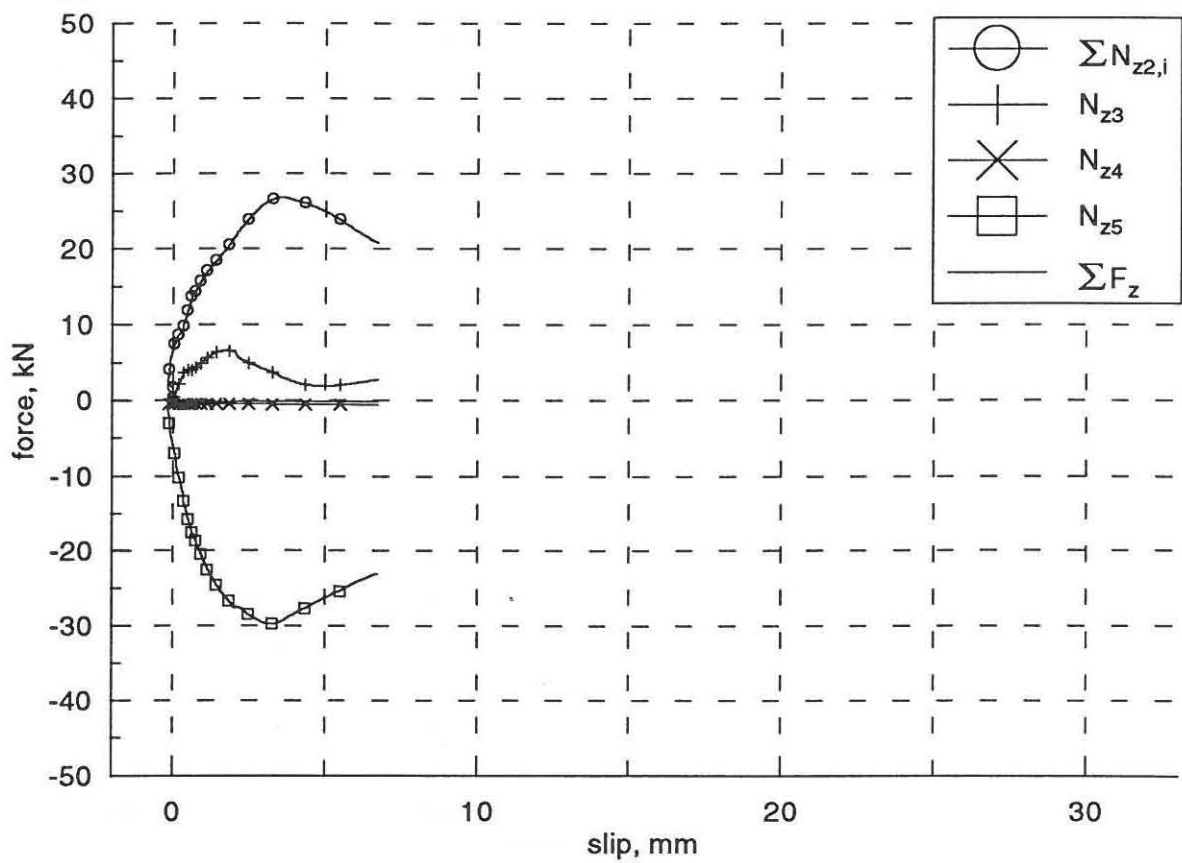
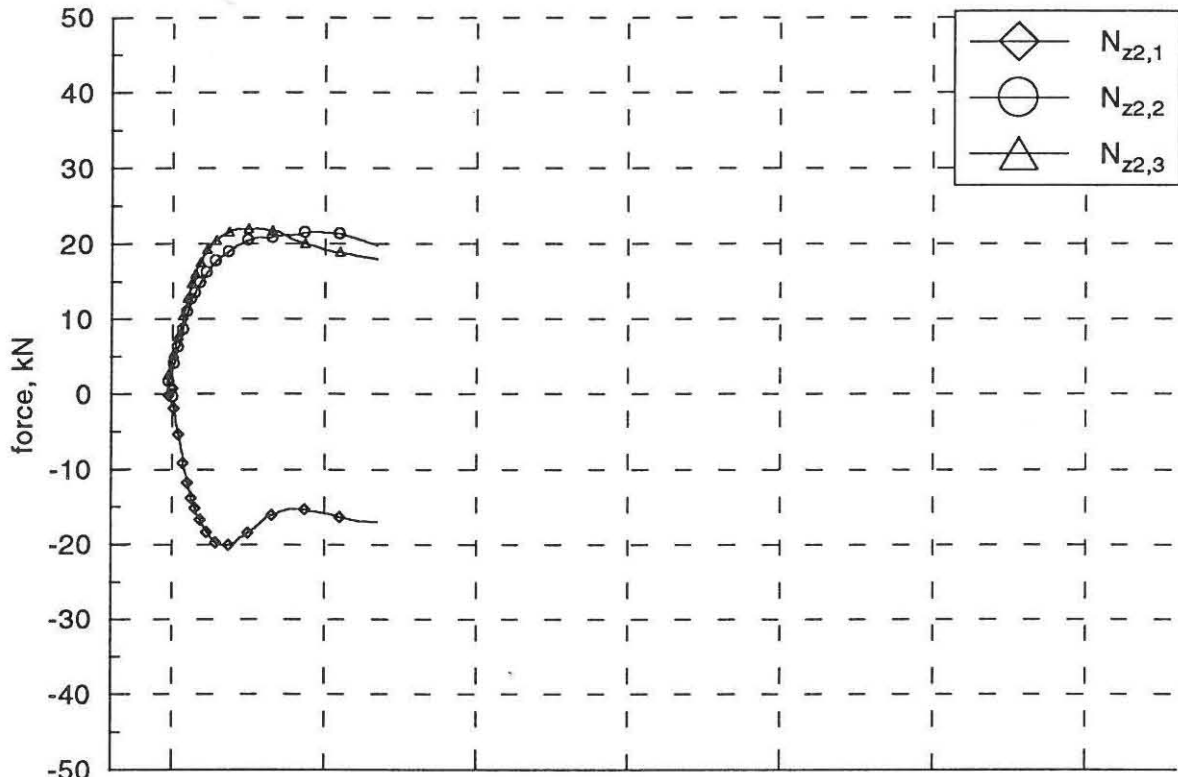
Forces in the z-direction.
specimen C1



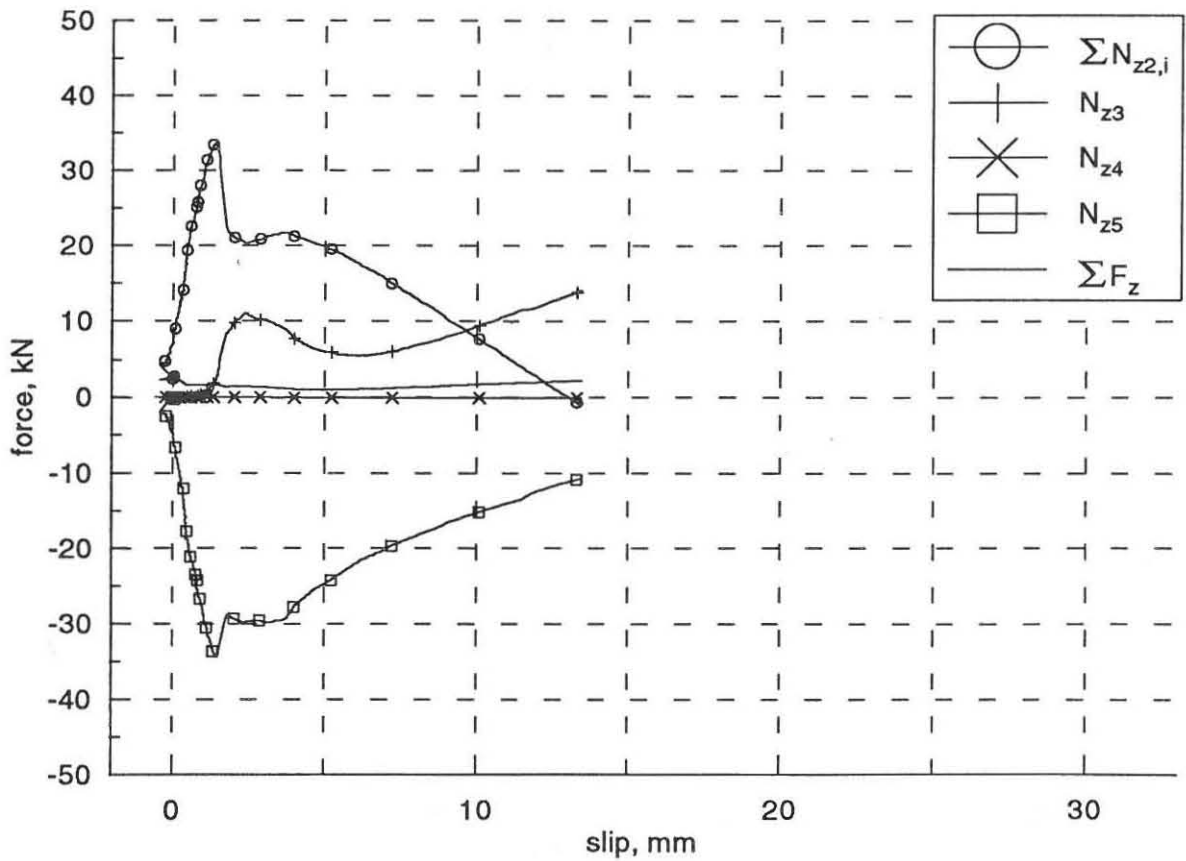
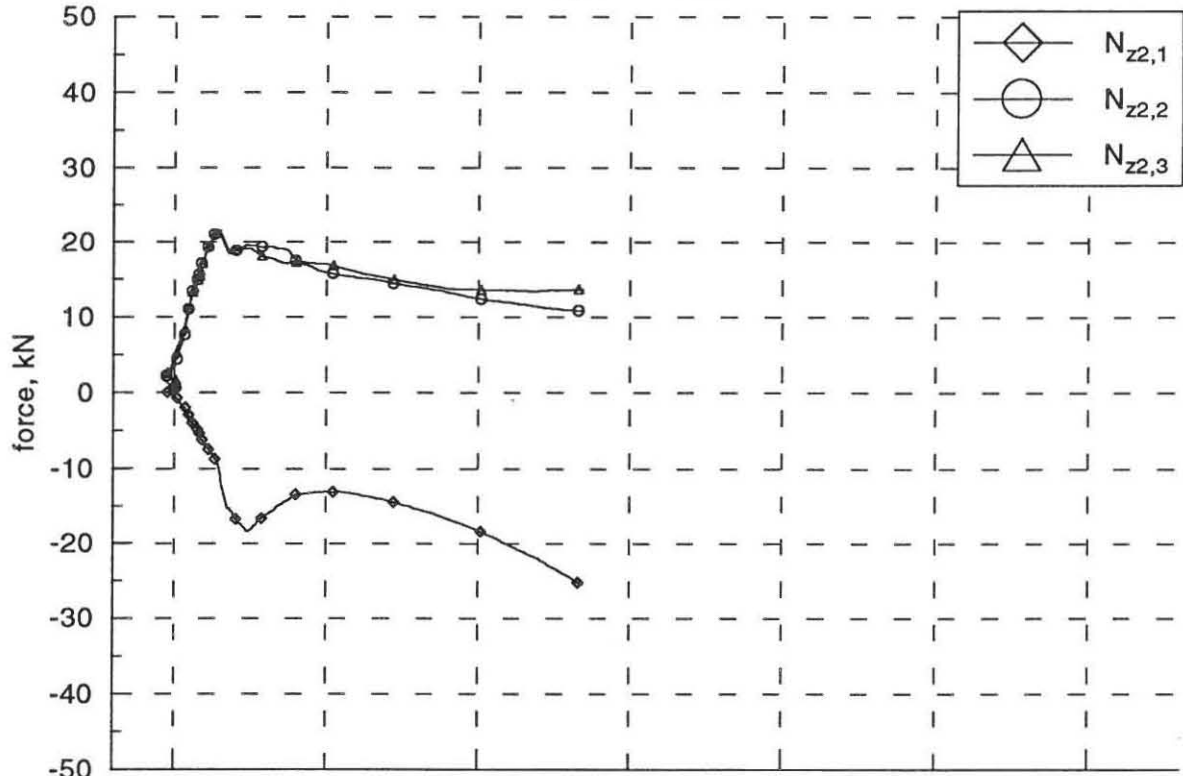
Forces in the z-direction.
specimen C2



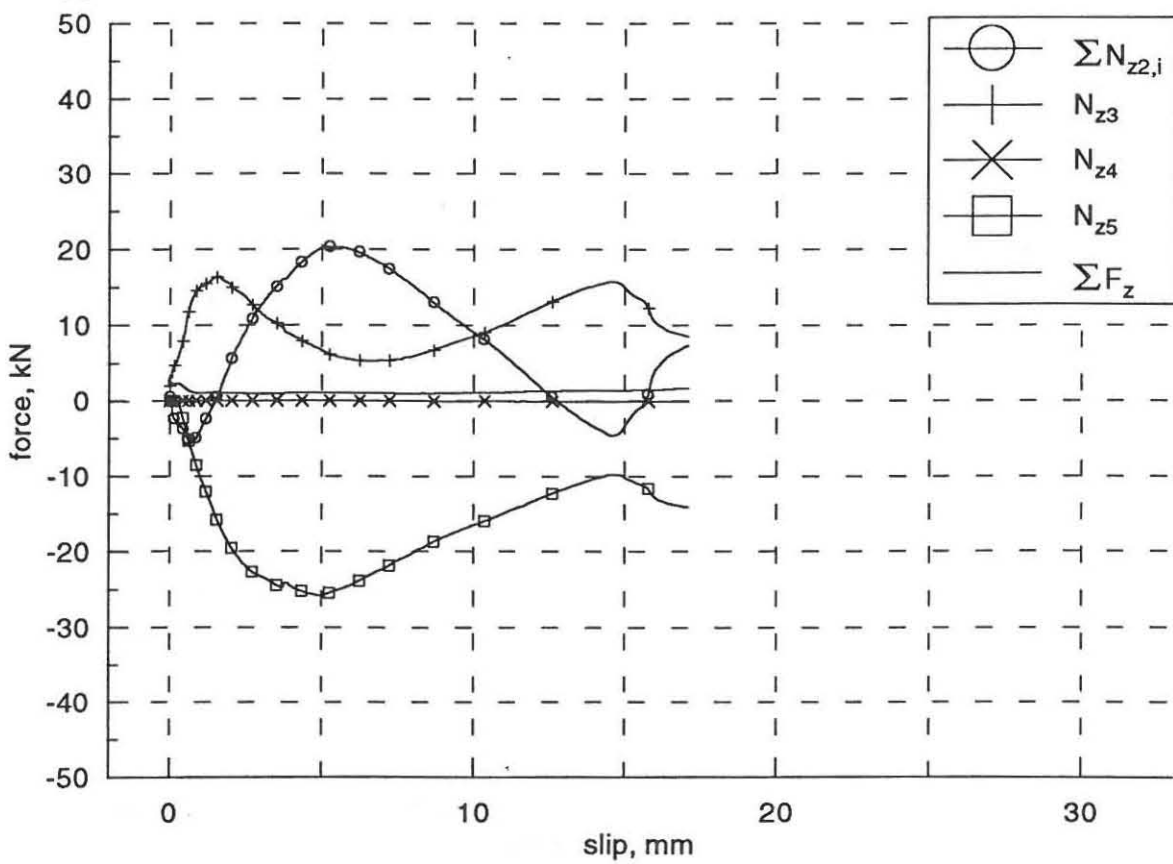
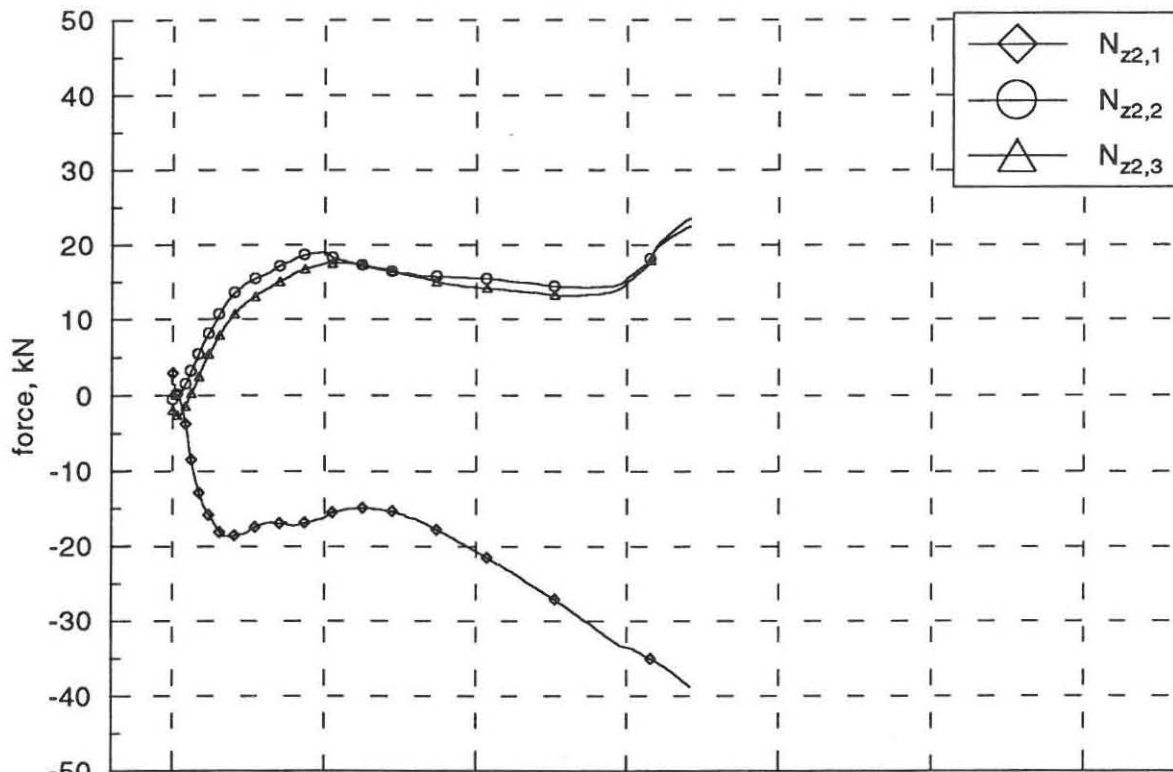
Forces in the z-direction.
specimen C3



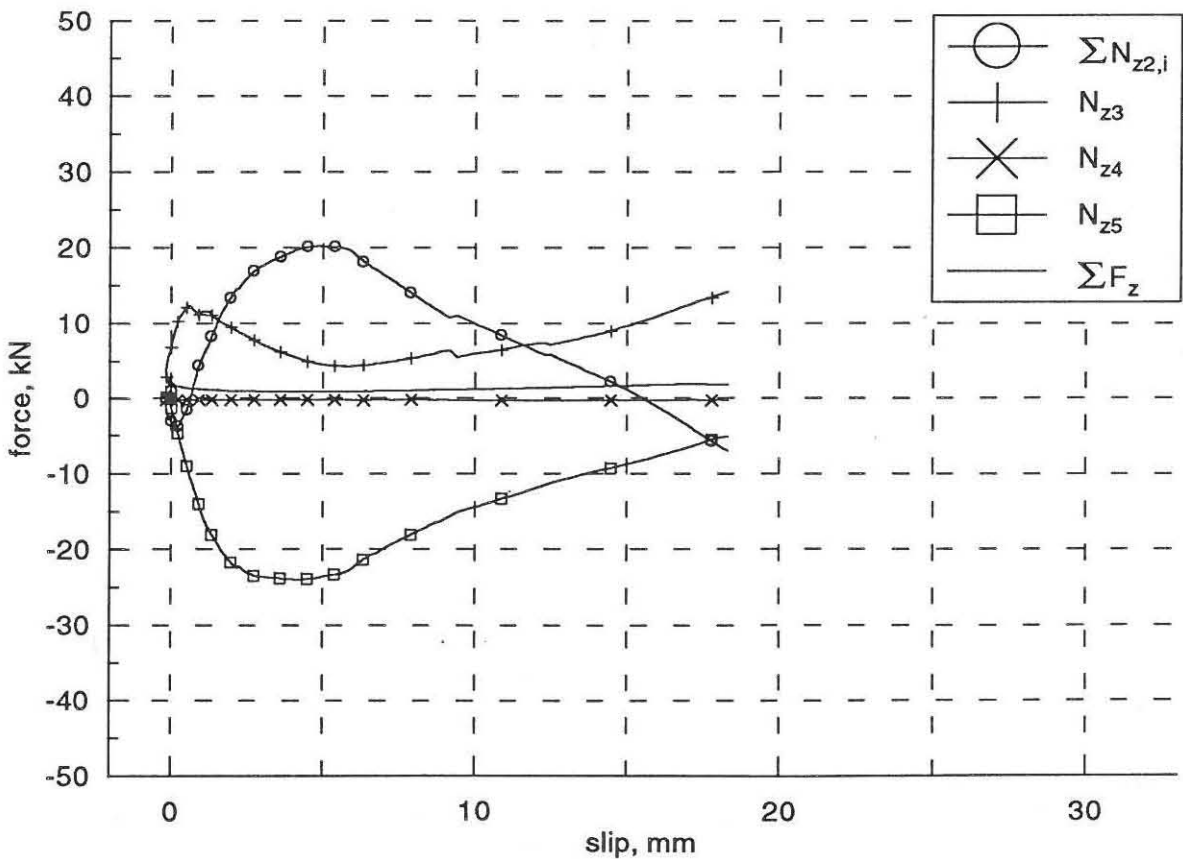
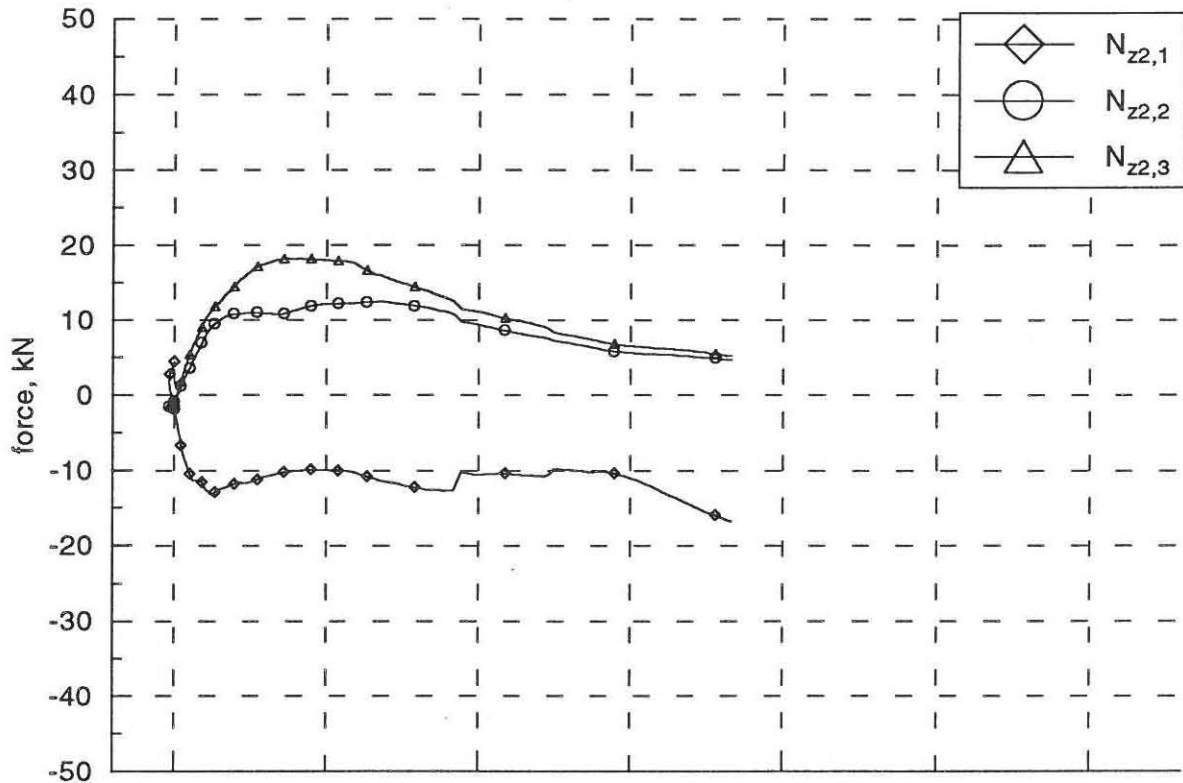
Foces in the z-direction.
specimen C4



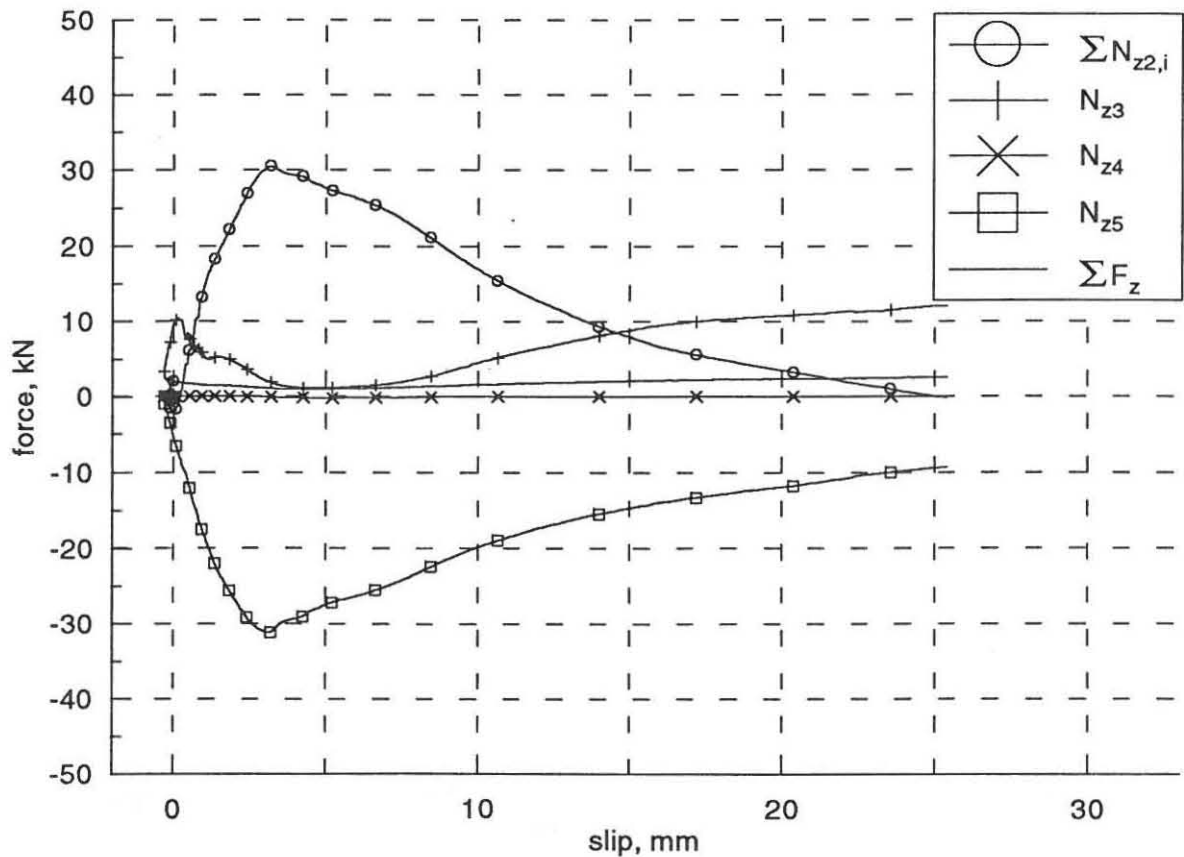
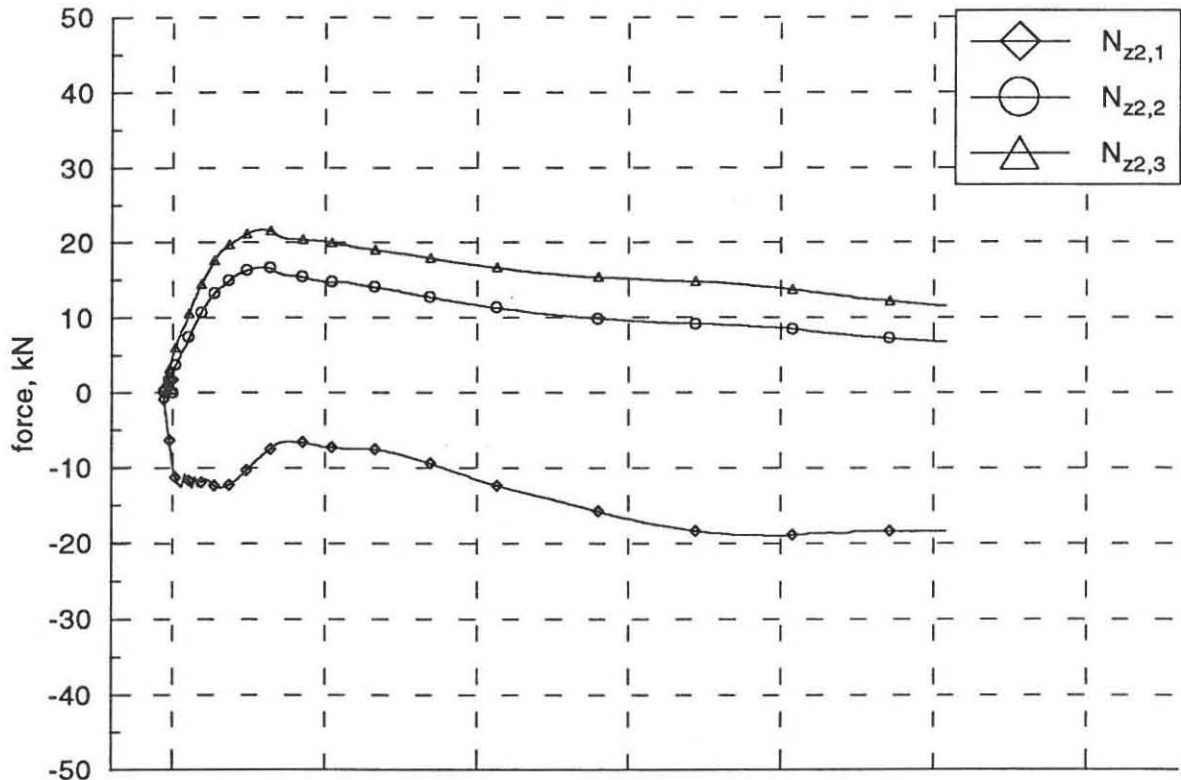
Forces in the z-direction.
specimen C5



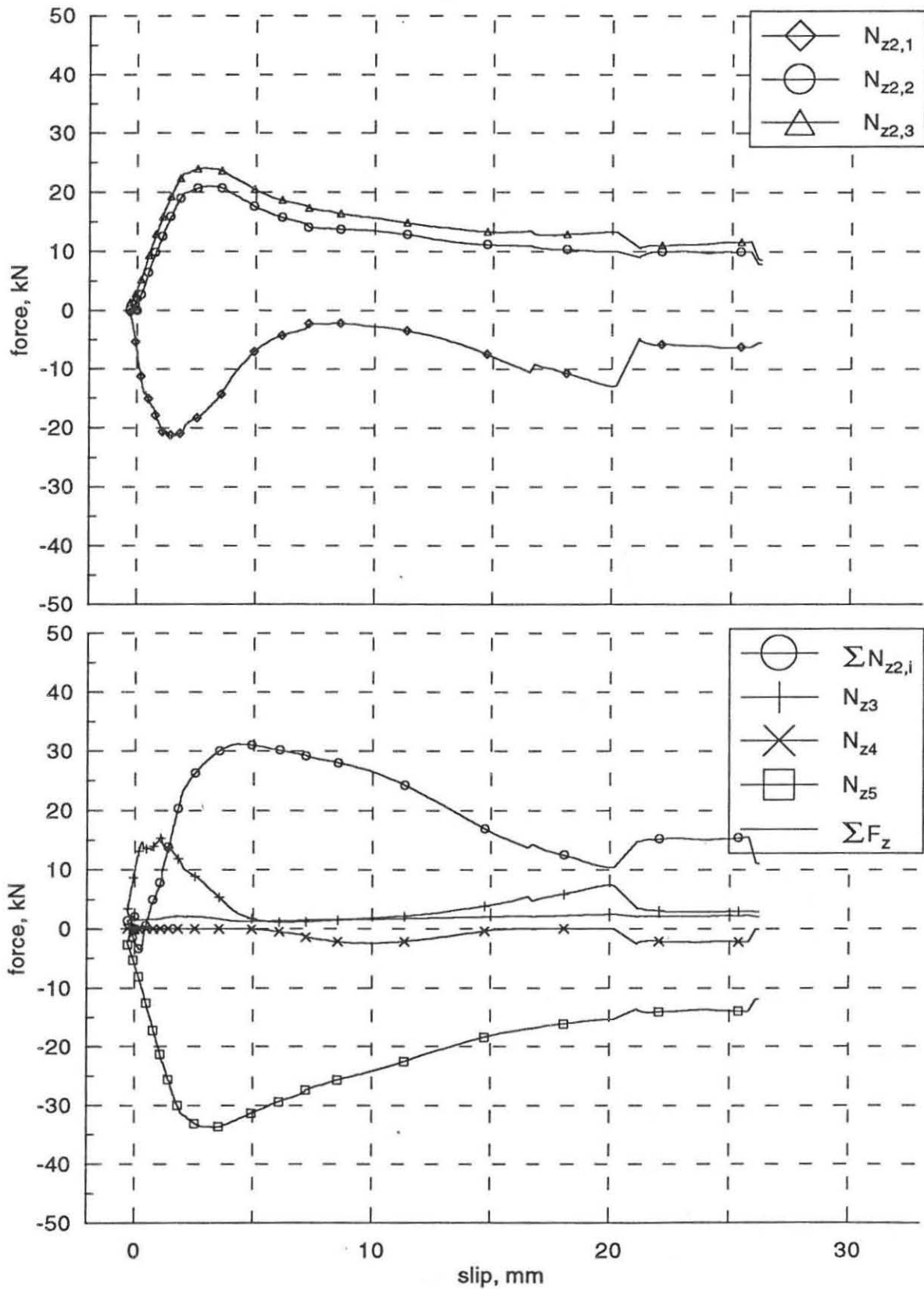
Forces in the z-direction.
specimen C6



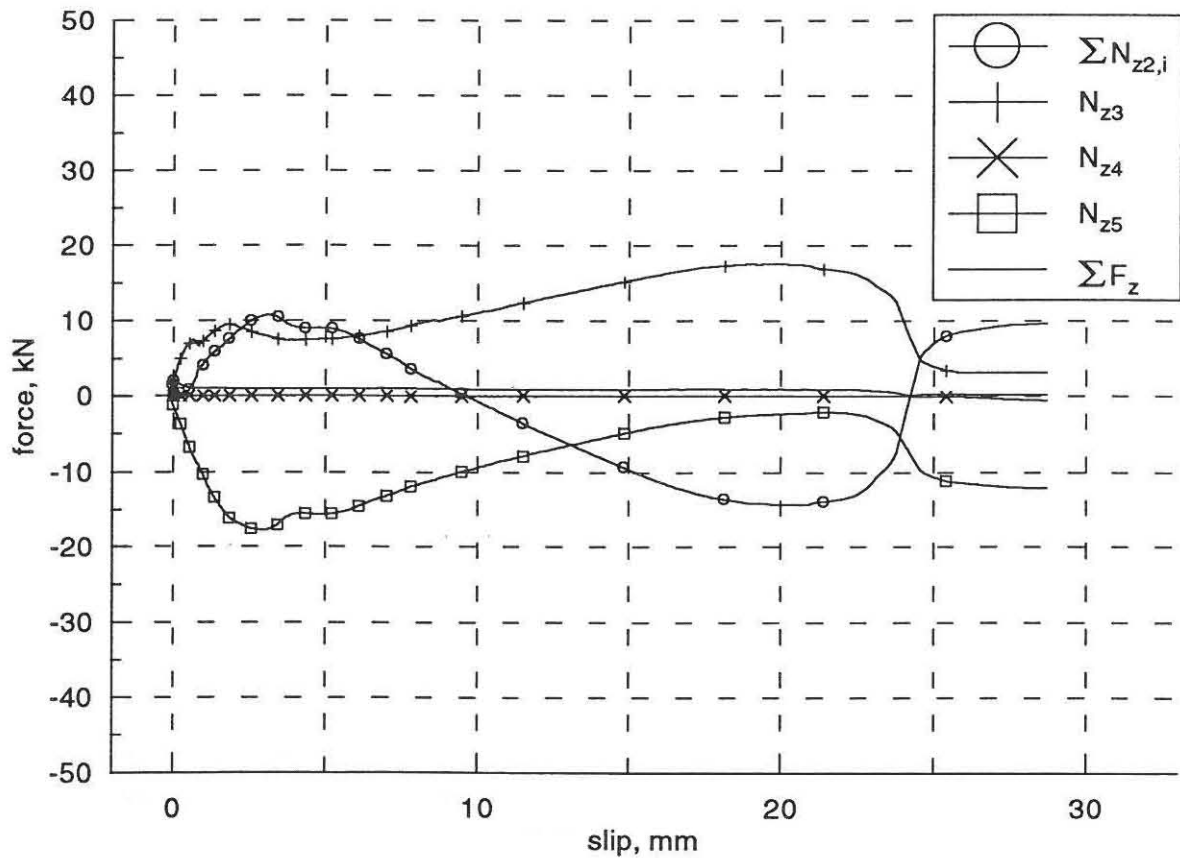
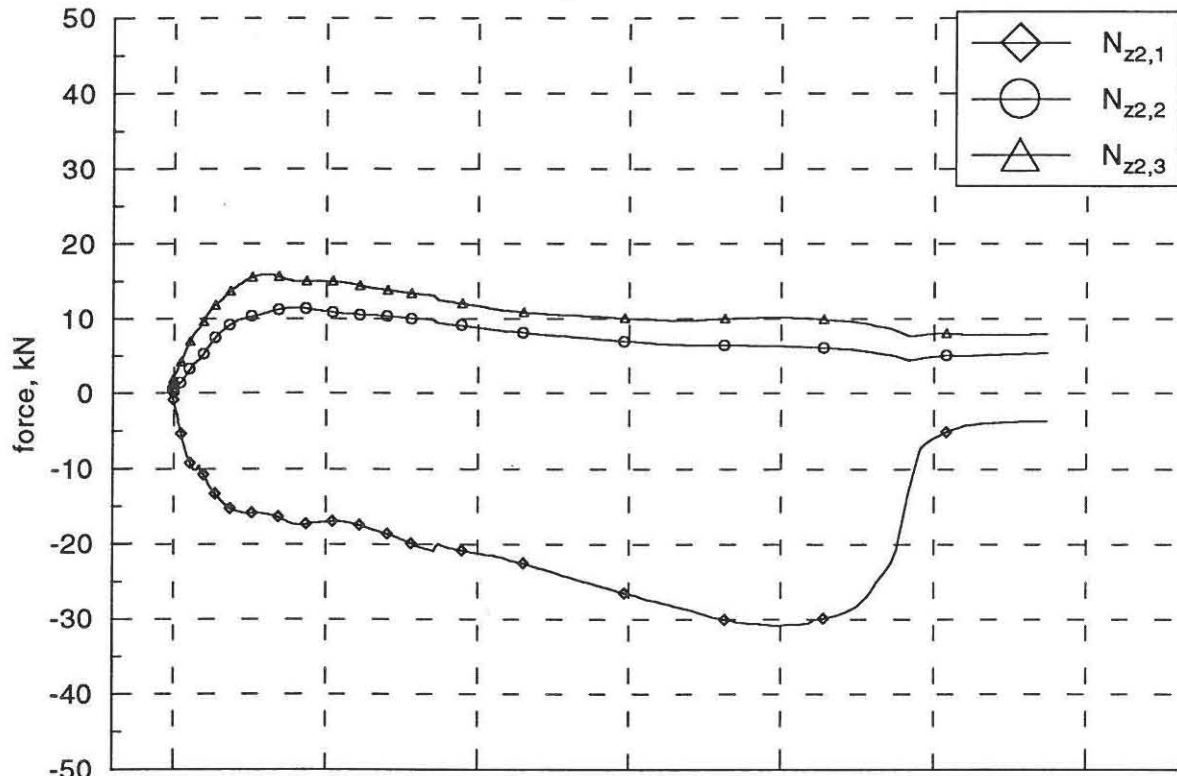
Forces in the z-direction.
specimen C7



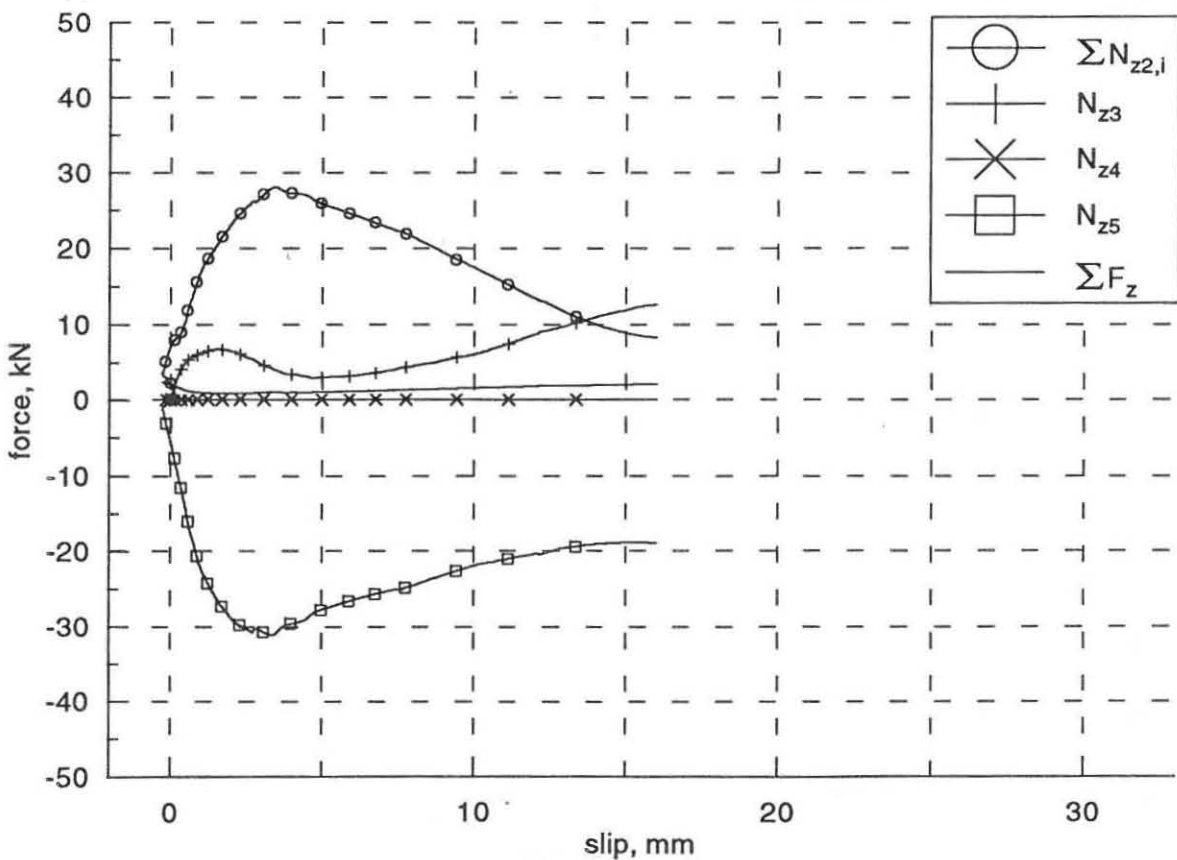
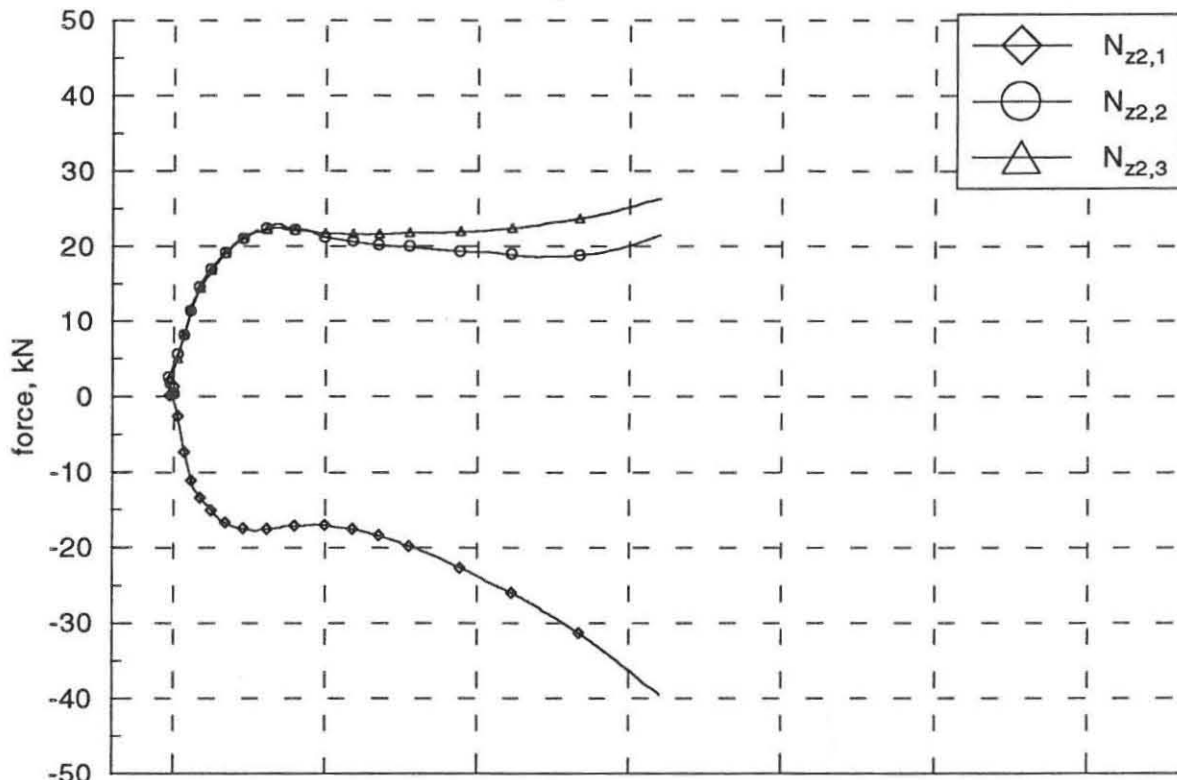
Forces in the z-direction.
specimen C8



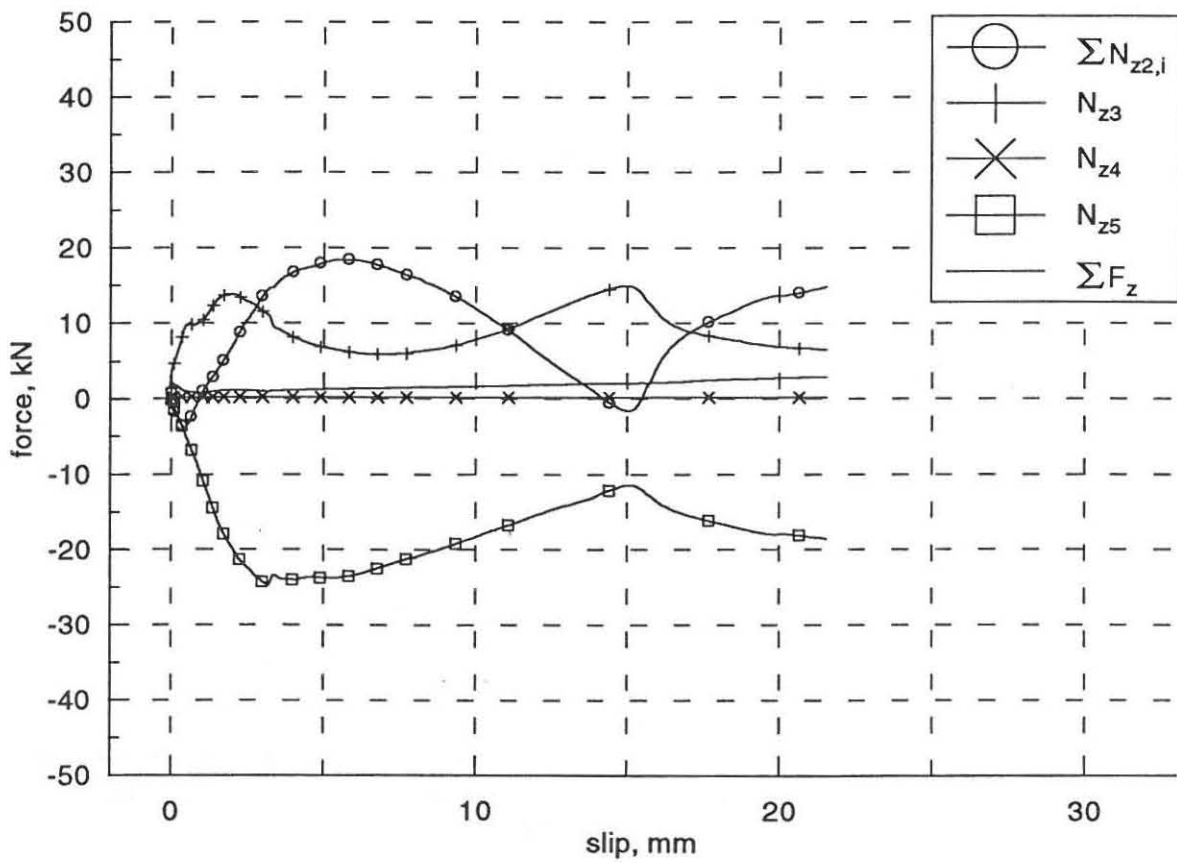
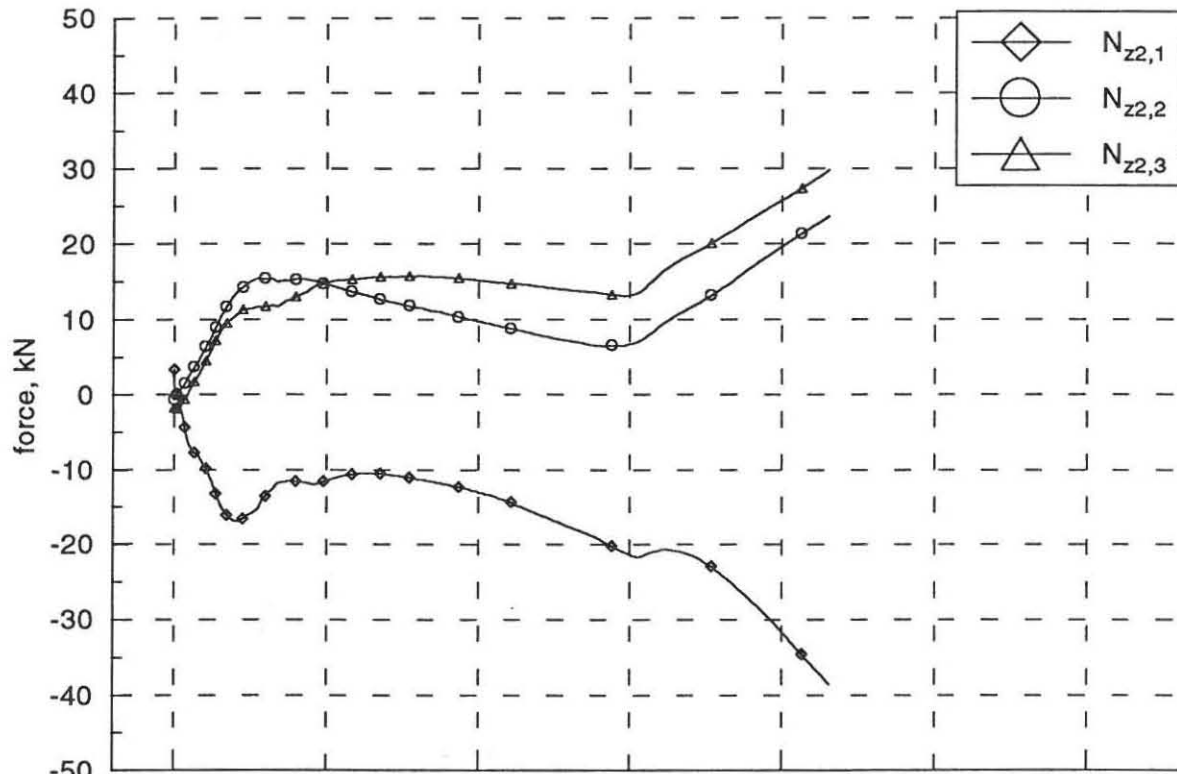
Forces in the z-direction.
specimen C9



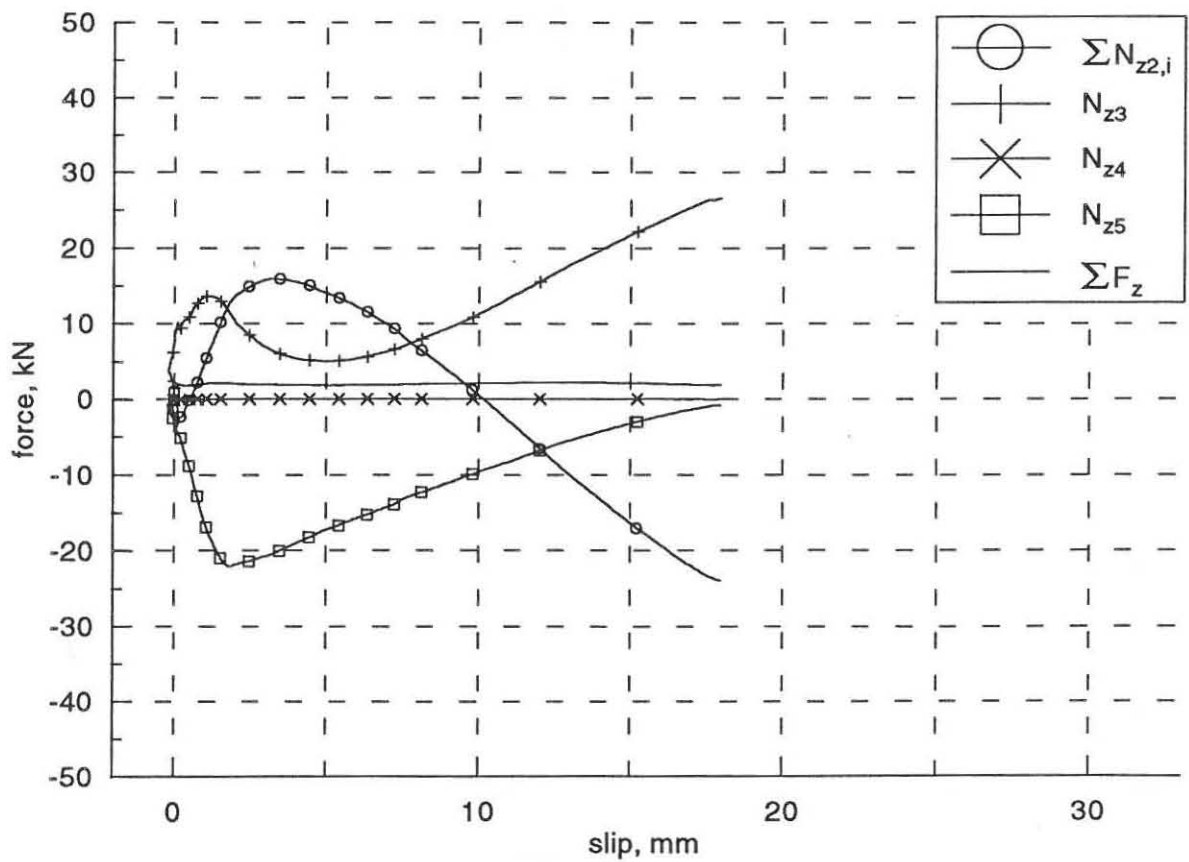
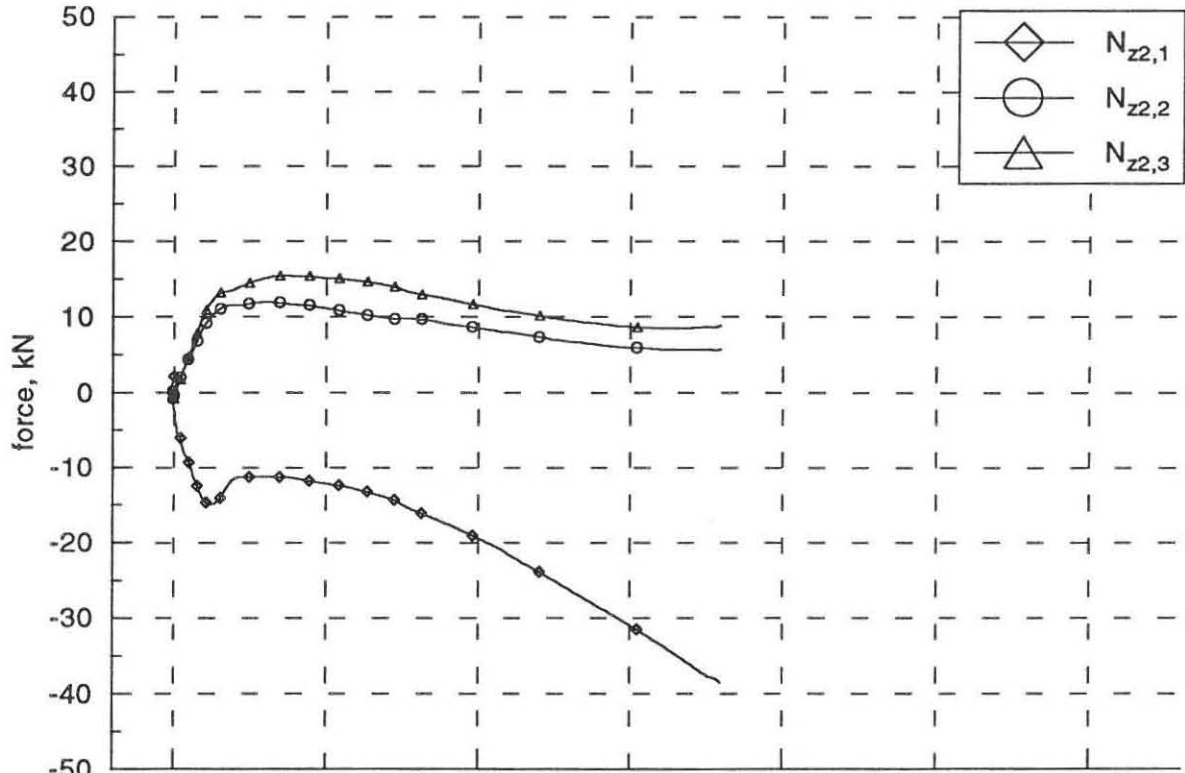
Forces in the z-direction.
specimen C10



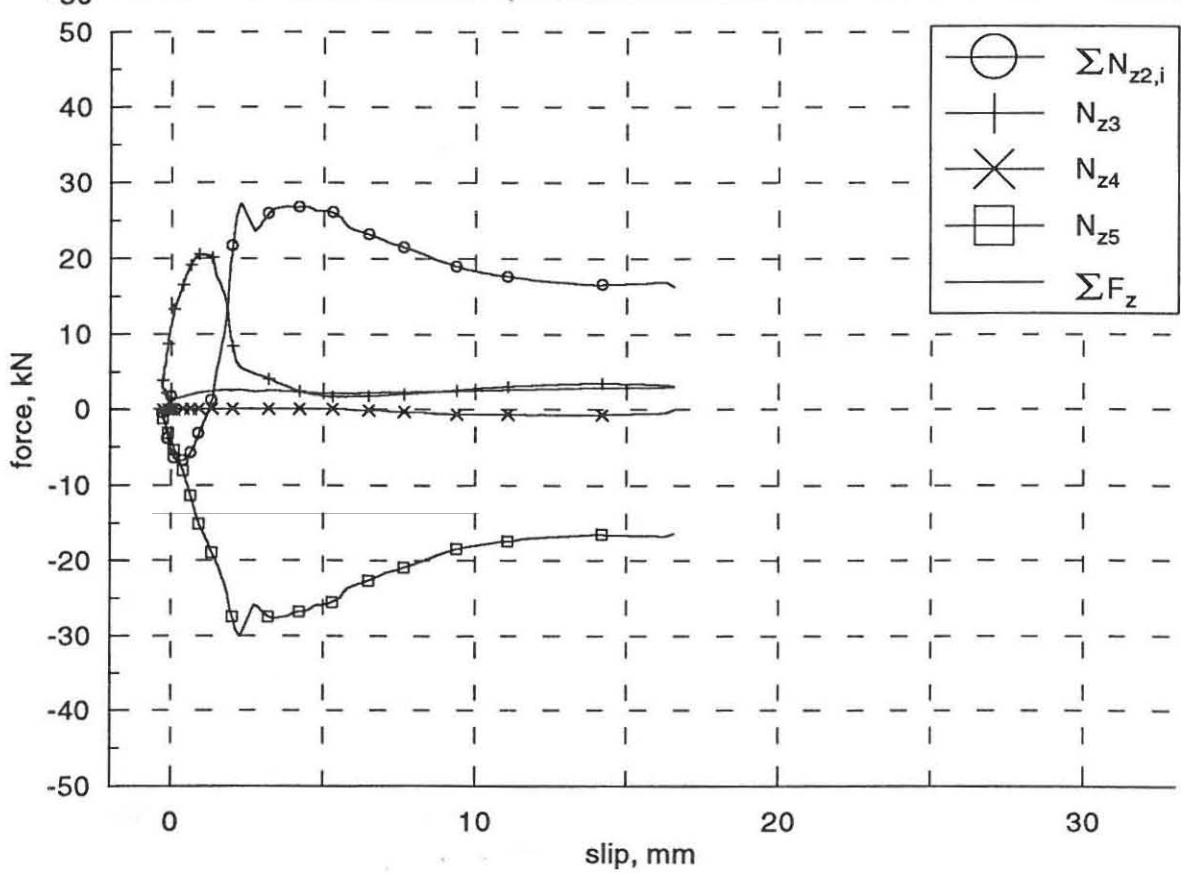
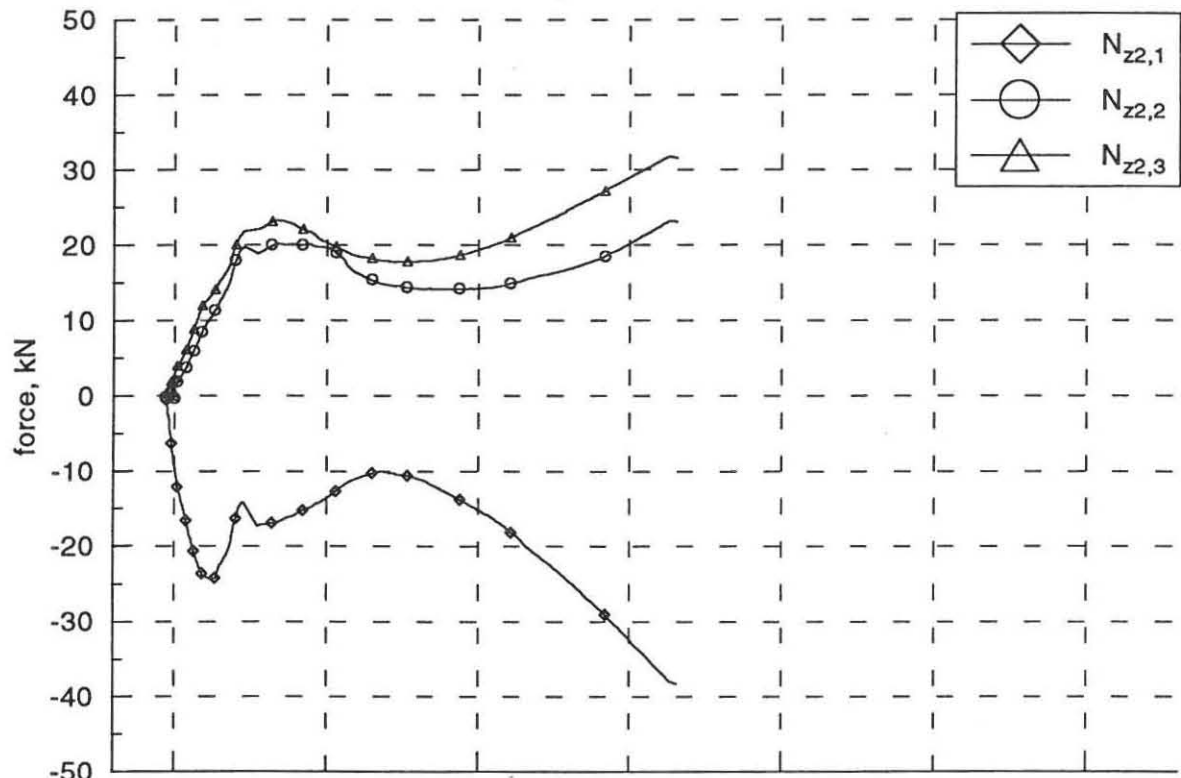
Forces in the z-direction.
specimen C11



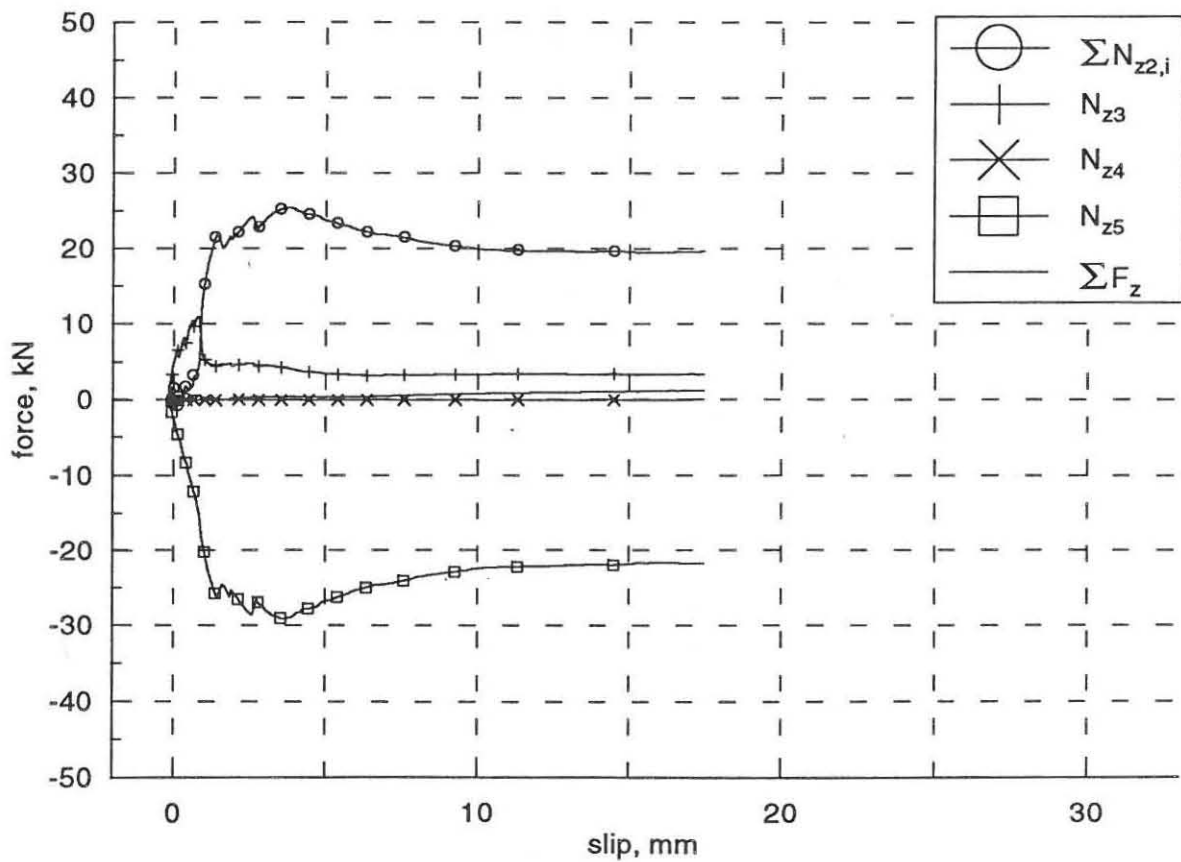
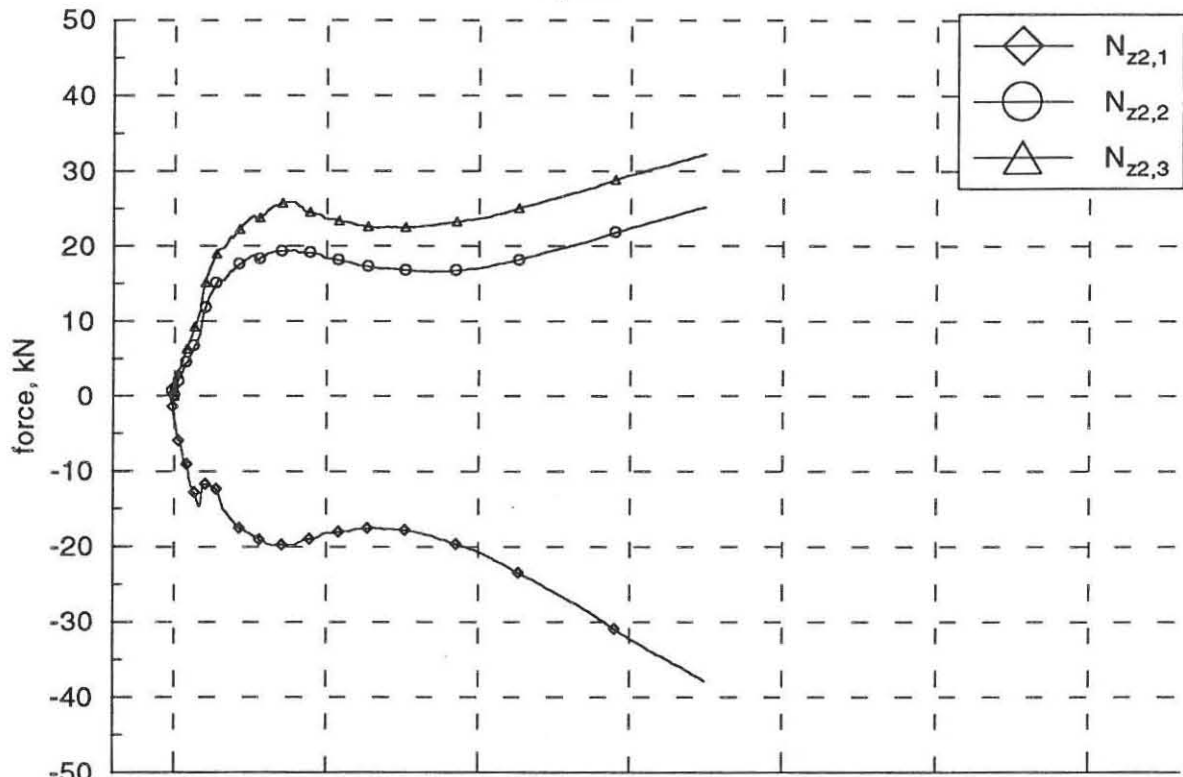
Forces in the z-direction.
specimen C12



Fores in the z-direction.
specimen C13

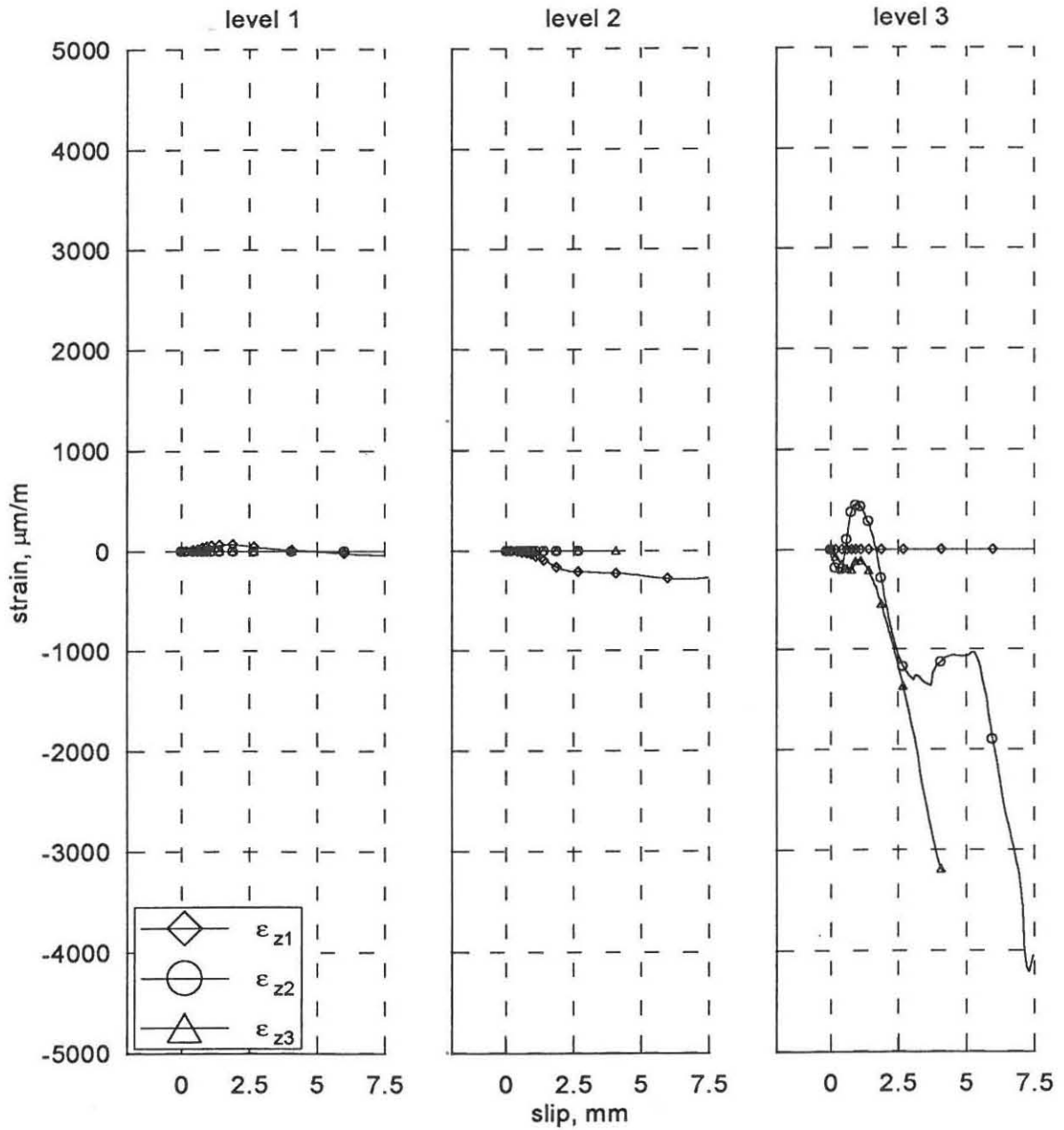


Forces in the z-direction.
specimen C14

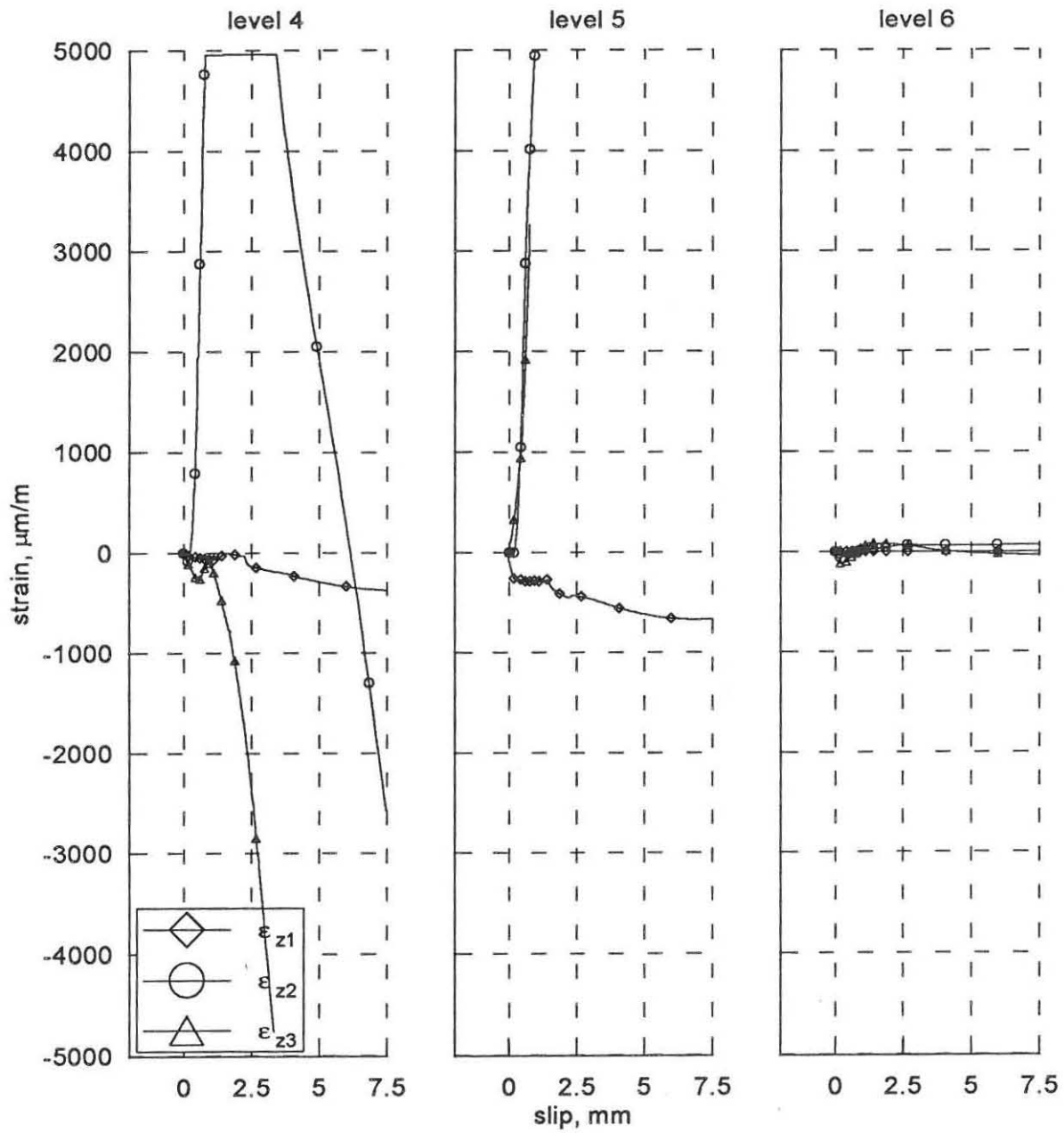


11.4 Strains of the headed stud connector: ϵ_{z1} , ϵ_{z2} & ϵ_{z3} .

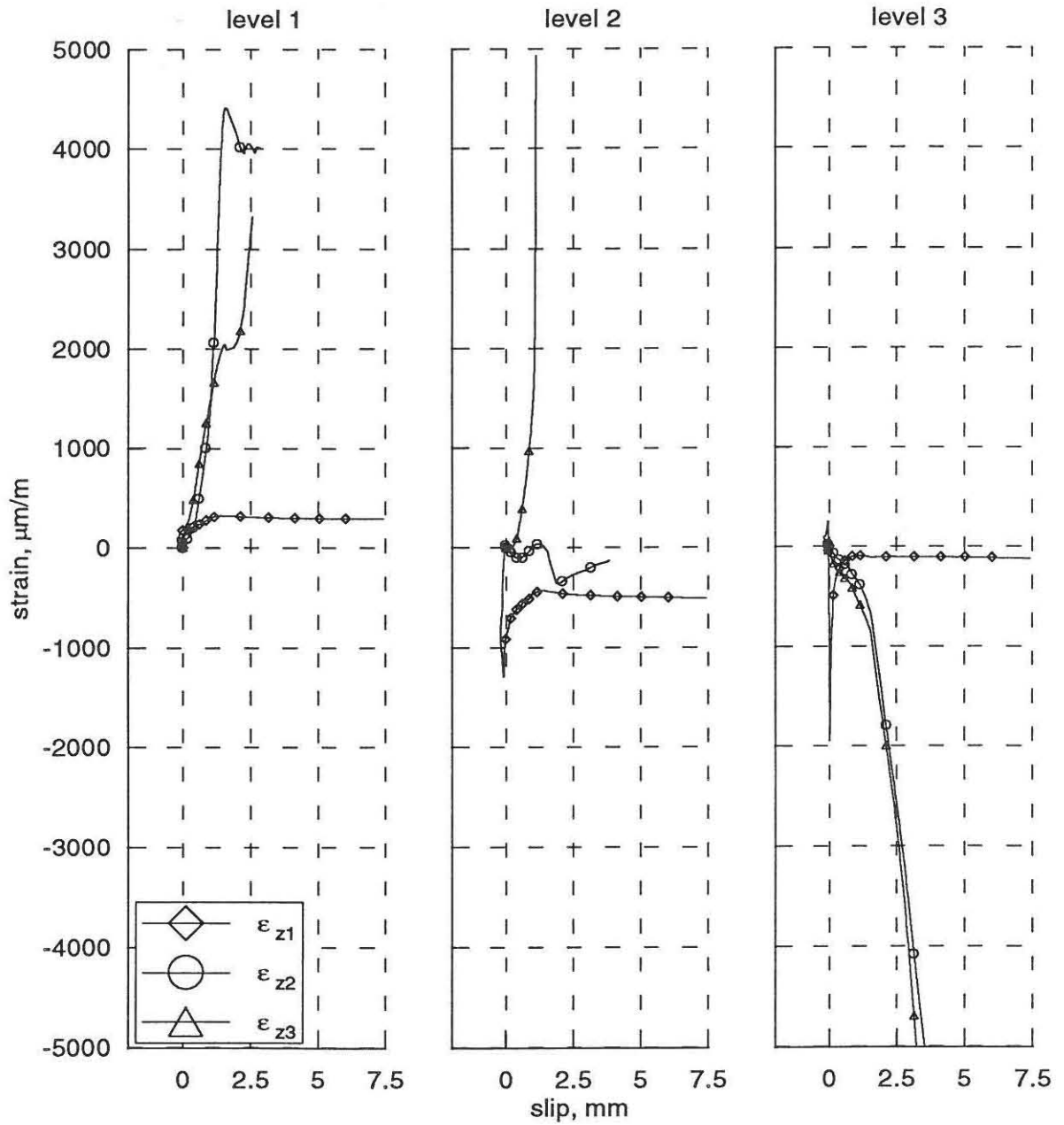
Strains of the headed stud connector.
specimen 2



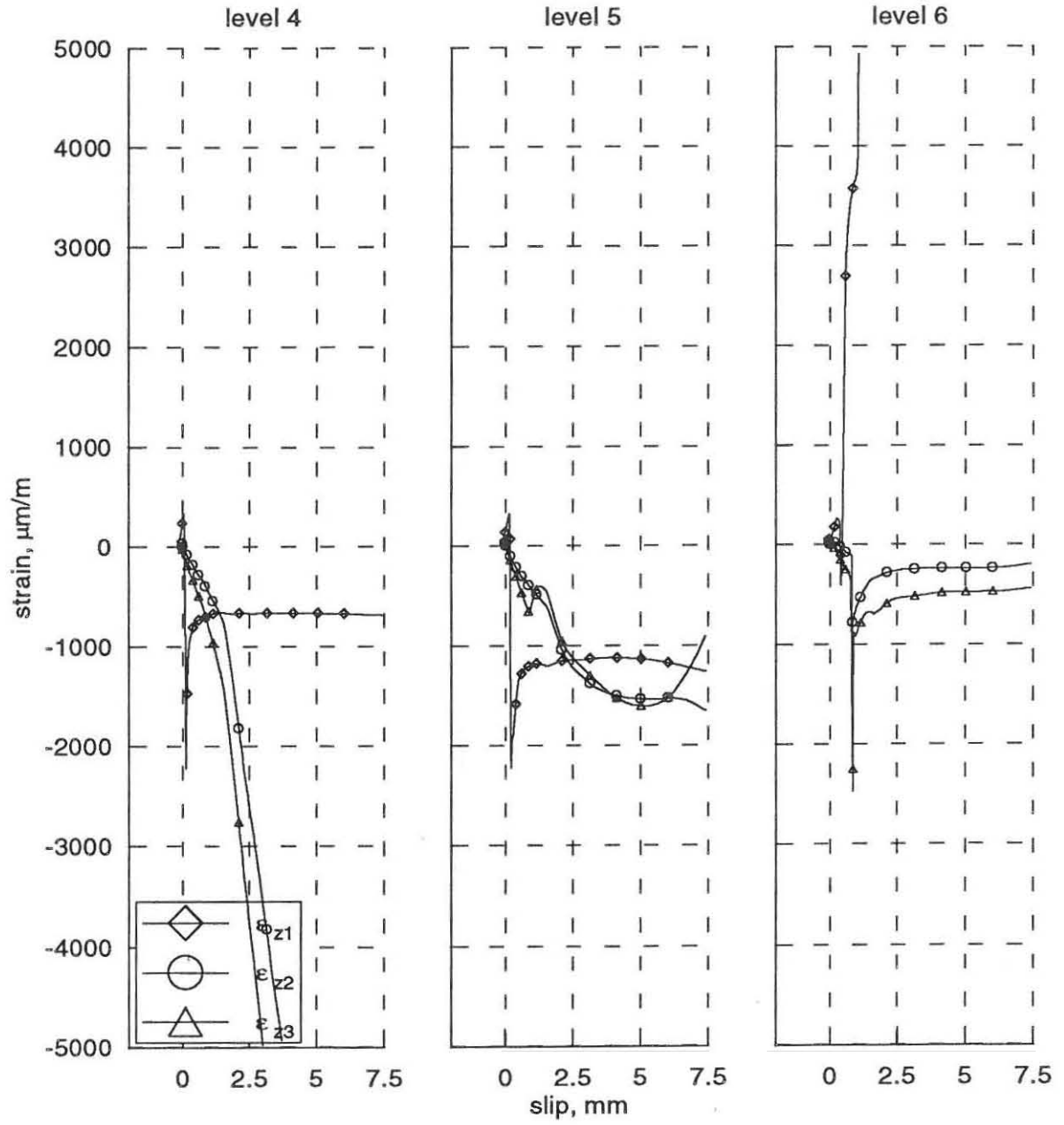
Strains of the headed stud connector.
specimen 2



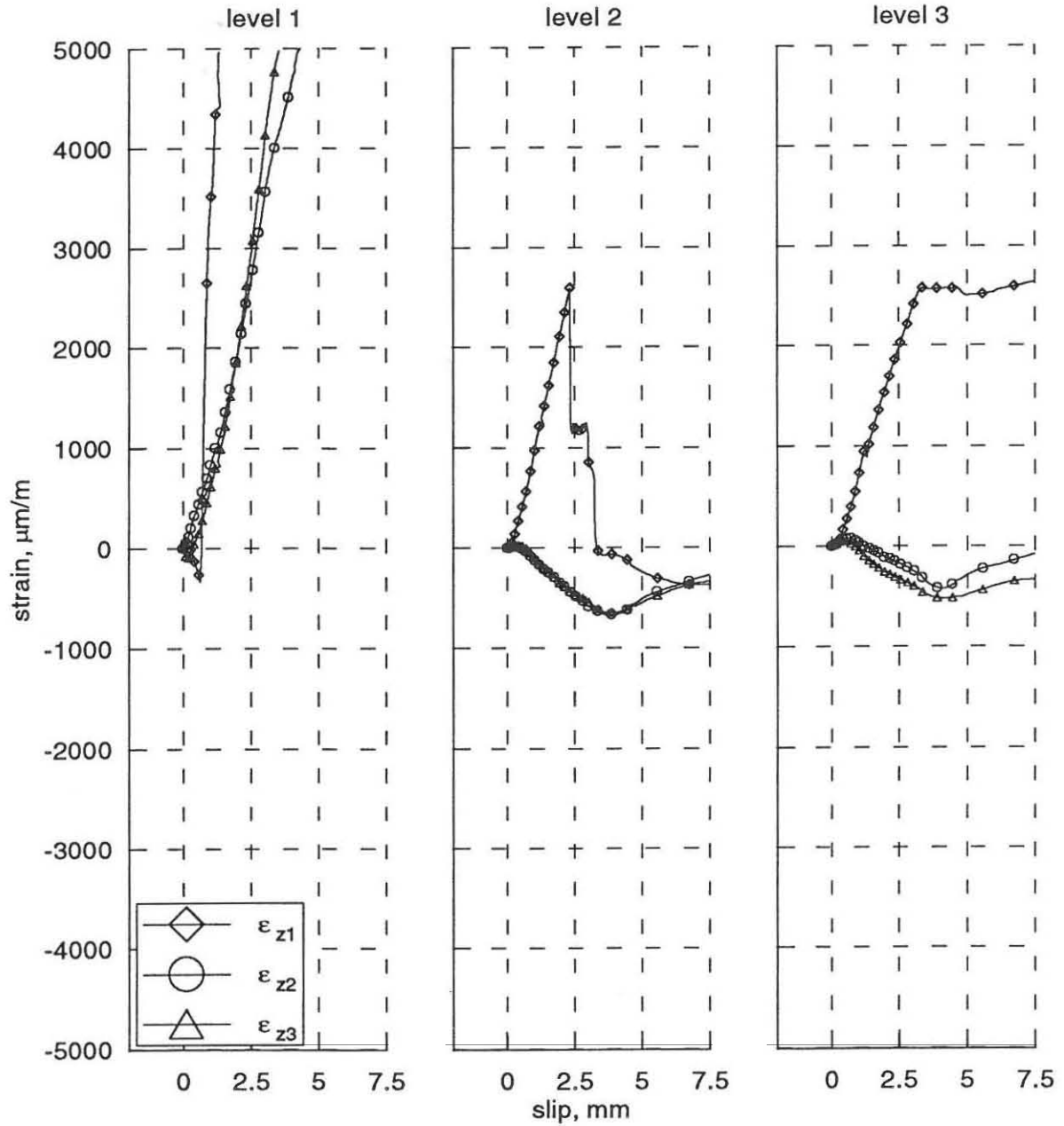
Strains of the headed stud connector.
specimen 3



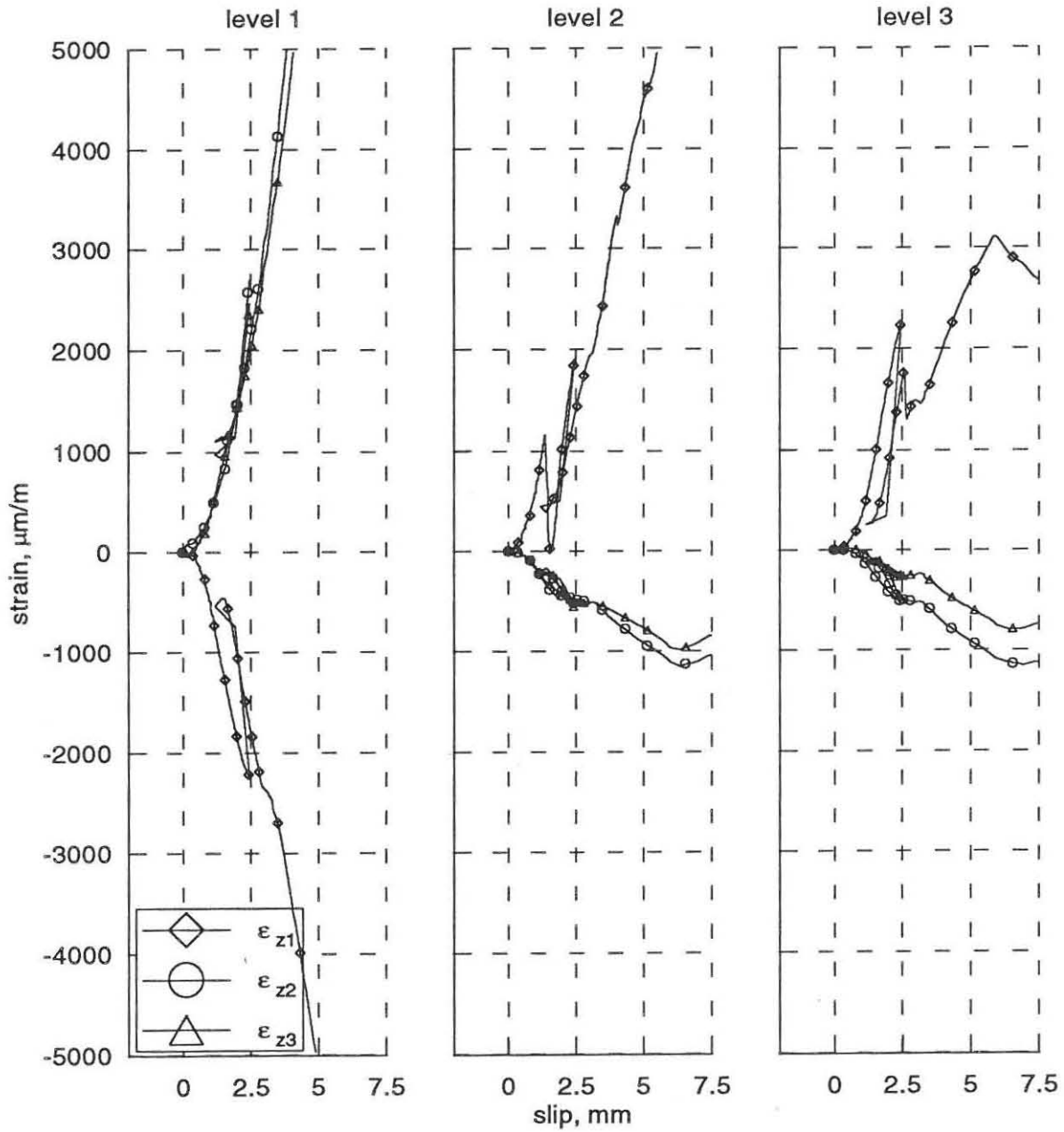
Strains of the headed stud connector.
specimen 3



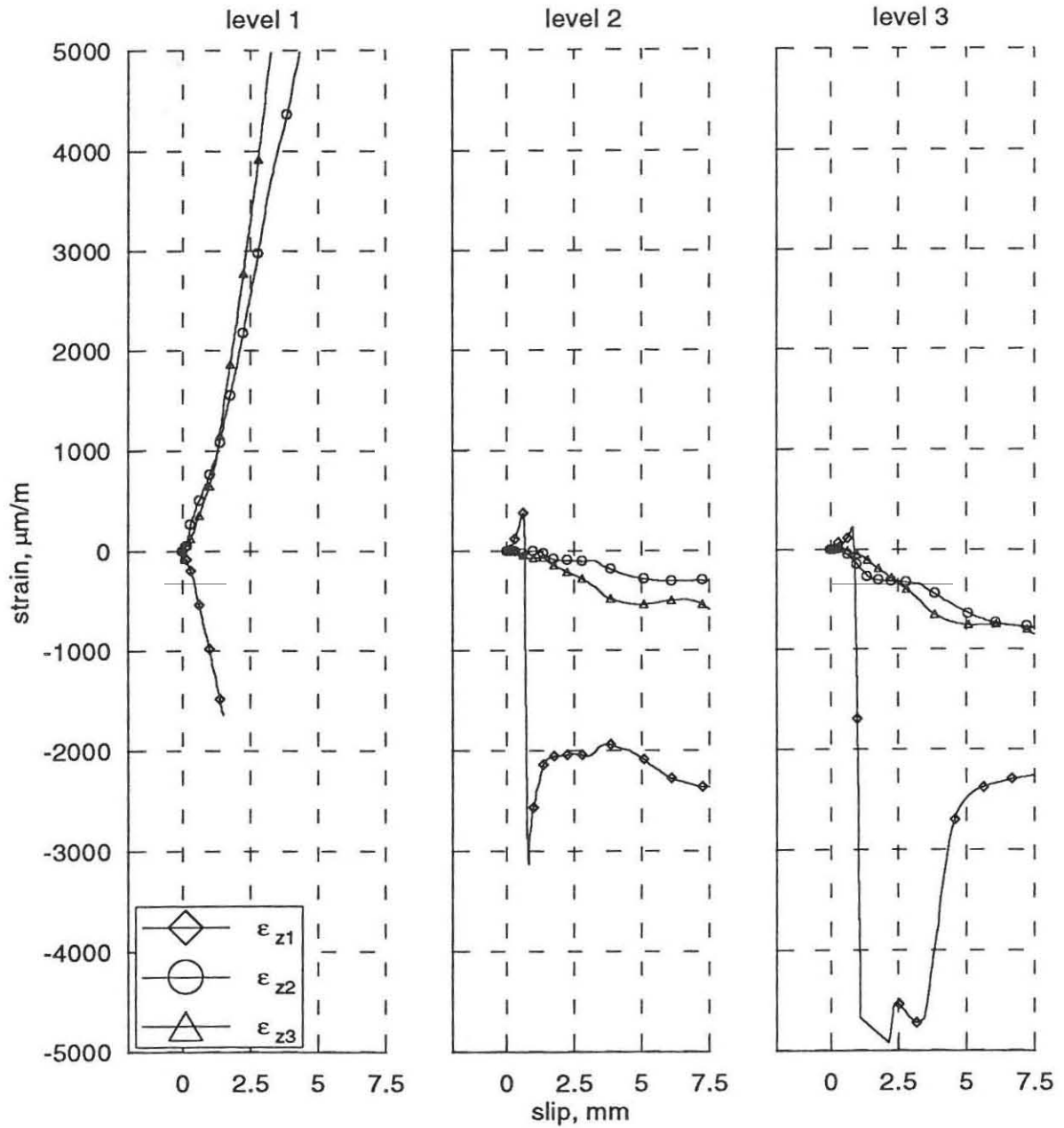
Strains of the headed stud connector.
specimen A1



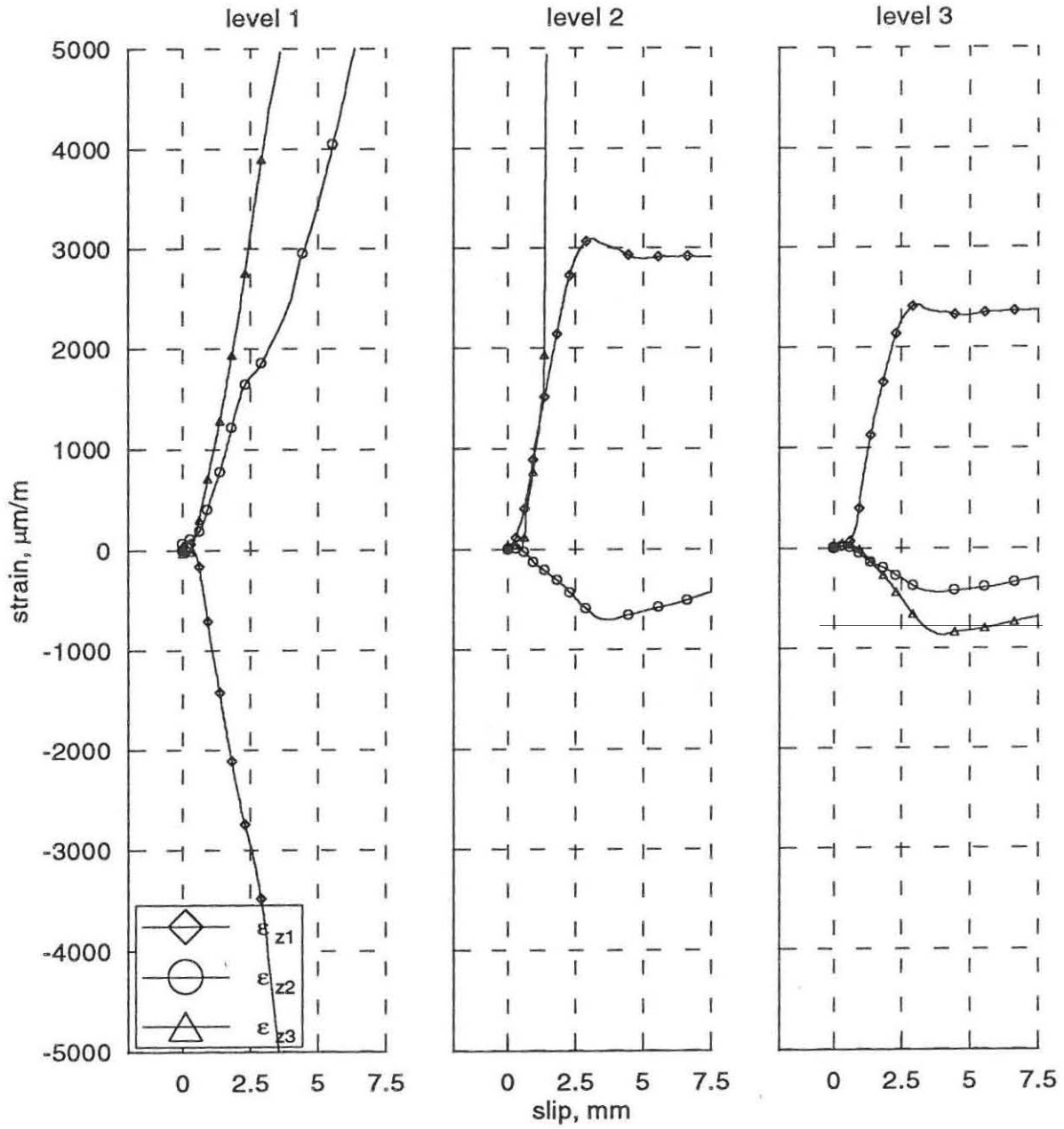
Strains of the headed stud connector.
specimen A2



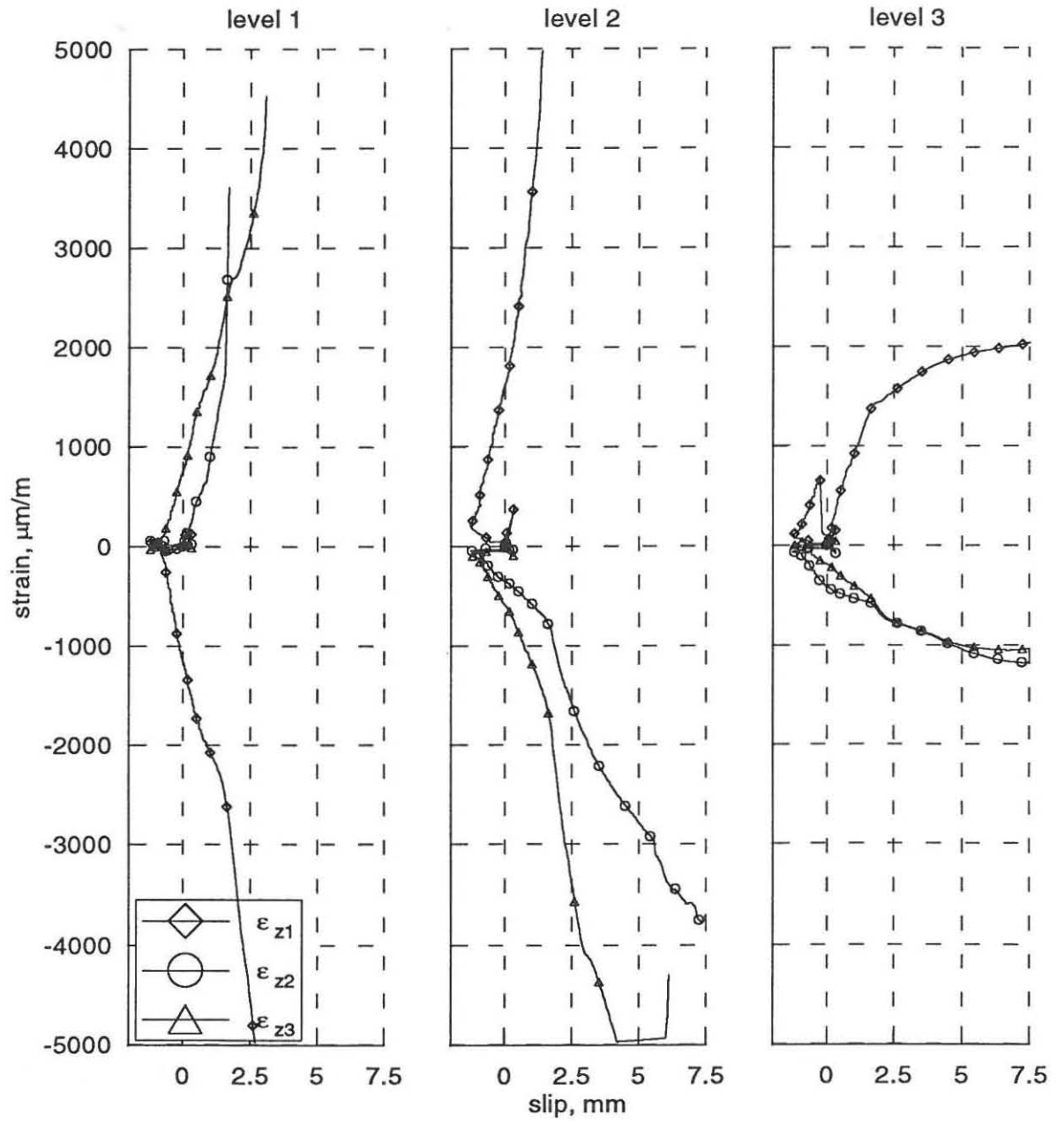
Strains of the headed stud connector.
specimen B1



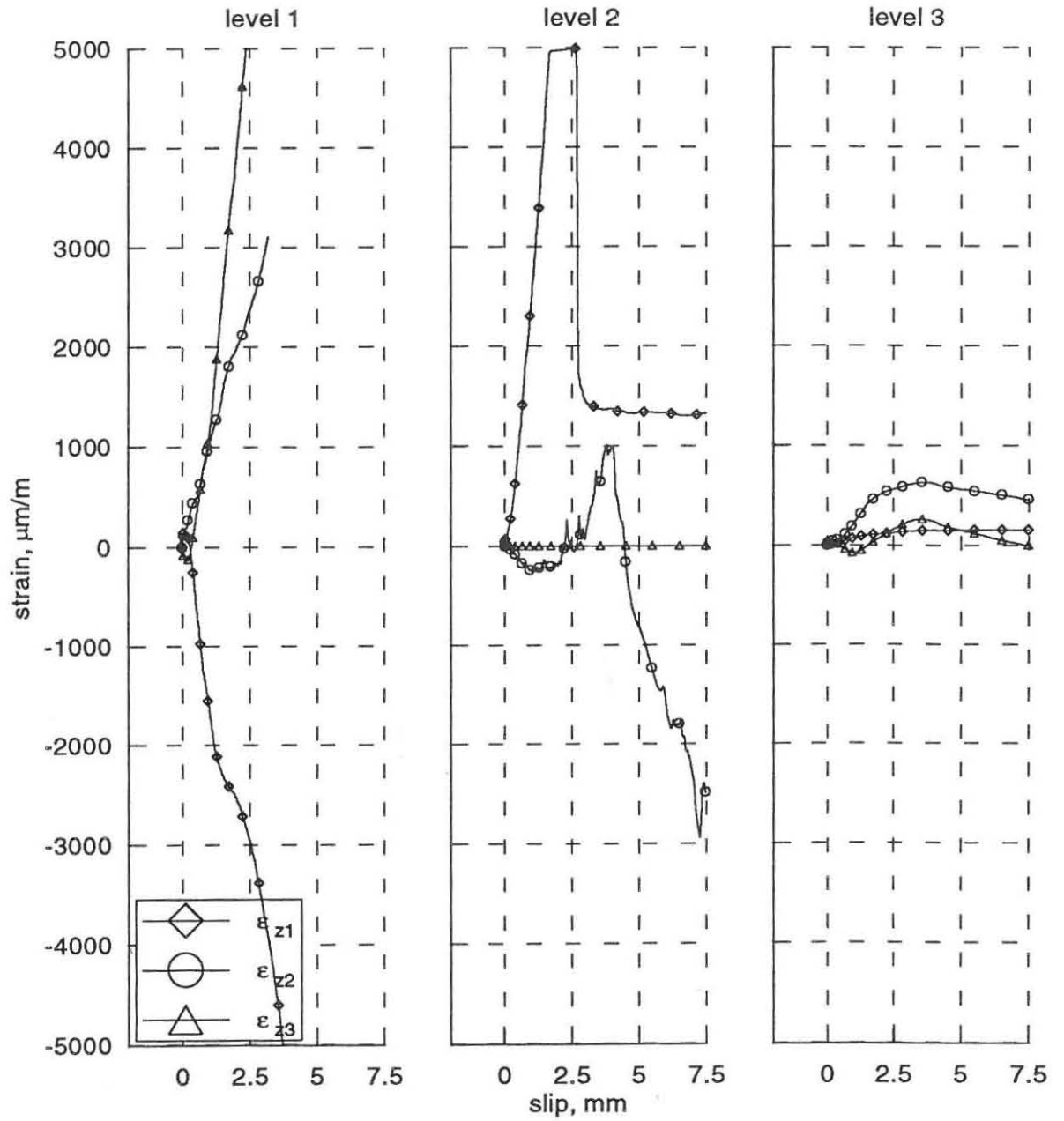
Strains of the headed stud connector.
specimen B2



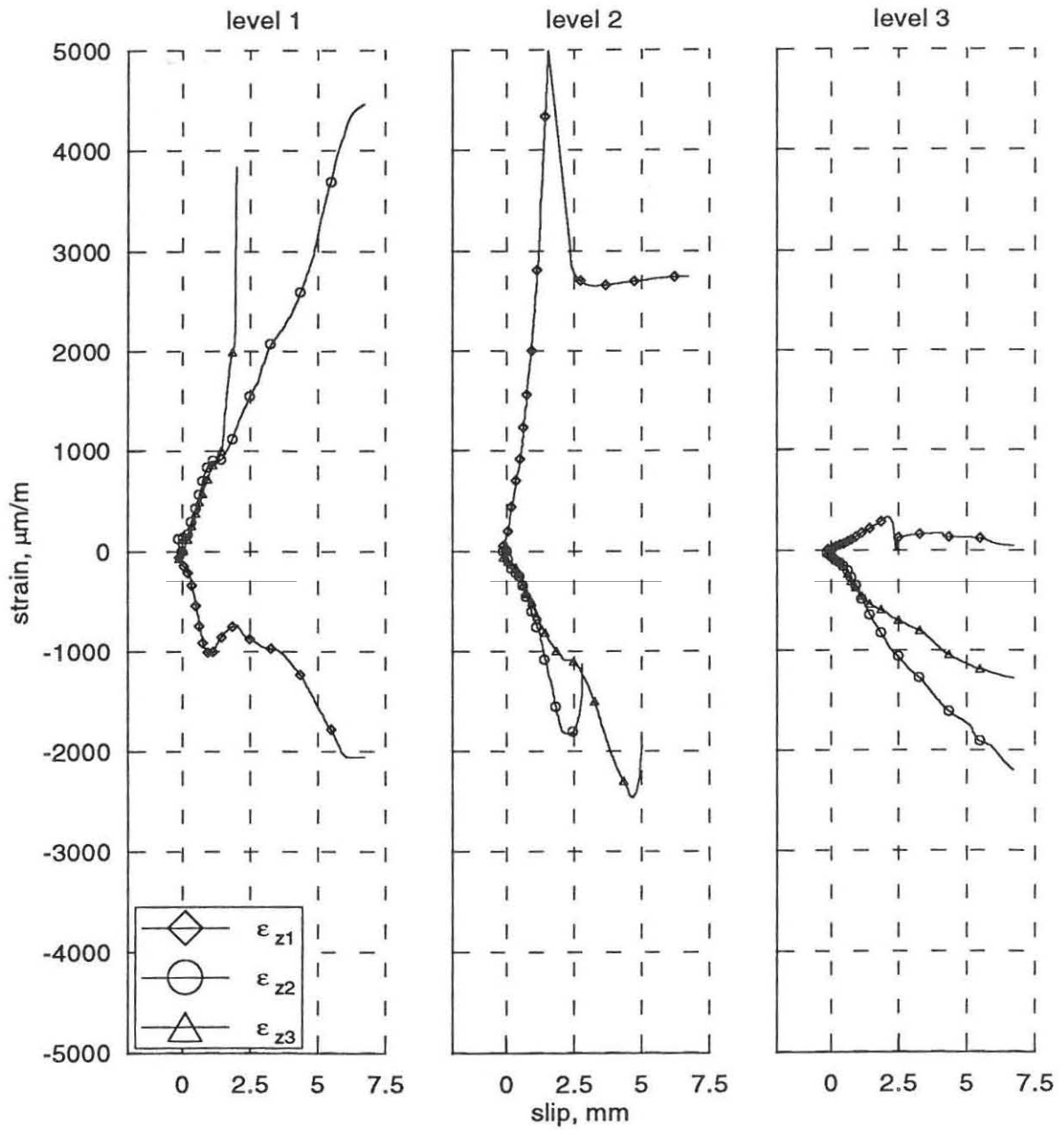
Strains of the headed stud connector.
specimen C1



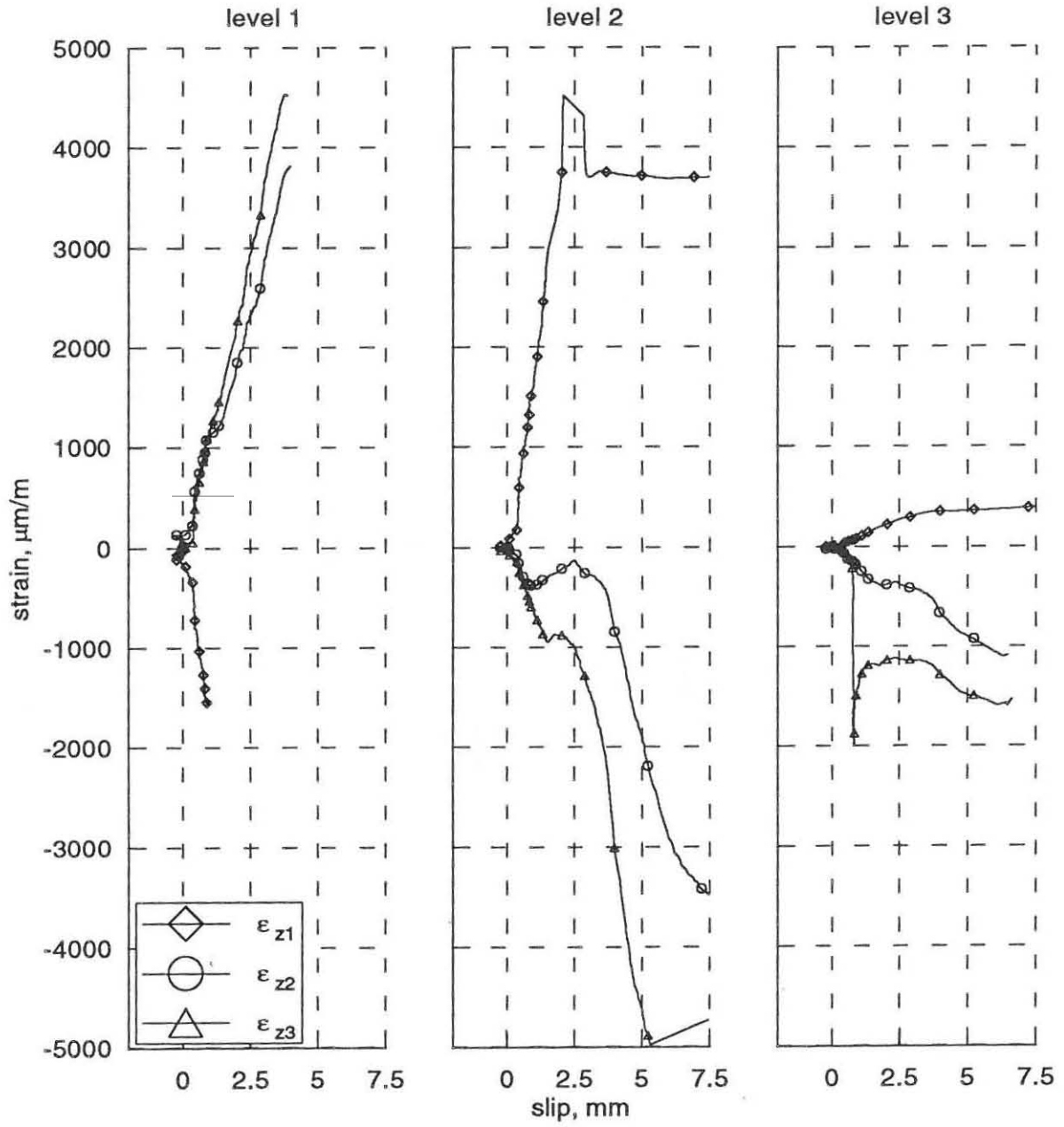
Strains of the headed stud connector.
specimen C2



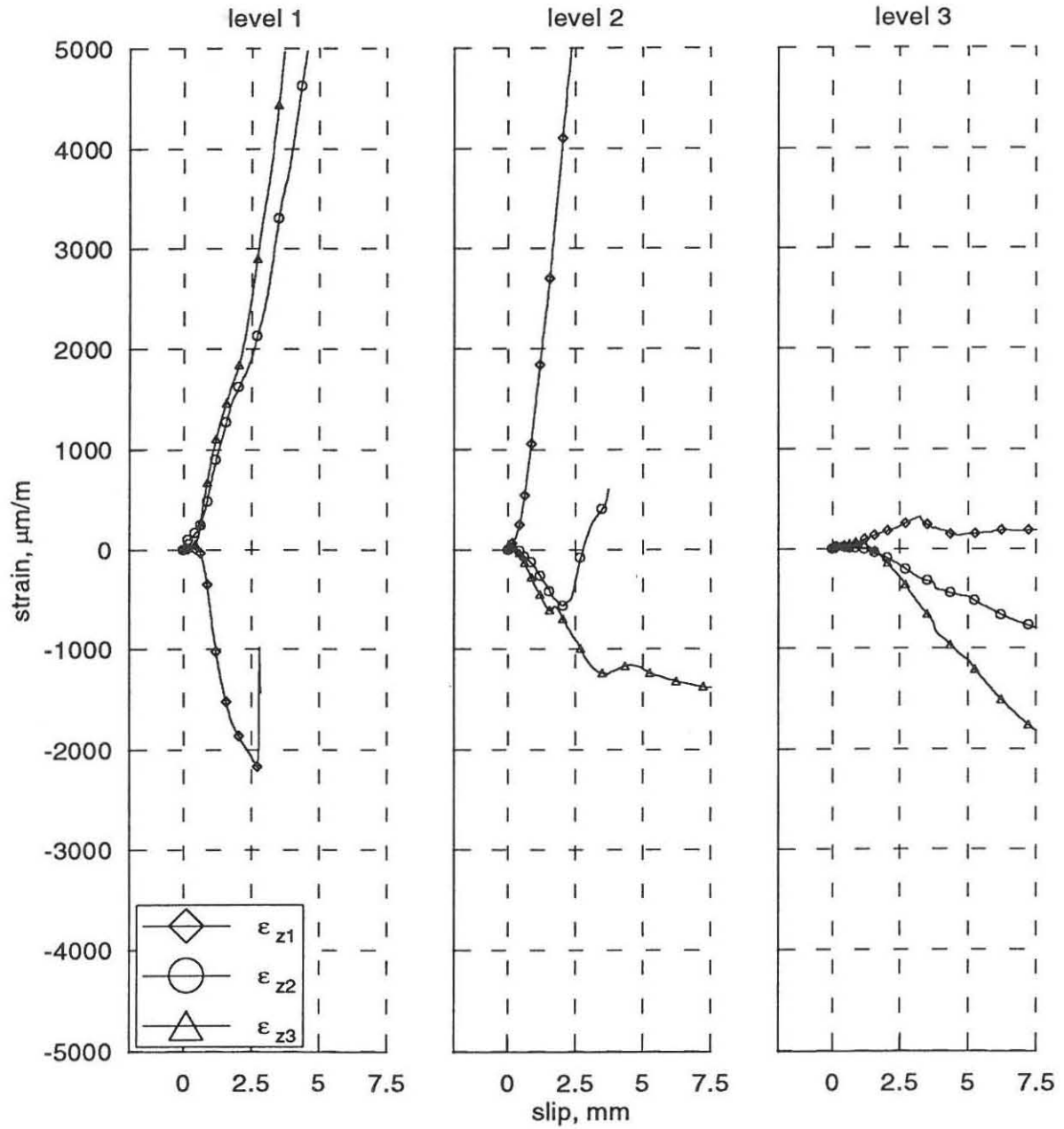
Strains of the headed stud connector.
specimen C3



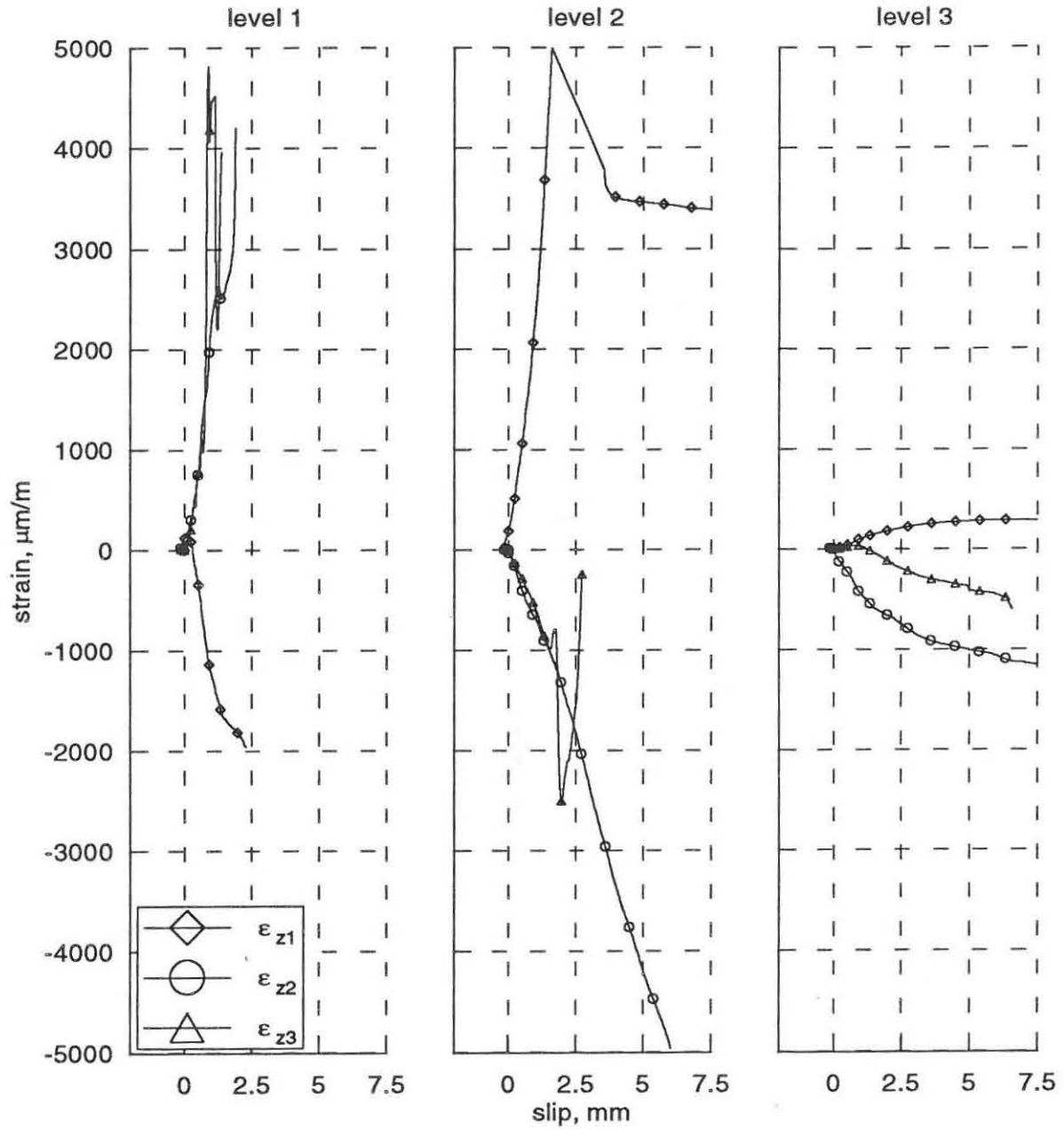
Strains of the headed stud connector.
specimen C4



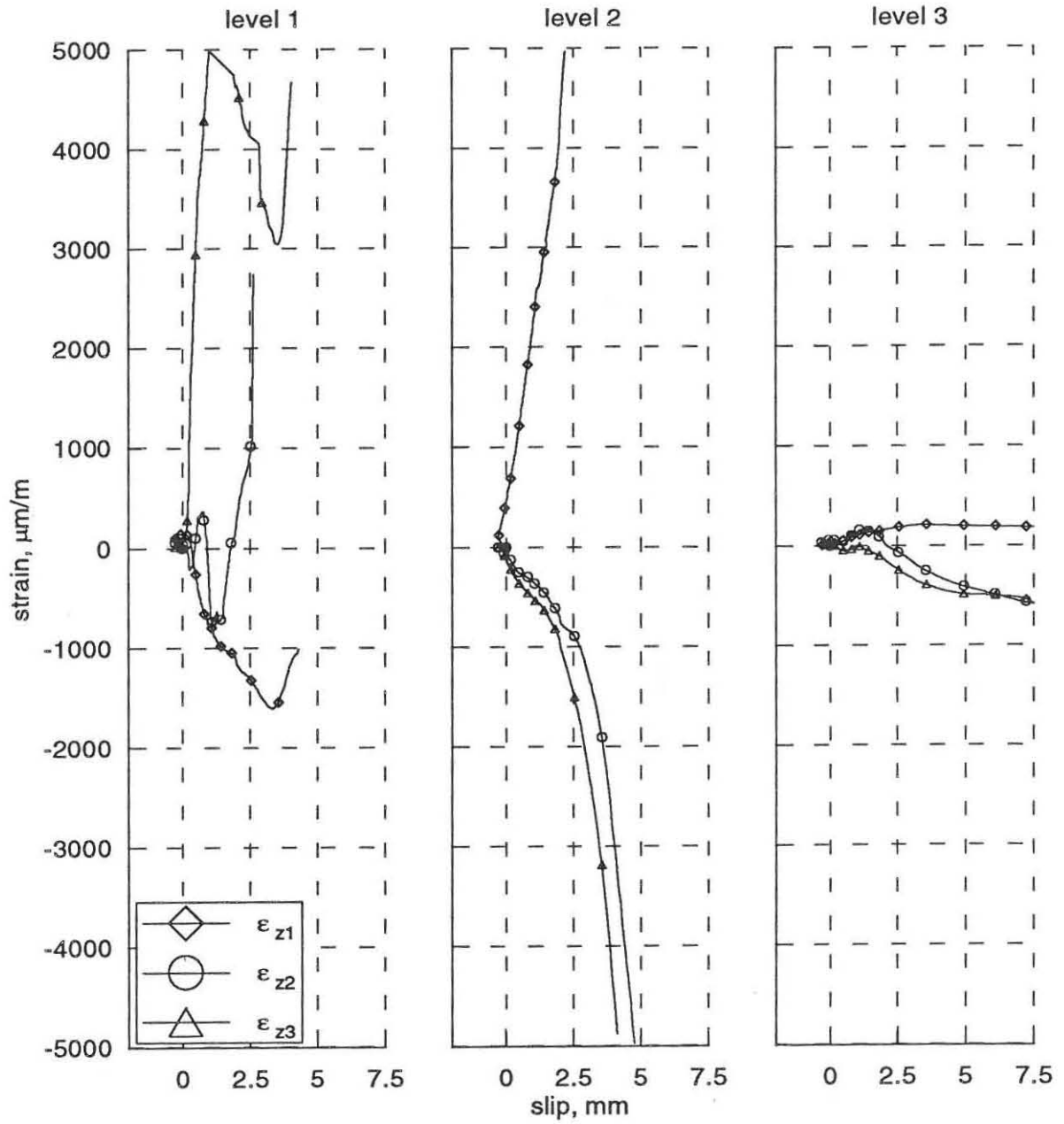
Strains of the headed stud connector.
specimen C5



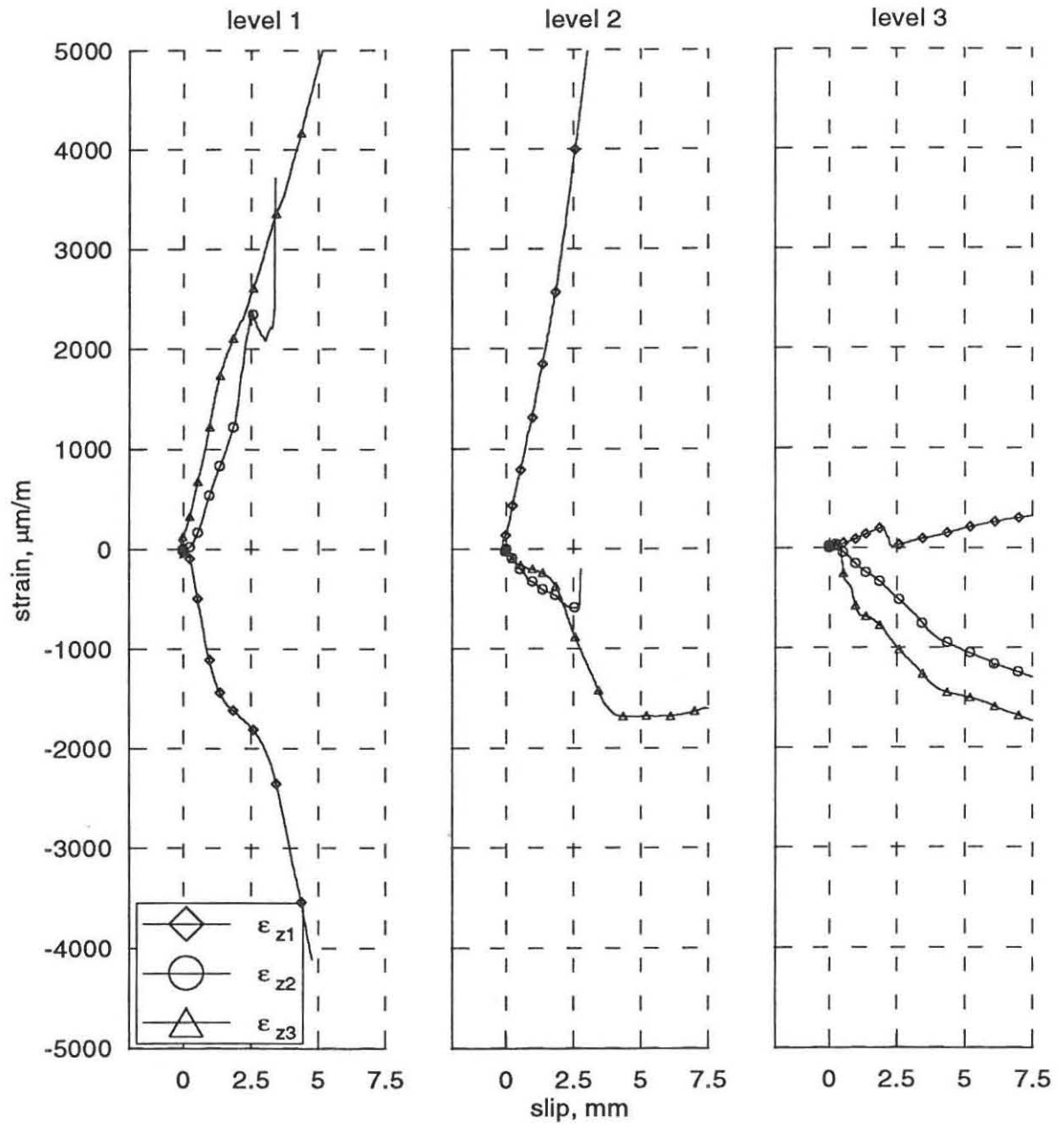
Strains of the headed stud connector.
specimen C6



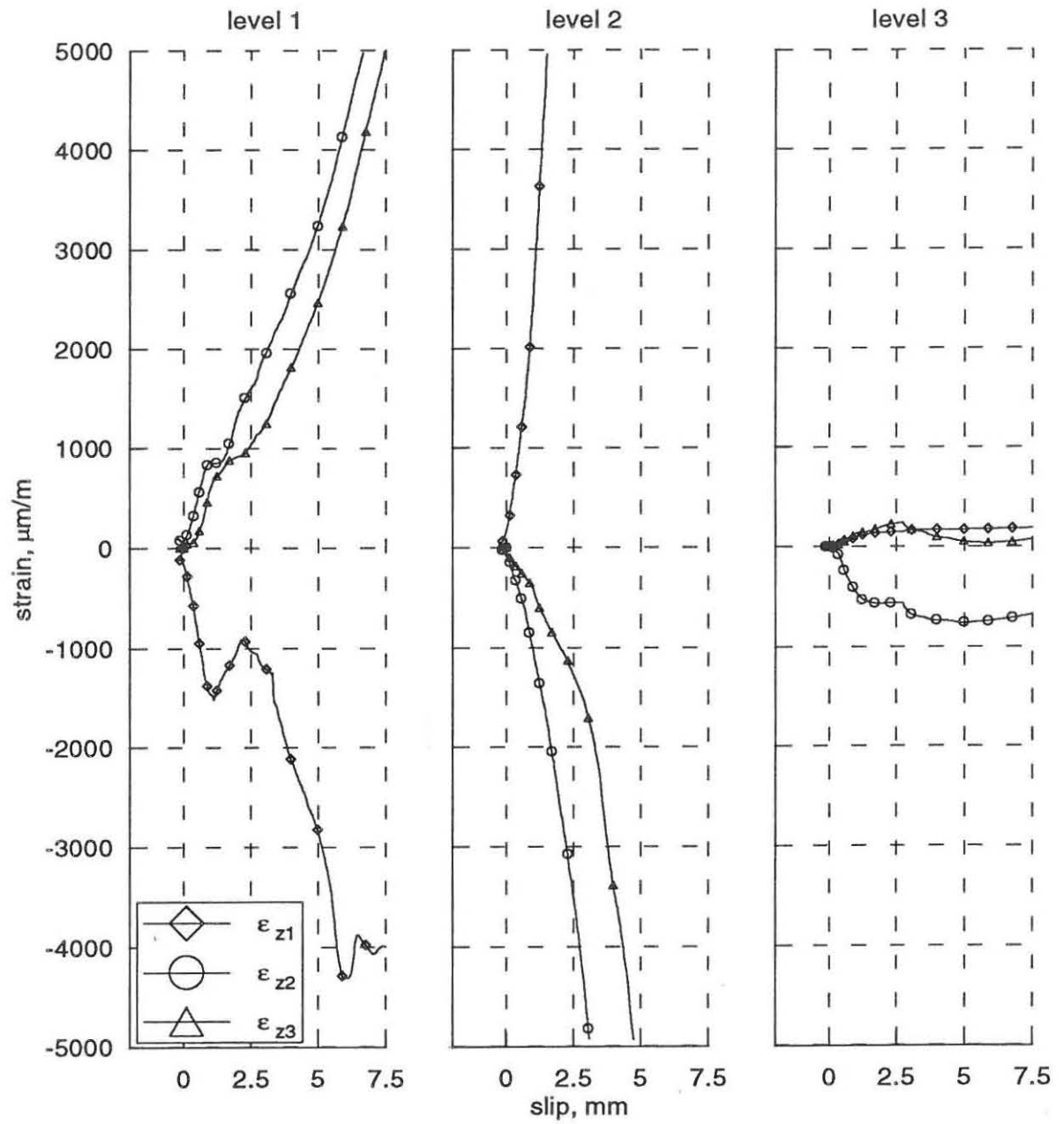
Strains of the headed stud connector.
specimen C8



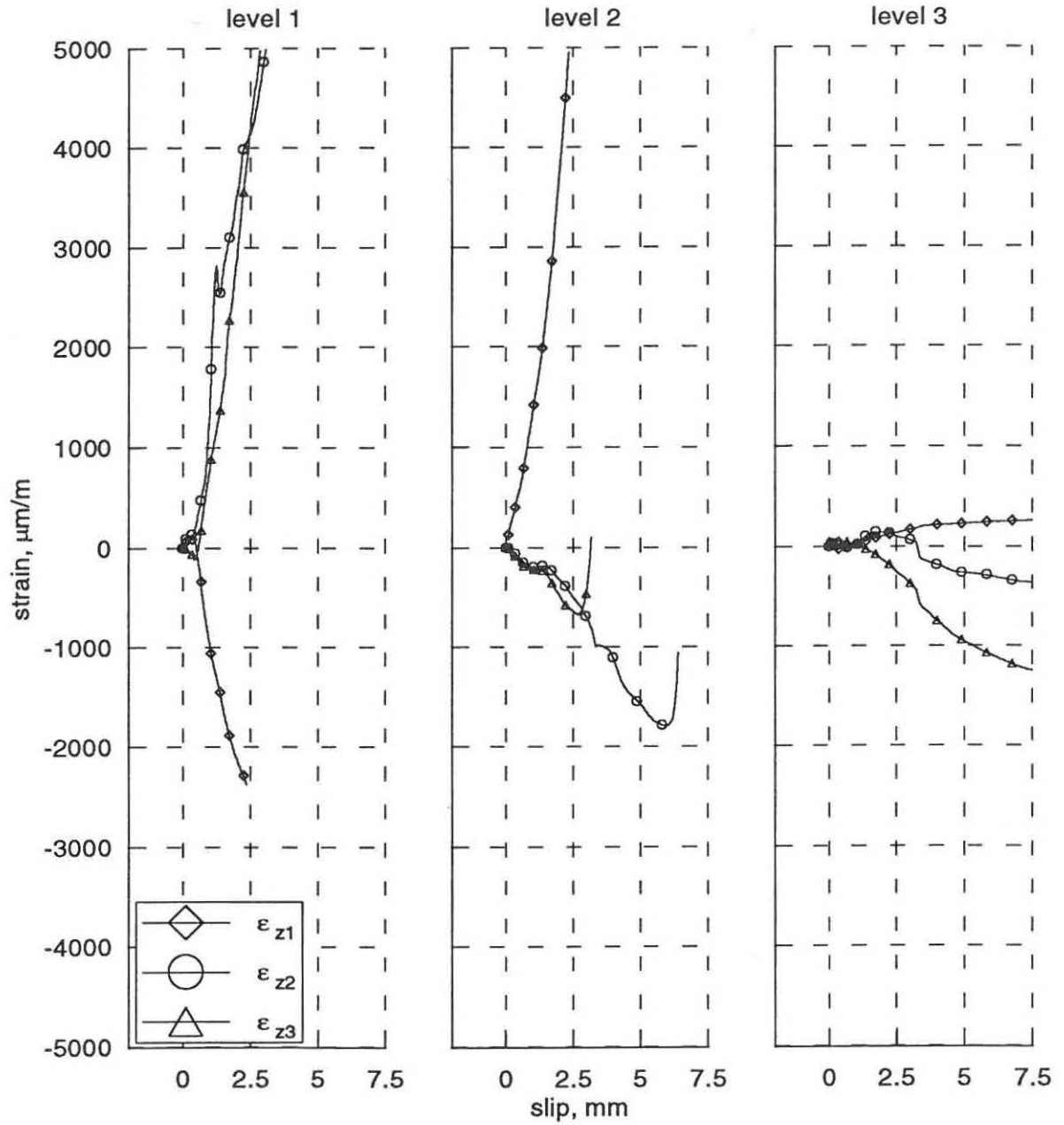
Strains of the headed stud connector.
specimen C9



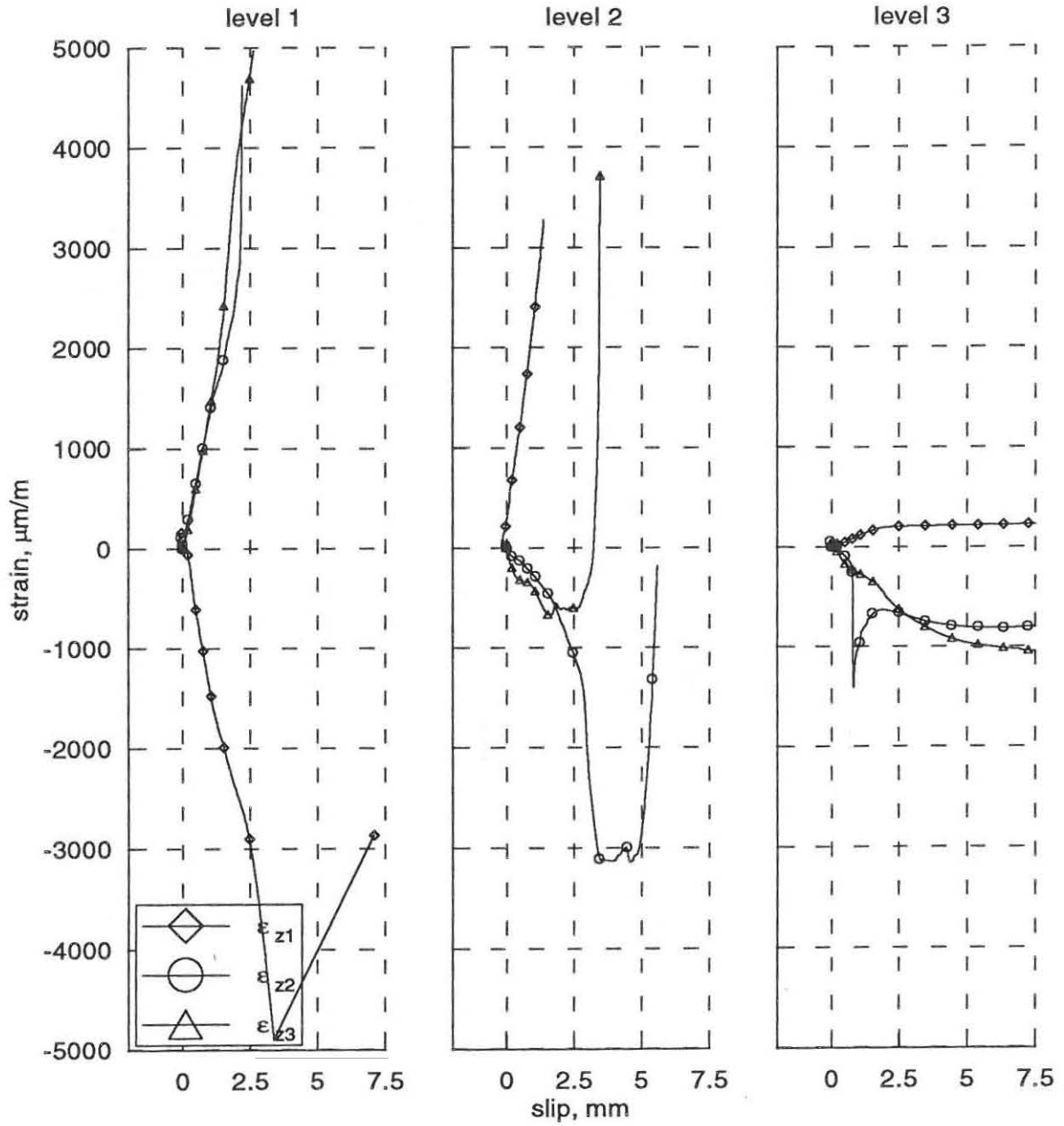
Strains of the headed stud connector.
specimen C10



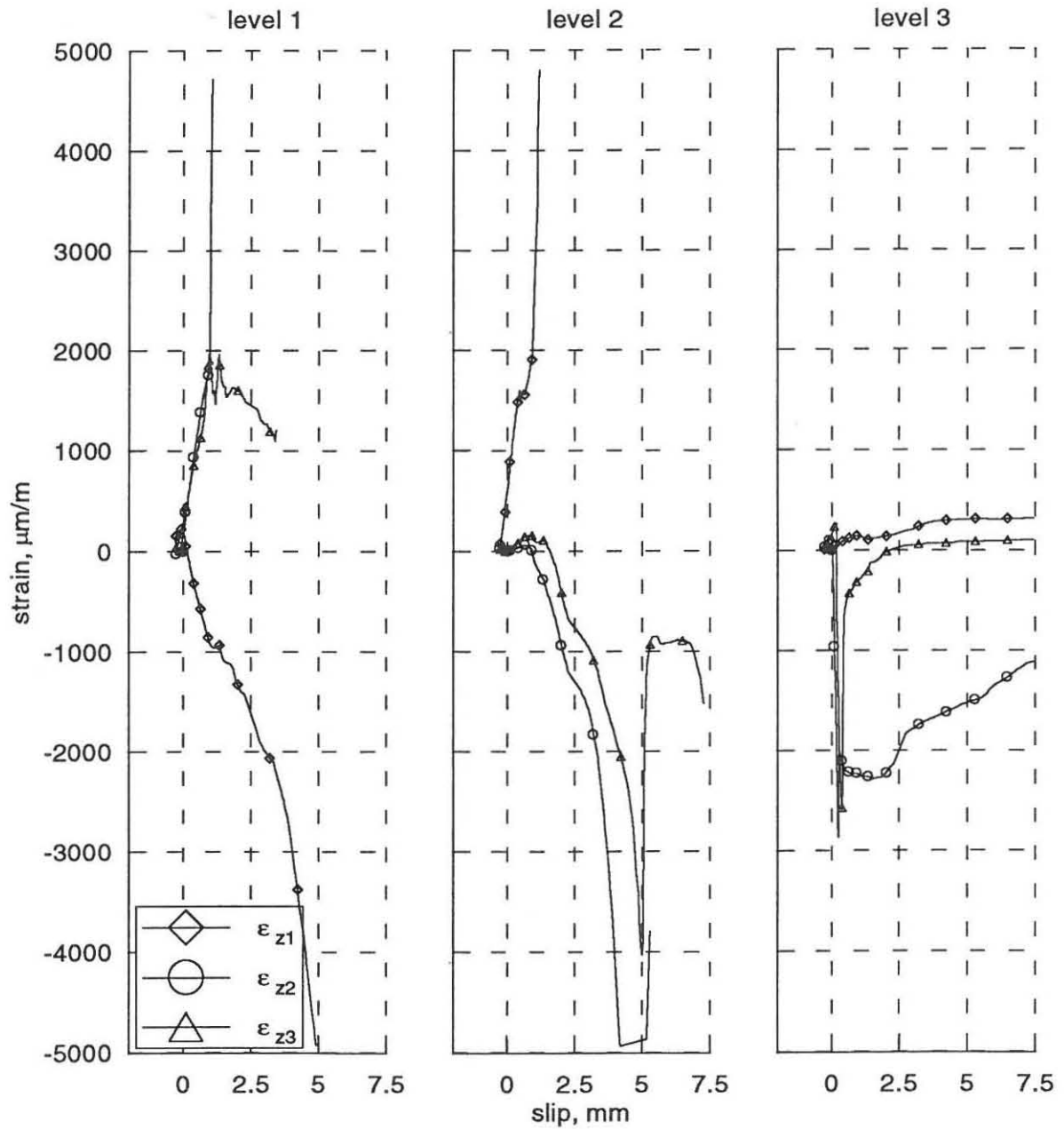
Strains of the headed stud connector.
specimen C11



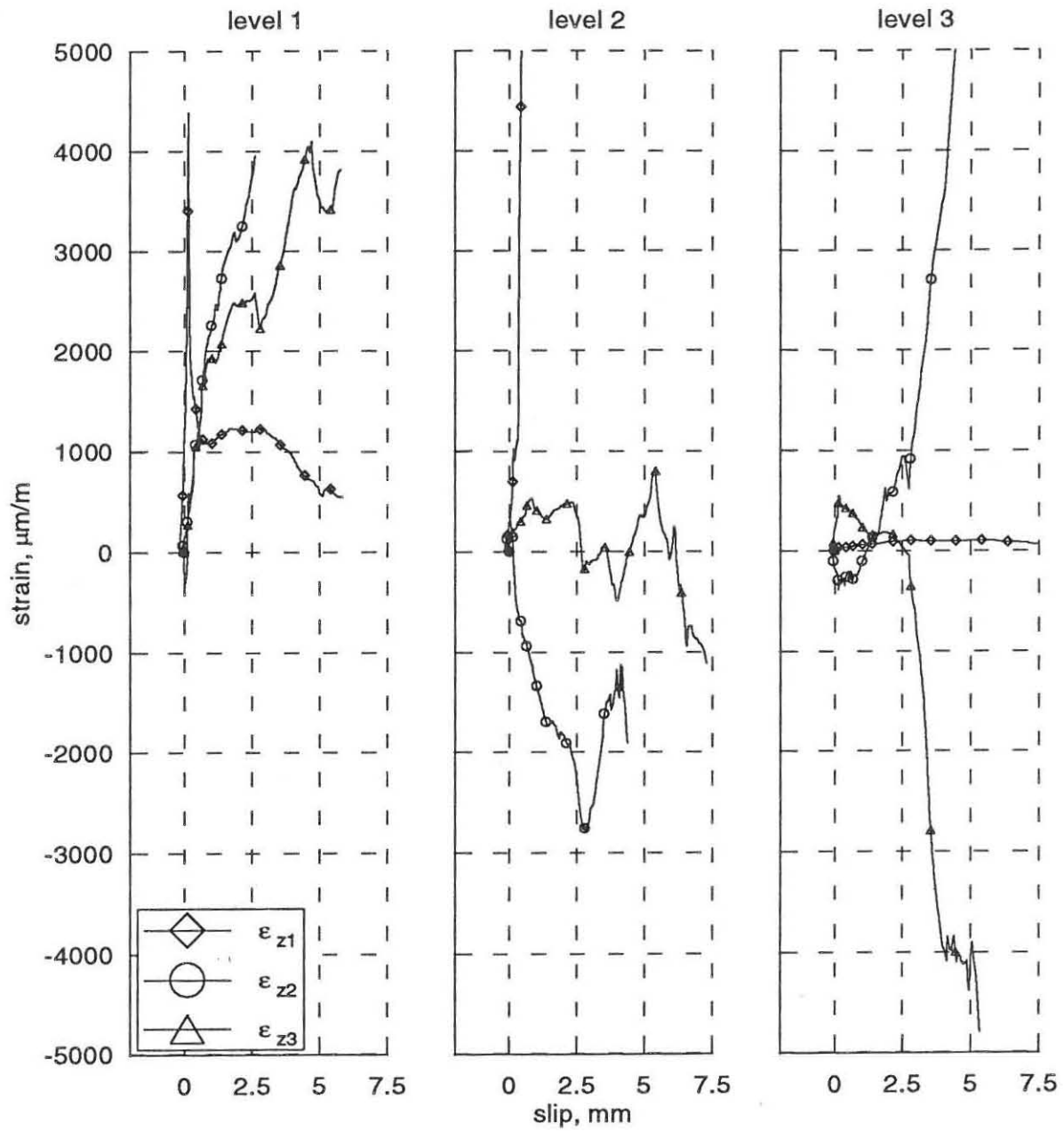
Strains of the headed stud connector.
specimen C12



Strains of the headed stud connector.
specimen C13

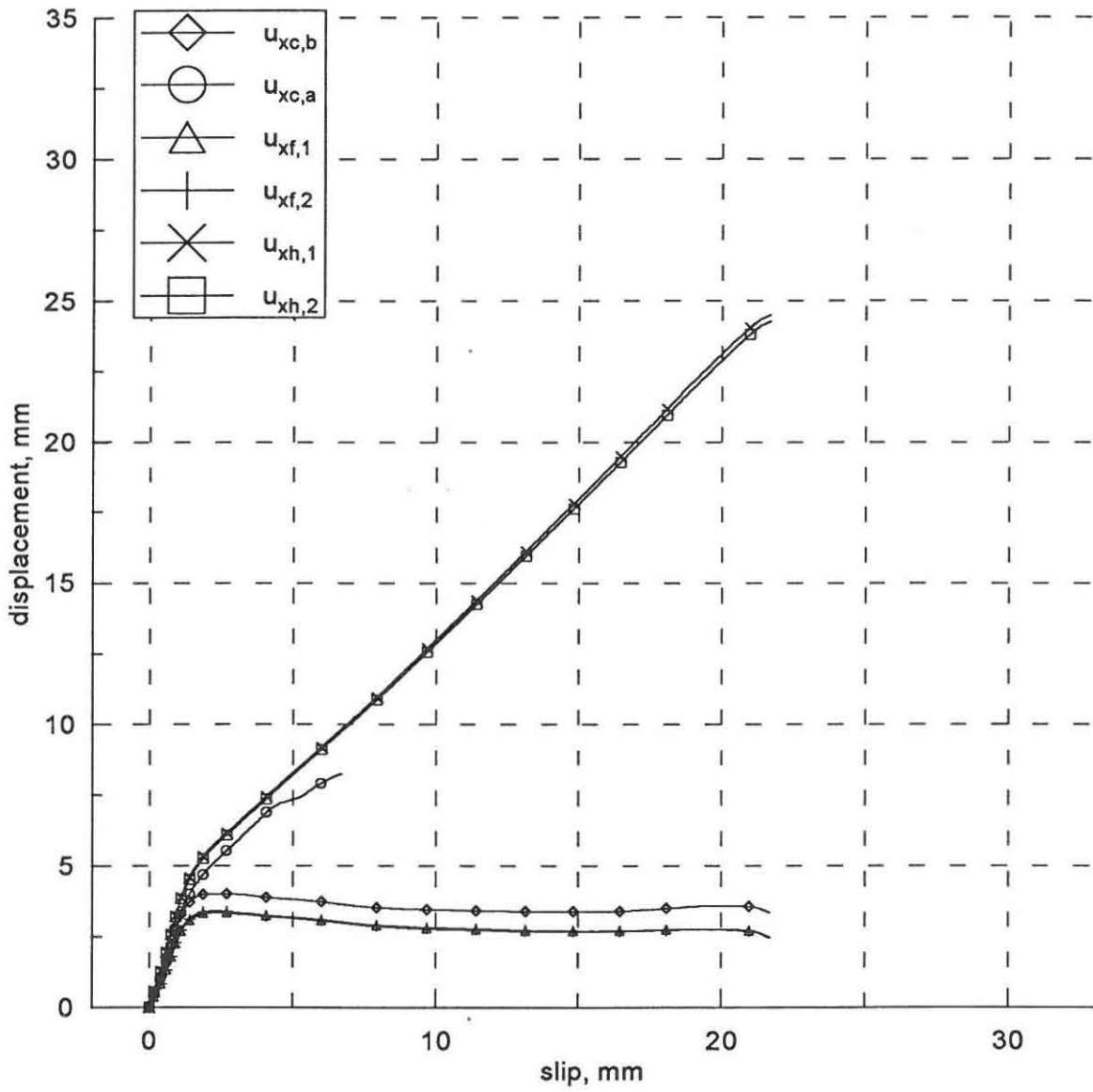


Strains of the headed stud connector.
specimen C14

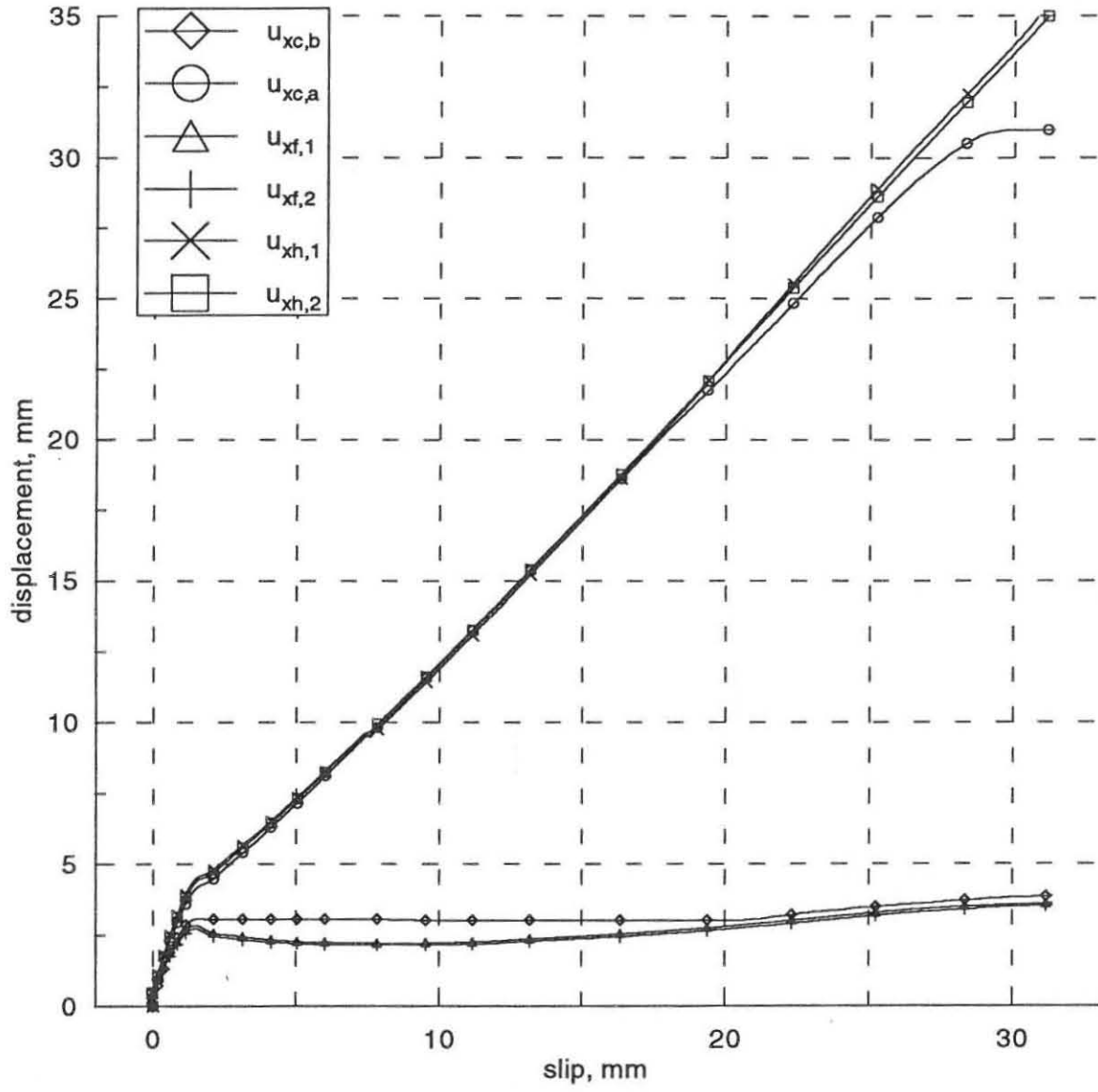


11.5 Displacements: $u_{xc,b}$, $u_{xc,a}$, $u_{xf,1}$, $u_{xf,2}$, $u_{xh,1}$ & $u_{xh,2}$.

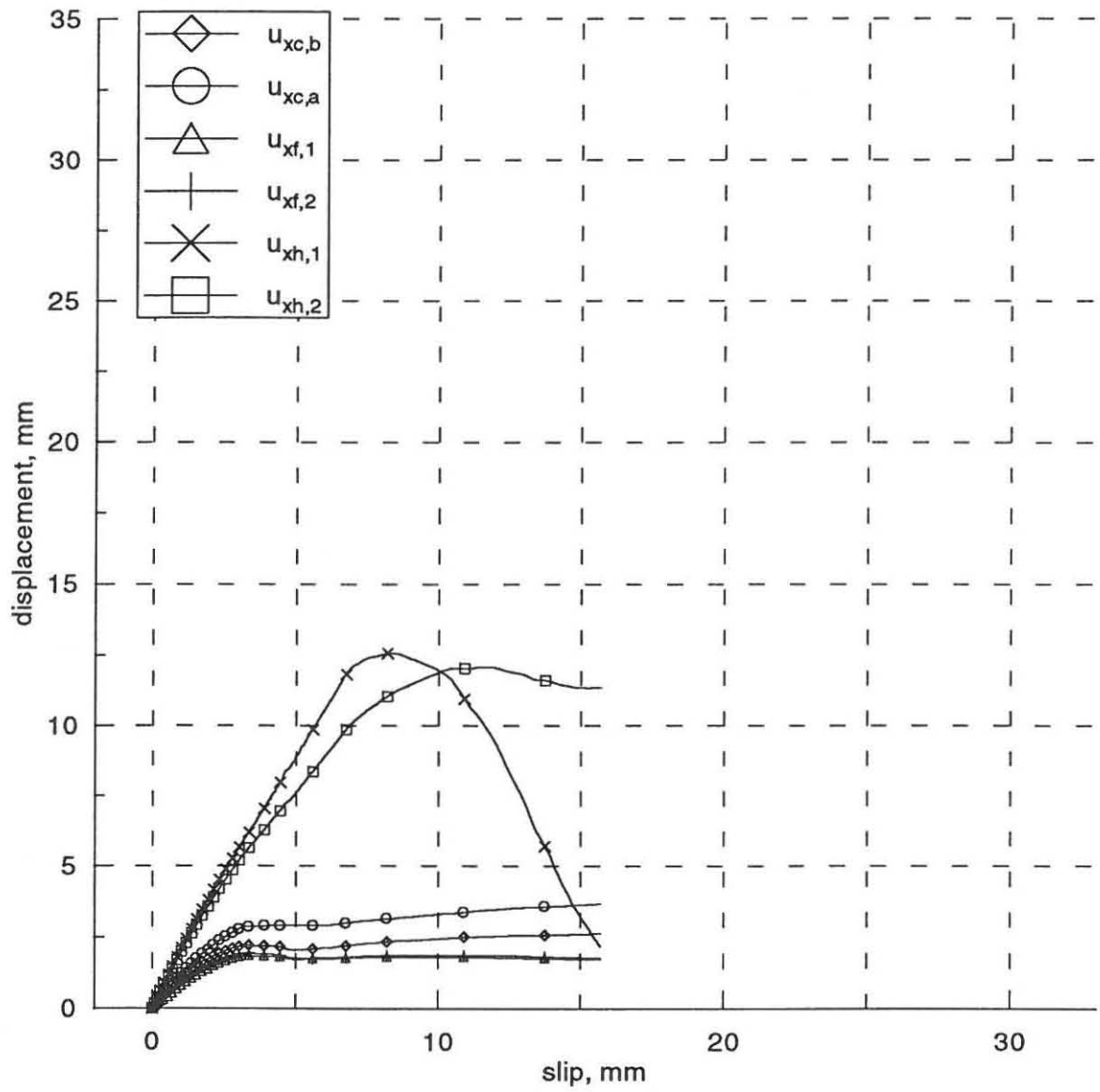
Displacements.
specimen 2

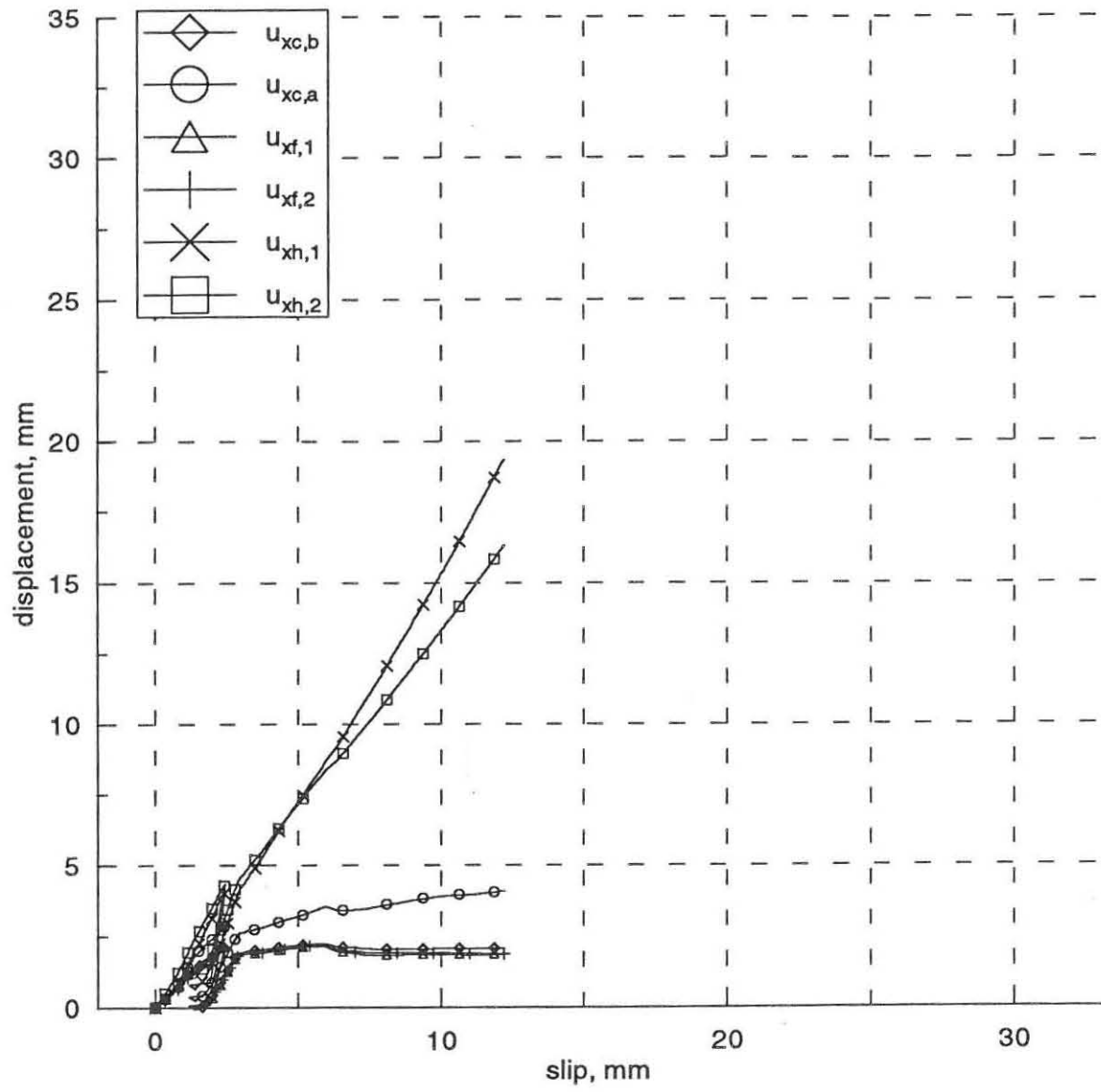


Displacements.
specimen 3

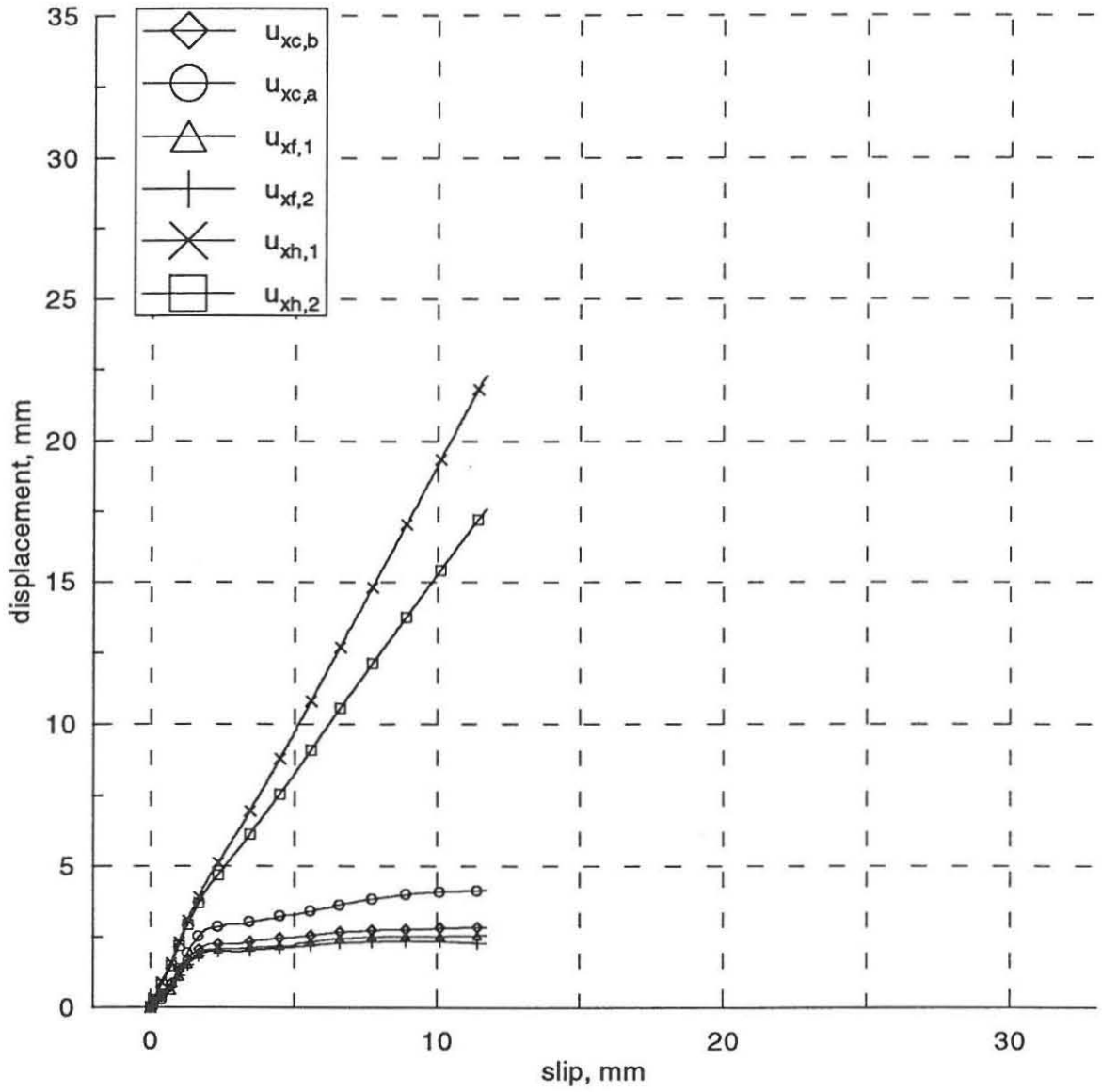


Displacements.
specimen A1

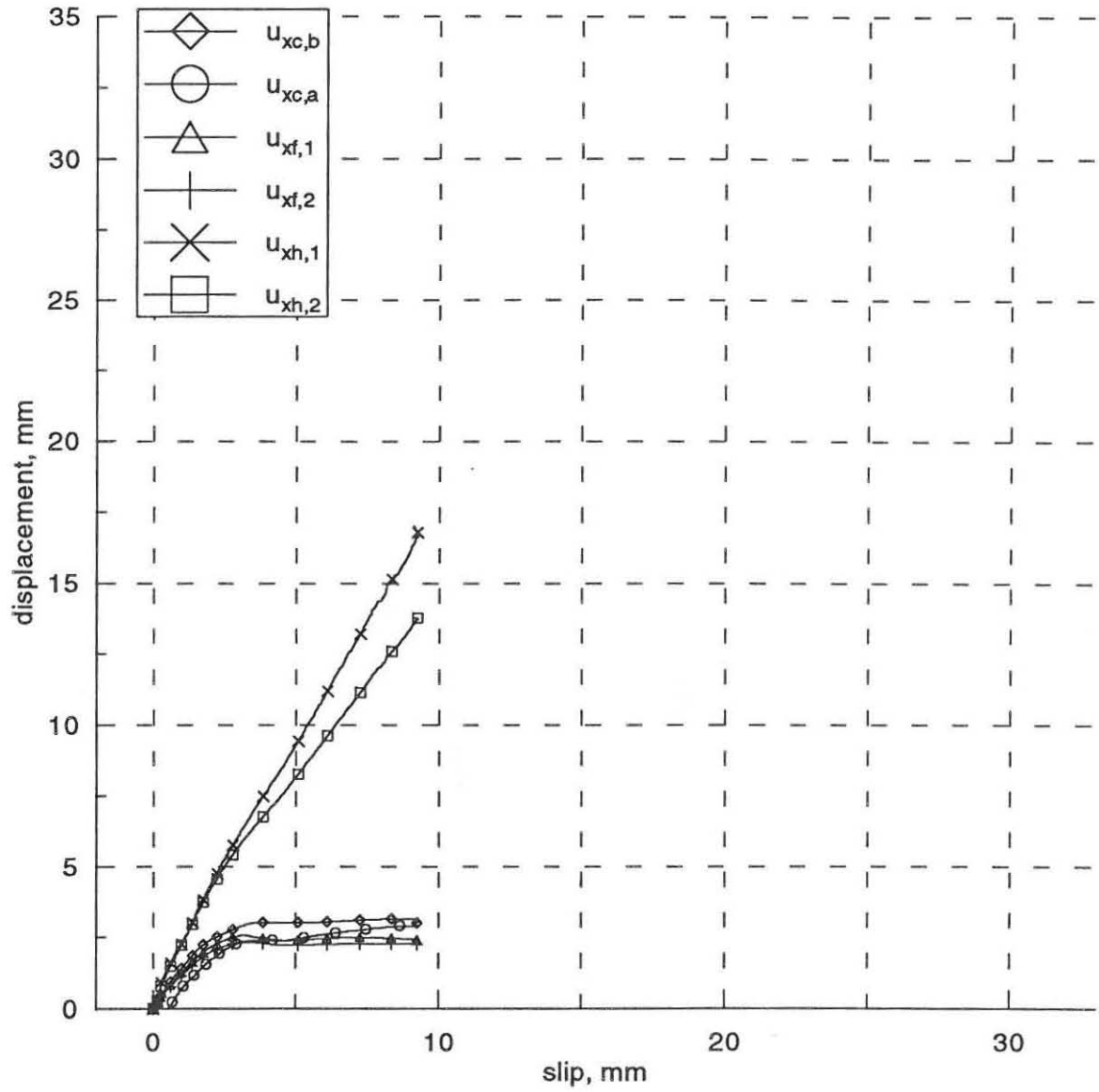


Displacements.
specimen A2

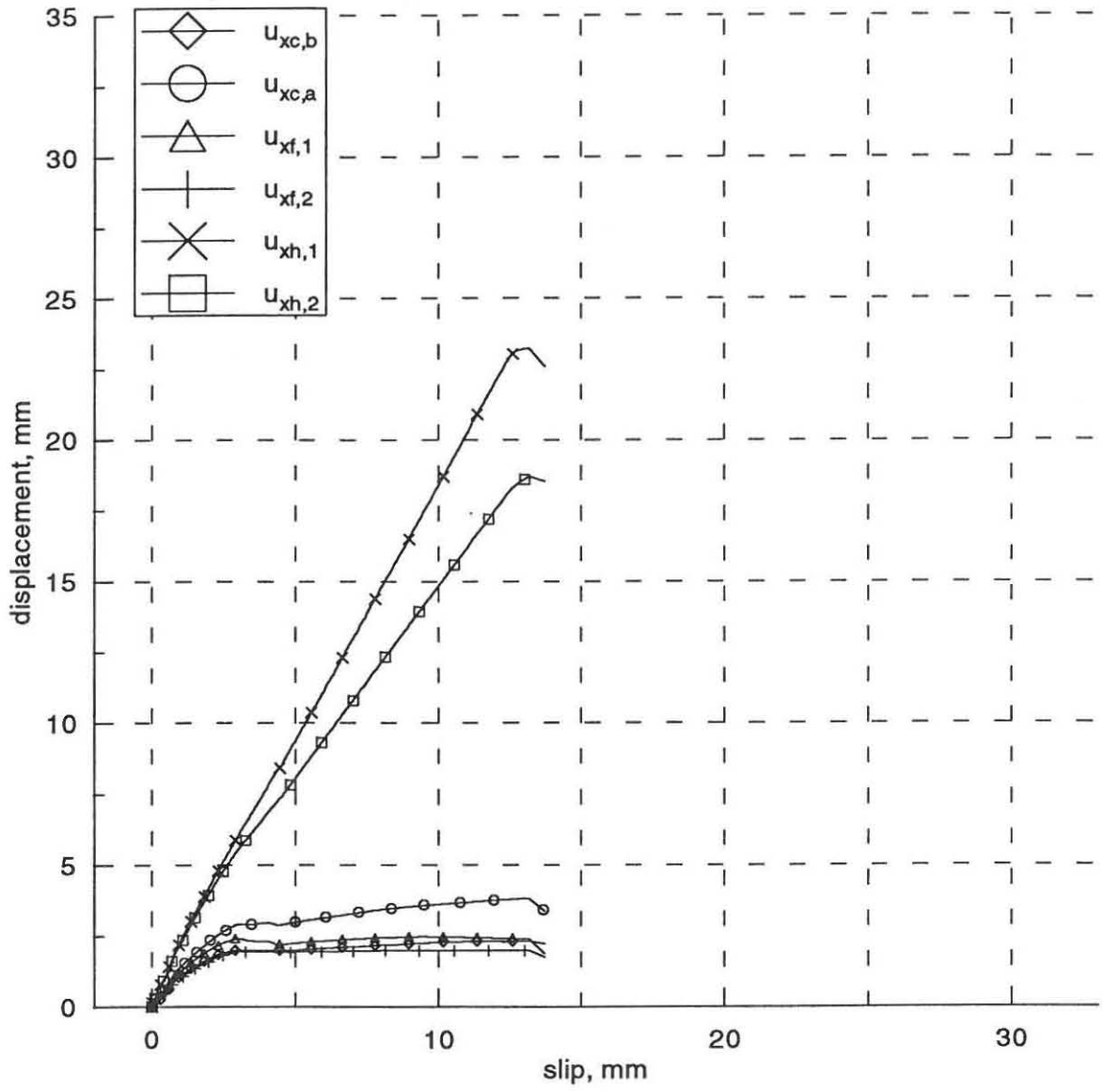
Displacements.
specimen A3



Displacements.
specimen B1

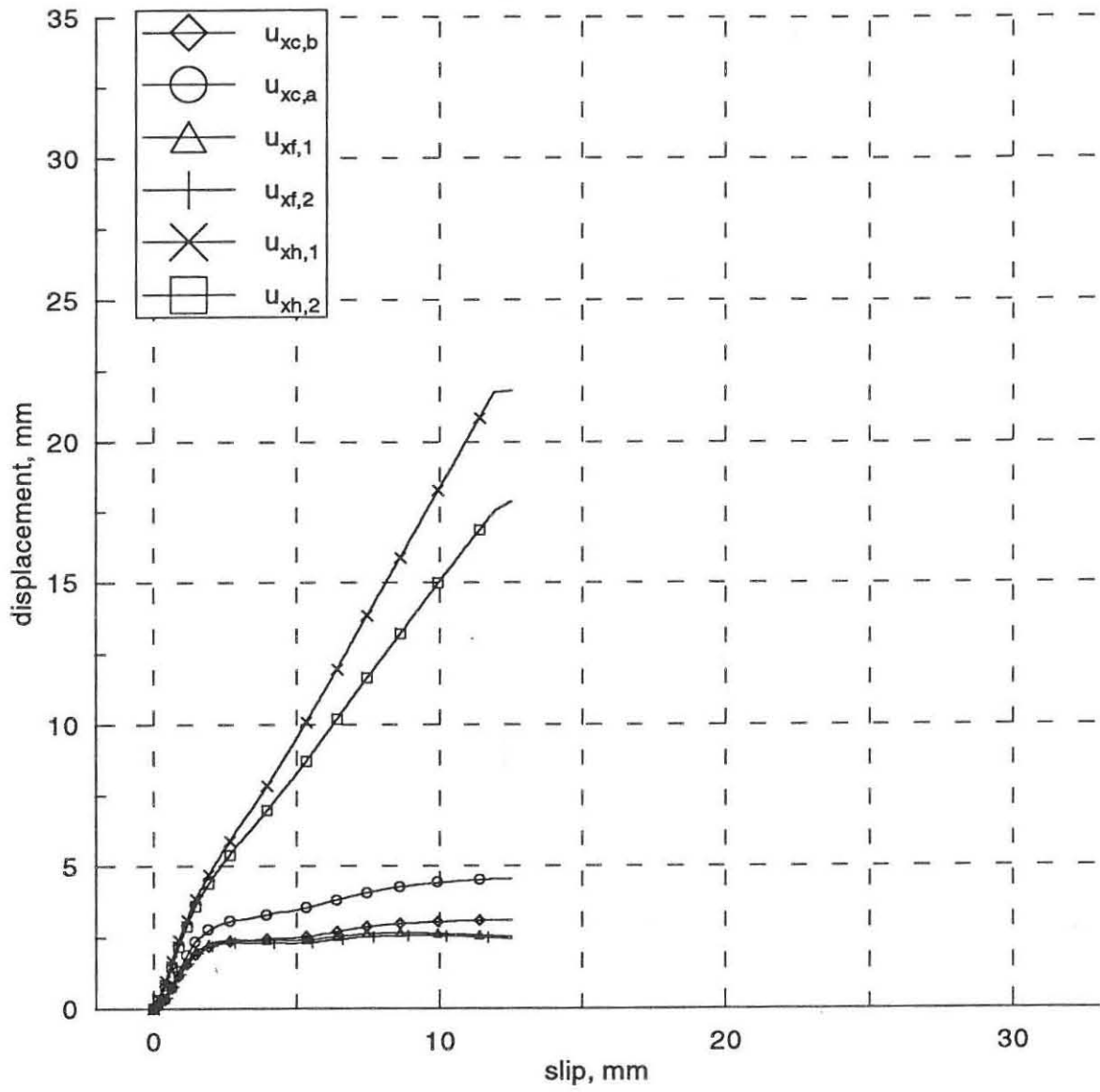


Displacements.
specimen B2

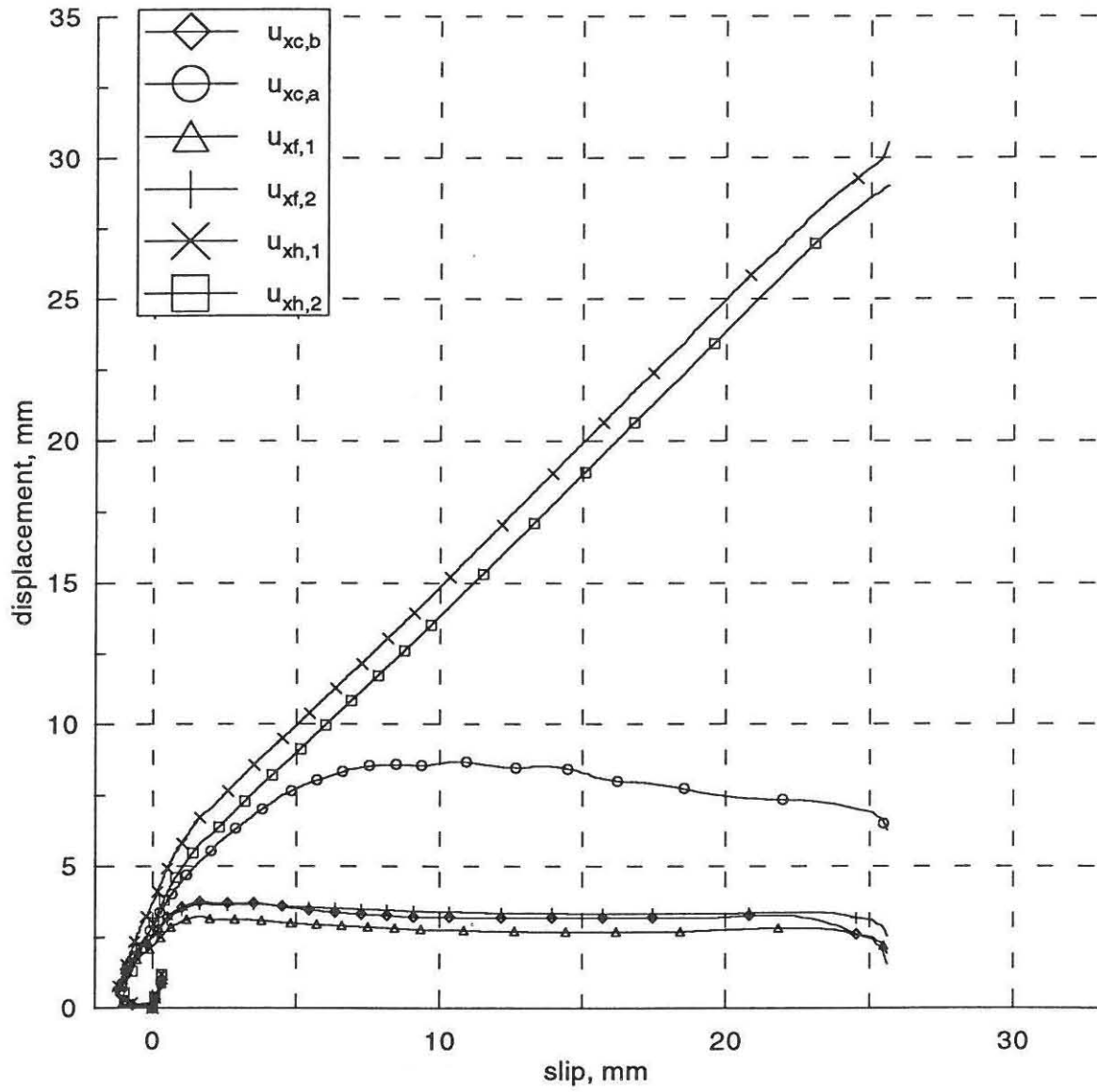


Displacements.

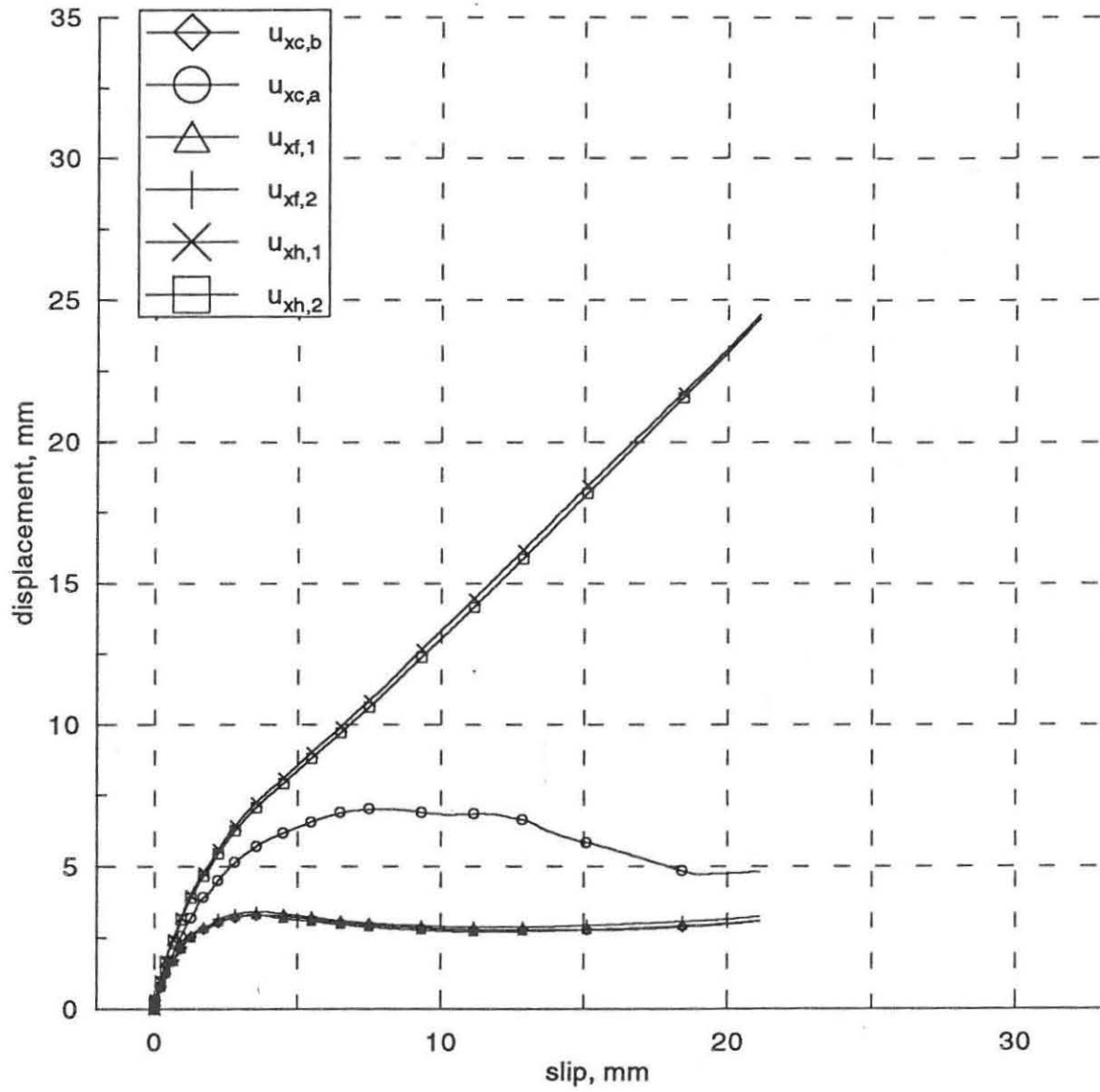
specimen B3



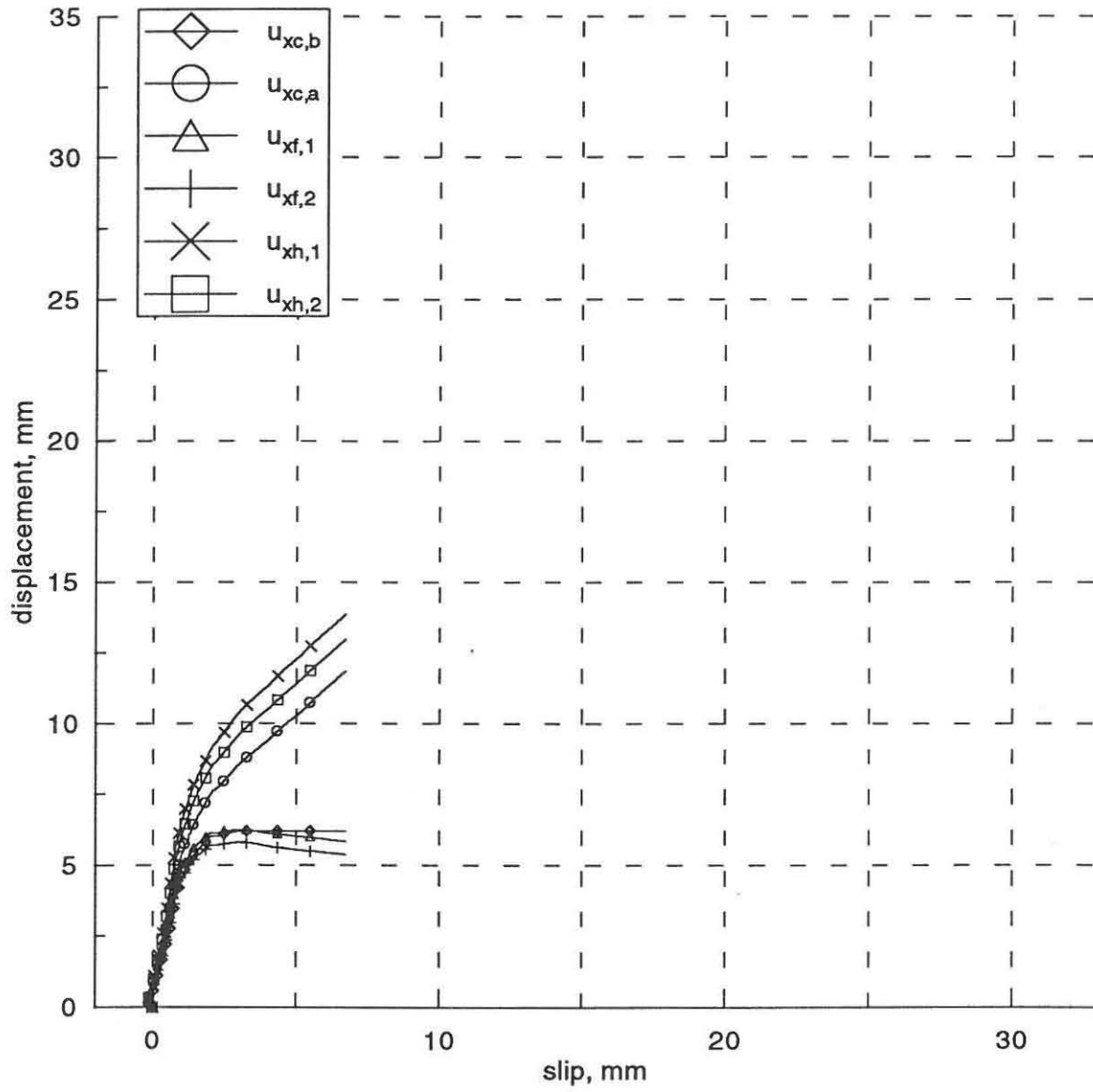
Displacements.
specimen C1



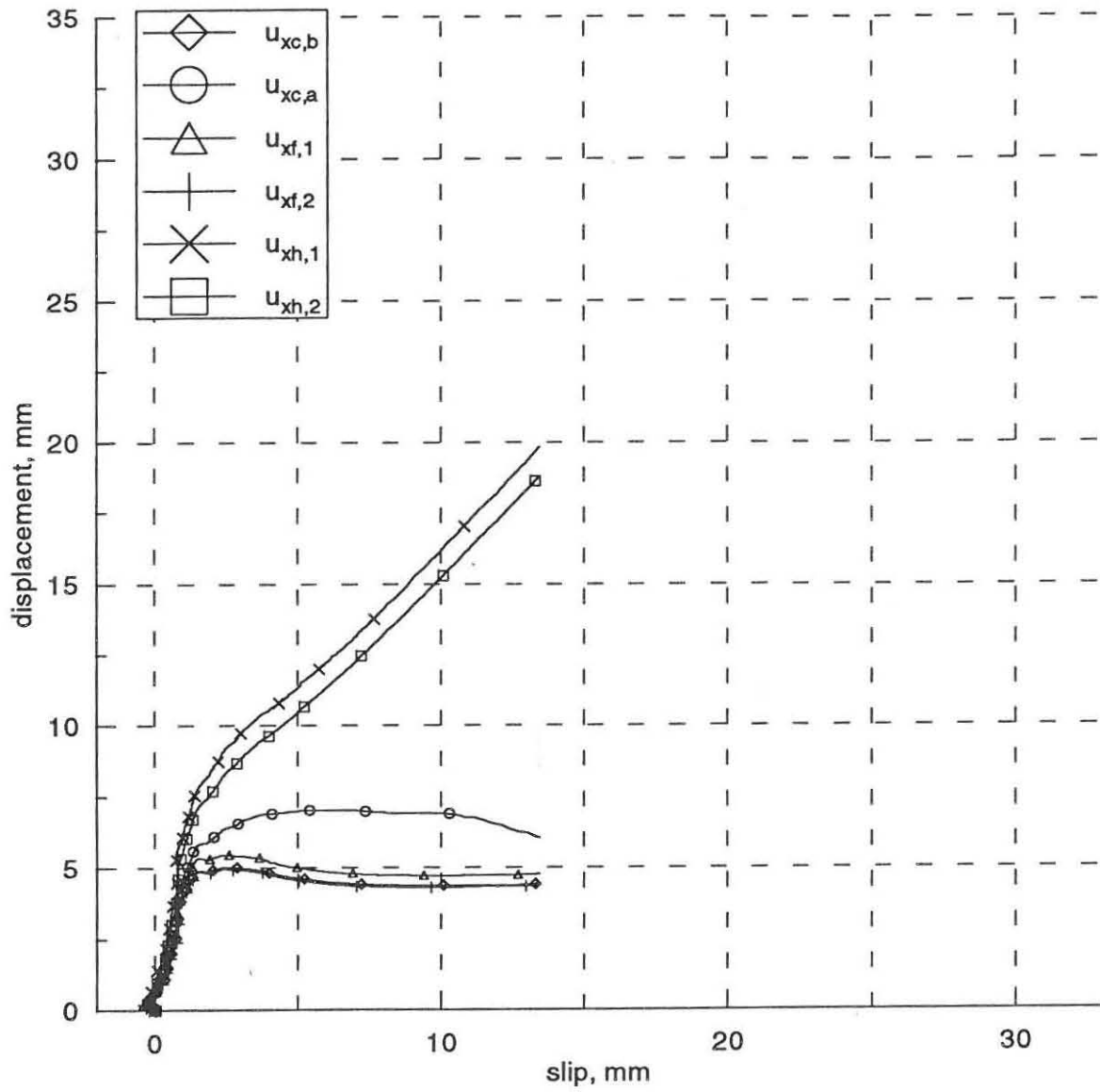
Displacements.
specimen C2



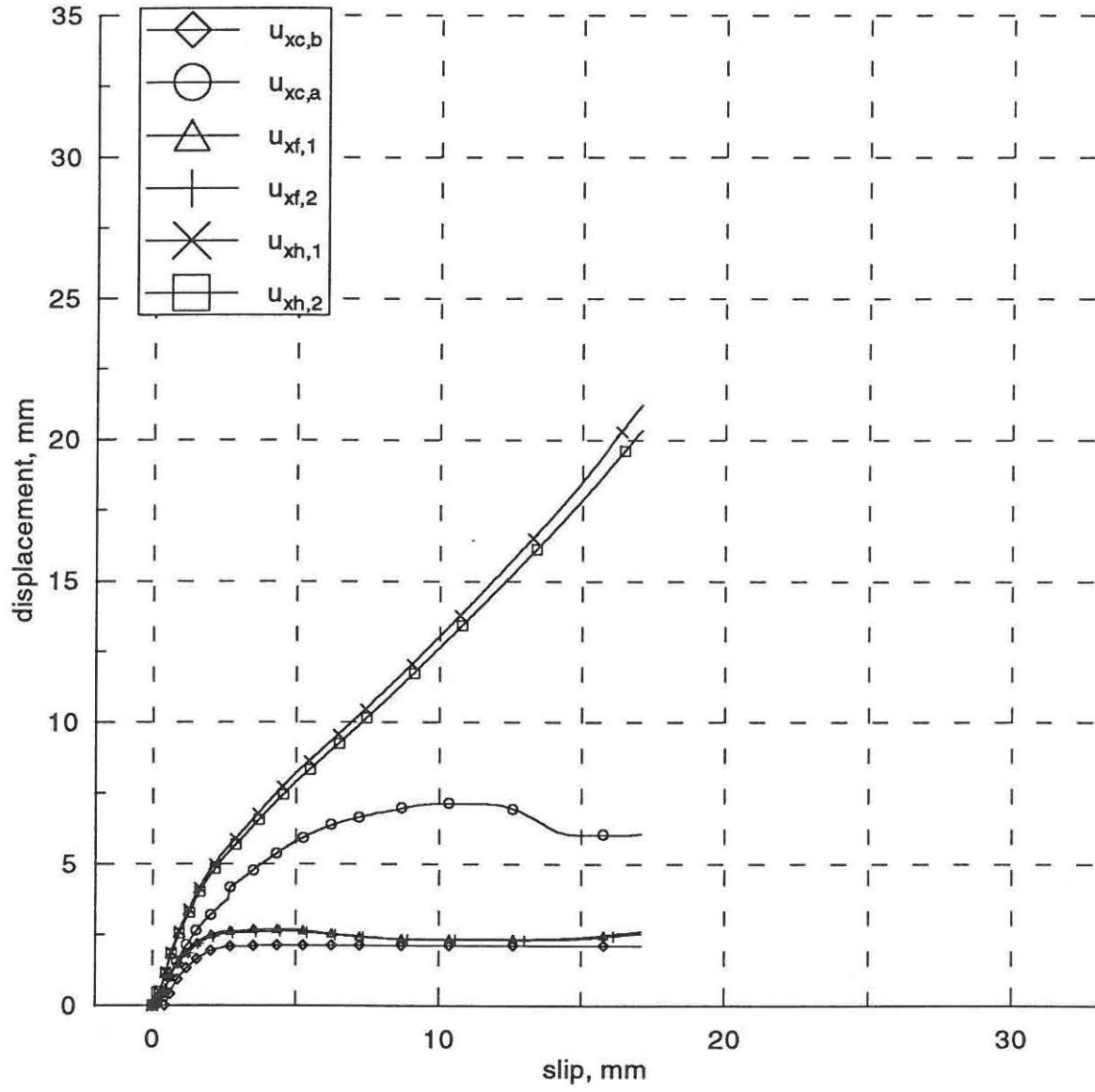
Displacements.
specimen C3



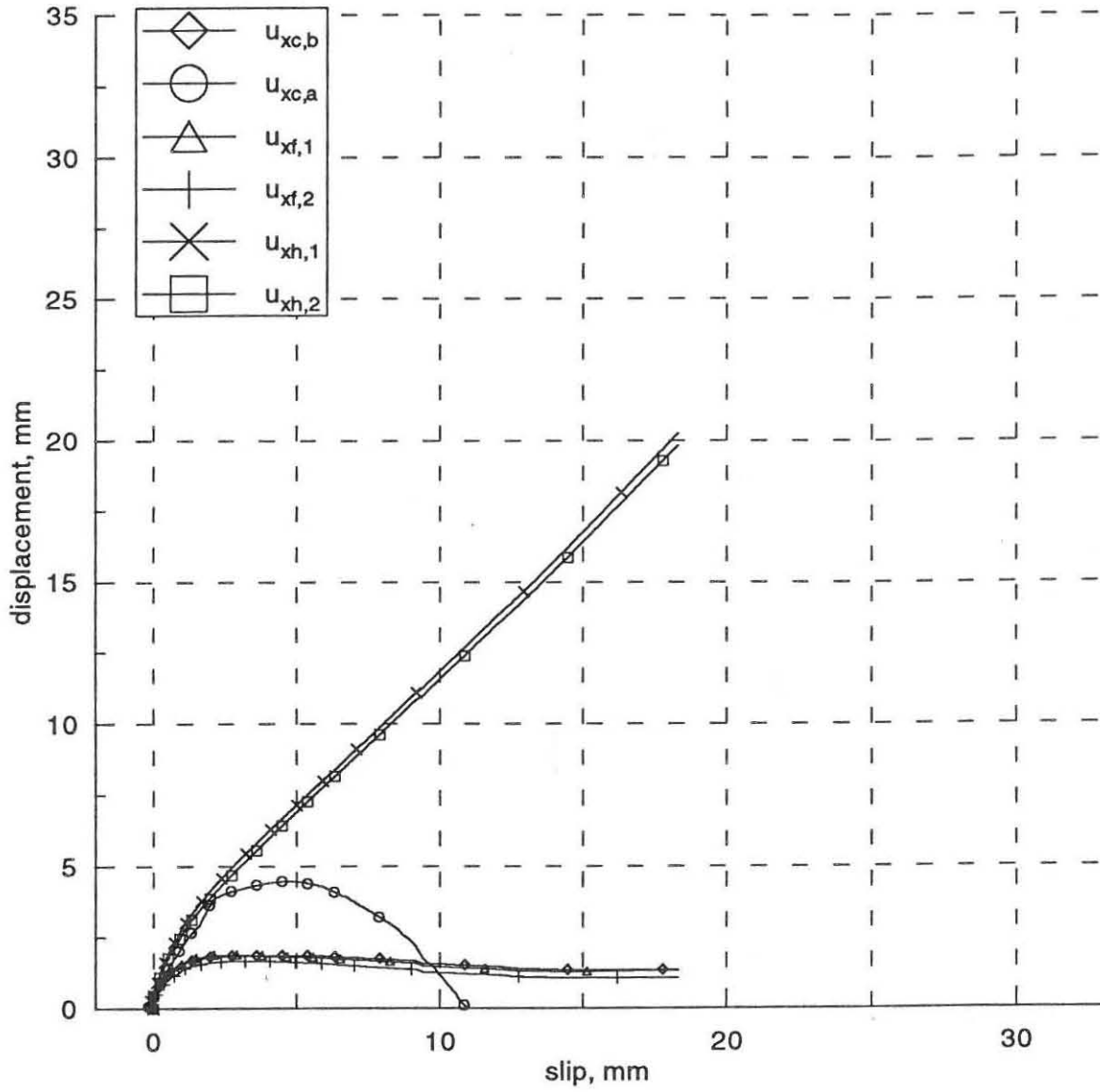
Displacements.
specimen C4



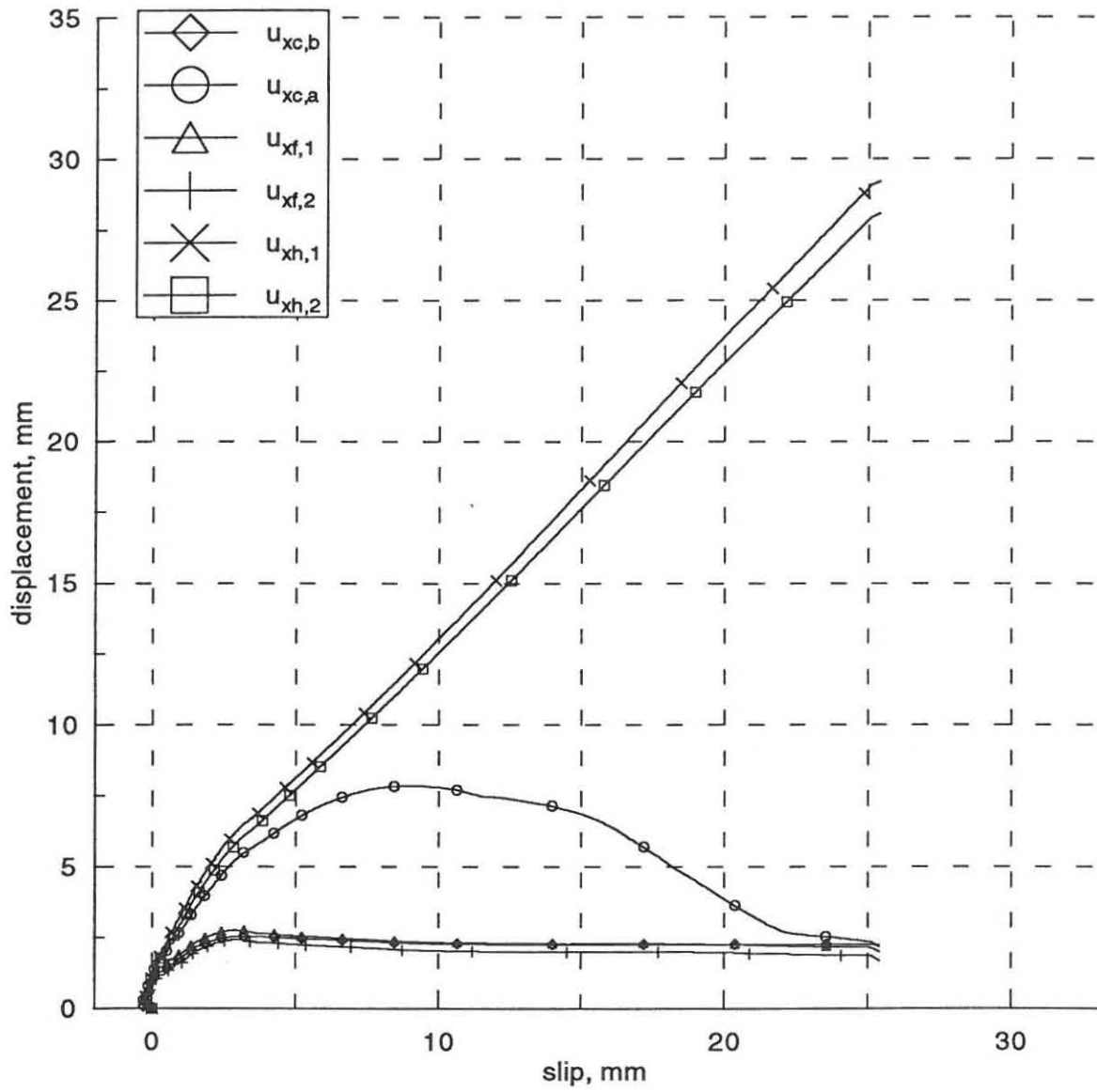
Displacements.
specimen C5



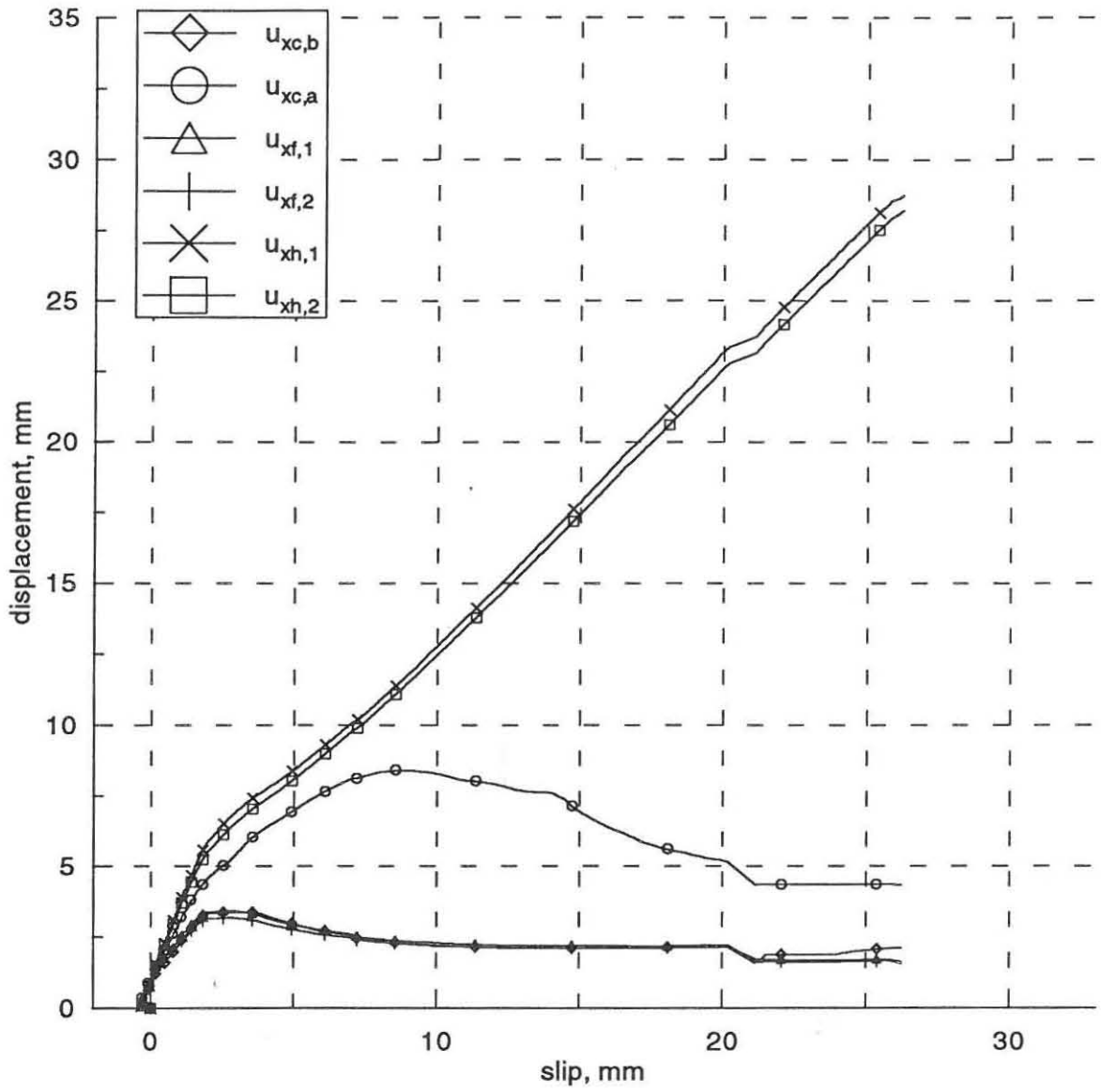
Displacements.
specimen C6



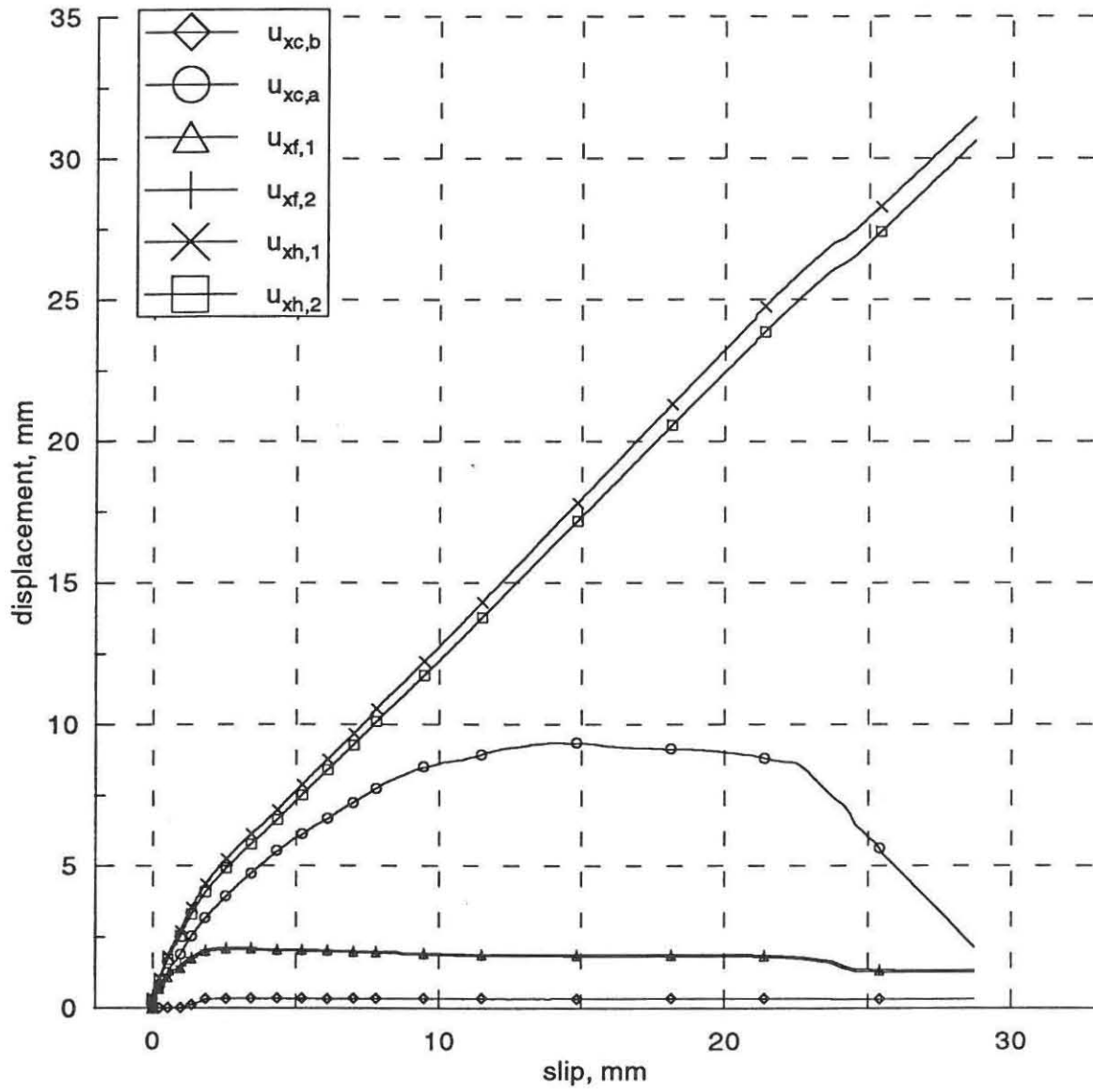
Displacements.
specimen C7



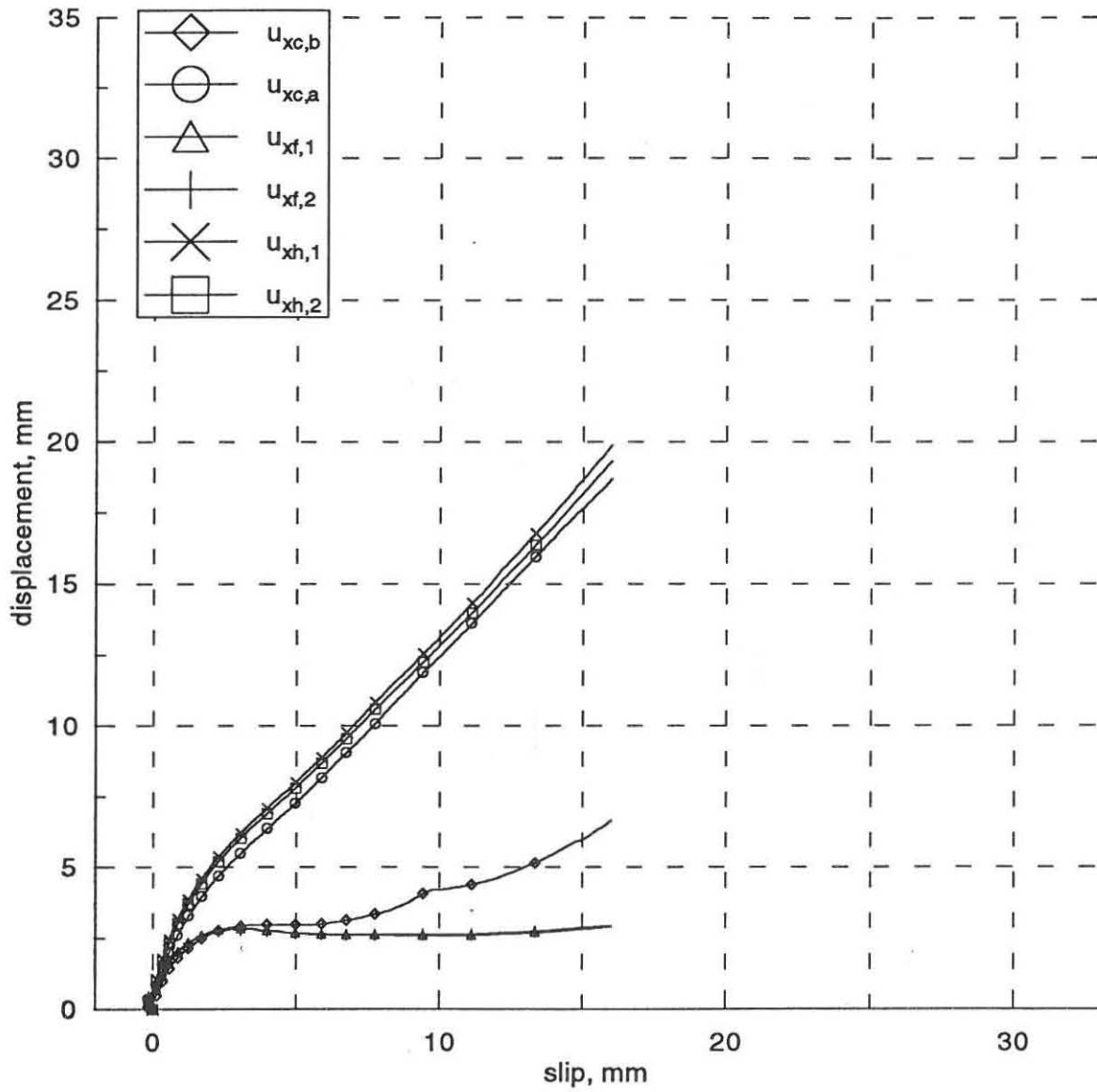
Displacements.
specimen C8



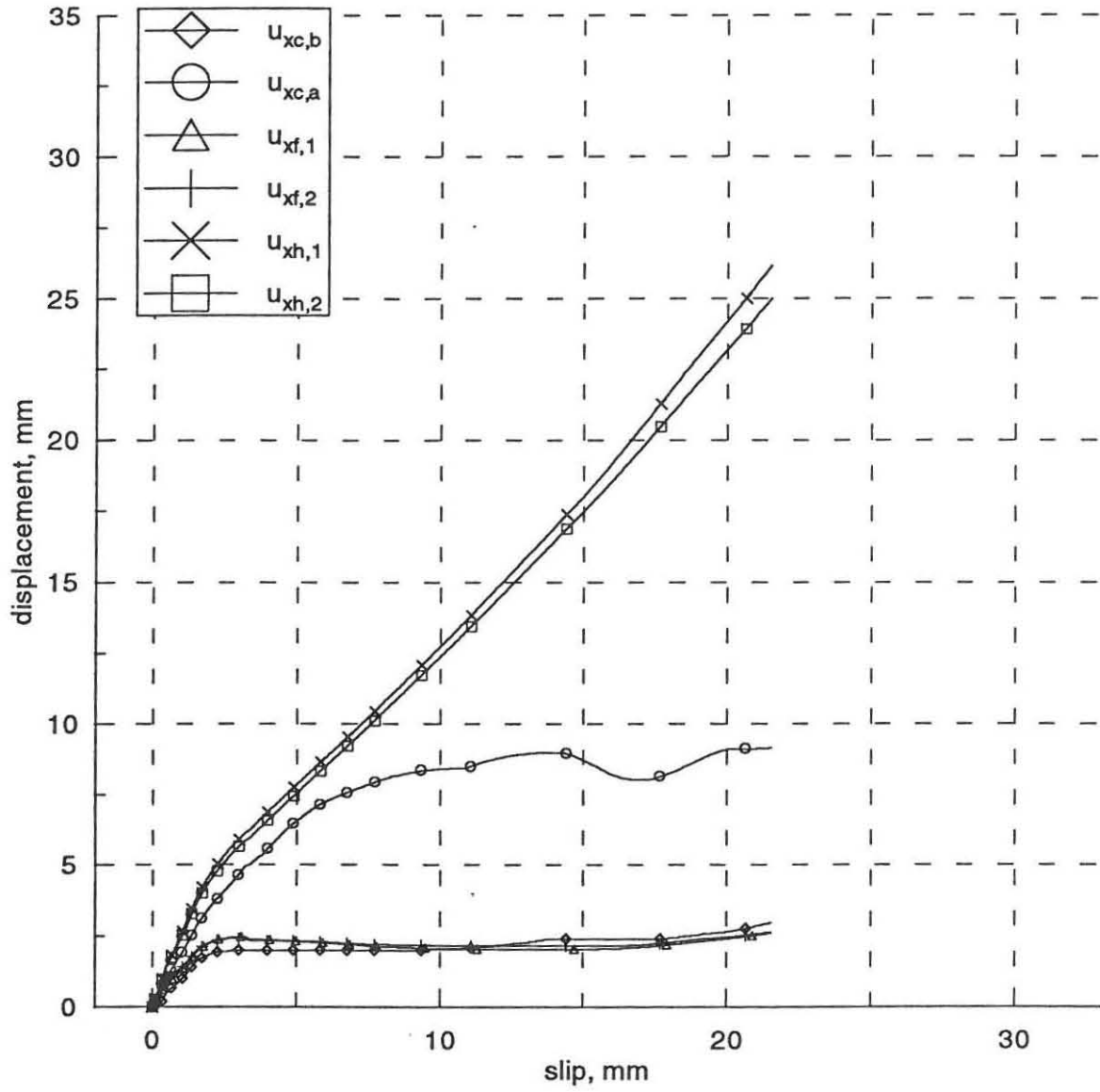
Displacements.
specimen C9



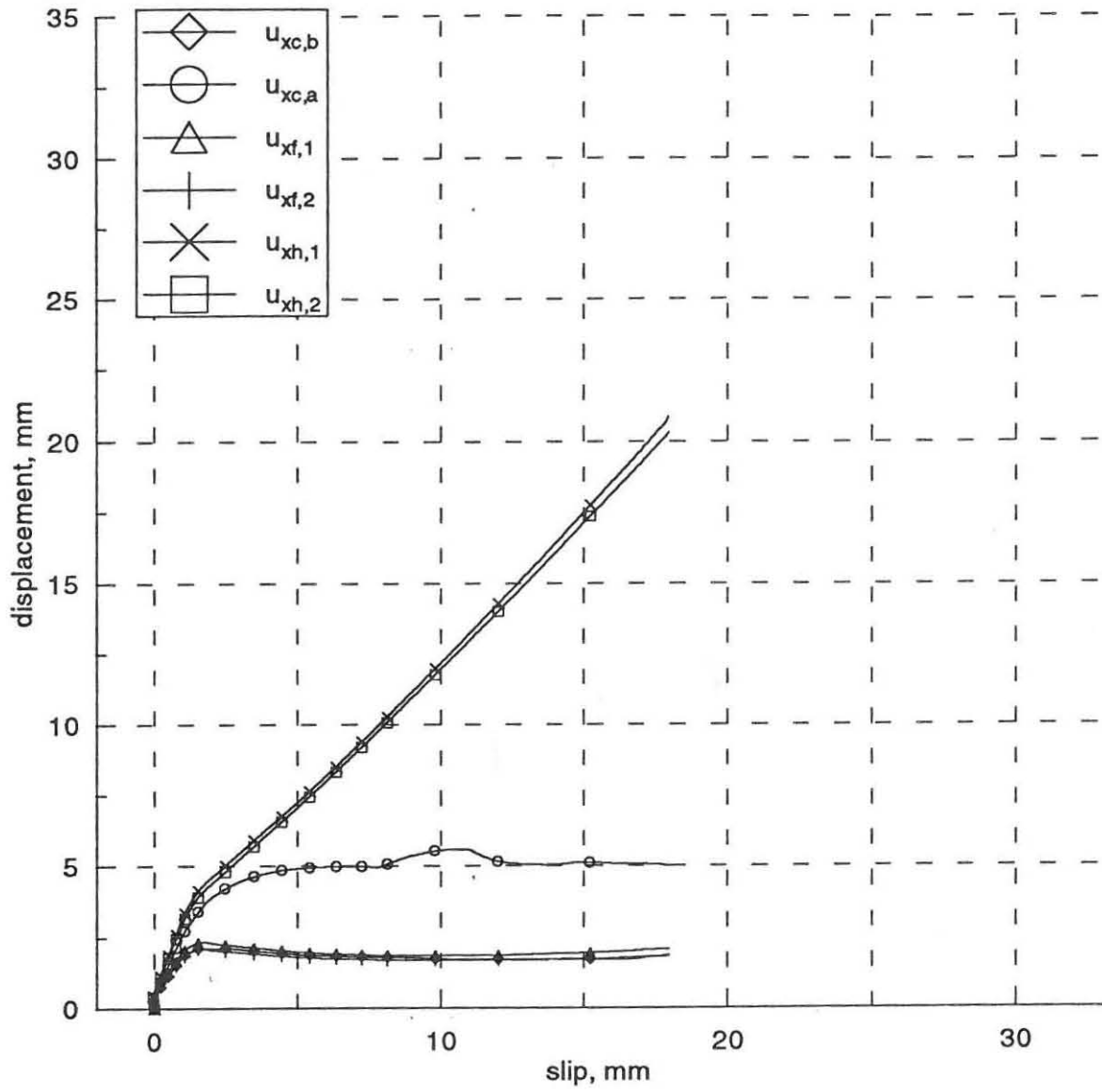
Displacements.
specimen C10



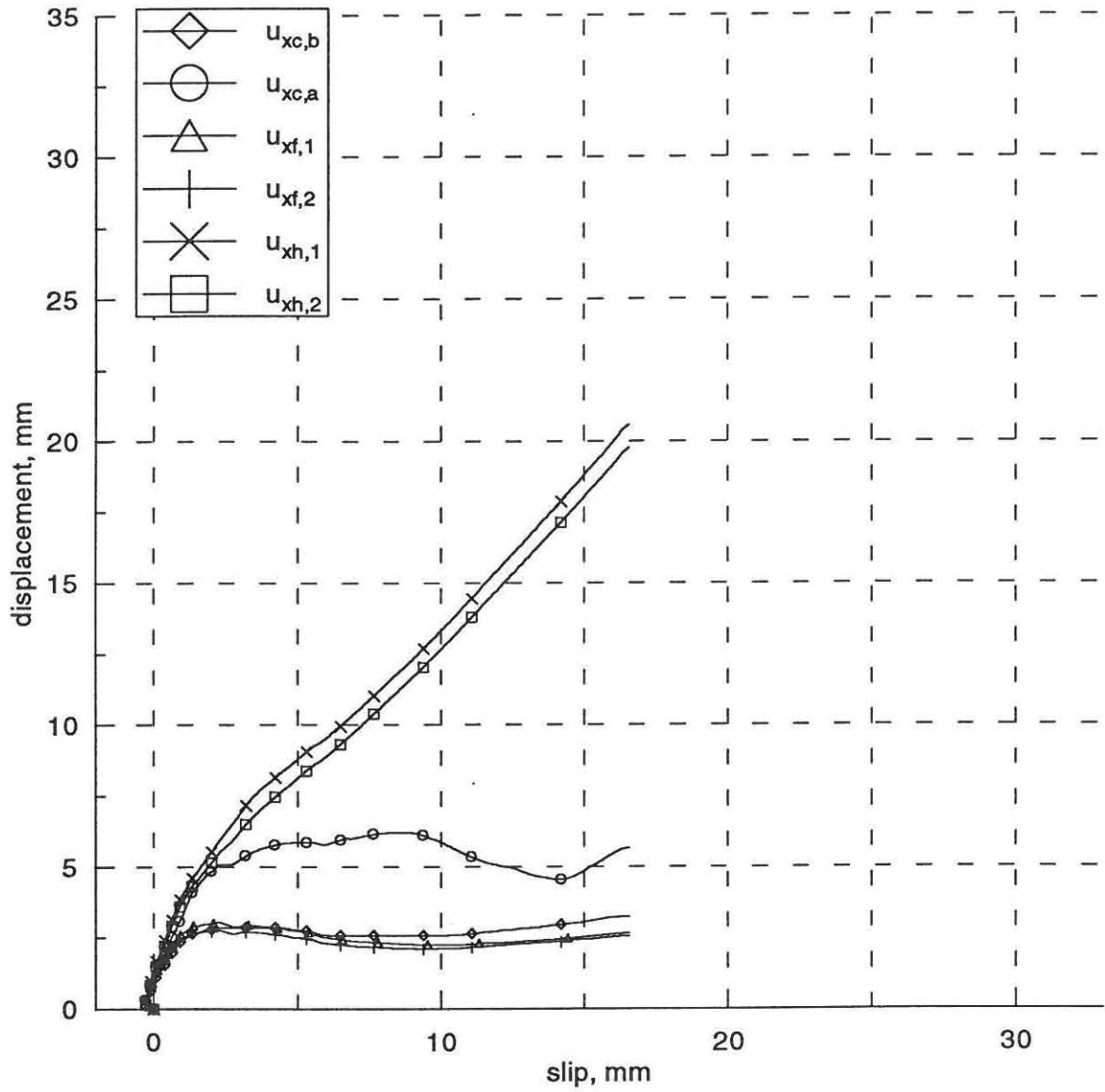
Displacements.
specimen C11



Displacements.
specimen C12



Displacements.
specimen C13



Displacements.
specimen C14

